LUMINESCENCE SENSITISATIONS OF NATURAL QUARTZ USING PRE-EXPOSURE DOSE AND THERMAL ACTIVATION TECHNIQUES

EBENEZER OLUBANJI ONIYA

Luminescence Sensitisation of Natural Quartz Using Pre-Exposure Dose and Thermal Activation Techniques

By

Oniya, Ebenezer Olubanji

(Matric No: 118223)

B. Sc (Hons) Physics (Ado Ekiti) M. Sc. (Ibadan)

A thesis in the Department of Physics

Submitted to the Faculty of Science

In partial fulfillment of the requirements

for the Degree of

Doctor of Philosophy

of the

University of Ibadan

DECEMBER 2014

CERTIFICATION

I certify that the work described in this thesis was carried out under my supervision by **Oniya Ebenezer Olubanji (118223)** in the Department of Physics, University of Ibadan, Nigeria.

.....

SUPERVISOR

I. A. Babalola
B.Sc, Ph.D (Ibadan)
Professor, Department of Physics,
University of Ibadan, Nigeria.

DEDICATED TO

GOD: My Alpha and Omega who always turn impossibilities to possibilities in my life.

My Father and Mother: Who made my coming to this world achievable.

Dupe: My love, for your patience, prayers, supports and encouragements.

Ini, Fise and Temmy: For all those times Daddy was away or too busy.

ACKNOWLEDGEMENTS

Words are inadequate to express my appreciations to God for the grace to complete this work against all the odds. I can say it loud that “weeping may endure for a night but joy cometh in the morning”. The way God has demonstrated HIS sovereignty and supremacy throughout the duration of study made it settled within me that any project that belongs to Almighty God will surely be accomplished. My Father and Redeemer, I thank you.

With pleasure, I express my immense gratitude to my supervisor, Prof. I. A. Babalola, and Dr N. N. Jibiri, who was co-opted to see to the completion of the work. Despite their tight schedules they patiently and diligently guided my thoughts. God will protect you for this kind gesture and efforts. I am equally grateful and can not but say a BIG thank you to Dr F. O. Ogundare who initiated this work and introduced me to luminescence world. I will continue to remember you as my mentor and academic tutor.

I wish to express my profound gratitude to Prof I. P. Farai, I. R. Obed, Dr A. A. Adetoyinbo, Dr (Mrs.) A. Ademola, Dr Adegoke, Dr Awe, Dr Ogunsola, Dr Otunla and the entire academic staff of Physics Departments University of Ibadan for their cooperation at various times.

I say special thanks to Prof. G. Kitis of Nuclear Physics Laboratory, Aristotle University of Thessaloniki, Greece and Dr. G. S. Polymeris of Institute of Nuclear Sciences, Ankara University, Turkey for their technical and academic assistance. I also register my profound appreciation to Dr. N. C. Tsirliganis and the entire member of staff of the Research Center ‘Athena’ (Athena R.C.) Greece, for the assistances and hospitality shown to me during my stay in their laboratory where I carried out the bench work.

I also express my untold appreciations to Prof I. R. Ajayi, Prof. N. O. Ajayi, Dr R. S. Fayose and all the entire member of staff of Physics and Electronics Department, Adekunle Ajasin University Akungba Akoko for their diverse encouragements and assistances rendered. I sincerely acknowledge my colleagues in the struggle, Dr. Benson Igboin, Dr. E. A. Afe, Dr. Busuyi Mekusi, Dr. Ayuba, Mrs. Igili and Dr. O. Olubosede for their wonderful supports, prayers and encouragements.

I am specially grateful to Adekunle Ajasin University and Education Trust Fund (ETF) Nigeria for the financial support offered in the framework of "2008 Education Trust Fund Academic Staff Training and Development" that was responsible for my sponsorship to Greece where I carried out the experimental work of this study.

I wish to acknowledge with due respect, Late Brother and Sister S. A. Adeyemi, Brother and Sister O. Ogunleye and Brother and Sister S. Balogun, Brother Paul Olpha and the leaders of Apostolic Faith, Youth Directorate Development, Ondo District for their great concern and prayers for the success of the research work.

This acknowledgment can be complete without appreciating my beloved wife, Dupe Oniya for the patience, tolerance and understanding she displayed during the course of this research. Your prayers and moral supports are acknowledged and appreciated, I love you my love.

Lastly, my immense appreciation goes to all that contributed to the success of the study, including you. Thank you all and God bless you.

TABLE OF CONTENTS

CHAPTER THREE: MATERIALS AND METHODS

CHAPTER FOUR: RESULTS AND DISCUSSIONS

LIST OF TABLES

LIST OF FIGURES

ABSTRACT

Luminescence sensitisation is an important stage in the application of quartz in pre-dose retrospective dosimetry and dating. The existing techniques for sensitisation in quartz are Pre-Exposure Dose (PED) and Thermal Activation (TA). Previous works were centred on combined actions of PED and TA with less attention given to the separate contributions of these techniques in pre-dose sensitisation of quartz. This work was undertaken to determine the separate contributions of PED and TA in sensitisations of 110^{o}C Thermoluminescence (TL) peak and Room Temperature Linearly Modulated Optically Stimulated Luminescence (RT-LMOSL) of quartz.

Two sets of quartz samples, one from Oro in Kwara State (S2) and the other from Ijero-Ekiti, Ekiti State (S4) with high sensitisation signals were used. Each of the two sets was divided into two parts; the first was unannealed while the second part was annealed, following standard procedures. Each of the unannealed and annealed samples was further divided into 38 aliquots required for the protocol. Fourteen aliquots each of unannealed and annealed samples were given PED and another set of 14 aliquots were without PED. The TL and RT-LMOSL measurements were carried out on each aliquot using an automated RISØ TL/OSL reader (model-TL/OSL–DA–15). Sensitisation reproducibility of repeated TL measurements on 10 different aliquots of each of the unannealed and annealed samples was quantified using Coefficient of Variation (CV). Data were analysed using descriptive statistics.

The sensitisation signals of the aliquots of unannealed samples without PED was higher than that of the aliquots with PED by factor of 76.0 % and 79.0 % for TL and RT-LMOSL respectively for S2 while the corresponding factors obtained for S4 were 45.0 % for TL and 14.0 % for RT-LMOSL. In annealed samples, the sensitisation signal of the aliquots with PED was rather higher than that of the aliquots without PED, by factor of 224.0 % for TL and 201.0 % for RT-LMOSL for S2 and for S4, it was by factor of 245.0 % for TL and 217.0 % for RT-LMOSL. The sensitisations reproducibility of aliquots of unannealed samples were found to be poor with CV of 33.5 % for S2 and 52.0 % for S4. This improved significantly in the annealed samples to CV 6.3 % for S2 and 9.0 % for S4.

Luminescence sensitisation by pre-exposure dose was dominant in annealed quartz samples. Therefore, only annealed quartz samples are recommended for pre-dose

retrospective dosimetry and dating. The use of 110^{o}C thermoluminescence peak signal in sensitisation corrections of unannealed quartz is not advisable.

Keywords: Quartz, Thermoluminescence, Optically stimulated luminescence, Pre-dose sensitisation, Thermal activation.

Word count: 411

NOTATIONS AND SYMBOLS

AD	Additive-dose
CCD	Computerized curve deconvolution
CW-OSL	Continuous-wave optically stimulated luminescence
ED	Equivalent dose
FWHM	Full width height maximum
Gy	Gray,S.I unit of absorbed dose (1J/kg)
HF	Hydrofluoric Acid
HR	Heating rates
IR	Infra-red
IRSL	Infra-red stimulated luminescence
LED	Light emitting diode
LM-OSL	Linear-modulation optically stimulated luminescence
MATAC	Multiple aliquot thermal activation curves
OSL	Optically stimulated luminescence
PMT	Photomultiplier tube
POSL	Pulsed- optically stimulated luminescence
RT	Room temperature
SAR	Single-aliquot regenerative-dose
TA	Thermal activation
TAC	Thermal activation curve.
TD	Test dose
TL	Thermoluminescence
TR-OSL	Time Resolved-optically stimulated luminescence
UV	Ultra-violet

CHAPTER ONE

INTRODUCTION

1.1. Background

Quartz is the second most abundant mineral in the continental crust of the Earth after feldspar (Preusser, *et al.*, 2009). It makes up 12.6% by weight of the Earth's crust as crystalline quartz and amorphous silica (Krbetschek, *et al*., 1997). This mineral exhibits Thermoluminescence (TL) and Optically Stimulated Luminescence (OSL) signals corresponding to amount of prior irradiations it received. Such luminescence signals have been used in retrospective dosimetry in the scope of accident dosimetry, dating geological and archaeological materials over the last 40 years (Wintle, 1973; Forman, *et al*., 1994; Duller, 1997; Krbetschek, *et al*., 1997; Prescott and Robertson, 1997; Roberts, 1997; Wintle, 1997; Preusser, *et al.*, 2009).

Mechanisms of quartz luminescence are full of complexity. As a result, many studies have been carried out by many workers on quartz in order to have better understanding of its luminescence for improved applications (Wintle, 1997; Bailey 2001; Preusser, *et al.*, 2009; Pagonis and Kitis, 2012; Kitis and Pagonis, 2013; Koul and Polymeris, 2013; Asfora et al., 2014; Ferreira de Souza, et al., 2014; Koul et al., 2014; Sadek, et al., 2014; Topaksu et al., 2014; Polymeris, 2015). However, such reports are very scanty on Nigerian quartz and quartz samples obtain from Africa as a whole. Pioneer works on TL characteristics of quartz from Southwestern Nigerian was reported by Ogundare *et al.*, (2006) on anomalous behaviour of thermoluminescence and its kinetic analysis (Ogundare and Chithambo, 2007a). More studies thereafter on Nigerian quartz using relative new luminescence method of Time Resolved OSL (TR-OSL) have also been reported (Ogundare and Chithambo, 2007b; 2008). Recently, universality study of thermal quenching effect and sensitisation of quartz of various origins that included Nigerian quartz have been reported (Subedi et al. 2011; Appendix 1; Appendix 2).

A very important feature of quartz luminescence property is an enhancement in its sensitivity as a result of combined actions of pre-exposure dose of previously received irradiation by the quartz sample and the subsequent thermal activation reading or annealing to an activation temperature. This characteristic termed pre-dose effect that is customarily allied with 110^{o}C TL peak of quartz has been well studied and

documented in the literature (Zimmerman, 1971; Chen 1979; Bailiff, 1994; Koul et al., 1996; Bailey, 2001; Li and Yin, 2001; Adamiec et al 2006; Galli et al., 2006; Koul 2008). The degree of pre-dose sensitisation is directly proportional to the quantity of the pre-exposure dose (Zimmerman, 1971). This forms the main reason behind the use of this technique in retrospective dosimetry. Pre-dose sensitisation is used to monitor the increase in the sensitivity of 110 ^{o}C TL peak resulting from pre-exposure dose rather than the accumulation of TL and OSL as in conventional luminescence methods (Bailif 1994; Koul et al., 2010). Also, the sensitisation of 110^{o}C TL glow-peak is the key instrument that is used in monitoring sensitivity changes of higher TL peaks and OSL signal of quartz as used in Additive-Dose (AD) and Single-Aliquot Regenerative-dose (SAR) methods of dating (Wintle 1997, Murray and Wintle, 2000; Wintle and Murray, 2006). Furthermore, this technique has been effectively utilized in authenticity testing of artefacts and firing temperature measurements of pottery materials (Bailiff, 1994; Koul et al., 1996; Galli et al., 2006; Li and Yin, 2001).

Apart from the pre-dose sensitisation, annealing of quartz at temperatures higher than 200^{o}C has been observed to result in enhancement of the TL sensitivity of the 110^{o}C glow peak (Yang and McKeever, 1990; Chen *et al*., 1994; Rendell *et al*., 1994; Han et al., 2000; Schilles, 2001, Li, 2002; Adamiec, 2005; Koul, et al., 2010). This sensitisation, unlike pre-dose effect, is independent of pre-exposure dose but rather reliant on annealing temperature and duration. Therefore, this type of sensitisation represents the sensitivity change caused by annealing process only. A viable proof of the existence of pure thermal sensitisation was the enhancement in sensitivity after a high temperature annealing of a synthetic quartz that was not expected in view of pre-dose sensitisation (Yang and McKeever 1990; Botter-Jensen *et al* 1995). This is because synthetic quartz, which is believed to have received insignificant level of irradiations in the past, is not supposed to display enhancement of sensitivity as a result of annealing to high temperature. In addition to their observations on synthetic quartz, Botter-Jensen *et al* (1995) and Larsen (1997) also established the sole thermal sensitisation of sedimentary quartz samples.

The long duration of annealing that was found to result in higher value of sensitisation was linked to a process caused by annealing only by Han et al., (2000). In another direction of thought, Chen and Li, (2000) who reported a similar observation proposed a modified Zimmerman's model with multiple R centres (each with different

life times leading to a more complex function of time and temperature) to explain their findings. Recently, Koul et al., (2010) tried to identify the possibility of pure thermal sensitisation in the pre-dose mechanism of the 110^{o}C TL peak of quartz by way of using different annealing temperatures and heating rates (HRs) for thermal activation process. The basis of incorporating different heating rates was on the premise of different time of heating that is associated with each heating rate. Theses authors also confirmed the sole thermal sensitisations in their study that involved three natural quartz samples and one synthetic.

In general, sensitivity change of the OSL has also been found to be parallel to that of 110^{o}C TL peak and that suggested a common mechanism for the two phenomena (Stoneham and Stokes, 1991; Franklin et al., 1995; Bøtter-Jensen et al., 1999; Jain et al., 2003; Koul and Chougaonkar, 2007). The similarity of the OSL and 110^{o}C TL peak sensitivities has made the latter a reliable monitoring tool for sensitisation of the OSL signal in various dating protocols (Aitken and Smith, 1988; Stoneham and Stokes, 1991; Stokes, 1994; Bøtter-Jensen et al., 1995; Wintle, 1997; Wintle and Murray, 1998; Murray and Roberts 1998; Chen and Li, 2000; Murray and Wintle, 2000; Wintle and Murray, 2006; Kiyak et al., 2007; 2008; Polymeris, et al., 2009).

Another issue of luminescence of quartz is the degree of sensitisation of 110^{o}C *TL* peak and *OSL* that changes from sample to sample. The complexity of this peak, just like other quartz luminescence properties, is always attributed to the different crystallization environments during formation of respective sedimentary quartz samples that varies from location to location (Deer et al., 2004; Preusser, *et al.*, 2009). Apart from this, 'sample to sample' variation in sensitisations, 'grain to grain' sensitisation variation has also been reported for the case of sedimentary quartz samples (Preusser, *et al.*, 2009), leading to the devising of a 'Single grain *OSL* attachment' to TL reader.

1.2 Justification of present study

Despite recent findings in the literature (Koul et al., 2010; Oniya et al., 2012a) coupled with other initial reports on the existence of pure thermal sensitisation of quartz, the conditions leading to thermal type of sensitisation is yet to be established in the literature. Hence, identification of conditions leading to pure thermal sensitisation

of quartz is important in the traditional pre-dose dating method. This is because there is possibility of erroneous age estimation in dating if pure thermal sensitisation happens to be the most prevalent mode of sensitisation in a sample to be dated using pre-dose dating technique.

Workers have tried to explain the reason for variations in sensitisation of quartz to be as a result of different grain to grain origin, and various irradiations, thermal and optical/bleaching histories that each grain might have possessed during transportation (Deer et al., 2004; Preusser, *et al.*, 2009). Each of these factors is widely known to be highly influential on pre-dose sensitisation. Ordinarily, the same degree of pre-dose sensitisation is expected from all the grains of any crystalline quartz. This assumption results from the fact that all the grains are from a common origin, and possess the same irradiations, thermal and optical/bleaching histories. Therefore, any variation in sensitisation that is exhibited by different grains of a crystalline quartz sample should arise from the intrinsic nature of the crystal and not from prevailing external factors. It is important to investigate this because such findings will definitely shed more light on the complex nature of quartz luminescence characteristics; and subsequently be of high assistance in all area of luminescence applications.

Simultaneous sensitisation study of various components of OSL signal and that of 110^{o}C TL peak of a Nigerian annealed quartz sample has not been conducted based on the available gathered data from the literature.

1.3 Aim and objectives of the study

This work was undertaken with the aim to study the pre-dose sensitisations of 110^{o}C Thermoluminescence (TL) peak and Room Temperature Linearly Modulated Optically Stimulated Luminescence (RT-LMOSL) of unannealed and annealed quartz.

The objectives of the study are as follows:

(1). Investigation of sensitisation of quartz grain of the same origin. This will reveal more information about the intrinsic nature of quartz luminescence properties and thereby improve luminescence dating techniques, mostly in sensitivity corrections of high TL peak and OSL component.

(2). Determination of the individual contributions of pre-exposure dose and thermal activation in pre-dose sensitisation. This will form criteria for selection of appropriate quartz for pre-dose technique and shed more light in luminescence characteristics of quartz generally.

(3). Correlation of pre-dose sensitisation of 110^{o}C TL peak and all components of OSL with a view to identifying which of the components of the OSL is associated with the 110°C TL trap in the two understudied Nigerian quartz samples. This will form a foundation upon which various dating protocols for Nigerian quartz could be based.

1.4 Thesis outlines

This thesis is organized in five chapters. Chapter 1 deals with the introduction. This is followed by justification of present study, aim and objectives of the study. Thesis outline concludes this chapter.

In Chapter 2, the basic concepts in luminescence are introduced including the band model, thermoluminescence (TL), OSL, dose estimation protocol, luminescence sensitivity and factors affecting sensitivity. Methods of computerised curves deconvolution are also presented. Brief description of retrospective dosimetry is presented in this chapter. Lastly, a description of the automated Riso TL/OSL reader system.

Chapter 3 presents the experimental description and preparations of the two quartz samples studied in this work. Followed by these is a Feldspar inclusion test on the two quartz samples studied is investigated. Furthermore, this chapter elucidates a list of TL/OSL protocols employed for the measurements undertaken in this work and their respective descriptions. A description of Computerised curves deconvolution analyses that were performed in this work concluded this chapter.

The results of the measurements carried out in this work are presented in chapter 4. The measurements are in two phases: (i) Reproducibility study of pre-dose sensitisation of the 110^{o}C TL peak and (ii) Modes of luminescence sensitisations in unannealed and annealed quartz samples. Each of these results is discussed. Respective

models are proposed and implication of results on retrospective dosimetry and general recommendations for luminescence studies are presented in this chapter.

Chapter 5 gives the conclusion and recommendation resulting from the pertinent findings of the study in luminescence dating and retrospective dosimetry generally.

CHAPTER TWO

LITERATURE REVIEW

2.1 Luminescence phenomena

Luminescence techniques that are employed in retrospective dosimetry involve stimulation of light from some insulators (called phosphors) that had been exposed to ionizing radiation earlier (Wintle, 1997). When the stimulation is achieved by application of heat at a linear heating rate, the technique is termed TL while known as OSL when it is accomplished by optical stimulation. The quantity of acquired dose due to the earlier exposure to radiation by the phosphors is estimated by measuring the amount of light emitted during the stimulation. This is based on the assumptions that the acquired dose is proportional to the quantity of the emitted light. Therefore, the measured acquired/equivalent dose is then utilized in retrospective dosimetry either in evaluation of date in archaeological and geological dating or reconstruction of accident dose in accident dosimetry.

The most widely used phosphor in retrospective dosimetry is quartz (Preusser et al., 2009). An important reason for this is its abundance in nature. This mineral is one of the more abundant rock-forming continental crust minerals (Ivliev et al, 2006). It is readily found in archaeological artifacts and geological materials like rocks and sediments (Preusser et al., 2009). Furthermore, quartz samples are always present in building bricks or blocks in which accident dose assessment could be based in the case of accident dosimetry.

Quartz, either in natural or synthetic form, does not exhibit perfect crystalline nature (Preusser, et al., 2009). This mineral generally contains a vast number of intrinsic and extrinsic point defects. Intrinsic defects are unoccupied sites (vacancies) and occupied sites that in a perfect crystal would be unoccupied (interstitials). On the other hand, extrinsic defects are impurities at sites that in a perfect crystal would be occupied (substitutional impurities) or unoccupied (interstitial impurities).

2.2 Energy band model

Theoretically, when electrons are excited in a perfect crystalline material that is free of defects by ionizing radiation, the excited electron will only reside in the conduction band for a moment say less than 10^{-8}s before it loses its excitation energy and drops back down to the valence band, where it recombines with a hole. However, in quartz (as it is in other phosphors) the existence of defects results in the creation of allowed energy states in the otherwise forbidden band gap. Therefore, instead of all the excited electrons to recombine directly with free hole at the valence band, electrons are rather trapped at these point defects known as trap centres. The free holes in valence band are also captured at recombination centres. The captured electrons remain trapped at the trap centres until thermal or optical excitation is applied to return the electrons to the conduction band. From where some fraction of the electrons will find their way to the recombination centre and recombine with the trapped holes. However, a fraction of the de-trapped electrons will be re-trapped at the trap centres. The diffusion time is very short and recombination can be regarded as instantaneous (Aitken, 1998).

When the recombination is radiative, luminescence signal is emitted and the total luminescence signal emitted is generally a function of the initial absorbed energy of the ionizing source (McKeever and Chen 1997). Meanwhile, a portion of all electron-hole recombination events take place without any light emission (non-radiative). The size of this fraction can vary between 0 and 1, depending on factors such as crystal temperature and type of impurity (Horowitz, 1984). Direct radiative transitions of electrons from conduction band to valence band do not contribute to luminescence signal described above. This is because such transition will give rise to radiation which has quantum energy greater or equal to the energy gap and consequently be absorbed by the material (self-absorption).

This mechanism for TL and OSL processes is better portrayed graphically using a simple band model shown in Figure 2.1. The electron and hole pairs created by irradiation with ionising radiation are trapped at trap centres; electrons being trapped at *T* traps while holes are captured at *R*-centre, *L*-centre or *K*-centre. While excited electrons at conduction band are trapped at T traps, some portion recombined directly with captured holes at L-centre or K-centre during irradiation. The trap *Ts* represents a

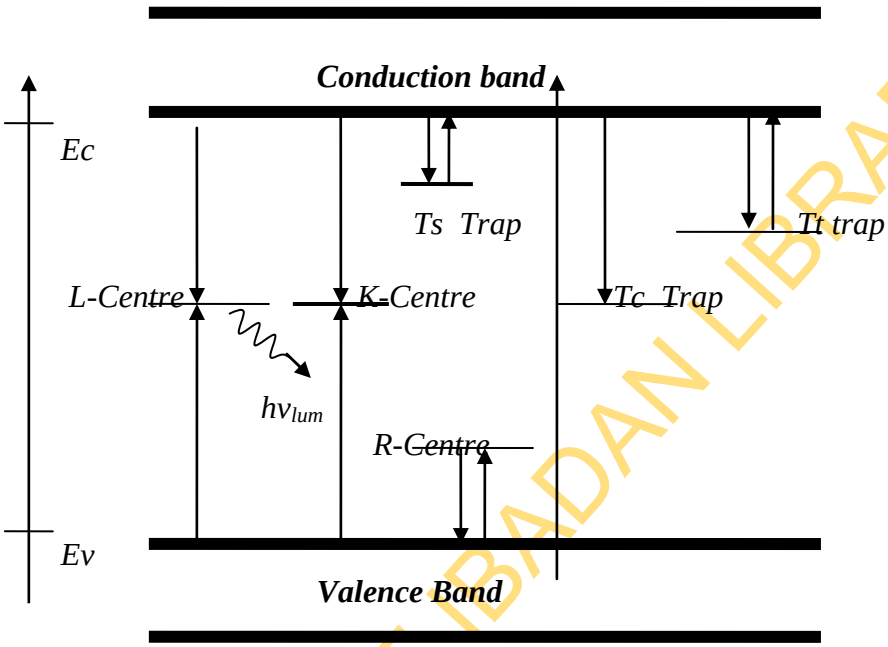

Fig. 2.1. Simple band model illustrating TL and OSL processes

shallow (unstable like 110^{o}C TL peak) trap from where the probability of thermal eviction/detrapping is high. *R*-centre is also unstable hole-trap. Whereas, *Tt* is the thermally stable trap in which the probability of thermal eviction (without both thermal and optical external stimulation) is negligible. Tc is extremely stable and deep trap which is thermally/optically disconnect. By stimulating the sample either thermally (TL) or optically (OSL), trapped electrons at Tt and Ts traps may gain sufficient energy to escape and be released into the conduction band. From where some of these released electrons can be retrapped at the any of *T* traps. The remaining will find their way to either *L*-centre or *K*-centre where they recombine with trapped holes. The recombination at *L*-centre is radiative, that is luminescence is emitted. This luminescent signal is what is employed in luminescence dosimetry. Conversely, the recombination at *K*-centre is non-radiative in which the energy release may be in form of heat or light with wavelengths that are outside the detecting window of the luminescence equipment.

2.3 Thermoluminescence

In case of TL, the stimulation by heat is applied by heating the material with a linear heating rate β (Ks^{-1}), resulting in the temperature varying as $T = T_0 + \beta t$, where T_0 is temperature at time $t = 0$ (K). The mathematical expressions describing TL processes .are presented below.

2.3.1 TL kinetic expressions

The rate of thermal release of trapped electrons into the conduction band at temperature *T* is $ns\exp\left(-\frac{E}{kT}\right)$ 2.1

where *n* is the number of trapped electron (cm^{-3}), *E* is the trap depth (eV) of the material (phosphor), *k* is Boltzmann's constant (eV/k) , and *s* is the frequency factor or attempt to escape frequency factor (sec^{-1}).

Assuming de-trapping and re-trapping of electron take place in the same trapping state, the intensity of *TL* signal is given by

$$I = -\frac{dm}{dt} = A_m m n_c \qquad 2.2$$

in which *m* is the concentration of recombination centres (hole in centres), (cm^{-3});

n_c is the concentration of free electrons in the conduction band, (cm^{-3});

A_m is the recombination probability ($cm^{-3}sec^{-1}$). From Eq. 2.2 it is evident that the recombination rate is proportional to the number of free electrons, n_c, and the number of active recombination centres, m.

The equation describing the rate of change of electrons in traps, n (cm^{-3}) is given by

$$\frac{dn}{dt} = -ns\exp\left(-\frac{E}{kT}\right) + n_c(N-n)A_n \qquad 2.3$$

where A_n ($cm^{-3}s^{-1}$) is the retrapping probability and N (cm^{-3}) is the total concentration of traps. By using Eq. 2.3, Randall and Wilkins (1945), Garlick and Gibson (1948) and May and Partridge (1964) respectively obtained First, Second, and General order kinetics for *TL* independently, which are equations governing TL processes. The expressions are:

First-order kinetics, $$I = -\frac{dn}{dt} = ns\exp\left(-\frac{E}{kT}\right) \qquad 2.4$$

Second-order kinetics, $$I = -\frac{dn}{dt} = n^2\frac{s}{N}e\exp\left(-\frac{E}{kT}\right) \qquad 2.5$$

General-order kinetics, $$I = -\frac{dn}{dt} = n^b s' e\exp\left(-\frac{E}{kT}\right) \qquad 2.6$$

where $s' = s/N$ and b = kinetic order, a parameter with values typically between 1 and 2

However, the general order kinetics is an interpolation between first and second order kinetics. It describes some experimental *TL* behaviour which does not correspond to any of first and second kinetics orders, but rather to a kinetics order between the two. Similar to this, Chen et al., (1981) suggested another order kinetic theory to describe these cases of intermediate kinetic order. This is called mixed order kinetic. It was given as:

Mixed order kinetics , $$I = -\frac{dn}{dt} = n(n+C)s'.e\exp\left(-\frac{E}{kT}\right) \qquad 2.7,$$

where $s' = s/(N+C)$, C is the concentration of electrons trapped at some kind of deep traps.

It follows from Eq. 2.4 that

$$\frac{dn}{dt} = -ns\exp\left(-\frac{E}{kT}\right) \qquad 2.8$$

If the sample is heated up so that the temperature is set at a linear rate β, so that $dT = \beta dt$, we can now substitute for dt in Eq. 2.8 and separate the variable to obtain.

$$\frac{dn}{n} = -\left(\frac{s}{\beta}\right)\exp\left(-\frac{E}{kT}\right)dT \qquad 2.9$$

At the start of the heating when $T = T_o$ let the number of trapped electrons be equal to n_o. When the temperature T has been reached there are n electron left in the trap. Now we can integrate Eqs. 2.9 between the limits to give

$$\int_{n_o}^{n}\frac{dn}{n} = -\frac{s}{\beta}\int_{T_o}^{T}\exp\left(-\frac{E}{kT'}\right)dT' \qquad 2.10$$

$$\ln\left(\frac{n}{n_o}\right) = -\frac{s}{\beta}\int_{T_o}^{T}\exp\left(-\frac{E}{kT'}\right)dT' \qquad 2.11$$

by finding the exponential of both side gives

$$n = n_o\exp\left[-\frac{s}{\beta}\int_{T_o}^{T}\exp\left(-\frac{E}{kT'}\right)dT'\right] \qquad 2.12$$

Substitution of Eqs. 2.12 into Eq. 2.4 yields

$$I(T) = sn_0\exp\left(-\frac{E}{kT}\right)\exp\left[-\frac{s}{\beta}\int_{T_o}^{T}\exp\left(-\frac{E}{kT^{'}}\right)dT^{'}\right] \qquad 2.13$$

which is the expression for the first order kinetics. With similar approach by starting from Eqs. 2.5, 2.6 and 2.7, the following equations are equally obtained for second, general and mixed order kinetics respectively (Pagonis et al., 2006)

$$I(T) = \frac{n_0^2 s}{N}\exp\left(-\frac{E}{kT}\right)\left[1+\frac{n_o(b-1)s}{N\beta}\int_{T_o}^{T}\exp\left(-\frac{E}{kT^{'}}\right)dT^{'}\right]^{-2} \qquad 2.14$$

$$I(T) = s"n_0\exp\left(-\frac{E}{kT}\right)\left[1+\frac{(b-1)s"}{\beta}\int_{T_o}^{T}\exp\left(-\frac{E}{kT^{'}}\right)dT^{'}\right]^{-\frac{b}{b-1}} \qquad 2.15$$

$$I(T)=\frac{s'C^2\alpha\exp\left[\left(\frac{s'C}{\beta}\right)\int_{T_o}^{T}\exp\left(-\frac{E}{kT'}\right)dT'\right]\exp\left(-\frac{E}{kT}\right)}{\left[\exp\left(\left(\frac{s'C}{\beta}\right)\int_{T_o}^{T}\exp\left(-\frac{E}{kT'}\right)dT'\right)-\alpha\right]^2} \qquad 2.16$$

where n_0 = number of trapped electrons at time $t = 0$ (m^{-3})

$s''=s'n_o^{(b-1)}$ is an empirical parameter acting as an "effective" frequency factor for general-order kinetics (in s^{-1}),

$\alpha=\frac{n_o}{n_o+C}$, but here C only takes positive value.

2.3.2 Glow curve

During *TL* measurements, the intensity of the emitted luminescence (*TL* response) is generally recorded and plotted against temperature; the resulted graph is called a glow-curve. Glow curve is a unique product of the TL measurement of a given phosphor. Since the temperature of measurement is increased linearly with time, the probability of detrapping increases. The intensity initially increases, then it reaches a maximum value at the rate of detrapping peaks, and then it drops to zero again. The drop in luminescent intensity is caused by depletion of the trap.

A glow curve may consist of a number of glow peaks having different heights, widths and shapes, each corresponding to different trapping levels. The TL belonging to each peak corresponds to trap centres within the crystal. The positions and shapes of the TL peaks are related to the characteristics of these traps, which are in turn typical of the crystal containing them. Thus, the TL glow curve represents a scan through the various types of trap present in the crystal from which information about the trap can be inferred.

The dose imparted on the sample is conventionally estimated by measuring height of desired peak or area under the peak or entire glow curve. A typical example of a glow curve is shown in Figure 2.2. By solving the kinetic equations stated above usually yields glow curves similar to the kinetic equation solved. Figure 2.3 presents glow curves obtained by solving first and second order kinetics Eqs. 2.13 and 2.14.

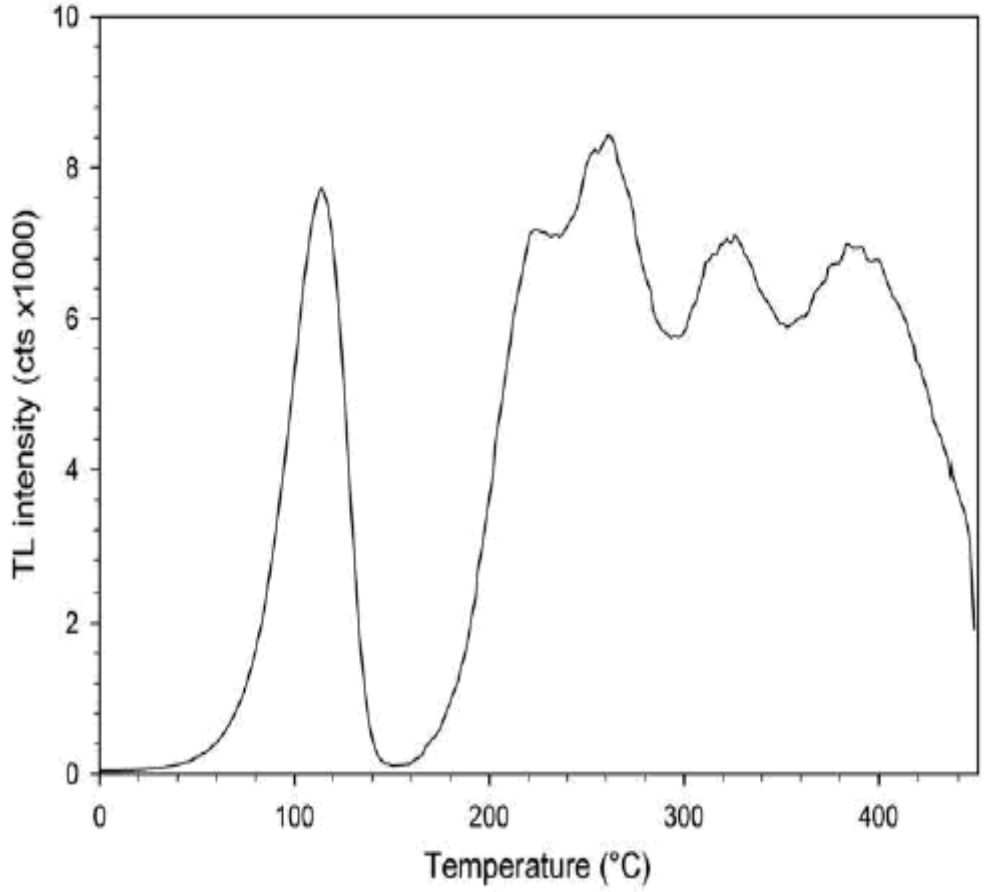

Fig. 2.2. Typical TL glow curve representing the photons released during the recombination at luminescence centres of previously trapped electrons. TL glow curve (heating rate 5 °C s−1) of quartz from Nigeria (GW1, Gumnior and Preusser, 2007)

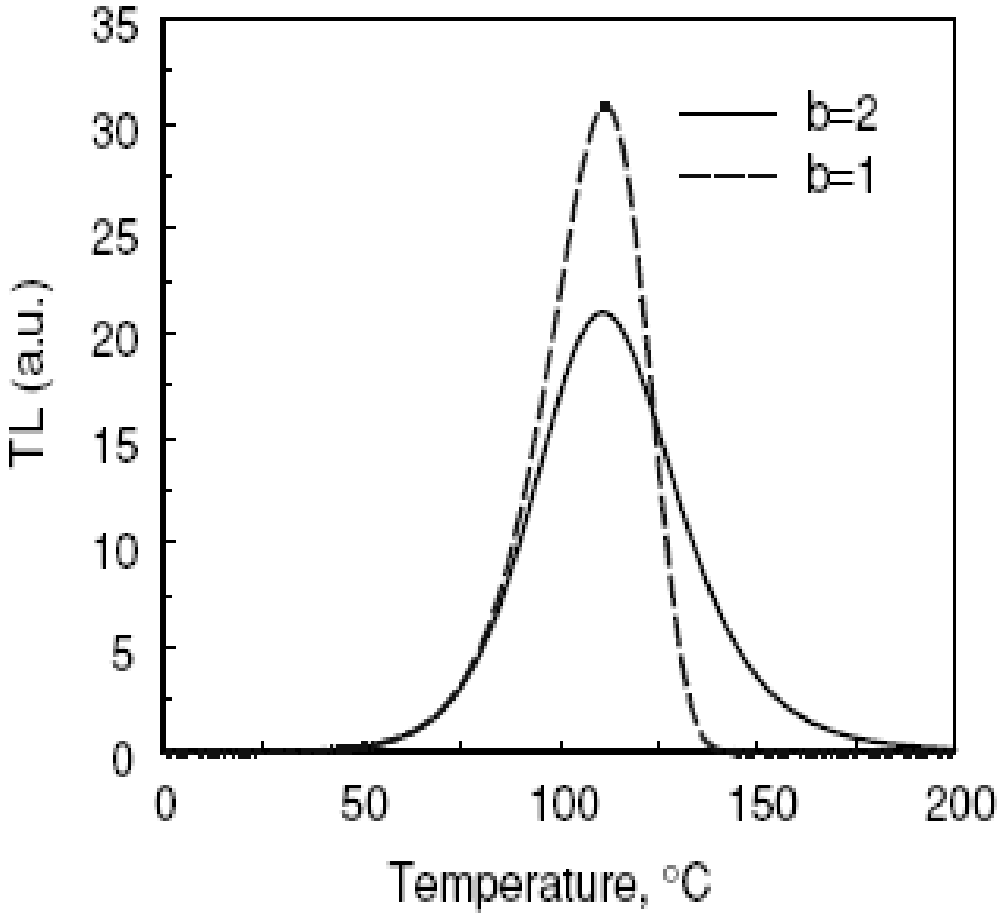

Fig. 2.3. Schematic comparison of TL glow peaks for first- and second-order kinetics. The parameters are E = 1 eV, s = 10^{12} s^{-1}, n_0 = N = 10^3 m^{-3}. (Pagonis et al., 2006)

2.3.3 Emission spectrum

As glow curve was defined as the plot of light intensity against temperature or time, emission spectrum is rather the graph of light intensity against wavelength. Emission spectrum is somewhat similar to TL glow curve. The light emitted during TL possesses a particular colour associated with recombination producing it. However, unlike glow curves, the colour dimension is not unique to TL, but is shared by all types of luminescence. While each TL peak in glow curve gives information about electron trap of the TL material under investigation, each peak in emission spectrum conveys information about recombination centre (hole trap). Particularly, emission spectrum of each glow peak of a glow curve is associated with the recombination/luminous center of that peak. Thus, glow peaks with identical emission spectra have the same recombination center. As a result, emission spectrum analyses provide adequate information about the recombination center that is responsible for each glow peak.

Quartz of various origins exhibit broad emission band in the blue, red and even around 990-1000nm. The different geological conditions of formation associated with each origin are apparently responsible for these various natures of glow curves and emission spectra (Jones and Embree 1976; Krbetschek et al., 1997; Preusser et al., 2009). However, the most frequently reported of all are the 380nm and 470nm which have their recombination centres linked to $[H_3O_4]^0$ and $[AlO_4]^0$ respectively. Optically stimulated luminescence (OSL) is believed to share the same emission band around 380nm. The wavelength emission from this center (380nm) is temperature dependent, while its luminescence is characterized by thermal quenching for all peaks in the family (Yang and McKeever, 1990; Wintle and Murray, 1999). Quartz TL peaks that are associated with the latter do not exhibit thermal quenching and do not bleach, unless the light wavelength is less than about 400 nm. Finally, the 470 nm emission of quartz has been found to remain almost unaffected by the pre-dose effect (Yang and McKeever, 1990; Koul and Chougaonkar, 2007). Examples of emission spectra are shown in Figures 2.4 and 2.5.

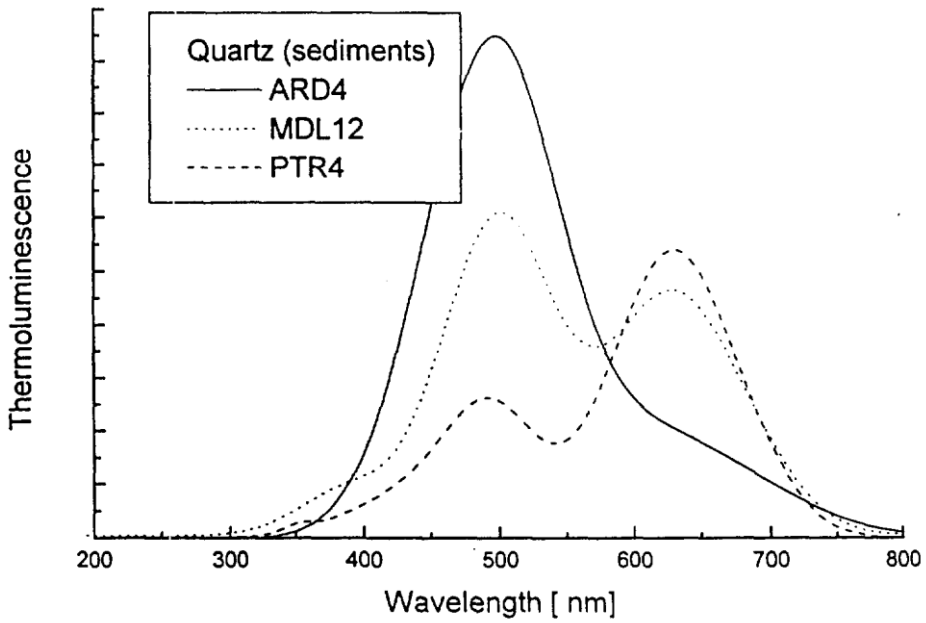

Fig. 2.4. Emission spectra at 190 – 210°C of quartz extracted from sediments; ARD 4: Thar deser, India (aeolian), MDL 12: Isrea (aeolian), PTR 4: California (marine-littoral). (after Singhvi and Krbetschek, 1996)

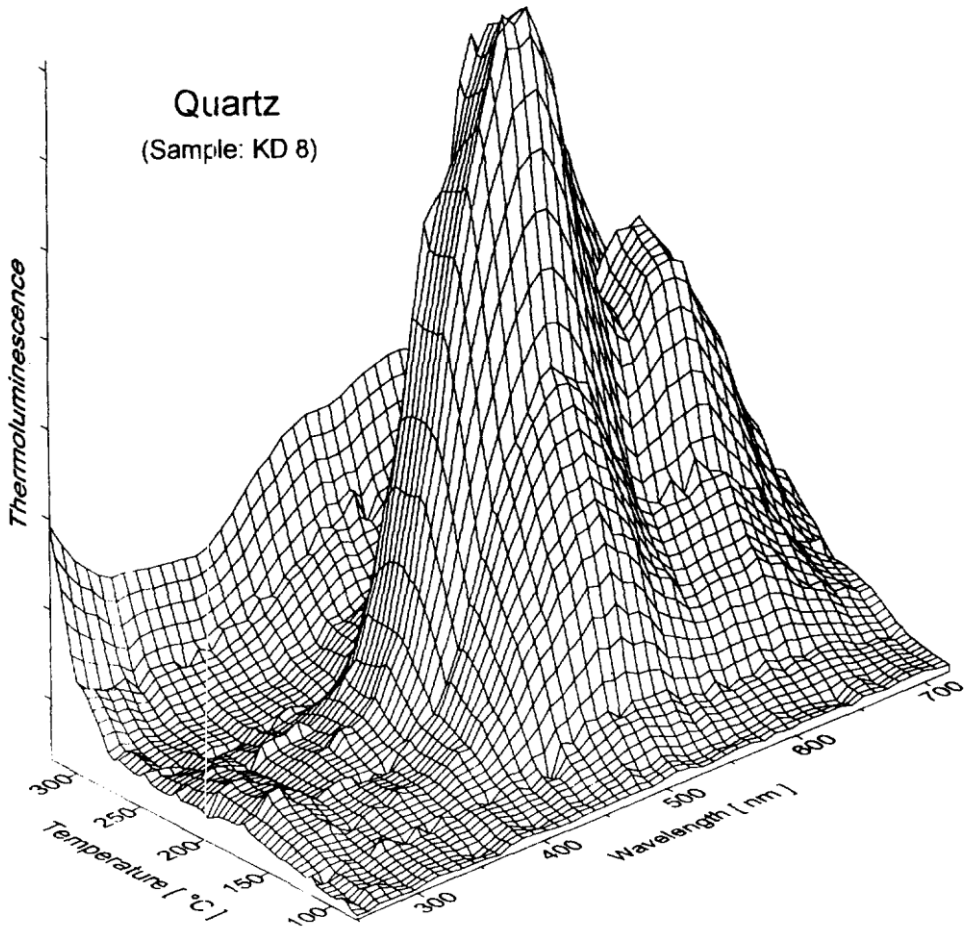

Fig. 2.5. Three-dimensional emission spectrum of an Aeolian/fluvial sample (KD 8) from the That desert, India (after Singhvi and Krbetschek, 1996).

2.4 Optically stimulated luminescence

Under optical stimulation, the irradiated phosphor is exposed to light (UV, visible or infrared) under a constant temperature and the OSL emission is recorded as function of stimulation time. The integral of the OSL emitted during the stimulation period is a measure of the dose of irradiation absorbed by the sample since it was last exposed to light. Unlike in the case of TL in which heat is applied only at a constant heating rate, there are three popular modes of stimulation in OSL. They are described below:

i. Continuous-wave OSL (CW-OSL):- this is a method in which thestimulation light intensity is kept constant and the OSL signal is monitored continuously throughout the stimulation period (Huntley et al., 1985),

ii. Linear-modulation OSL (LM-OSL):- in this method, the stimulation intensity is ramped (increased) linearly while the OSL is measured (Bulur 1996),

iii. Pulsed-OSL (POSL):- the stimulation source is pulsed and the OSL is monitored only between pulses in this method. This method has been developed into time-resolved OSL (TR-OSL) which provides information about luminescent centres (Bailiff, 2000; Chithambo and Galloway, 2000).

The plot of OSL signal recorded as a function of time is called OSL curve. Typical examples of CW-OSL and LM-OSL curves obtained experimentally are presented in Figures 2.6 and 2.7 respectively. More considerations will be devoted on CW-OSL and LM-OSL in this work.

2.4.1 CW-OSL

Just like it is with TL, the transitions of charge between energy levels during irradiation and subsequent optical stimulation of a phosphor can be described by a series of non-linear, coupled rate equations. p (s^{-1}) which is the rate of stimulation of electrons from the trap is related to the incident photon flux Φ and the photoionisation cross-section σ by

$$p(E_o) = \Phi\sigma(E_o) \qquad 2.17$$

where E_o is the threshold optical stimulation energy required for charge release and a return of the system to equilibrium.

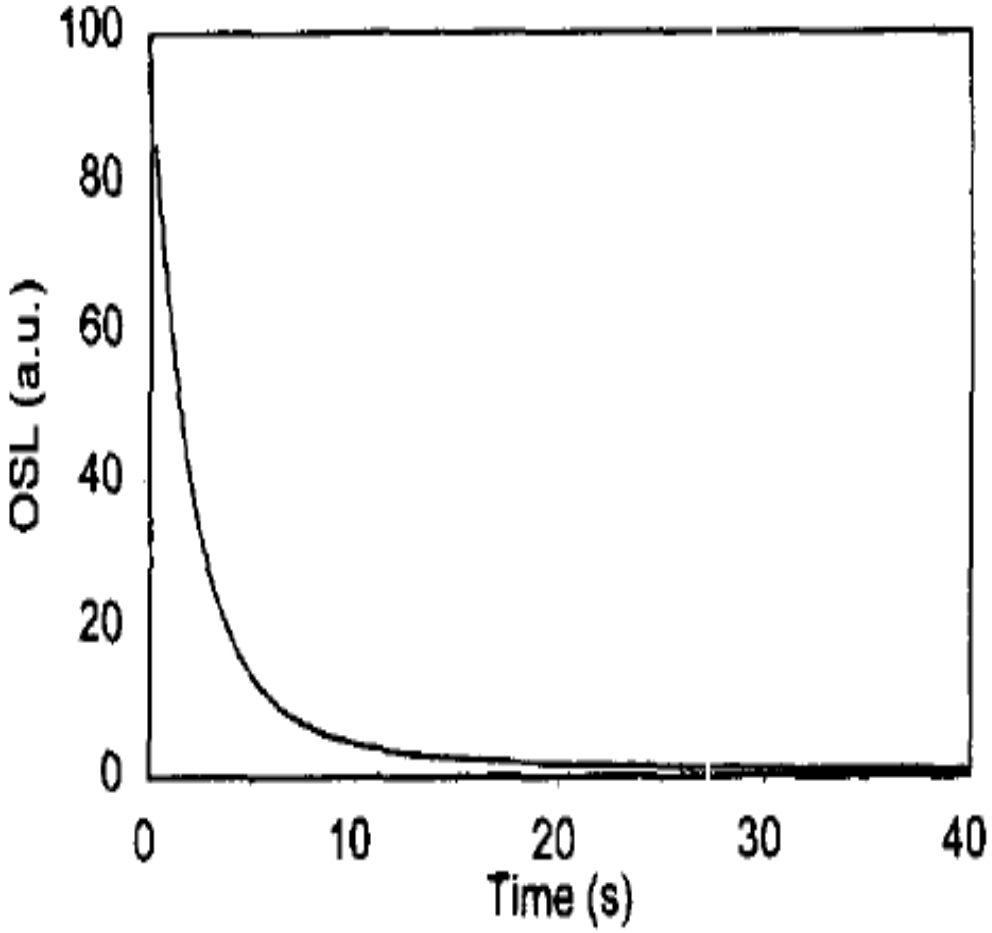

Fig. 2.6. Typical OSL decay curve from a sedimentary quartz samples given a beta dose of 2 Gy obtained using a green light wavelength band of 420 – 550 nm producing 16 mW/cm^2 at the sample position (Botter-Jessen, 1997)

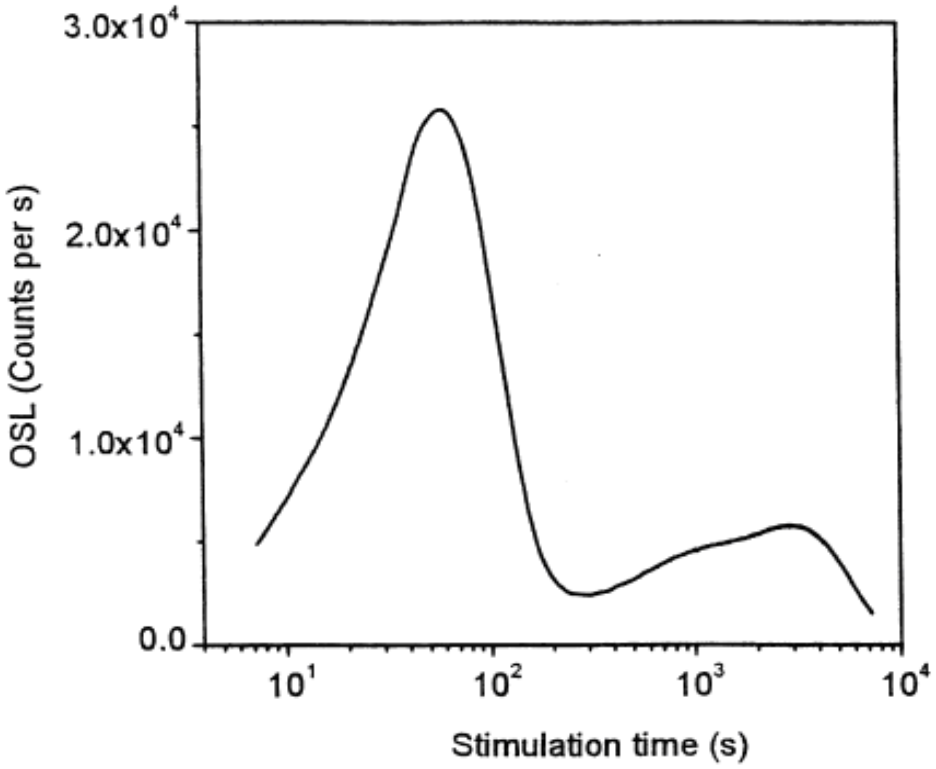

Fig. 2.7: An example of exposing a heated and dosed quartz sample to linearly increasing blue LED stimulation from 0 to 20 mW/cm2 over 7200 s. (Botter-Jessen et al., 2000).

The first-order kinetic describing CW-OSL is given as

$$I_{OSL} = -\frac{dm}{dt} = -\frac{dn}{dt} = np \qquad 2.18$$

with the solution of

$$I_{OSL} = n_o p \exp(-tp) = I_o \exp(-t/\tau_d) \qquad 2.19$$

where I_o is the initial OSL intensity at $t = 0$ and τ_d is the CW-OSL decay constant (Botter-Jessen et al., 2003a, McKeever et al., 1997).

The second order kinetics is given by Chen and McKeever (1997) as

$$I_{OSL} = \frac{n^2 p}{NR} = -\frac{dn}{dt} \qquad 2.20$$

Where $R = A/A_m$

after integration it is presented as

$$I_{OSL} = I_o \left(1 - \frac{n_o pt}{NR}\right)^{-2} \qquad 2.21$$

where $I_o = n_o^2 p / NR$.

For general order kinetics, Eq. 2.21 becomes

$$I_{OSL} = I_o \left(1 - \frac{n_o pt}{NR}\right)^{\frac{b}{1-b}} \qquad 2.22$$

with $I_o = n_o^b p / NR$

Chen and Leung, (2002) later worked on this and considered CW-OSL to be best fitted by a so-called "stretched exponential" of the form:

$$I_{OSL} = I_o \exp\left\{-\left(\frac{t}{\tau_d}\right)^{\beta}\right\} \qquad 2.23$$

with $0 < \beta < 1$.

Figure 2.8 shows a typical example of OSL curves of first and second order obtained by solving Eqs 2.19 and 2.21.

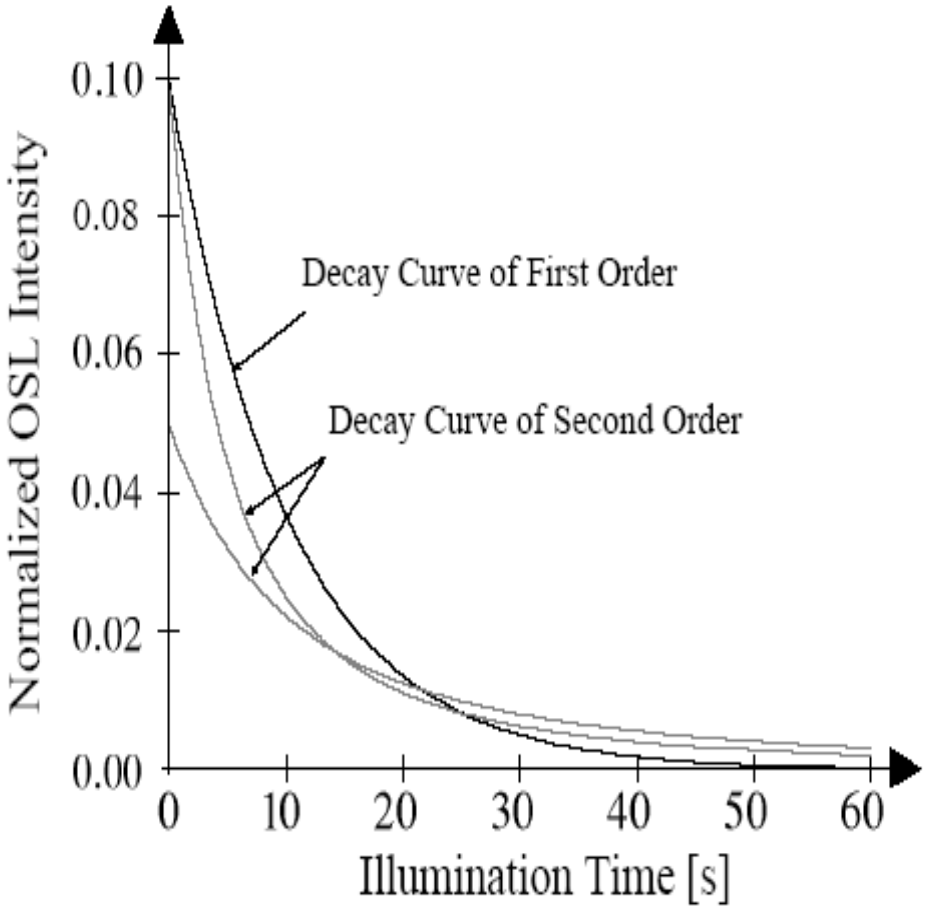

Fig. 2.8. OSL curves of first and second order.

2.4.2 LM-OSL

A linear increase in the intensity $\Phi(t)$ of optical stimulation at a fixed wavelength is employed in LM-OSL unlike in the case of CW-OSL in which steady stimulation intensity Φ is applied. By the adoption of this mode of stimulation we have

$$\Phi(t) = \Phi_0 + \beta_\Phi t \qquad 2.24$$

with $\beta_\Phi = d\Phi / dt$ and $\Phi = \Phi_0$ at time $t = 0$.

Therefore, the OSL signal is observed with series of peaks, with each peak corresponding to the optical release of charge from different trap types. Consequently, traps with large photoionisation cross-section at the particular wavelength used in stimulation are emptied first leaving those with small photoionisation cross-section to be emptied at later time of stimulation. This behaviour is well portrayed by the position of each peak in LM-OSL curves. Unlike the case of TL, the depletion of all the traps starts at the same time at the beginning of stimulation of LM-OSL however with different depletion rates. Meaning that all the peaks normally originate from the beginning of the OSL curve (at time t = 0) irrespective of their peak position. This is contrary to the case of TL in which each peak starts from different point depending on the positions of the respective peak in the glow curve. In general, LM-OSL is now becoming more popular than CW-OSL because the former gives more information about the traps involved in OSL measurements than the later (Botter-Jenson et al., 2003a).

To illustrate the shape of an LM-OSL curve mathematically, we consider the intensity of optical stimulation is ramped from zero to a maximum value Φ_m. Hence Φ now takes the new form $\Phi(t) = \gamma t$ for LM-OSL.

Therefore

$$p = \sigma\gamma t \qquad 2.25$$

By substituting Eq. 2.25 into Eq. 2.18 results in the first order kinetics of LM-OSL

$$I_{OSL} = -\frac{dn}{dt} = \sigma\gamma t n \qquad 2.26$$

from which a Gaussian function

$$n = n_0 \exp\left(-\frac{\sigma\gamma}{2}t^2\right) \quad 2.27$$

is obtained. Hence,

$$I_{OSL} = n_0\sigma\gamma t \exp\left(-\frac{\sigma\gamma}{2}t^2\right) \quad 2.28$$

following Whitley and McKeever, 2001, Eq. 2.28 may be written as

$$I_{OSL} = \gamma t \sum_{i=1}^{k} n_{0i}\sigma i \exp\left(-\frac{\gamma\sigma_i}{2}t^2\right) \quad 2.29$$

if there are *k* traps of type-*i*.

Eq. 2.29 describes simple sum of first order LM-OSL curves that represent several traps that are being emptied simultaneously at different rates.

2.5 Dose response

An essential element in any dating method is the graph of TL/OSL intensity versus dose known as dose response (McKeever and Chen, 1997). This provides data calibration parameters that are used to estimate natural luminescence signal which is converted into an equivalent dose. The response curve of a dosimeter should be proportional to dose; even ideally linear over dose range of interest. However, dose response of quartz is not always linear with dose because of sensitivity changes. It is rather known to have a non-linear growth curve with, quite often, a faster than linear dependence that is superlinear/supralinear, and slower than linear which is known as sublinear growth. A very important factor that determines the dose response curve is the competitions of electron among the electron traps during 'excitation stage' and a 'readout stage' of luminescence (Chen and McKeever, 1997).

Chen and McKeever, (1997) presented a linearity index f (D) that can be used to estimate dose linearity of any material as follows:

$$f(D) = \frac{(TL_i / D_i)}{(TL_1 / D_1)} \quad 2.30$$

where $TL_i(D)$ is the sample TL response corresponding to dose D_i, and D_1 is the normalization dose in the initial linear region, $f(D_1)$ is the sample TL response

corresponding to dose D_1, (by this definition $f(D)>1$, $f(D)=1$, and $f(D)<1$ respectively imply supralinearity, linearity and sublinearity).

Dose response of quartz is associated with saturation at high dose of irradiation. Saturation is normally brought about by absolute filling up of the electron traps from high irradiation dose at which response to subsequent dose is not possible. However, very high dose of irradiation can destroy the electron trap thereby causing decrease of the response. The effect is known as radiation damage. Typical dose responses for four electron traps/peaks (P1, P2, P3 and P4) of Brazilian quartz are shown in Figure 2.9 (Sawakuchi and Okuno, 2004). The peaks exhibit a common pattern up to ~30 kGy, with a fast initial supralinear growth. After that dose the peaks P3 and P4 saturate and the peak P2 decays continuously until 500 kGy and becomes constant. The peak P1 cannot be resolved after ~20 kGy due to the high intensity of the peak P2. However it seems to behave like the peak P2.

2.6 Luminescence sensitivity

Luminescence sensitivity of a given sample is defined as the amount of luminescence emitted per unit sample mass in response to a fixed laboratory dose (Furetta, 2003). Ideally, this phenomenon is expected to be constant for quartz but it is not in practice. Quartz of diverse kinds and origins possess different luminescence sensitivity. Better still, change in sensitivity stands as the most widely encountered problem in luminescence dating applications (Murray and Roberts, 1998). This attribute among other features of quartz that vary from 'samples to samples' are ascribed to different crystallization environments during formation of quartz samples (Deer et al., 2004; Preusser et al., 2009).

Apart, there are even some treatments that cause enhancement (sensitisation) or decrease (de-sensitisation) in luminescence sensitivity of quartz of the same kind and origin. Such could arise from prevailing external factors that the quartz sample either naturally or inadvertently exposed to in nature or those that are as a result of artificial or premeditated treatments in the laboratory during or prior to luminescence readouts; like radiaztion exposure, thermal treatments and optical stimulation e.t.c. (Bailey, 2001). The remaining part of this section will be devoted to considering some factors leading to sensitivity changes of quartz.

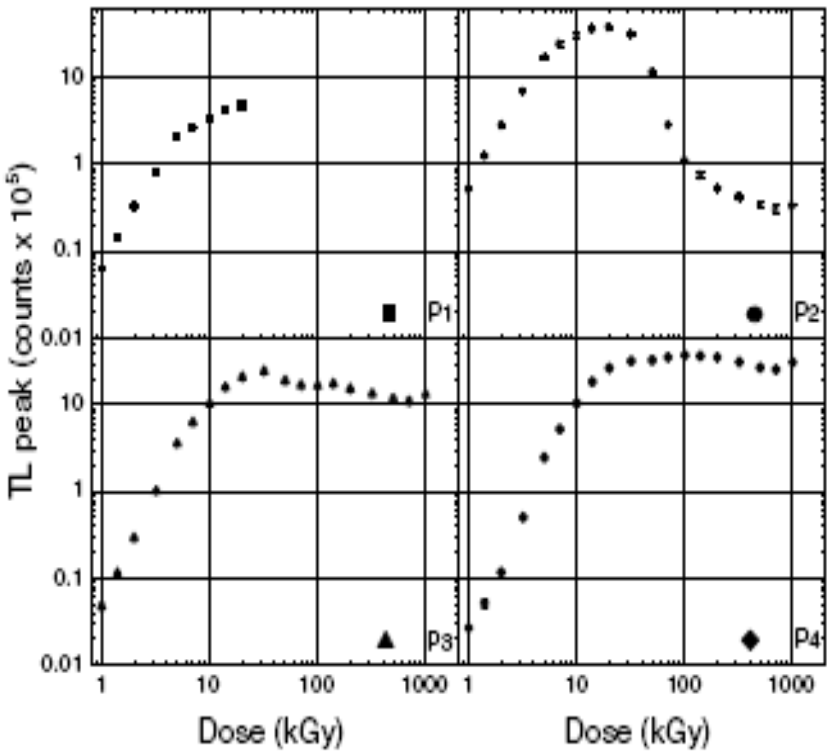

Fig. 2.9. Dose response of the TL peaks (P1, P2, P3 and P4) of Brazilian natural quartz exposed to γ rays of ^{60}Co in the range 1–1000 kGy. Heating rate used: 1°C/s. (Sawakuchi and Okuno, 2004)

2.6.1 Competitions during irradiation and stimulation

Various traps usually compete to trap free electrons that are produced during irradiation or stimulation. This process is known as competition. The nature of competitions depends on intrinsic nature of each respective luminescence material and some other external factors that cause alterations in the sensitivity of a given sample like radiation exposure, thermal treatments and optical stimulation (Bailey, 2001). By employing the model of Figure 2.1 as an example, traps *Ts*, *Tt* and *Tc* will contend among themselves for electrons during irradiation stage in which electrons are raised from the valence band into the conduction band. The manner of charge trafficking during irradiation is illustrated in Figure 2.10. The fraction of the total excited electrons to be trapped into each of the electron traps depends on their respective trapping probabilities.

The influence of competitions is most apparent during the stage of stimulation like TL readout. Figure 2.11 illustrates charge trafficking during the early temperature of heating; say to about 150^{o}C in which 110^{o}C TL peak is evicted. Due to competitions between Ts and the relatively thermal stable traps, it is obvious that only a portion of the electrons released from Ts trap to the conduction band can find their way to the L or K centre where recombination with hole takes place while the remaining fraction are shared among Tt and Tc traps. In this case, traps Tt and Tc are competitors and their degree of competitions depends on the level of their initial fillings. Therefore, there is a reduced competition at higher dose levels of saturation. In that case, the released electrons can only be involved in the recombination which will yield a relative enhanced 110^{o}C TL signal. The mode of charge trafficking reduces to what is contained in Figure 2.12 when heating is continued to higher temperature beyond 110^{o}C TL peak. Trap Ts in not taking part here and it is the turn of eviction of electrons in Ts which represent all thermally stable electron traps. Trap Tc is the only competitor with respect to traps Tt. Trap Tc is always potential competitor because it has a very deep depth that makes it to be thermally/optically disconnected always. Disconnected in the sense that once electrons are trapped into Tc trap, they can never be freed or evicted for re-trapping into any of the T traps or recombination with holes at recombination centre.

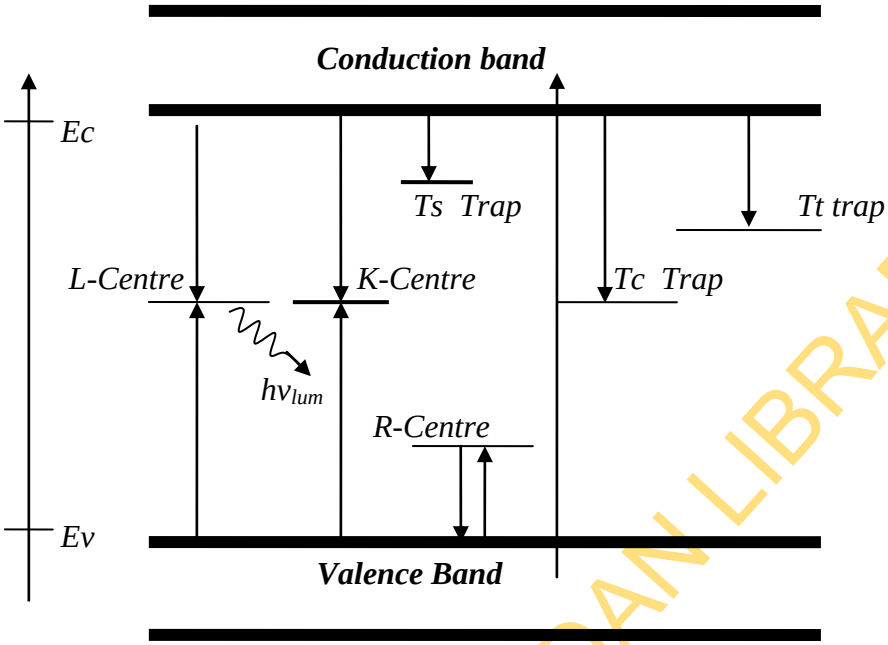

Fig. 2.10. Transitions taking place during excitation stage in the same energy scheme as that shown in Figure 2.1.

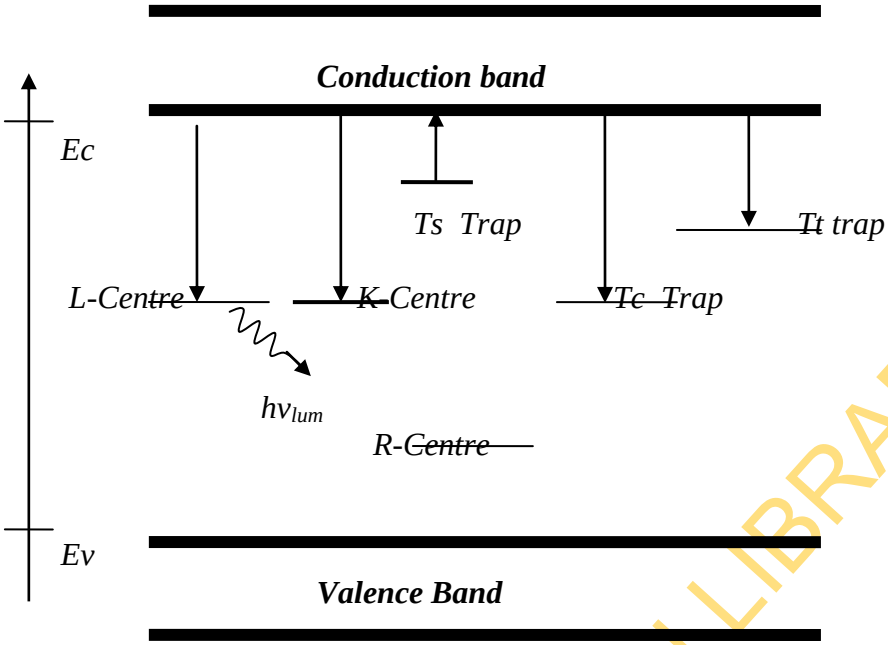

Fig. 2.11. Schematic competition of free charges among the electron traps during early state of heating (TL) up to ~150^{o}C

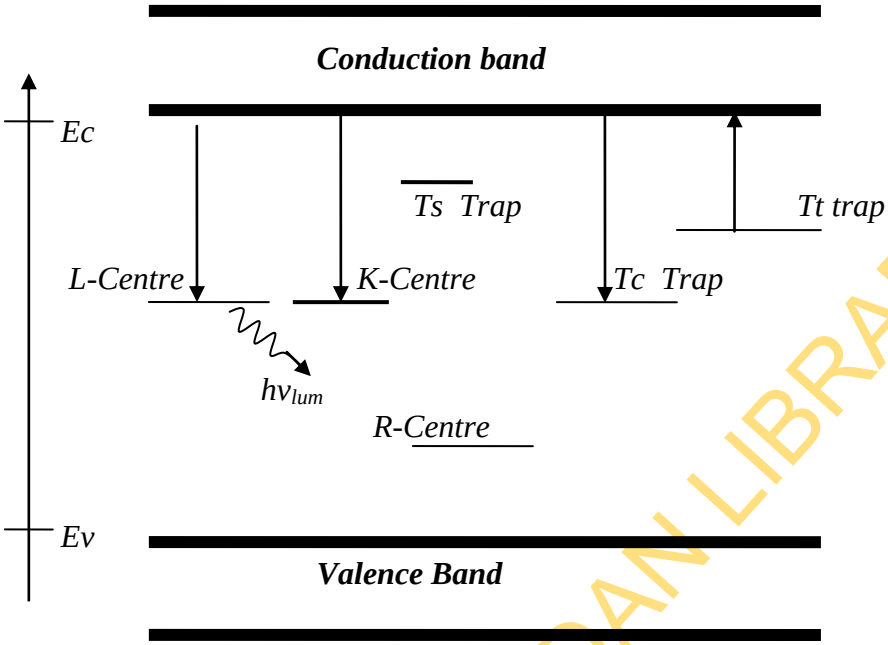

Fig. 2.12. Schematic competition of free charges among the electron traps during late state of heating (TL) from ~150 - 500^{o}C

The mechanism of competition explained above for TL is similar for the case of OSL except for the mode of stimulation that differs. This procedure of competition has been used to explain the enhancement of the luminescence sensitivity and then the phenomenon of suparlinearity (Chen et al., 1988) in the framework presented below explanations.

During readout, electrons released from, say trap Ts, could be re-trapped in competitor traps Tt or Tc or recombine in L or K centres at low doses of irradiation. This competition thereby causes reduction in luminescence signal. Increase in sensitivity that is paramount to suparlinearity, is expected at higher dose of irradiation. This is because almost or absolute saturation of competitor traps Tt and Tc at higher dose levels will result into a reduced or no competition at all. Consequently, nearly all evicted electrons from Ts trap will be available for recombination at L-centre or K-centre leading to enhanced sensitivity.

2.6.2 Luminescence sensitisation

One of the major challenging problems in quartz luminescence world is the issue of sensitivity changes (sensitisation). This is because adequate knowledge of this is required mostly in the regenerative-dose and pre-dose techniques where series of irradiations and thermal reading are employed. Moreover, quartz that is widely used in this task exhibits complex sensitivity nature. As a result, the issue of luminescence sensitivity has been a major point of attraction, both in the past and in the present, to many researchers. Two main causes of sensitisation in quartz are classified as pre-dose and thermal sensitisations.

2.6.2.1 Pre-dose sensitisation

Generally, sensitisation is an effect recognized to be the increase in the luminescence intensity of a phosphor to a certain test-dose (TD) of irradiation as a result of some treatment of the sample like heating, irradiation etc. Pre-dose sensitisation of quartz has been widely believed to be an enhancement of sensitivity as a combined result of irradiation and annealing. This implying that sensitivity changes in the 110^{o}C TL peak result only when the sample has been pre-exposed to a dose of

irradiation and subsequently heated to a given temperature; typically 500^{o}C (Chen and McKeever 1997). Sensitivity change of the OSL also has been found to be parallel to that of 110^{o}C TL peak and that suggested a common mechanism for the two (Stoneham and Stokes, 1991,). Franklin et al (1995) established that the electrons from the OSL traps combine with same luminescence centres as those from 110^{o}C TL peak. Many researchers have confirmed the similarity of the OSL and 110^{o}C TL peak sensitivities (Stoneham and Stokes, 1991, Murray and Roberts 1998, Wintle and Murray, 1998).

Pre-dose sensitisation was first discovered by Fleming and Thompson (1970) and the first model to explain the phenomenon was proposed by Zimmerman (1971). Her model was later amended by Chen (1979) to accommodate superlinearity of 110^{o}C TL peak.

2.6.2.1.1 Pre-dose model

The amended model of Zimmerman (1971) by Chen (1979) consists of two electron trapping states, Ts and Tc (the competitor Tc represents both Tt and Tc in Figure 2.1) and two hole states R-centre (the reservoir) and L-centre. During the excitation (see Figure 2.13) by administration of TD of ionizing radiation, electrons are raised from the valence to the conduction band. A fraction of this is trapped at the trapping state Ts and remaining at competitor trap, Tc. The holes go preferably to the reservoir R-centre. However, there is a non-negligible probability of the holes going to L-centre. Thus, the first thermally freed electrons can recombine with them during the heating (first heating to about 150^{o}C) and this results in the emission of the TL of the unsensitised material. The annealing (or TL reading), typically to 500^{o}C following the application of a high dose, empties all the electrons from Ts, yielding a rather high 110^{o}C TL peak signal. The significance of the thermal treatment to ~500^{o}C is to thermally release holes from the reservoir R, to the luminescence centre L. Zimmerman ascribed the reason for the higher response/signal observed, when a subsequent TD is given, to this increase in the concentration of holes in the luminescence centres by probability of radiative recombination. In attempt to improve on this model, more than one reservoir centres have been introduced to this model and that have been employed to account for most of the TL and OSL experimental observations (Bailey, 2001; Adamiec et al 2006)

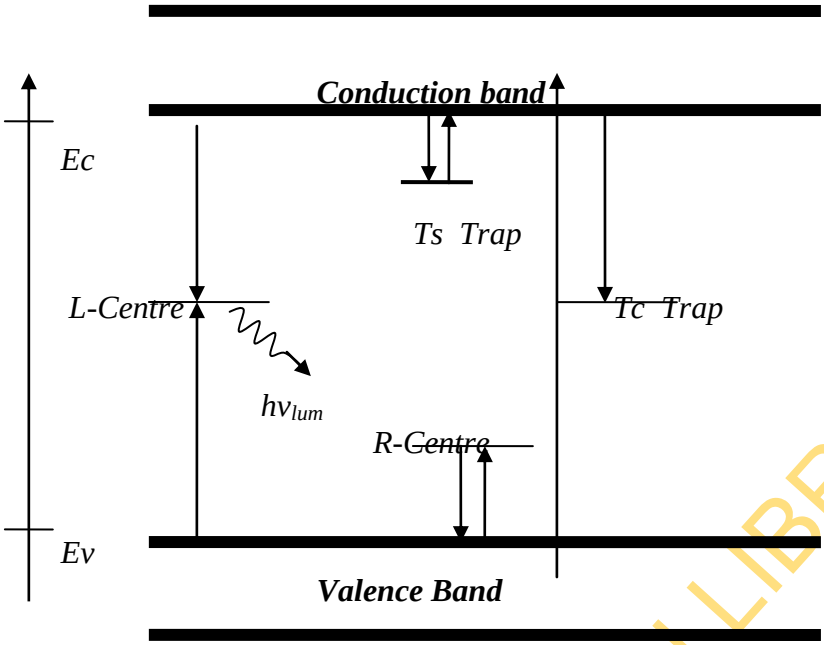

Fig. 2.13. Pre-dose sensitisation schematic band model.

Two major factors that can cause desensitisation of pre-dose effect after thermal activation are (i) radiation or dose quenching and (ii) ultra-violet (UV) reversal.

2.6.2.1.2 Radiation quenching

The effect called radiation or dose quenching is a desensitisation phenomenon that is observed in pre-dose effect. This occurs if the sensitivity to a TD following pre-exposure dose and thermal activation of a sample (Baillif 1994) that is expected to increase rather decreases with irradiation dose. This effect is quite different from radiation damage that results from annihilation of electron traps by very high dose of irradiation.

Two different models have been used to explain radiation quenching effect. Using the Zimmerman (1971) model, Aitken, (1985) attributed radiation quenching effect to the removal of holes trapped at L-centres as recombination occurs during irradiation leading to diminution in sensitivity of subsequent luminescence measurement. This model is contrary to a model of Bailey, (2001) in which he proposed that recombination is allowed at the R-centre unlike the model of Zimmerman, (1971) and that the concentration of holes trapped at both L- and R-centres increases with dose. Using these, he argued that it is an increase in competition for free charge, during both irradiation (TD) and during heating (TL readout) from the R-centres that produces the quenching effect.

However, by considering the sequence of pre-dose technique of dating of Bailiff, (1994), the recombination that occurs during heating to ~150^{o}C that is meant for removal of 110^{o}C TL peak which, follows laboratory calibration beta-dose, definitely contributes to radiation quenched sensitivity also. What makes this proposition viable is the level of the depletion of trapped holes at L centre resulting from this which is measurable and quantifiable if the pre-heat TL is recorded.

2.6.2.1.3 UV Reversal

UV reversal, as described by Zimmerman (1971), is the substantial sensitivity decrease that is always observed once an irradiated and annealed sample is illuminated by UV light. And a repeated high temperature annealing increases the sensitivity back

to nearly the same level as the previous one following the first high-temperature annealing. Zimmerman (1971) suggested that the UV reversal is associated with the transfer of holes from L-traps to R-traps during exposure of sample to UV light.

The detail of her model is presented as follows: When the sample is exposed to UV light the electrons in the valence band are excited. Because they acquire too much energy to be trapped by the R traps they are preferentially captured by L traps. The holes transferred to the valence band are then trapped by R traps, decreasing the sensitivity. Another model proposed by McKeever (1991) linked UV reversal with the optical release of electrons from deep traps which then recombine with trapped holes in $(H_3O_4)^0$ centres, thereby reducing the concentration of recombination centre.

2.6.2.2 Thermal sensitisation

Apart from the pre-dose sensitisation, annealing of quartz at temperatures higher than 200^{o}C has been observed to result in enhancement of the TL sensitivity of the 110^{o}C glow peak (Han et al., 2000). The effect of this sensitisation is not limited to annealing temperature only but also to duration of the annealing. Longer duration of heating (annealing time) generally results in higher value of the sensitisation. This sensitisation represents the sensitivity change caused by annealing process only and should not be confused with pre-dose process. This phenomenon is based on some workers findings on thermal sensitisation. This fact was supported by the enhancement in sensitivity after a high temperature annealing of a synthetic quartz that was observed, which was supposed not be in view of pre-dose sensitisation (Yang et al 1990). This is because synthetic quartz, which is believed to have received insiginificant level of irradiations in that past, is not supposed to display enhancement of sensitivity as a result of annealing to high temperature based on pre-dose mechanism.

McKeever et al (1983) observed that both TL and radioluminescence (RL) were affected in the same way, indicating that the sensitivity changes were due to alterations to the recombination centres (RL is the luminescence generated in material during exposure to nuclear radiation). Changes to the emission spectra that were also observed by Hashimoto et al (1994) confirmed these alterations to the recombination centres. Botter-Jensen *et al* (1995), in their study was able to establish the sole thermal sensitisation of sedimentary and synthetic quartz samples also. This was observed in

OSL and phototransferred TL (PTTL) of quartz to follow the same pattern of sensitisation after high temperature annealing. They suggested a model to explain thermal sensitisation which is based on that of McKeever et al (1983) (alterations to the recombination centres) and removal of competitors at high temperature annealing.

2.6.2.2.1 Thermal sensitisation model

The Botter-Jensen *et al* (1995) model contain three trapping states. As being seen in Figure 2.14, a shallow electron trap Ts represents 110^{o}C TL peak and all those shallow trap centres in the real material. The electron tap centres Tt represents all the optically active trap centres that are depopulated during OSL measurements and thermal stable traps in quartz (e.g 325^{o}C TL peak). Tc represents the thermally deep electron traps that do not empty either optically or thermally during TL or OSL measurement.

The model has two recombination centres L-centre and K-centre in which L-centre is radiative and K-centre none-radiative. Based on the assumption that annealing at high temperature alters recombination centres, concentration of L-centre is increased relatively to that of K-centre for annealed case in this model. This is achieved by either increasing L concentration or reducing K-centre concentration. Also, to model the removal of competitors at high temperature annealing, the concentration of Tc was reduced. By applying all these in the model, the following as observed experimentally were simulated (Botter-Jensen *et al* 1995; Larsen 1997):

i. OSL and PTTL sensitivity changed due to annealing temperature,

ii. Temperature shift of the photo-transferred 110^{o}C TL peak, and

iii. Dose response of OSL in sedimentary quartz.

The agreement between these and experimental results supports the hypothesis that thermal sensitisation observed in quartz is due to alterations to the concentrations of the recombination centres and trap centres and not to pre-dose effect only. These findings also suggested the impact of purely thermal sensitisation in pre-dose and regenerative dose methods.

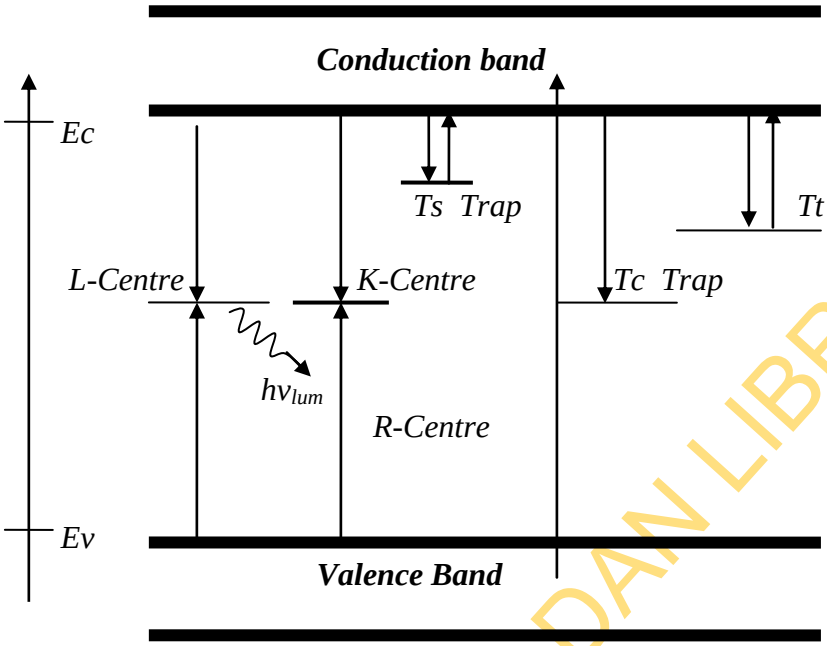

Fig. 2.14. Thermal sensitisation schematic band model

Also, the duration of the annealing has been observed to affect the degree of thermal sensitisation (Han et al., 2000). Longer time of annealing was found to result in higher value of the sensitisation and that was linked to a process caused by annealing only. Nevertheless, Chen and Li, 2000 who reported a similar observation has proposed a modified Zimmerman's model with multiple R centres (each with different life times leading to a more complex function of time and temperature) to explain their findings.

2.6.2.3 Thermal activation curve

The plot of thermally induced luminescence sensitisation as a function of thermal activation temperature (TAT) is often called thermal activation curve/characteristic (TAC). This is, however, referred to as multiple aliquots thermal activation curve (MATAC) when multiple aliquots are involved. TAC gives room for easy comparison of sensitisation associated with each TAT. An example of TACs is depicted in Figure 2.15. As observed in Figure 2.15, TAC is usually characterized by peak at maximum TAT. The 'late activation' and 'early activation' referred to in the figure are due to different heating rates employ for activation. Aitken (1985) points out that the temperature at which the sensitivity maximum of the TAC is reached depends on the time spent at high temperature. If the heating rate is slow, and more particularly, if the maximum temperature is held for, say, a minute before cut off, then the maximum will shift downwards in temperature.

The phenomenon behind the usual decrease in value of the sensitivity beyond the highest TAT in MATAC of quartz 110^{o}C TL peak has been an issue of concern in quartz luminescence research. According to Aitken (1985), this is referred to as thermal deactivation which, he presumed to be due to a direct thermal eviction of holes from L-centres into the valence band. Conversely, this is contrary to the pre-dose model in which L-centre is assumed to be much further from the valence band so that once a hole is captured at L-centre, it cannot be thermally released back to the valence band. Figel and Geodicke (1999) proposed a model which takes care of the possibility of thermal eviction of holes from L-centres into the valence band. These authors argued that recombination of electron trapped at high TL peaks beyond the

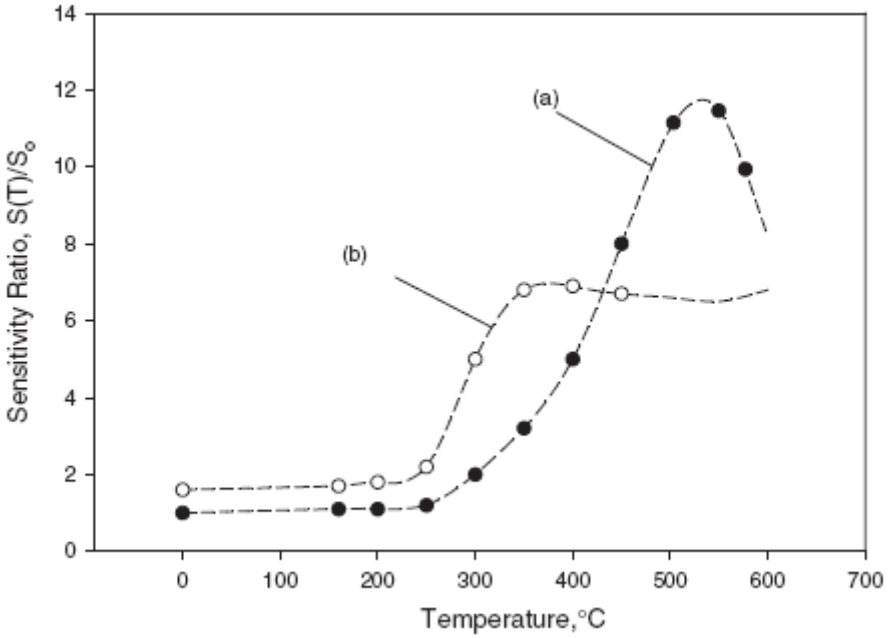

Fig. 2.15: TAC of Fleming and Thompson (1970) redrawn. Curves (a) and (b) show the 'late activation' and 'early activation' phenomena, respectively'

maximum TAT during further thermal activation will lead to depletion of already enriched trapped holes at L- centres. Consequently, a reduced TL sensitivity will follow. Based on this later model, it is envisaged that the structure of glow curve of thermal activation TL if recorded (which is quantifiable measure of the recombination process) should be related to TAC. Lastly, a model of probable recombination of electron at L-centres during subsequent irradiation after thermal activation was proposed by Chen and Pagonis (2003) to explain this nominal decrease of sensitisation after TAT. This model was experimentally confirmed recently (Appendix 2)

2.6.2.4 Heating rate effects

If different heating rates (β) are used during TL readout, the position of the maximum glow-peak temperature (Tm) is known to shift towards higher temperature with increasing β (Kitis et al., 1993). Furthermore, there is always a drastic reduction of TL signal as the β increases. The later diminution has been attributed to thermal quenching effect. The effect of β is better portrayed in Figure 2.16

Kitis et al., (1993) presented explanation to account for the shifting of Tm with β. At a low heating rate β_1, the time spent by the phosphor at a temperature T1 is long enough so that an amount of thermal release of electrons depending on the half-life at this temperature could take place. As the heating rate increases to $\beta_2 > \beta_1$ the time spent at the same temperature T1 decreases and therefore the thermal release of electrons is also decreased. So, a higher temperature T2 is needed for the same amount of thermal release to take place at β_2. In this way the whole glow-peak is shifted to higher temperatures as the heating rate increases in a manner depending on the half-life and the time spent at each temperature.

2.6.2.5 Thermal quenching

Thermal quenching is an effect known to cause decrease in TL and OSL signals as measurement temperature is increased. In other words, it is the loss of luminescence efficiency with increasing measurement temperature. This effect has been reported for both quartz TL (Wintle, 1975) and quartz OSL (Smith et al., 1990; Spooner, 1994)

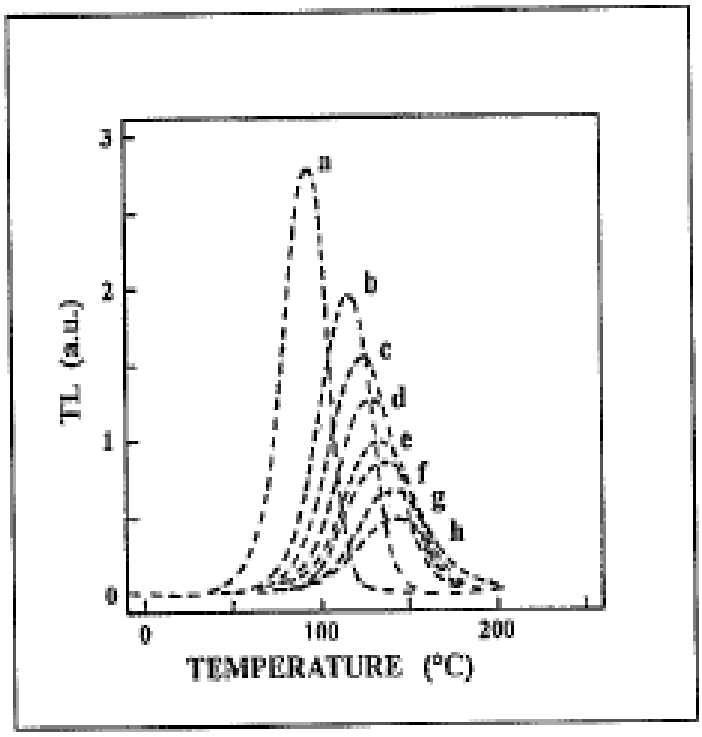

Fig. 2.16: Experimental glow-peak shapes of the 110°C TL peal of Norwegian quartz obtained by heating rates in °C/s: a = 2, b = 8, c = 20, d = 30, e = 40, f = 50, g = 57, h = 71

This effect is only obvious in TL when the measurement is taken with different heating rates. As the heating rate increases the glow-peak is shifted to higher temperatures and the integral of the glow-peak, which measures the luminescence efficiency, decreases. Apart from the reduction in the TL peak (area and peak height) that is caused by this effect, the shape of the peak is distorted (Kitis et al., 1993). This consequently affects the kinetic order since the high temperature side of the glow peak is afflicted more than the lower temperature side. However, in the case of OSL, the effect is noticeable when the OSL is measured at a given elevated temperatures. (Wintle, 1975; Petrov and Bailiff, 1996).

Two models have been used to explain the thermal quenching mechanism; Schön-Klasens (McKeever et al., 1997) and Mott-Seitz models (Mott and Gurney, 1948). The reduction of luminescence efficiency with Schön-Klasens model is ascribed to a progressive loss of L-centres due to thermal ionisation of trapped holes into the valence band. Conversely, in Mott-Seitz model an increase in the probability of non-radiative recombination centre relaxation is predicted for higher temperatures, rather than a reduction in the concentration of L-centres. With this, electrons that are captured to the excited states of L-centres from the conduction band are thermally assisted to undergo non-radiative transition to the ground state. Thus, the probability of non-radiative recombination increases with temperatures. The recombination energy that ought to be given out as light is absorbed by the lattice in this case. This model is generally more adopted than the former (Bailiff, 1994; Bailey 2001).

The empirical expression for the reduction in radiative intensity due to thermal quenching is of the form (Curie, 1963)

$$\eta = \frac{1}{1 + Ce^{-W/kT}} \qquad 2.31$$

where η is luminescence efficiency, C is dimensionless quantity, W (in eV) is the activation energy and T is the temperature (K).

In view of Mott-Seitz model (Bøtter-Jensen et al., 2003a) W is the energy barrier necessary for an excited state electron to transition non-radiatively to the ground state, with the emission of phonons (Nanjundaswamy et al., 2002).

2.6.2.6 Temperature lags

Another effect that has to do with measuring temperature in TL is termed temperature lags or thermal lagging. In practice, the thermocouple that measures the temperature of the sample during TL measurements is usually fixed to the heating element in many of the TL/OSL readers. This meaning that the thermocouple measures the temperature of the heating element rather than that of the sample. However, when physical information from the glow curves is to be extracted, it is essential to know the sample's temperature rather than that of the heating element. Differences in the temperature of the heating element and that of the sample that is known as temperature lags, have been studied by many workers (Taylor and Lilley, 1982; Gotlib et al., 1984; Betts and Townsend, 1993; Betts et al., 1993; Piters and Bos, 1994; Facey, 1996;).

The major causes of this effect are, non-ideal thermal contact between the heater element and the sample (in case of contact heating TL reader), the temperature gradient across the sample and effects of the inert exchange gas in the chamber that is applied in order to avoid chemiluminescence (light from oxidation) (Piters and Bos, 1994). Theoretical studies in this direction have contributed to the possibility of making necessary correction to this effect. (Gotlib *et al* 1984; Betts and Townsend 1993; Piters and Bos 1994).

Kitis and Tuyn (1998) provided equation that can be used for evaluation of the temperature lag between the heating element and the dosimeter to be:

$$T_j = T_i - c\ln\left(\frac{\beta_i}{\beta_j}\right) \qquad 2.32$$

where T_i is peak maximum temperature at very low heating rate β_i, T_j is the corrected peak maximum temperature at heating rate β_j and $c = \frac{T_{m2} - T_{m_1}}{\ln 2}$. T_{m1} and T_{m2} are the peak maximum temperature for the first two lower heating rates β_1 and β_2. These authors demonstrated that Eq. 2.32 can be used for correction of both first and general order kinetics. However, temperature lag correction is mostly necessary when thermal quenching parameters are to be calculated.

2.6.2.7 Feldspar inclusion

Inclusion of substantial quantity of feldspar in quartz material to be used for luminescence dating or study is always problematic. This is because feldspar is relatively more sensitive than quartz (Duller, 1997). Therefore, its considerable inclusion in quartz will definitely undermine the overall result of the experiment. Usually, this is checked by exposing aliquots to infrared (IR) at ambient temperatures, in order to check if there is an infrared stimulated luminescence (IRSL) signal. This is possible because feldspar is highly sensitive to IR stimulation and whereas to which quartz is insensitive. Thus, IRSL enables discrimination between the presence of the two. Alternatively, or in addition, a light microscope is normally used to estimate level of infections (Spooner and Questiaux, 1989; Duller, 2003).

2.7 Computerised curves deconvolution

Glow curves obtained from TL measurements, of quartz in particular, are usually of several overlapping glow peaks in nature. This consequently makes separation of the composite peaks to their individual glow peak difficult, since this is required for analyses. In reality, the 110^{o}C TL peak of quartz is always isolated and glaring, but the thermal stable peaks are the major problem of overlapping. On the other hand, a complete composite nature of all the components of LM-OSL curves is always observed in nature. One major contribution to this feature is the fact that the entire components originate from the beginning of the OSL curve, at t = 0.

What is desirable in basic research and luminescence applications is the individual peak/component of the glow or OSL curve. This is due to the reason that evaluation of the charge stored in respective trap, which corresponds to each peak/component, is obtained from the area under each peak/component. Furthermore, important information, like trapping parameters, about the traps and subsequently about the crystal in general are deduced from the shape of each glow peak or OSL component. Therefore, it is essential to separate each glow or OSL curve into their individual glow peak or component respectively.

The computerized curve deconvolution (CCD) analysis is the general term used for doing this. CCD has proved to be promising and more easily applied than the experimental approach that is used determining the number of peaks in a complex TL

glow curve of quartz (Horowitz and Yossian, 1995; Kitis et al., 1998; Kitis, 2001, Afouxenidis et al., 2012). There is no available experimental procedure for isolating the components of OSL curve. Analytical expressions used for CCD are based on the TL and OSL kinetic equations. However, the expressions are transformed to the forms that have some experimental measurable parameters unlike the conventional kinetic equations. n_0 and s are replaced with I_m and T_m in TL kinetics, whereas, n_0 and s replaced with I_m and t_m in LM-OSL kinetics. T_m is the temperature at glow-peak maximum intensity, I_m while t_m is the time, t, at component maximum intensity, I_m for LM-OSL.

General order kinetics for both TL and LM-OSL are often used for CCD. This is because both general and mixed orders reduce to first order form for TL and LM-OSL cases when the order of kinetics b =1.00001. The transformed expressions of general order for TL and LM-OSL are as follows:

for TL

$$I(T) = I_m b^{\frac{b}{b-1}} \exp\left(\frac{E}{kT}\frac{T-T_m}{T_m}\right) \times \left[(b-1)(1-\Delta)\frac{T^2}{T_m^2}\exp\left(\frac{E}{kT}\frac{T-T_m}{T_m}\right) + Z_m\right]^{-\frac{b}{b-1}} \quad 2.33$$

with $2kT/E$, $\Delta_m = 2kT_m/E$, $Z_m = 1+(b-1)\Delta_m$ and the frequency factor s is calculated using

$$s = \frac{\beta E}{kT_m^2}\exp\left(\frac{E}{kT_m}\right)\left[1+(b-1)\frac{2kT_m}{E}\right]^{-1} \quad 2.34$$

And for LM-OSL

$$I(t) = I_m \frac{t}{t_m}\left(\frac{b-1}{2b}\left(\frac{t}{t_m}\right)^2 + \frac{b+1}{2b}\right)^{\frac{b}{1-b}} \quad 2.35$$

The quality of the fit produced by fitting any of these equations to experimental curve is normally tested with figure of merit (FOM) defined by Balian and Eddy (1977) as

$$FOM(\%) = 100 \times \frac{\sum_j |I_j - I(T_j)|}{\sum_j I_j} \qquad 2.36$$

where I_j and $I(T_j)$ are the experimental and fit intensities in channel j respectively.

The background signal is usually simulated by an equation of the form

$$BKG_{LM} = \alpha + ct \qquad 2.37$$

where α is the average in the first few seconds of a zero dose LMOSL measurement, and c is a constant.

2.8 Retrospective dosimetry

The term 'Retrospective Dosimetry' generally has to do with determination of the dose of absorbed radiation to environment or locally available material in situations where conventional, synthetic dosimeters were not in place at the time of radiation exposure. Luminescence retrospective dosimetry is applied in dating (of archaeological and geological materials) and accident dosimetry. The quantity of interest in these two areas of applications is absorbed or equivalent dose, *ED* (in Gy). In dating, the age of the material is evaluated by measuring the *ED* that the materials received from radiation owing to the natural background, since they were last heated (as in TL) or exposed to sunlight (as in OSL), depending. Thereby, the age is calculated by dividing the *ED* by the dose rate (in Gy/s) of the natural background. In accident dosimetry, the goal is to reconstruct *ED* as a consequence of a radiation accident.

The techniques used in accident dosimetry and dating applications are identical. Both TL and OSL are routinely used in retrospective dosimetry; even in some cases, the two approaches are used as complementary methods

There are three major methods generally employed in calculating *ED* in luminescence retrospective dosimetry. They are additive-dose, regenerative-dose and pre-dose methods (Wintle, 1997; Bøtter-Jensen et al., 2003a).

i. **Additive-dose method:-** in this, the dose response curve (from which *ED* is evaluated) is constructed from measurements of luminescence signals due to

both naturally/accidentally-received-dose and those from additional artificial doses that are added on the naturally/accidentally-received-dose using multiple aliquots.

ii. **Regenerative-dose method**:- this method is based on giving series of laboratory dose D_i on a single aliquot of the sample to be dated following pre-heating and OSL measurements. This procedure is repeated for number of times and by varying the regeneration doses, a dose response curve (also known as a growth curve) showing how the OSL signal grows with radiation dose can be constructed. Interpolating the natural OSL signal onto this growth curve provides way of estimating *ED*. This method in particular is popular in luminescence dating. It must be noted here that the ED that are calculated in this method and previous method, are from the charges that are trapped at the thermally stable traps of the material. Thermally stable is the sense that the electrons that are captured in them remain trapped for a long period of 10^8 years at 20^{o}C. For quartz, traps that are only depleted at 200^{o}C and above are considered to be thermally stable. The 325^{o}C TL peak that is often used for both TL and OSL dating in quartz and has a lifetime of about $3x10^7$years (Chen and McKeever 1997).

iii. **Pre-dose method**:- Unlike it is with the first two methods, *ED* estimation is achieved by employing thermally unstable trap, 110^{o}C peak in quartz that has half-life of about 2 hours at RT. This is made possible by taking the advantage of changing in sensitivity of this peak due to previous irradiations and thermal treatments. Thus, the sensitivity changes serve as a memory tool that records past irradiations from which *ED* estimation is made. It must be noted here that apart from its application in retrospective dosimetry, pre-dose technique has been effectively utilized in authenticity testing of artefacts and firing temperature measurements of pottery materials (Bailiff, 1994; Koul et al., 1996; Galli et al., 2006; Li and Yin, 2001).

2.9 TL/OSL reader

The most widely used instrument for measuring TL and OSL is "The Risø automated TL/OSL reader". Both TL/OSL measurement and beta irradiation facilities

are included in its compartment. The remaining part of this chapter is dedicated to the full description of this reader.

2.9.1. The Risø automated TL/OSL reader

The basic components of the Risø TL/OSL reader are as follows:

i. a light detection system

ii. a heating system for TL measurements

iii. optically stimulation units for OSL measurements and

iv. a beta irradiator facility.

The reader is a computer-controlled system. It enabled measurement of both TL and OSL. With the system, up to 48 samples can be individually:

i. heated to any temperature between room temperature and 700^{o}C,

ii. irradiated by a beta source (^{90}Sr/^{90}Y) mounted on the reader and

iii. optically stimulated by various light sources *in situ*.

The emitted luminescence is measured by a light detection system which comprised of a photomultiplier tube and suitable detection filters. A schematic diagram of the system is shown in Figure 2.17

Either 9.7 mm diameter aluminium disc or stainless steel cups are used as sample holders for all measurements. While aluminium disc can only be used for TL measurement up to 500^{o}C, stainless steel cup which can withstand higher temperature is used for measurements that required heating to 700^{o}C. To ensure that the sample are fastened to the aluminium disc, fine grains samples are mounted on it by deposition through suspension method (Aitken, 1998), while silicone oil/grease/spray is used as a glue for loose grains.

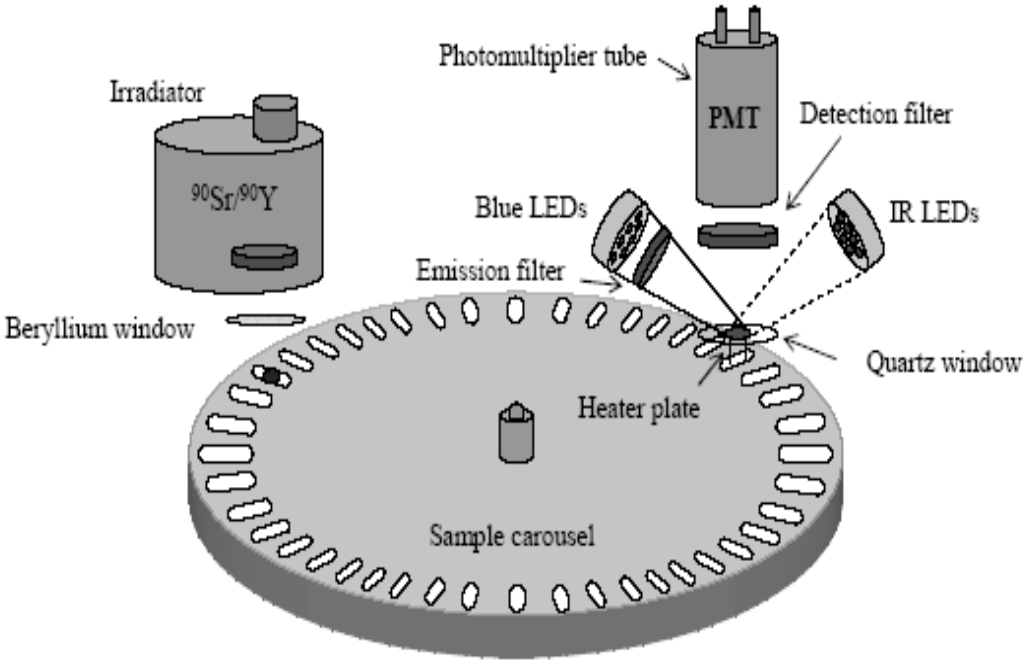

Fig. 2.17: Schematic diagram of the Risø TL/OSL luminescence reader used for the measurements

Samples in discs or cups are loaded onto an exchangeable sample carousel that could accommodate up to 48 samples. The sample carousel is then placed in the sample chamber. The chamber had a nitrogen atmosphere maintained by a nitrogen flow. The sample carousel rests on a motor driven turntable, which enables rotation (in steps) of the sample carousel. Rotation is computer controlled and position holes drilled though the carousel in close proximity to the sample positions enable the system to keep track of the position of the carousel using optoelectronics and a stepper motor. An infrared light emitting diode (LED) is positioned underneath the turntable, which is switched on during rotation. The measurement is initiated by moving a given sample to the measurement position located directly underneath the light detection system. The sample is then lifted through slots in the sample carousel into the measurement position. In the measurement position the sample can be stimulated thermally and/or optically. Thermal stimulation is obtained by linearly increasing the temperature of the heater strip and optical stimulation is provided by different light sources focused onto the sample position. In both cases, the emitted luminescence is measured by the light detection system during the stimulation.

2.9.1.1 Heating system

The heating element that is combined with lift mechanism is located directly underneath the photomultiplier tube. The heating element functions as heater for heating the samples and as well as elevator for lifting the sample into the measurement position. The heater strip is made of Kanthal (a high resistance alloy) which is U-formed to provide good heat transmission to the sample and to lift it securely and reproducibly into the measurement position. Heating is accomplished by feeding a controlled current through the heating element. Feedback control of the temperature employs an Alumel-Cromel thermocouple mounted underneath the heater strip. Heating is provided by a non-switching continuous full sine wave generator operating at 20 kHz. The heating system is able to heat samples to 700^{o}C at linear heating rates from 0.1 to 30 K/s. The heating strip can be cooled by a nitrogen flow which also protects the heating system from oxidation at high temperatures.

2.9.1.2 Optical stimulation system

The reader is equipped with a choice of two stimulation sources as shown in Figure 2.18). They are:

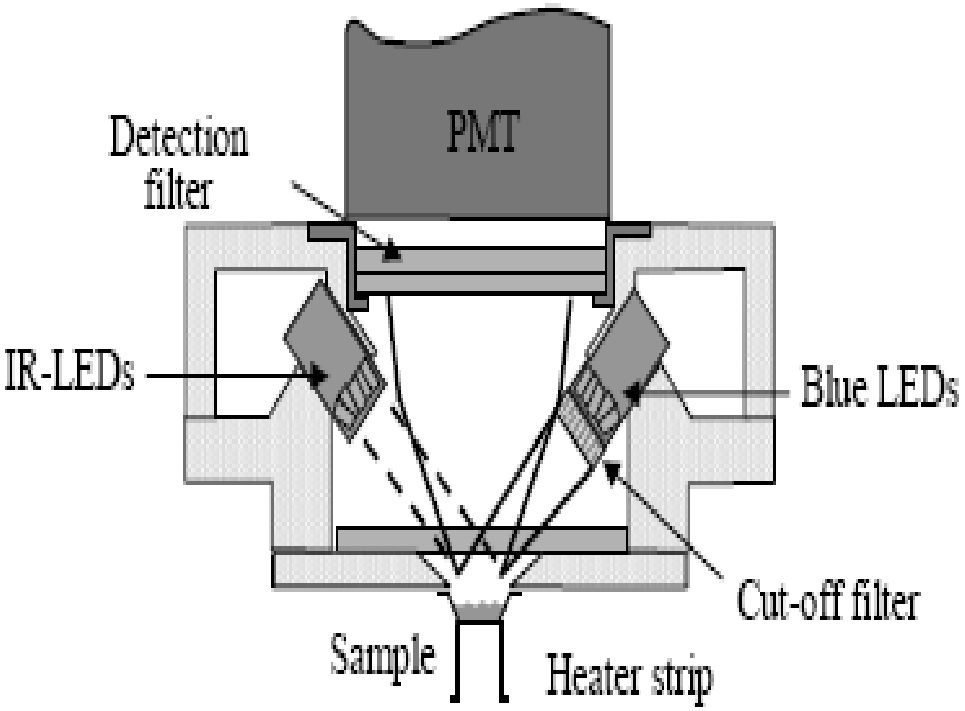

Fig. 2.18: Schematic diagram of the combined blue and IR LED OSL unit. The unit contains 28 blue LEDs (in 4 clusters) emitting at 470 nm delivering »40 mW/cm2 at the sample and 21 IR LEDs (in three clusters) emitting at 875 nm delivering »135 mW/cm2 at the sample.

i. blue light emitting diodes (LEDs) and

ii. infrared (IR) LEDs

Stimulation at different intensities is possible with the blue LEDs. This is achieved by varying the stimulation intensity as a function of stimulation time. The array of LEDs is equipped with an optical feedback servo-system to ensure the stability of the stimulation power for the delivered light intensity by the blue LEDs. Stimulation in CW-mode as well as LM-mode is possible. The LEDs are arranged in clusters, which are mounted concentrically in a ring-shaped holder located between the heater element and the photomultiplier tube. The holder is designed in such a way that all individual diodes are focused on the sample. The distance between the diodes and the sample is approximately 20 mm.

2.9.1.2.1 Blue LEDs

The blue LEDs (NISHIA type NSPB-500s) are with a peak emission at 470 nm (FWHM = 20 nm). They have an emission angle of 15 degrees and a power output of ≈ 2 cd at 20 mA (Botter-Jensen et al.,1999). The energy fluence rate at a distance of 2cm is 19mW/cm^2. The blue LEDs are usually arranged in 4 clusters each containing seven individual LEDs. The total power from 28 LEDs is > 40 mW/cm2 at the sample position (Botter-Jensen et al., 2003b). To reduce the amount of directly scattered blue light reaching the light detection system, a green long pass filter (GG-420) is incorporated in front of each blue LED cluster. The filter effectively attenuates the high energy photons from the blue LEDs at the cost of approximately 5% attenuation of the peak centred on 470 nm. Figure 2.19 displays the measured LED emission spectrum compared with the published transmission curve for the GG-420 filter and the U-340 detection filter.

2.9.1.2.2 Infrared LEDs

Infrared (IR) stimulation in the region 800-900 nm can stimulate luminescence from most feldspars (but not from quartz at room temperature) probably by a thermal assistance mechanism (Hutt et al., 1988). This has the important advantage that a wider range of wavelengths for the detection window becomes available. The IR LEDs used here emit at 875 nm, which is close to the IR resonance wavelength at 870 nm found in most feldspars (Botter-Jensen et al., 2003b). The IR LEDs are arranged in 3 clusters

each containing seven individual LEDs. The maximum power from the 21 IR LEDs is approximately 135mW/cm^2 at the sample position (Botter-Jensen et al., 2003b).

2.9.1.3 Photon detector system

A photomultiplier tube (PMT) and suitable detection filters constitute the essential components of the light detection system of the Riso reader. While the PMT detects emitted luminescence, the importance of the detection filters is to define the spectral detection window and to shield the PMT from scattered stimulation light.

2.9.1.3.1 Photomultiplier tube

The light sensitive component in the PMT is the cathode. This is coated with a photoemissive substance CsSb and other bialkali compounds are commonly used as substitute for this material. Typically, ten photons in the visible range striking the cathode are converted into one to three electrons. Electrons emitted from the photocathode were accelerated towards a series of dynodes maintained at a positive voltage relative to the photocathode. Electrons with sufficient velocity striking the dynode will eject several secondary electrons from the surface. The PMT attached to the Riso TL/OSL luminescence reader is a bialkali EMI 9235QA PMT, which has maximum detection efficiency at approximately 400 nm, making it suitable for detection of luminescence from both quartz and feldspar. The PMT is operated in “photon counting" mode, where each pulse of charge arising at the anode is counted. As the stimulation sources have to be placed between the sample and the PMT the sample-to-PMT cathode distance in the Riso TL/OSL luminescence reader is 55 mm, giving a detection solid angle of approximately 0.4 steradians.

2.9.1.3.2 Detection filters

Detection filters define detection window for the PMT and thereby preventing unwanted light and scattered stimulation light from reaching the PMT. This is important because the spectral stimulation and detection windows must be well separated since the intensity of the stimulation light is ~ 1018 orders of magnitude larger than the emitted luminescence. Quartz has a strong emission centred on 365 nm (near UV) and many types of feldspars have a strong emission centred on 410 nm (violet). In Figure 2.20 emission spectra from several samples of sedimentary quartz and K feldspars are shown. A commonly used detection filter is Hoya U-340 (Figure 2.19), which has a peak transmission around 340 nm (FWHM = 80 nm).

2.9.1.4 Beta irradiator

A schematic drawing of the irradiator unit is shown in Figure 2.21. It is a detachable beta irradiator located above the sample carousel. The irradiator normally accommodates a 90Sr/90Y beta source, which emits beta particles with a maximum energy of 2.27 MeV. The source strength is about 40 mCi, which gives a dose rate in quartz at the sample position of approximately 0.075 Gy/s at the time of measurements in this research. The source is mounted into a rotating, stainless steel wheel, which is pneumatically activated. The source-to-sample distance should be as small as possible to provide the highest possible dose rate at the sample, however any spatial variations in dose rate across the source will be accentuated at small source-to-sample is instances, so a compromise is required. The distance between the source and the sample is 5 mm. A 0.125 mm beryllium window is located between the irradiator and the measurement chamber to act as vacuum interface for the measurement chamber. The cross-talk, i.e. the percentage of dose given to an adjacent non-irradiated sample is, on average, 0.1735 2±0.0004% for a 4 mg mono-layer coarse grain quartz sample using the new 48-sample carousel. The 2nd nearest sample only receives 0.0042±0.002% of the primary beta dose.

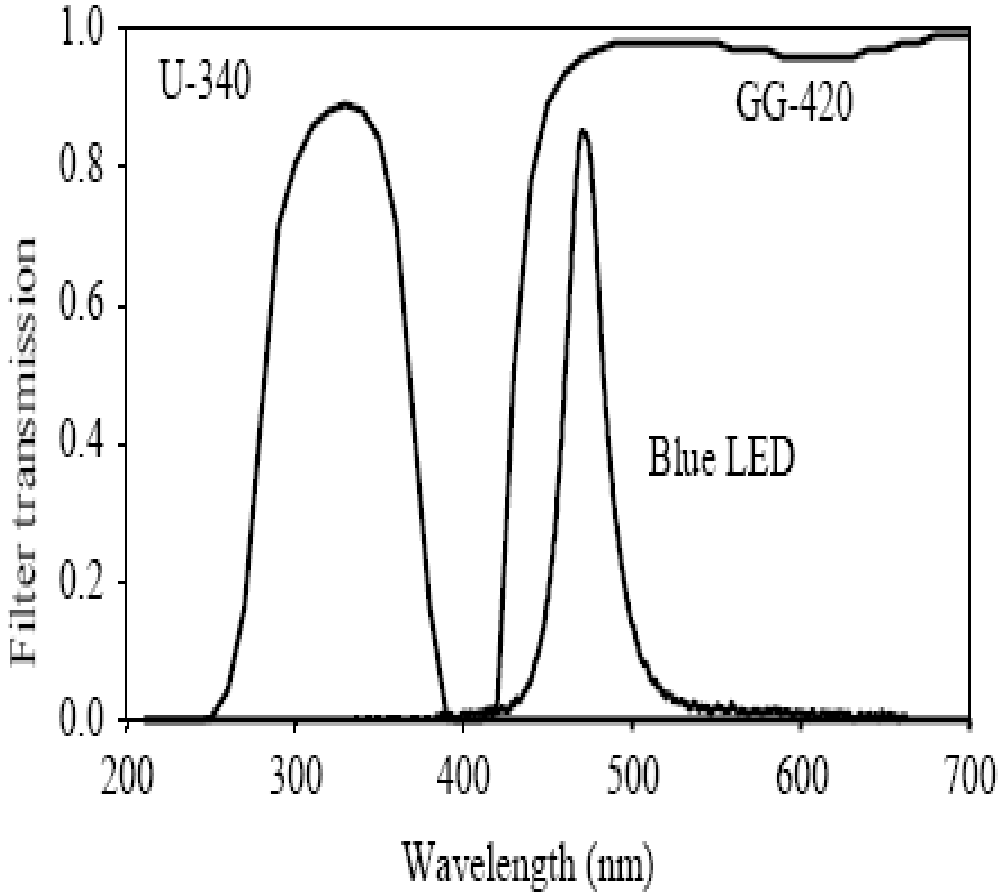

Fig. 2.19: The emission spectrum of blue LEDs. Also shown are the transmission curves for the GG-420 green long pass filter (cut-off filter in front of the blue LEDs) and the Hoya U-340 filter (detection filter in front of the PMT); after Botter-Jensen et al. (1999).

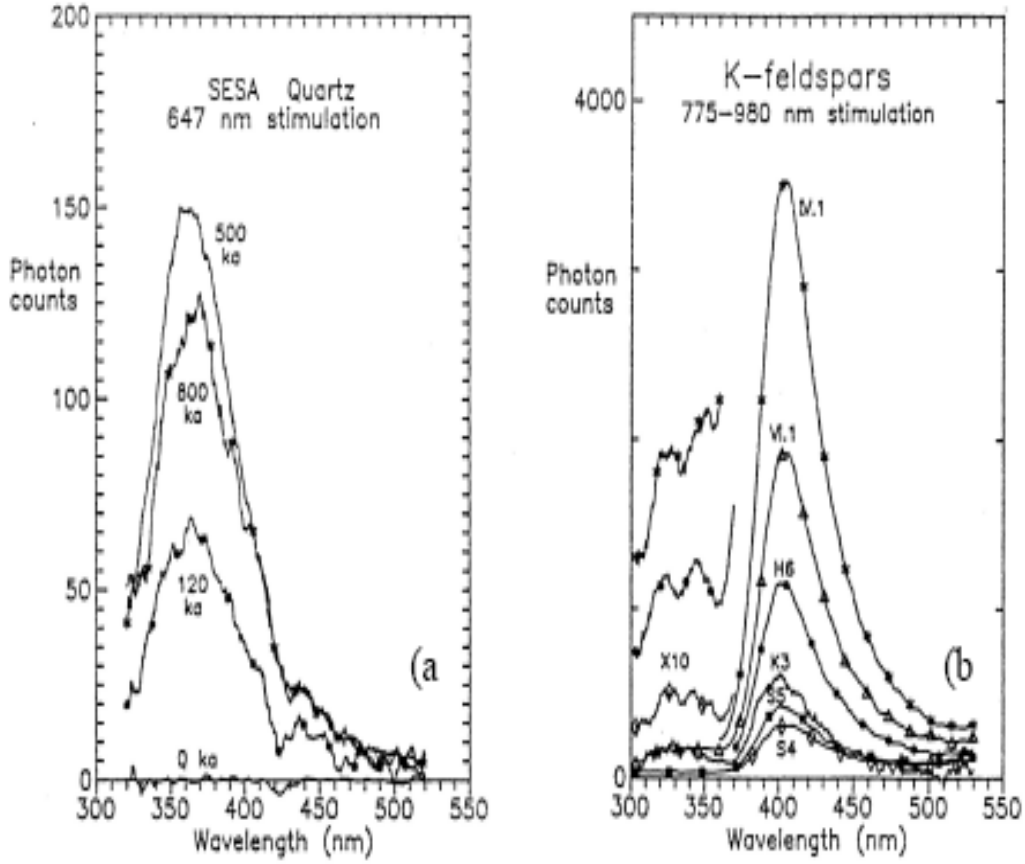

Fig. 2.20: Emission spectra of sedimentary quartz and K feldspars (from Huntley et al., 1991). (a) Emission spectra of several sedimentary quartz samples from South Australia obtained for stimulation using the 647 nm line from a Krypton laser. (b) Emission spectra of several sedimentary K feldspars using IR diode stimulation.

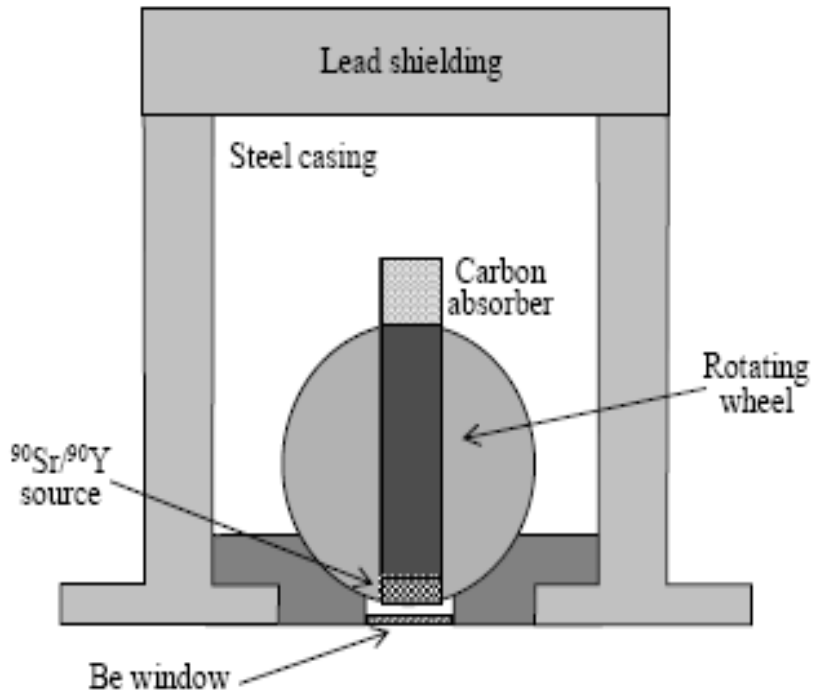

Fig. 2.21: Schematic diagram of the cross section of the beta irradiator. The $^{90}Sr/^{90}Y$ source is placed in a rotating stainless steel wheel, which is pneumatically activated. The source is shown in the *on* (irradiating) position. When the source is off the wheel is rotated 180^{o}, so that the source points directly at the carbon absorber.

CHAPTER THREE

MATERIALS AND METHODS

3.1 Sample collection

The original quartz samples used were large crystal quartz. This was done in order to guarantee the same radiation, optical and thermal histories for quartz grains obtained from the same large crystal instead of using sedimentary quartz grains that could have different origins. This is because it is likely that grains of various sizes to originate from different source areas and their mixing may be due to diverse transport modes (short and long distance transport, respectively) (Preusser et al., 2009). Individual grains may have experienced a different sedimentary history; some grains may have been transported over long distances and repeatedly been recycled while others may originate more-or-less directly from in-situ weathered bedrock. This complex origin in known to cause differences in the concentrations of point defects among individual quartz grains; this plays a role in the highly variable luminescence characteristics of single grains (Preusser et al., 2009).

The quartz samples used were twelve in numbers and were collected from southwestern Nigerian. In the preliminary measurements, only two of the samples that possessed highest sensitivity (Figure. 3.1) and at the same time found to be among those that passed feldspar contamination test (Figure. 3.2) were selected for this study. The first of the samples was from Oro, in Kwara State and named S2, whereas the other was from Ijero-Ekiti in Ekiti State named S4 all from part of Nigerian basement complex. They were large crystals of hydrothermal origins which occurred in veins associated with metamorphic rocks. The two quartz samples were clear rock crystal.

3.2 Sample preparation

Grains of dimensions 90-150μm were obtained from each of the natural crystal quartz samples after, smashing in an agate mortal, sieving and rinsed in acetone. Each of the two selected sample types was divided into two. The first sets were unannealed while the second sets were annealed at 900 ^{o}C for 1 hour and allowed to cool immediately to the room temperature in the air. This annealing temperature was selected because it is higher than the temperature of about 870^{o}C, where an irreversible

phase change takes place in quartz (Preusser et al., 2009). Therefore, the set of annealed samples represent quartz grains extracted from fired quartz-grained inclusion materials like ceramics, potteries, fired sediments and bricks, metallurgy ovens, and other highly fired objects for dating. On the other hand, the unannealed samples represent set of samples to be dated that have not been artificially heated beyond irreversible phase change temperature (870^{o}C) like sedimentary quartz grains that are extracted from sediments or overbank deposits. All the aliquots (sub-samples) used for the measurements were of equal mass (about 5mg).

3.3 Instrumentation

The TL and OSL measurements were carried out using the automated Risø TL/OSL reader (model TL/OSL DA-15) systems at Archaeometry Laboratory, Cultural and Educational Technology Institute (C.E.T.I.), R.C. "ATHENA", Xanthi, Greece. An overall description of the readers was presented in section 2.9.

3.4 Feldspar inclusion test

It was considered necessary to confirm weather there was no feldspar inclusion in the two quartz samples used in this study. This was undertaken by conducting Infra-Red Stimulation Luminescence (IRSL) measurements on samples with dose of Natural + 5Gy. Quartz is known not to be sensitive to infra-red stimulation, while feldspar is (Preusser et al., 2009). The result of this is shown in Figure 3.2. It was evidence from this that S2 and S4 were not infected with feldspar while S5, S11 and S12 were contaminated.

3.5 Experimental procedures

The TL/OSL measurements carried out in this work were executed in two phases, namely:

i. Reproducibility study of pre-dose sensitisation of the 110 ^{o}C TL peak.

ii. Study on luminescence sensitisations in unannealed and annealed quartz samples

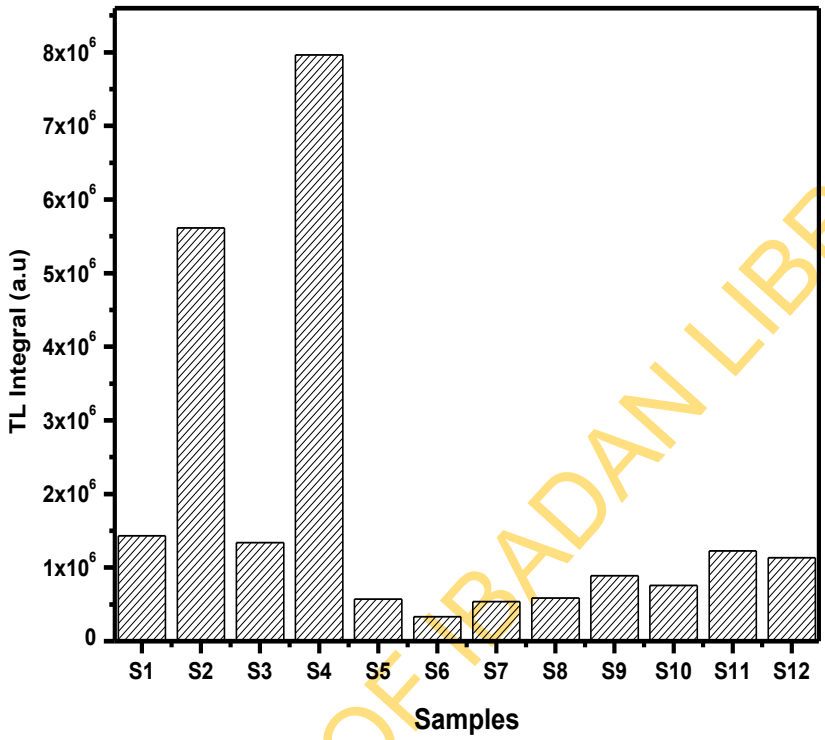

Fig. 3.1: Luminescence sensitivity of all the samples to 5Gy dose of radiation

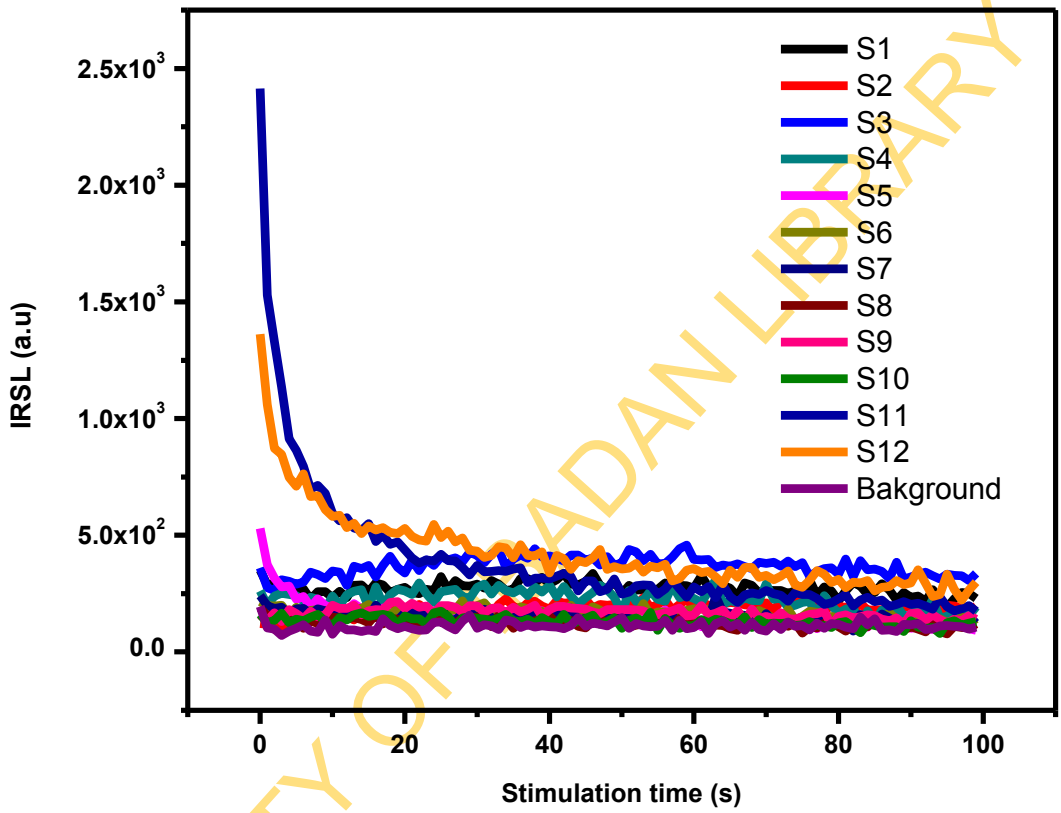

Fig. 3.2: Infra-Red Stimulation Luminescence (IRSL) curves of all the samples to test for feldspar contamination.

All measurements were done in a nitrogen atmosphere with different constant heating rates as indicated in the measurement protocols, up to a maximum heat temperature of 500^{o}C. The test dose and range of doses administered to each of the quartz samples are accordingly indicated in the respective experimental protocols presented in following subsequent sections.

3.5.1 Reproducibility study of pre-dose sensitisation of the 110 ^{o}C TL peak

Unannealed and annealed sample were used in this section by following the sequence of the experimental protocol presented below.

3.5.1.1 Measurement protocols

Step 1: A TD was given to a sample.

Step 2: TL readout up to 180 ^{o}C.

Step 3: TD and TL readout up to 500 ^{o}C.

Step 4: TD and TL readout up to 500 ^{o}C.

Step 5: TD and TL readout up to 500 ^{o}C.

Step 6: Repeat steps 1 to 5 for 10 different aliquots of the same quartz sample.

A dose of 2Gy was the TD administered to unannealed S2 and S4 while 1 and 0.5 Gy dose were given to their annealed counterpart respectively. At least 20 aliquots were prepared for the complete run of the above protocol for each of the samples making a total of 40 set of runs.

3.5.1.2 Description of the protocol

i. Steps 1 and 2 measured the sensitivity Sn_{01} of the TL glow-peak at "110 ^{o}C" acting additionally as a mass normalization.

ii. Step 3 measured (a) the sensitivity Sn_{02} of the TL glow-peak at 110 ^{o}C and (b) acts as a thermal activation up to 500^{o}C for the sample to ensure that all the stable straps that are used for TL and OSL dating are completely depleted.

iii. Step 4 measured (a) the sensitivity Sn_{1} of the TL glow-peak at 110 ^{o}C and (b) acts as a thermal activation for the sample again.

iv. Step 5 measured the further sensitisation Sn_{2} of the TL glow-peak at 110 ^{o}C.

v. Step 6 allowed sensitisation test among 10 different aliquots of the same quartz kind.

3.5.2 Study on luminescence sensitisations in unannealed and annealed quartz samples

Both unannealed and samples annealed at 900 ^{o}C were used in this section by following the sequence of the experimental protocol presented below.

3.5.2.1 Measurement protocol

Part A

Step 1: TD was given to an aliquot.

Step 2: TL readout up to 180^{o}C at heating rate of HR_i (^{o}C/s).

Step 3: Another TD was given to the same aliquot

Step 4: TL (S_{n0}) readout up to 500^{o}C at heating rate of HR_i (^{o}C/s)

Step 5: Steps 3 and 4 were repeated four times on the same aliquot leading to signals S_{n1}, S_{n2}, S_{n3} and S_{n4} respectively.

Step 6: Another TD was given to the same aliquot

Step 7: TL (S_{n5}) readout up to 500^{o}C at heating rate of 2^{o}C/s

Step 8: Steps 1-7 were repeated for fresh aliquot and new HR_i (Taking HR_i= 0.25, 0.5, 1, 2, 5, and 10^{o} C/s)

Part B

Step 1: TD was given to a fresh aliquot.

Step 2: TL readout up to 180^{o}C at heating rate of HR_i (^{o}C/s).

Step 3: TL readout up to 500^{o}C at heating rate of HR_i (^{o}C/s)

Step 4: Steps 3 was repeated four times more on the same aliquot

Step 5: Another TD was given to the same aliquot

Step 6: TL (S_{n1b}) readout up to 500^{o}C at heating rate of HR_i (^{o}C/s)

Step 7: Another TD was given to the same aliquot

Step 8: TL (S_{n2b}) up to 500^{o}C at heating rate of 2^{o}C/s

Step 9: Steps 1-8 were repeated for fresh aliquot and new HR_i (Taking HR_i= 0.25, 0.5, 1, 2, 5, and 10^o C/s)

Part C

Step 1: TD was given on an aliquot.

Step 2: TL readout up to 180^{o}C at heating rate of HR_i (^{o}C/s).

Step 3: Another TD was given to the same aliquot

Step 4: OSL (S_{n0}) measurement at RT for 1000s

Step 5: TL readout up to 500^{o}C at heating rate of HR_i (^{o}C/s)

Step 6: Steps 3-5 were repeated four times more on the same aliquot leading to OSL signals S_{n1}, S_{n2}, S_{n3} and S_{n4} respectively.

Step 7: Steps 1-6 were repeated for fresh aliquot and new HR_i (Taking HR_i= 0.25, 0.5, 1, 2, 5, and 10^o C/s)

Part D

Step 1: TD was given to an aliquot.

Step 2: TL readout up to 180^{o}C at heating rate of HR_i (^{o}C/s).

Step 3: OSL measurement at RT for 1000s

Step 4: TL readout up to 500^{o}C at heating rate of HR_i (^{o}C/s)

Step 5: Step 4 was repeated four times more on the same aliquot

Step 6: Another TD was given to the same aliquot

Step 7: OSL (S_{n1b}) measurement at RT for 1000s

Step 8: TL readout up to 500^{o}C at heating rate of HR_i (^{o}C/s)

Step 9: Steps 1-8 were repeated for fresh aliquot and new HR_i (Taking HR_i= 0.25, 0.5, 1, 2, 5, and 10^o C/s)

The same TD of 7.5Gy was for both S2 and S4 unannealed samples while 1 and 0.5 Gy were used for S2 and S4 annealed samples respectively.

3.5.2.2 Descriptions of the protocol

Part A

i. Steps 1and 2 were meant for mass normalization.

ii. TD of Steps 1and3 served as pre-exposure dose (these added to the naturally acquired dose for unannealed samples).

iii. Step 4 measured the unsensitised TL (named as S_{n0}) and at the same time serves as thermal activation to 500^{o}C for the next TL of step 5.

iv. Step 5 measured four (4) sensitised successive cycles TL namely; S_{n1}, S_{n2}, S_{n3} and S_{n4} respectively. Each TL also serves as thermal activation to 500^{o}C for the next successive cycle TL.

v. TD of step 6 served as a pre-exposure dose for step 7.

vi. Step 7 measured TL (Sn_5) sensitisation resulting from successive cycles of irradiations and TL readouts of (i) to (v) and heating rates. Note this step 7 is always read at 2^{o}C/s heating rate.

vii. Step 8 meant to observe the effect of different levels of thermal activation resulting from different heating rates.

Part B.

The description of Part B is just like that of Part A above. The only difference comes from the fact that intermediate irradiations of Part A step 3 were missing. That was devised to observe pure thermal sensitisation contribution which TL (S_{n1b}) of step 6 represented while TL (S_{n2b}) of step 8 is similar to its counterpart of Part A step 7 as described in (vi) above

Parts C and D

Parts C and D that are for OSL, are similar to Part A and Part B respectively, but instead of TL, RT-LMOSL measurements were employed to measure the sensitivity as indicated in the protocol.

3.6 Computerised curves deconvolution analyses

The RT-LMOSL curves were analyzed through a Computer Glowcurve Deconvolution Analysis (CGDA) using a general order kinetics expression proposed of Bulur (1996) and later modified by Kitis and Pagonis (2008) into an expression containing only the peak maximum intensity I_m and the corresponding time t_m. These two variables can be extracted directly from the experimental OSL curves. The modified expression used in the computerized procedure is:

$$I(t) = I_m \frac{t}{t_m}\left(\frac{b-1}{2b}\left(\frac{t}{t_m}\right)^2 + \frac{b+1}{2b}\right)^{\frac{b}{1-b}} \qquad 3.1$$

where b is the order of kinetics.

This latter expression was used providing thus the best test of the first order model assumption correctness for the quartz LM-OSL, since the values of b were selected to be 1.0001.

The background signal was simulated by an equation of the form

$$BKG_{LM} = \alpha + ct \qquad 3.2$$

where α is the average in the first few seconds of a zero dose LMOSL measurement, and c is a constant.

The non-zero intensity value at T = 0 or RT in TL and t = 0 in RT LMOSL, was considered to be included in the CGDA analysis in order to accomplish good fit. The value of this now-zero intensity can be observed to be dependent on sample and the entire TL glow curve or OSL curve integral which is a function of applied dose or sensitization factor. See figures 1 to 4 in Kiyak et al, (2007), figure 3 in Polymeris et al., (2009), figures 2 and 3a in Jain et al., (2003) and figures 1 and 2 in Appendix 1). However, this unwanted signal is of insignificant value in TL dating since it can be easily excluded from the desired TL peak generally. Equally, this value is not observed in LMOSL received at 125^{o}C of one of the present understudied samples which would have made evaluation of fast component used in OSL dating difficult (Oniya et al., 2012a). Hence, the unwanted initial signal is in this work attributed to the signal arising from the decay of extremely shallow traps that decay in RT. Because (i) they decay in RT and do not require optically stimulation (ii) the signal is eliminated by pre-heat to 180^{o}C and elevated LMOSL measurement at 125^{o}C in this work. Therefore, in the same direction with Kitis et al., (2010) that this non zero intensity value could be due to

the presence of phosphorescence, a first order phosphorescence component of the form, $I(t) = I_o \exp[-\lambda \cdot t]$, was included in the CGDA analysis. The decay rate, λ, was numerically adjusted until good fits were achieved for all signals.

All curve fittings were performed using the software package Microsoft Excel, with the Solver utility (Afouxenidis et al., 2012), while the goodness of fit of all the curves fitted was tested using the Figure Of Merit (FOM) of Balian and Eddy (1977) given by.

$$FOM = \sum_i \frac{|Y_{Exper} - Y_{Fit}|}{A} \qquad 3.3$$

where Y_{Exper} is the experimental glow-curve, Y_{Fit} is the fitted glow-curve and A is the area of the fitted curve. The FOM values obtained were less than 1% for the RT curves.

CHAPTER FOUR

RESULTS AND DISCUSSIONS

4.1 Introduction

Results and discussions of TL/OSL measurements on the two quartz samples investigated in this study, as described in chapter three, are presented in this section.

4.2 Reproducibility study of pre-dose sensitisation of the 110^{o}CTL peak

According to the experimental protocol of section 3.5, the sensitivity Sn_{01} is the "natural" sensitivity obtained without any treatment. The sensitivity Sn_{02} is due to the heating up to 180 ^{o}C, for which the sensitisation is considered to be negligible. So, 180 ^{o}C is generally adopted as the temperature used to erase the TL glow-peak at 110 ^{o}C in most of the TL/OSL protocols (Polymeris et al., 2009). The sensitivities Sn_1 and Sn_2 are due the first and second thermal activation up to 500 ^{o}C respectively.

4.2.1 Sensitisation in unannealed samples

Figures 4.1 and 4.2 present glow curves of S2 and S4 samples respectively. The most interesting observation could be seen from the different level of sensitisation that took place in various aliquots of the same quartz sample. In these figures, curve (a) represents the glow-curve of natural TL (NTL) plus the test dose (Sn_{02}, step 3, without any thermal activation). Both curves (b) and (c) correspond to the glow-curve after the first thermal activation (Sn_1, step 4). However, since the sensitisation level is not the same throughout all the aliquots of each quartz sample, curve (b) corresponds to the aliquot for which the minimum sensitivity Sn_1 of 110 ^{o}C TL peak occurred, while curve (c) stands for aliquot with maximum Sn_1 sensitivity. The degree of scatter of the pre-dose sensitisation of the 110 ^{o}C TL peak in 10 aliquots for the two understudied quartz samples is better illustrated in Figures 4.3 and 4.4, for unannealed S2 and S4 samples respectively. To demonstrate that the above scattered is as a result of

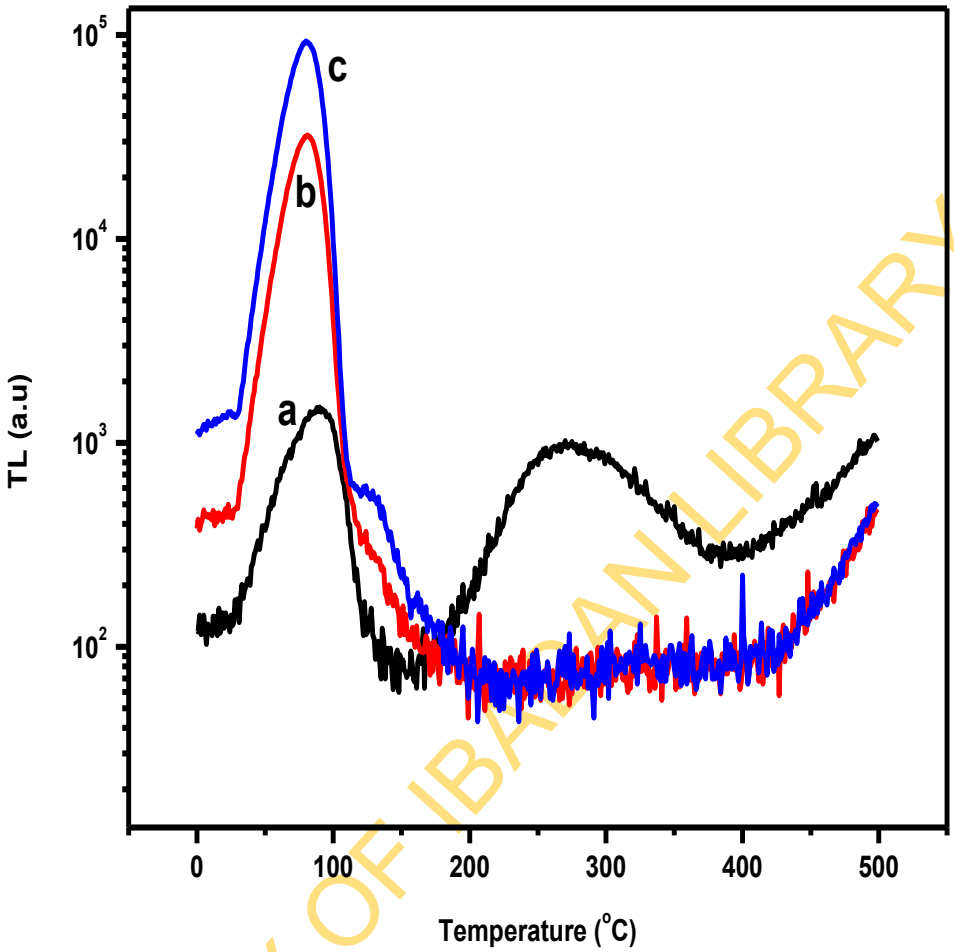

Fig. 4.1: TL glow curves for unannealed S2 samples. Curve (a) corresponds to the sensitisation without previous thermal activation (Sn_{02}). Both curves (b) and (c) correspond to the glow-curve after the first thermal activation (Sn_1) indicating the minimum and maximum sensitisation respectively.

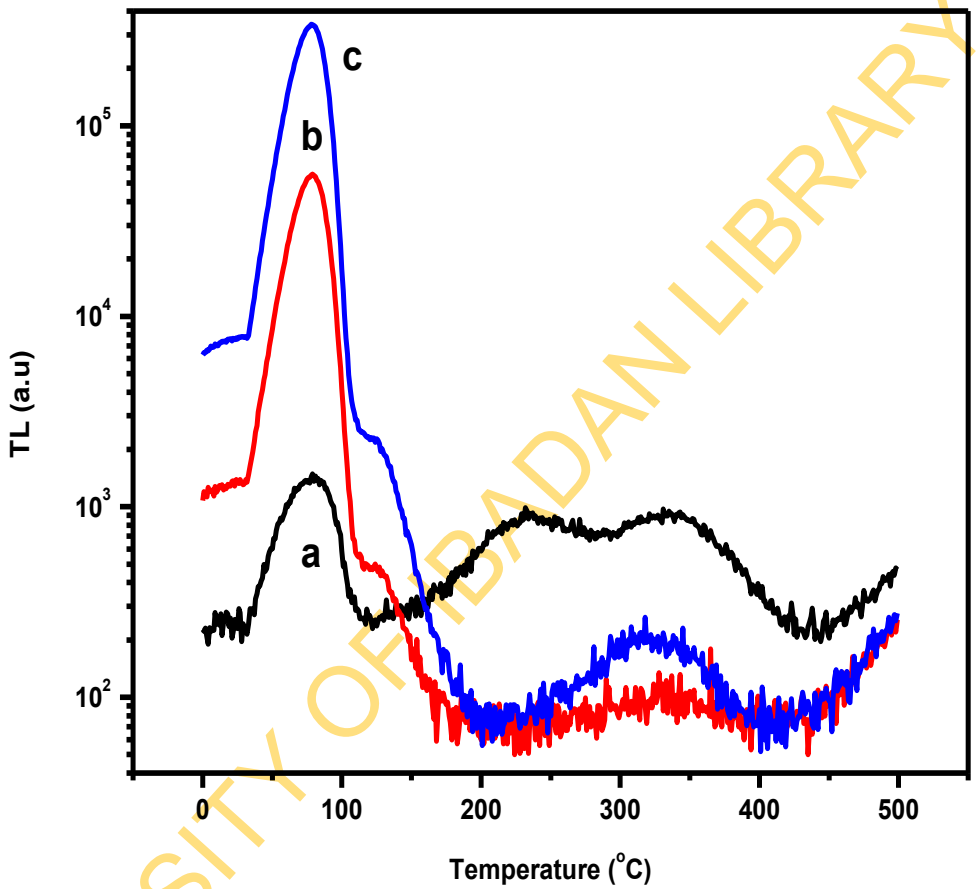

Fig. 4.2: TL glow curves for unannealed S4 samples. Curve (a) corresponds to the sensitisation without previous thermal activation (Sn_{02}). Both curves (b) and (c) correspond to the glow-curve after the first thermal activation (Sn_1) indicating the minimum and maximum sensitisation respectively

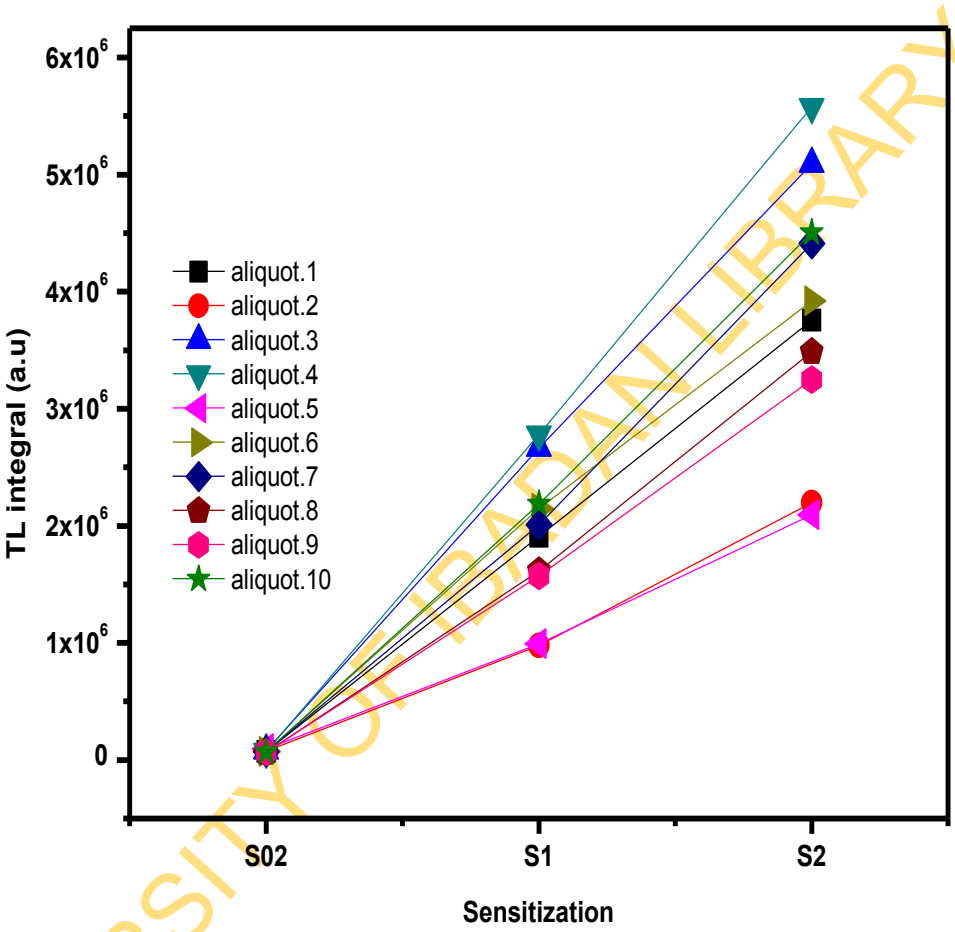

Fig. 4.3: The sensitisations resulting from three successive irradiations and luminescence readings for 10 aliquots for unannealed S2 sample

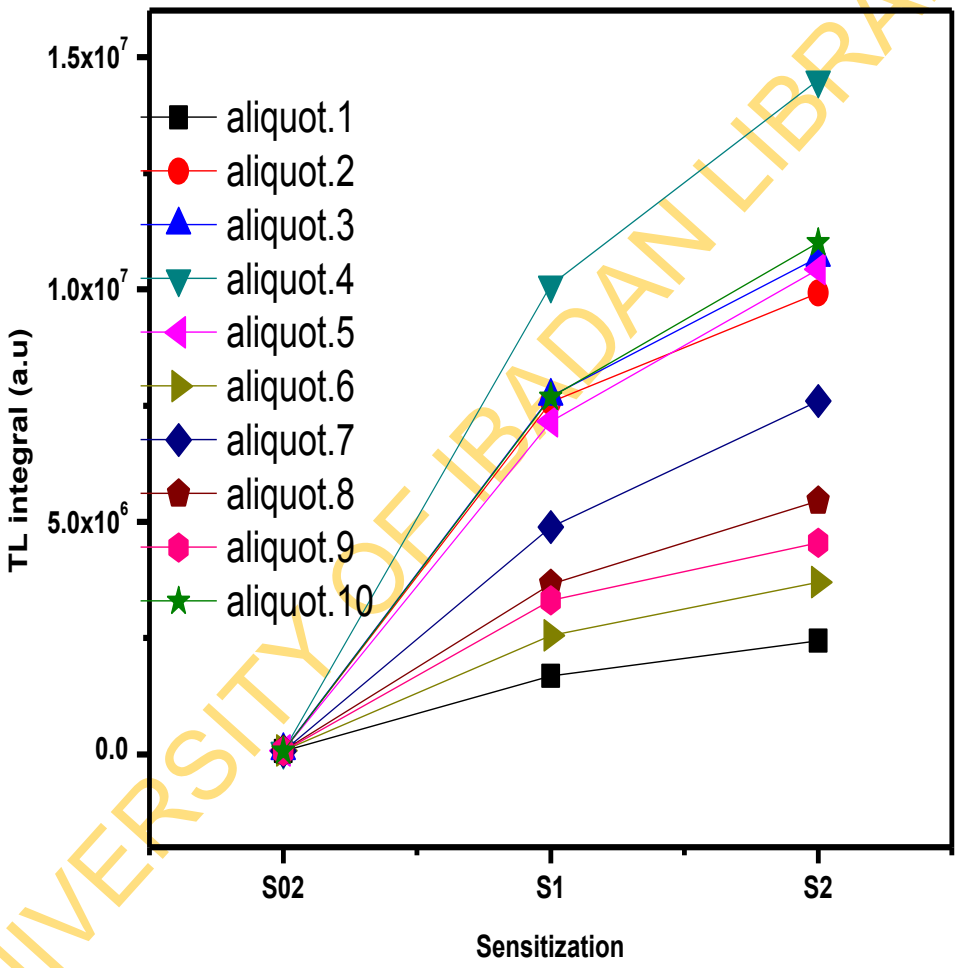

Fig. 4.4: The sensitisations resulting from three successive irradiations and luminescence readings for 10 aliquots for unannealed S4 sample.

sensitisation, unsensitised glow curves from two measurements on two aliquots for each of the two understudied samples are presented in Figure 4.5 and 4.6 respectively. It is clear from these curves that the responses were excellent for S2 and S4 samples. The Coefficient of Variation (CV), defined as the ratio of standard deviation to the mean, in all cases were less than 5%

Normalisation is routinely employed in luminescence studies and dating for the purpose of attaining good reproducibility (Murray and Roberts, 1998). To observe the influence of normalization on the sensitisation reproducibility, all sensitivities were normalized over the "natural" sensitivity Sn_{01}; this ratio of artificial sensitivities over the "natural" sensitivity (i.e. normalization) will be called sensitisation factor hereafter. The results concerning the reproducibility of the pre-dose sensitisation effects are summarized in Table 4.1. The second column *[nS_{01} (%)]* describes CV of sensitisation of 10 aliquots. This column represents the reproducibility of unnormalized and unsensitised signal of the two samples. As seen here, the level of scatter is much in S2 than S4. In the cases of the unannealed quartz the sample reproducibility can be also measured through their NTL signal. This is shown in the third column *[NTL (%)]*.

The excellent reproducibility of fourth column *[Sn_{02}/Sn_{01}]* in Table 4.1 is a product of normalization that enhances level of reproducibility among different luminescence measurements. The normalization improved the CV from 12.44 to 1.46% and 5.40 to 1.06% for S2 and S4 samples respectively. It should be recalled that since the pre-heat was only to 180 ^{o}C up to stage S_{02}, the reproducibility here represents unsensitised signals. Of main interest were the results of column *[Sn_1/Sn_{01}]*, which gave the variation of the sensitisation factor due to first thermal activation up to 500 ^{o}C. High levels CV up to 33.7 and 51.99% were introduced into reproducibility by sensitisation even after normalization for S2 and S4 samples respectively which indicated that normalization to first thermal activation is not ideal to improve sensitisation reproducibility. Although, slight variations in the sensitisation between different aliquots of the same quartz type for the two quartz types could be expected. Of truth, this variation was well beyond expectation, based on the original state and origin of the samples, as well as, on the good reproducibility resulted from unsensitised values

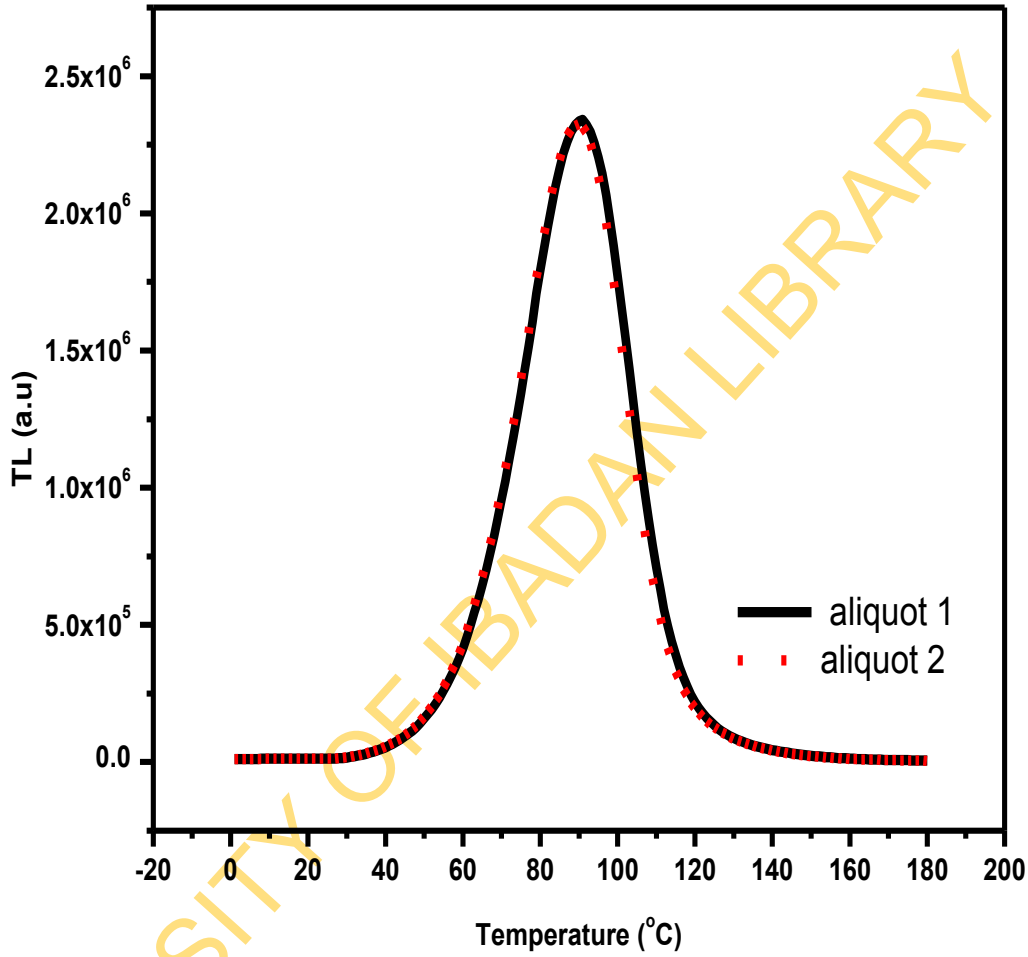

Fig. 4.5: TL test of two runs for S2 samples

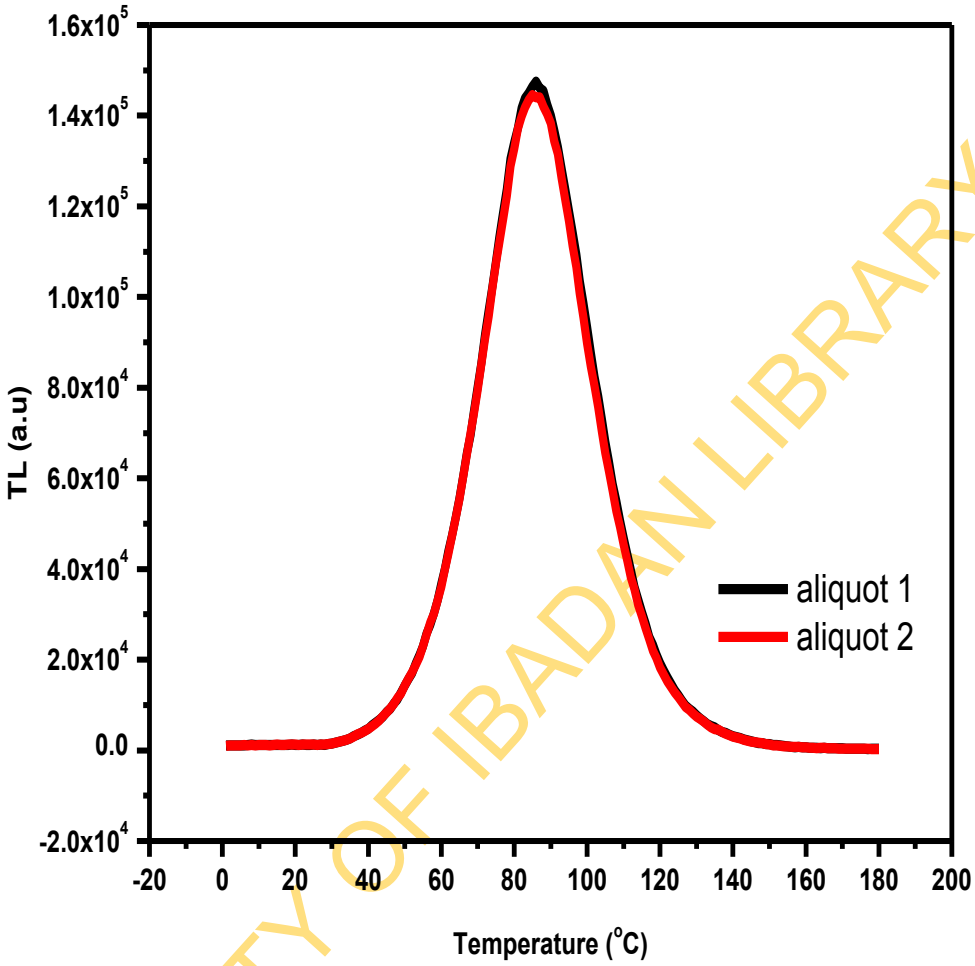

Fig. 4.6: TL test of two runs for S4 samples.

Table 4.1: Coefficient of Variation (CV) of Reproducibility sensitisation of 10 aliquots of S2 and S4 quartz samples.

Quartz Sample	Sn_{01} (%)	NTL (%)	Sn_{02}/Sn_{01} (%)	Sn_1/Sn_{01} (%)	Sn_2/Sn_{01} (%)	Sn_2/Sn_1 (%)
S2 Unannealed	12.44	6.60	1.46	33.74	31.51	6.39
S4 Unannealed	5.40	7.5	1.06	51.99	51.31	4.67
S2 Annealed	6.55	--	0.72	6.29	7.78	3.24
S4 Annealed	12.03	--	1.23	9.00	9.86	2.00

Keys: Sn_{01} = "natural" sensitivity, NTL = natural TL signal,
Sn_{02}/Sn_{01} = normalised sensitivity, Sn_1/Sn_{01} = 1st normalised and sensitised sensitivity,
Sn_2/Sn_{01} = 2nd normalised and sensitised sensitivity,
Sn_2/Sn_1 = ratio of the 1st and 2nd sensitised sensitivities.

(second to fourth columns, in Table 4.1). The results of column *[Sn_2/Sn_{01}]*, which provides the variation of the sensitisation due to second thermal activation up to 500 ^{o}C, possesses exact poor reproducibility as it is in column *[$nS2/Sn_{01}$]*. Normalization of the second sensitisation to the first sensitisation, rather to the unsensitised signal of Sn_{02}, shows the effect of TL readout up to 500^{o}C on the sensitisation reproducibility. This is represented in the last column, *[Sn_2/Sn_1]*, in Table 4.1. It is apparent from this that TL readout to 500 ^{o}C improved the CV in sensitisation reproducibility from 31.51 to 6.39% and 51.31 to 4.67% respectively for S2 and S4 samples.

4.2.2 Sensitisation in annealed quartz

The results for annealed quartz samples are also shown in Figures 4.7 and 4.8. The degree of scatter of the pre-dose sensitisation of the 110 ^{o}C TL peak in 10 aliquots for the two quartz samples annealed at 900^{o}C are shown in Figures 4.9 and 4.10. As could be observed from theses figures, outstanding enhancement in reproducibility of pre-dose sensitisation by annealing becomes apparent as compared to the case of unannealed samples. The comparison of this sensitisation reproducibility for the two cases of unannealed and annealing is presented in Table 4.1.

In this Table 4.1, while annealing increased the sensitisation reproducibility of un-normalized signal of S2 from CV of 12.44 to 6.55%, annealing rather worsen the sensitisation reproducibility of S4 from CV of 5.39 to 12.03% (Column *[Sn_{01} (%)]*). However, the sensitisation reproducibility became excellent after normalization for the two samples after annealing as expected.

Column *[Sn_1/Sn_{01}]*, also here, provides the variation of the sensitisation factor due to first thermal activation up to 500 ^{o}C for the case of annealed samples. Notably, it comes out that annealing at 900^{o}C for an hour surprisingly removed the high levels of CV observed in the case of unannealed samples from 33.7 to 6.29% and 51.99 to 9.00% for S2 and S4 samples respectively. Exact good reproducibility as in column *[Sn_1/Sn_{01}]* is recorded in column, *[$nS2/Sn_{01}$]* for the case of sensitisation due to second thermal activation up to 500 ^{o}C. Lastly, a good sensitisation reproducibility was demonstrated in column, *[Sn_2/Sn_1]*, and it is an indication of the effect of TL readout up to 500^{o}C on the sensitisation reproducibility as anticipated (column *[Sn_{02}/Sn_{01}]*).

4.2.3 Discussion

The sensitisation of a quartz sample is influenced by its thermal and radiation history (Preusser et al., 2009). The original quartz samples were not of sedimentary origin, but instead large crystals of hydrothermal and metamorphic origins which occurred in vein-associated metamorphic rocks. Consequently, the different grains of the same sample were subjected to the same conditions of both heating and irradiation. Therefore, based on their origin, similar pre-dose sensitisation was expected for various aliquots derived from these samples. In order to explain the large variation in the sensitisation observed in case of various aliquots of a sample the following phenomena are proposed.

The sensitisation of the same quartz samples after annealing does not yield the same discrepancy as compared to unannealed case, indicating the importance of heating to reduce the CV of the sensitisation. The most probable cause could be the gridding and milling of the samples. In general, any treatment of quartz by mechanical actions such as grinding, milling, crushing, sawing and cutting, may result in the production of defect structures (McKeever, 1985; Ranjbar, et al., 1999; Takeuchi, et al., 2006; Takeuchi and Hashimoto, 2008). These procedures result mostly in the formation of defects such as dislocations in the outer surface of the grains (Ranjbar, et al., 1999). The surface alterations following a prolonged grinding, which results in significant changes in the physical and chemical characteristics of the material, have been reported in the literature (Battaglia, et al., 1993). Formation of free radicals results from the production of large amounts of new fracture surfaces in small quantities of the material. These new surfaces create broken bonds which lay in regions a few nm below the surface.

The defect creation is related to the methods and conditions of treatment (Bartnitskaya et al., 1992). The influence of crushing and milling on TL seems to be minimized if HF treatment is applied, since the near-surface layer is usually removed by HF etching (Bartnitskaya, et al., 1992). In the present study, HF etching was not applied because removal of feldspar was not necessary since the samples are not of sedimentary origin. Therefore the creation and presence of these defects affect the TL

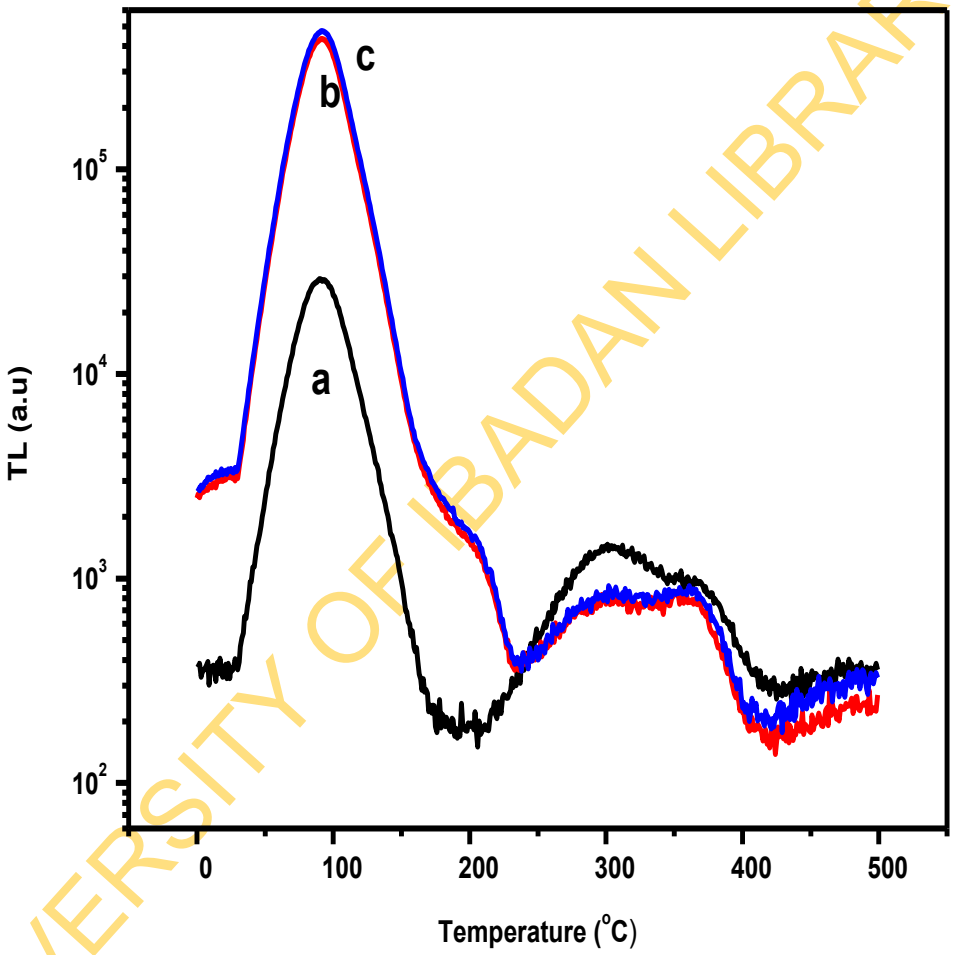

Fig. 4.7: TL glow curves for annealed S2 samples. Curve (a) corresponds to the sensitisation without previous thermal activation (Sn_{02}). Both curves (b) and (c) correspond to the glow-curve after the first thermal activation (Sn_1) indicating the minimum and maximum sensitisation respectively.

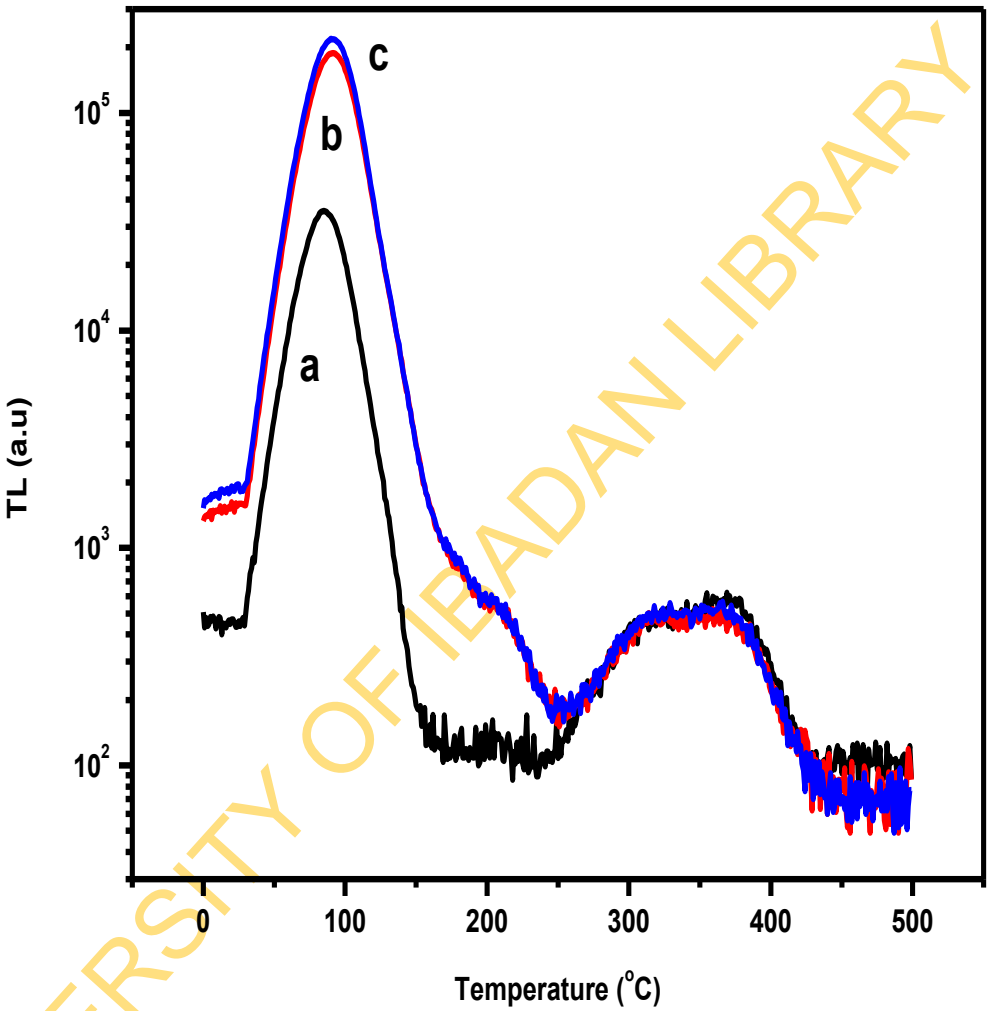

Fig. 4.8: TL glow curves for annealed S4 samples. Curve (a) corresponds to the sensitisation without previous thermal activation (Sn_{02}). Both curves (b) and (c) correspond to the glow-curve after the first thermal activation (Sn_1) indicating the minimum and maximum sensitisation respectively

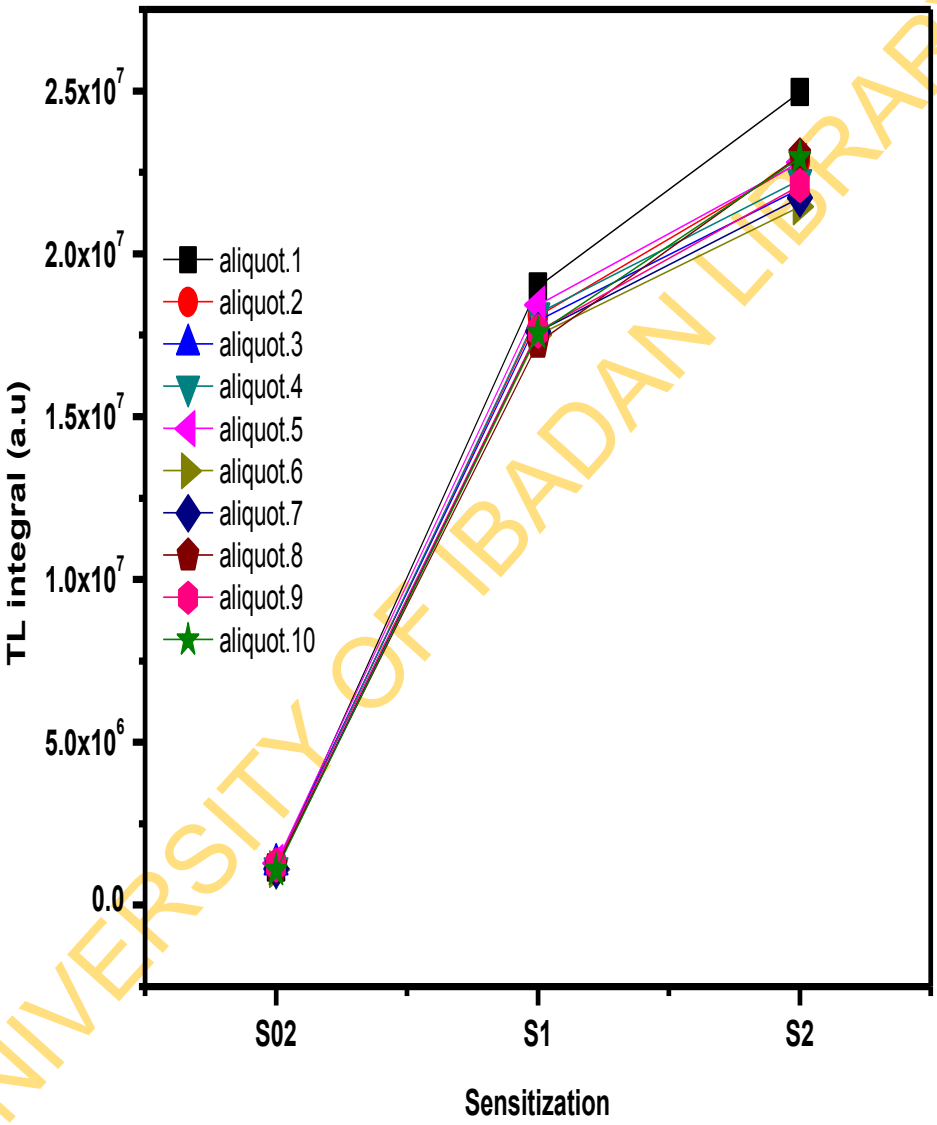

Fig. 4.9: The sensitisations resulting from three successive irradiations and luminescence readings for 10 aliquots for annealed S2 sample.

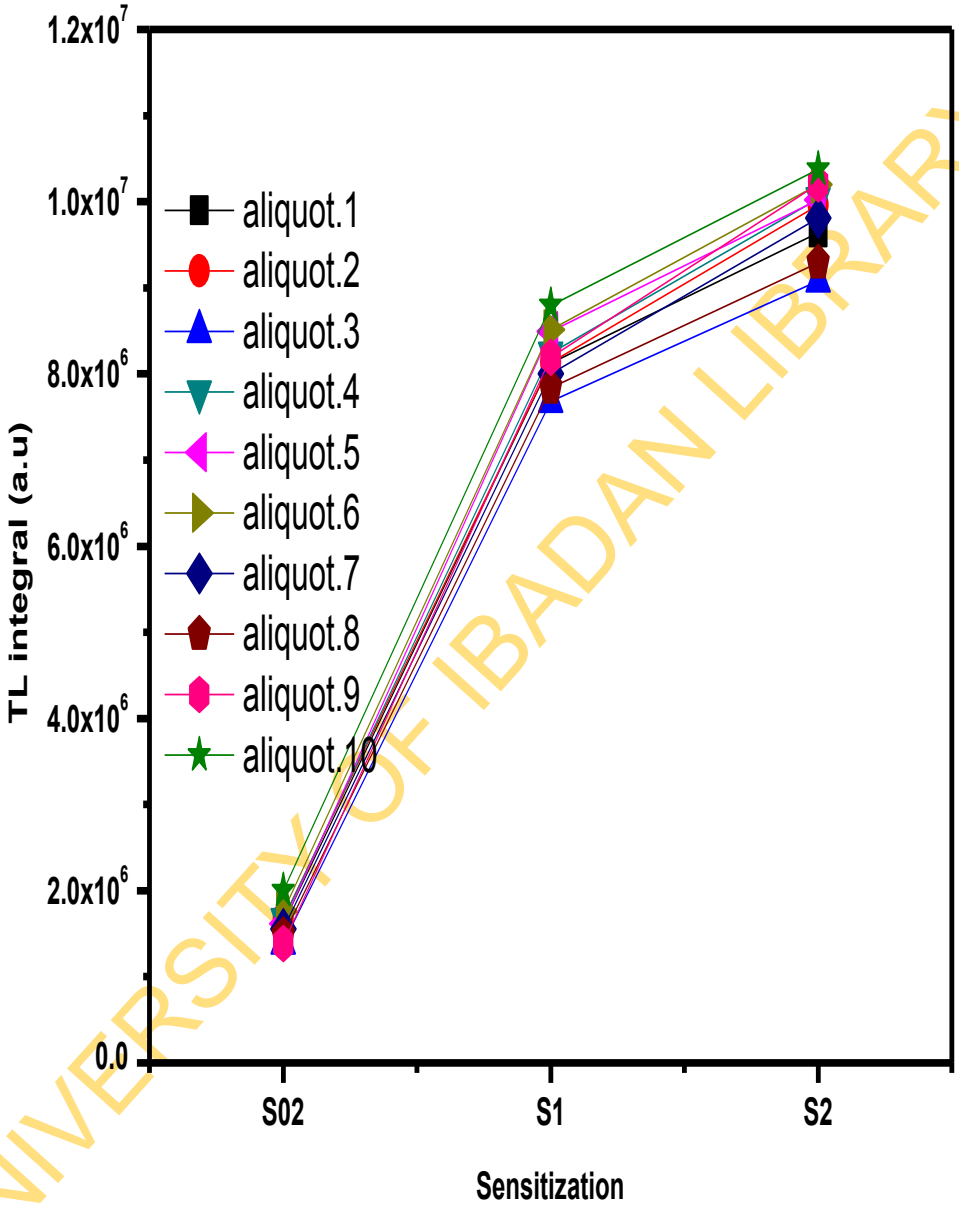

Fig. 4.10: The sensitisations resulting from three successive irradiations and luminescence readings for 10 aliquots for annealed S4 samples.

sensitivity of the unannealed samples. However, certain changes occurring in the quartz lattice with heating at 500^{o}C, such as annealing of these defects, result in dilution of grinding effects. Therefore, in the case of the annealed samples the sensitisation is much more uniform for all aliquots of the same quartz sample. This latter argument is further supported by the column *[Sn_2/Sn_1]* of Table 4.1 of the unannealed samples case. Besides the large variation of the sensitisation factor Sn_1 due to first thermal activation up to 500 ^{o}C in all quartz samples, the ratio Sn_2/Sn_1 of various aliquots is consistent. Therefore, it seems that heating up to 500 ^{o}C, even though instantaneous, could merely anneal the dislocations, resulting thus in much more uniform sensitisation ratio Sn_2/Sn_1.

4.2.4 Implications of results

The fact that 110 ^{o}C TL peak in quartz is not stable, a number of applications aside pre-dose dating technique, have been proposed by taking advantage of either its sensitivity or sensitisation. Among these, Stokes (1994) suggested the applicability of the 110 ^{o}C TL peak as a sensitivity correction in a single-aliquot additive dose protocol. A linear relationship between sensitivity changes in the 110 ^{o}C TL peak of quartz and in its OSL emission was reported first by Stoneham and Stokes (1991) providing evidence for a strong link between the two luminescence signals. Consequently, one expects that similar CV of sensitisation is expected also for the OSL emission of the same quartz samples. However, implications of this high CV of sensitisation to OSL are limited due to single aliquot procedures applied. The same insignificant implication applies to the pre-dose dating technique, which is theoretically based on pre-dose sensitisation. Because it also involves single aliquot procedure and of the actuality that the technique was originally established on observations on heated quartz extracted from pottery (Zimmerman, 1971) that is identical to annealed quartz.

Nevertheless, the 110 ^{o}C TL peak in quartz is used in order to perform mass reproducibility check and correction in many multiple-aliquot protocols, such as the foil technique (Michael, et al., 1997). In the framework of similar protocols, a second TL measurement is performed after the main measurement for each aliquot used. The same dose is applied to all aliquots. The intensity of the 110 ^{o}C TL peak of all these second TL measurements is used for both mass reproducibility monitoring and correction. Based on the results presented so far in the present study, this procedure could be successfully applied only in the case of heated quartz, although still a relatively increased error is expected. Unfortunately, special caution should be exercised while

applying this specific mass reproducibility correction procedure in the case of geological, unannealed quartz samples, since it could result in erroneous equivalent dose estimation.

4.2 Study on luminescence sensitisations in unannealed and annealed quartz samples

Experimental protocols of section 3.3.2 in chapter three were employed to obtain all experimental results presented below.

4.2.1 Sensitisations of 110^{o}C TL peak and RT-LMOSL of unannealed and annealed samples

The representative glow curves from measurements performed on unannealed and annealed S2 and S4 samples using Part A of the experimental protocol are shown for the two samples in Figures 4.11 to 4.14 respectively. Their counterparts of RT-LMOSL curves, using Part C of the protocol, are shown in Figures 4.15 to 4.18. It is evident from these figures that the two phenomena, 110^{o}C TL peak and RT-LMOSL curves, exhibit nearly identical sensitisation pattern both in unannealed and annealed samples of the two quartz samples.

Deconvolution to the respective components of the whole RT-LMOSL curves for the two samples is presented in Figures 4.19 to 4.22. Each of the two unannealed samples has four different RT-LMOSL components namely; 1st component (C1), 2nd component (C2), 3rd component (C3) and 4th component (C4) while these increased to five, components, 1st component (C1), 2nd component (C2), 3rd component (C3), 4th component (C4) and 5th component (C5) in annealed samples. The increase in number of RT-LMOSL components from 4 to 5 following annealing is not a new idea. A similar increase in number of TL glow peaks of some Nigerian quartz after annealing has been reported (Oniya et al., 2012b). Therefore, the number of RT-LMOSL components that are associated with optical release of charge from each different trap types that are also responsible for TL peaks is expected to increase too after

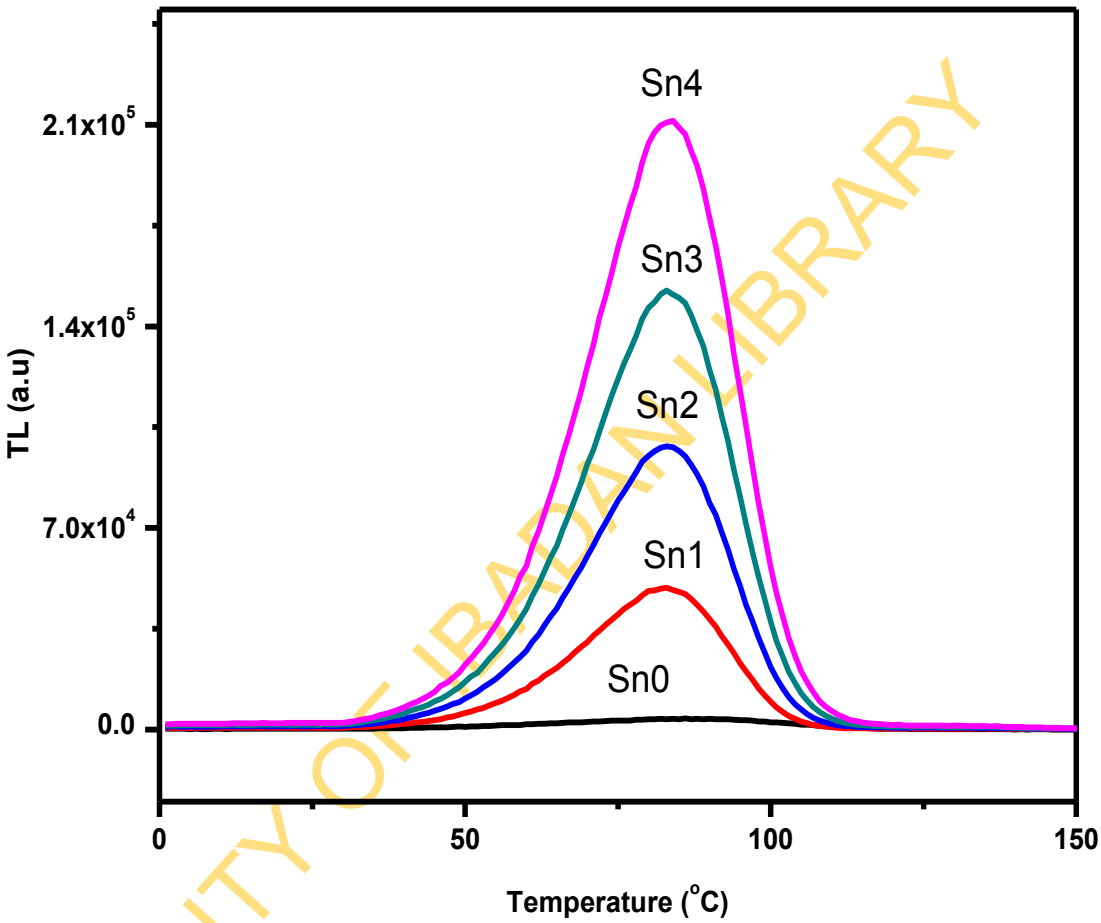

Fig. 4.11: Glow curves showing sensitisations resulting from successive irradiations and TL readings of unannealed S2 sample. Curves S_{n0}, S_{n1}, S_{n2}, S_{n3}, S_{n4} represent unsensitised, 1st sensitised, 2nd sensitised, 3rd sensitised, 4th sensitised, luminescence readings respectively.

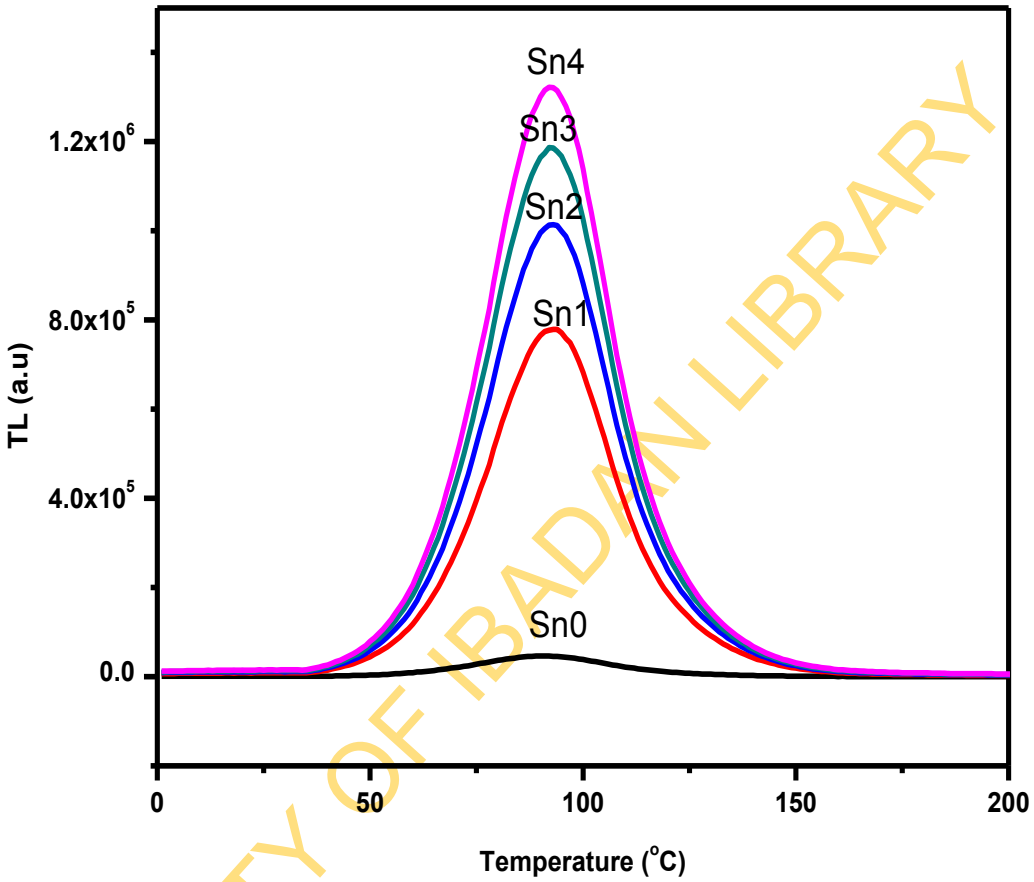

Fig. 4.12: Glow curves showing sensitisations resulting from successive irradiations and TL readings of annealed S2 sample. Curves S_{n0}, S_{n1}, S_{n2}, S_{n3}, S_{n4} represent unsensitised, 1st sensitised, 2nd sensitised, 3rd sensitised, 4th sensitised, luminescence readings respectively.

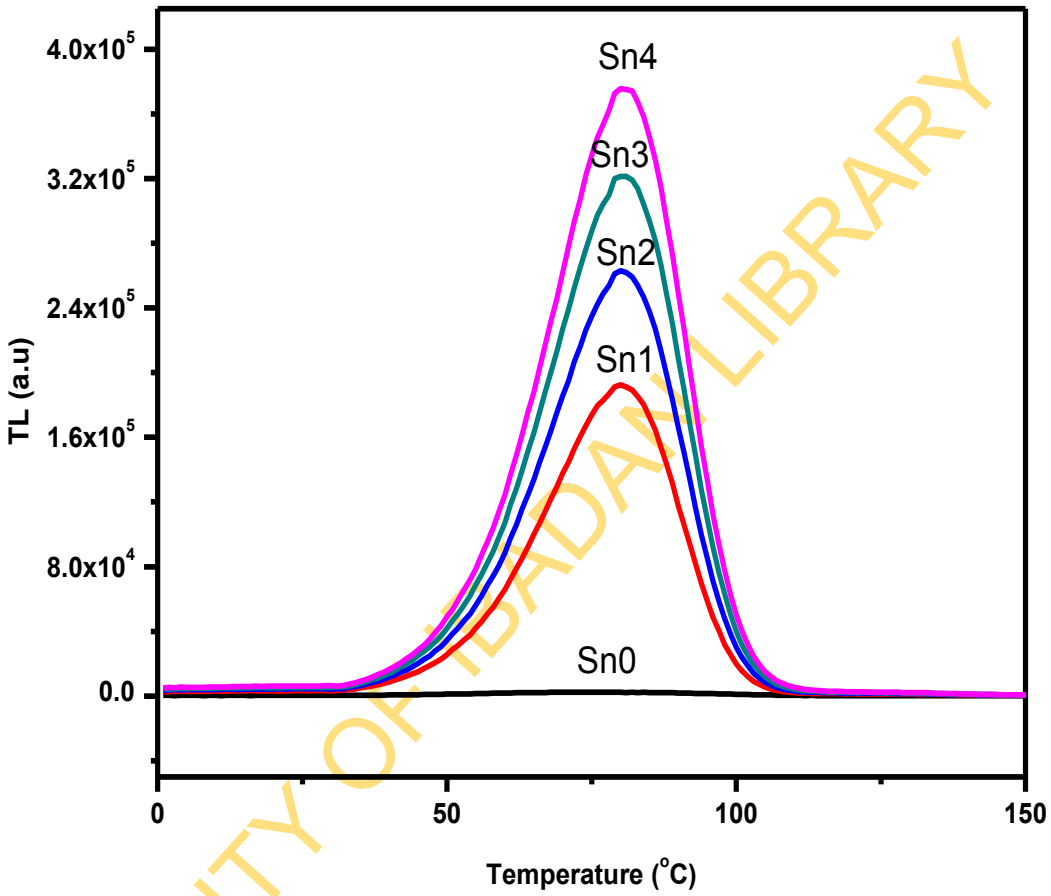

Fig. 4.13: Glow curves showing sensitisations resulting from successive irradiations and TL readings of unannealed S4 sample. Curves S_{n0}, S_{n1}, S_{n2}, S_{n3}, S_{n4} represent unsensitised, 1st sensitised, 2nd sensitised, 3rd sensitised, 4th sensitised, luminescence readings respectively.

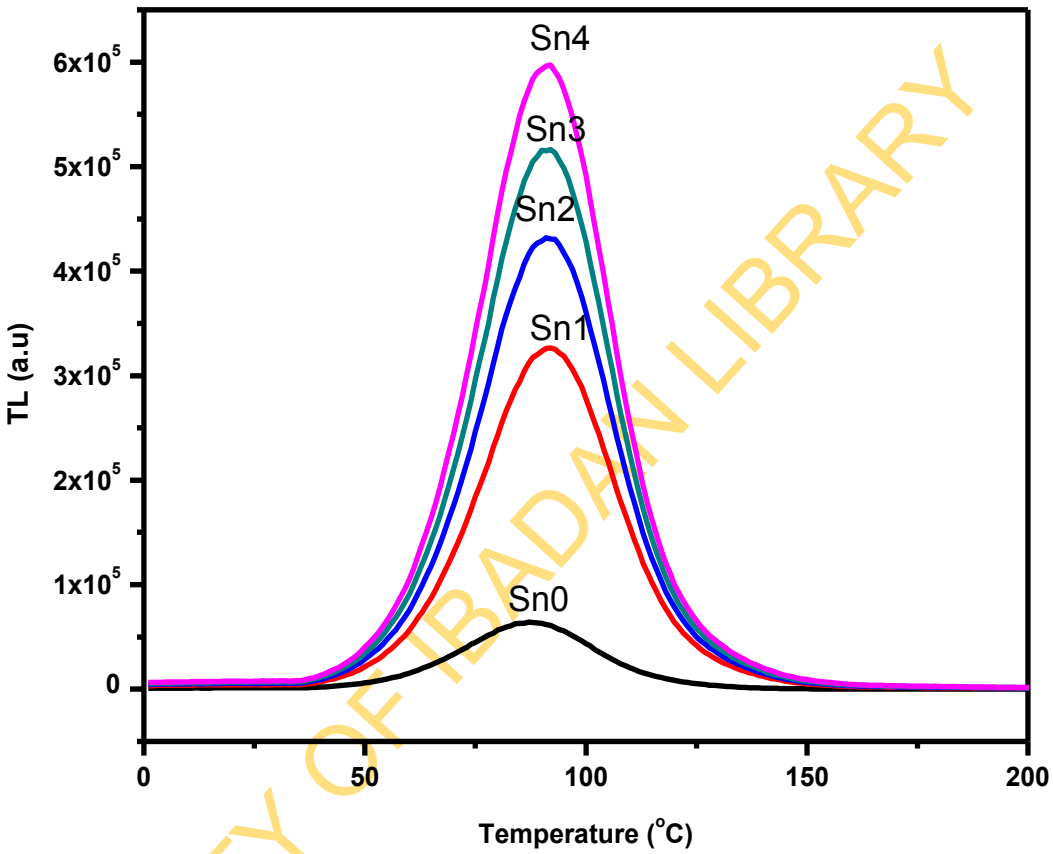

Fig. 4.14: Glow curves showing sensitisations resulting from successive irradiations and TL readings of annealed S4 sample. Curves S_{n0}, S_{n1}, S_{n2}, S_{n3}, S_{n4} represent unsensitised, 1st sensitised, 2nd sensitised, 3rd sensitised, 4th sensitised, luminescence readings respectively.

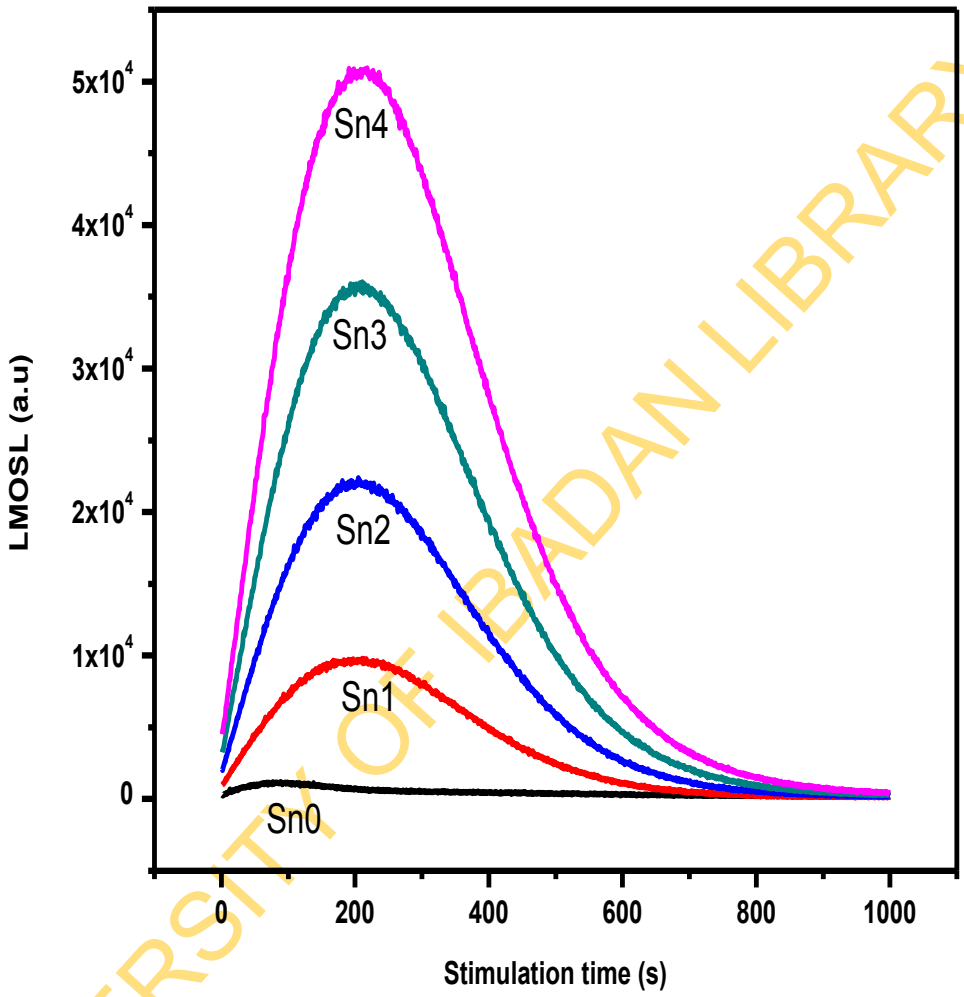

Fig. 4.15: OSL curves showing sensitisations resulting from successive irradiations and LMOSL readings of unannealed S2 sample. Curves S_{n0}, S_{n1}, S_{n2}, S_{n3}, S_{n4} represent unsensitised, 1st sensitised, 2nd sensitised, 3rd sensitised, 4th sensitised, luminescence readings respectively.

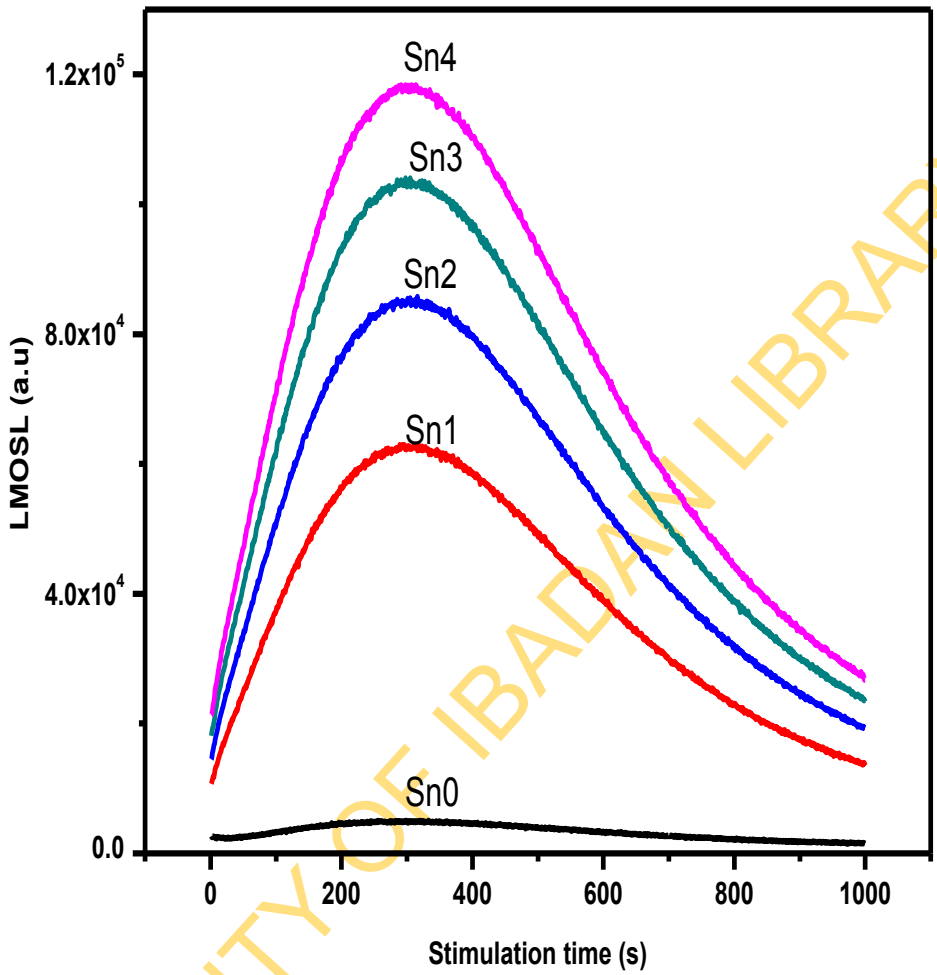

Fig. 4.16: OSL curves showing sensitisations resulting from successive irradiations and LMOSL readings of annealed S2 sample. Curves S_{n0}, S_{n1}, S_{n2}, S_{n3}, S_{n4} represent unsensitised, 1st sensitised, 2nd sensitised, 3rd sensitised, 4th sensitised, luminescence readings respectively.

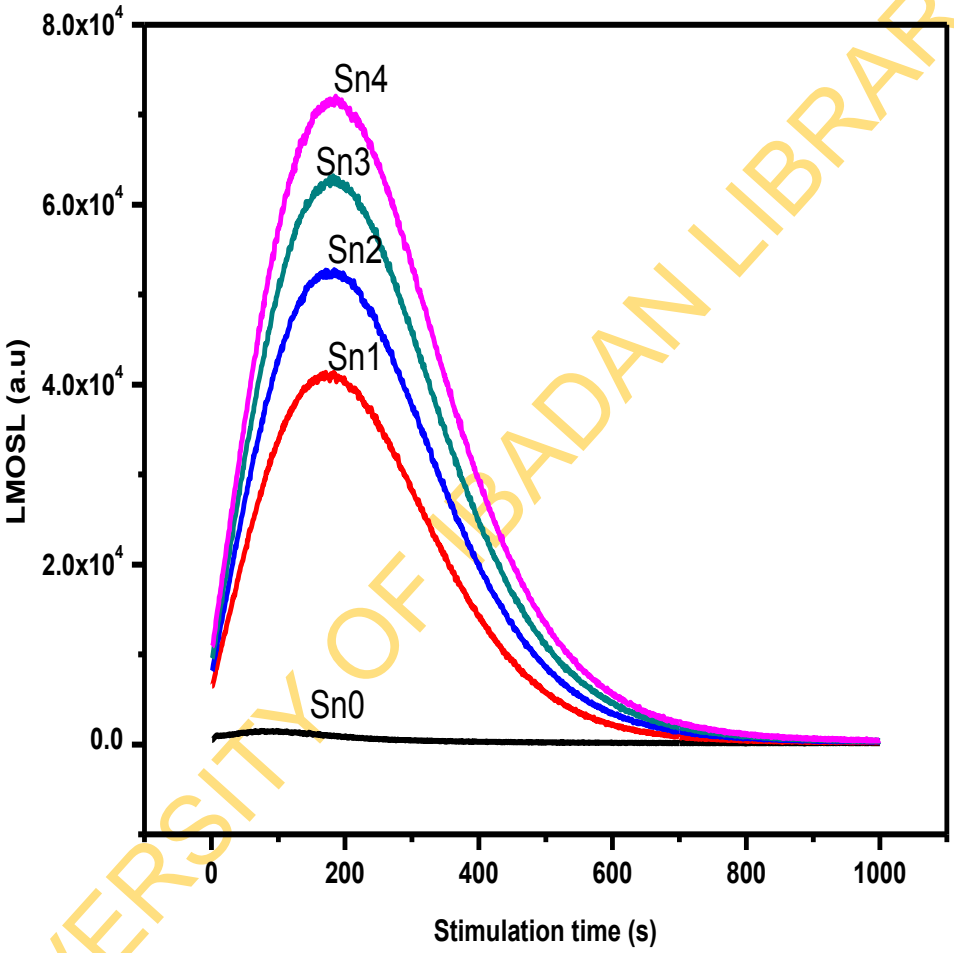

Fig. 4.17: OSL curves showing sensitisations resulting from successive irradiations and LMOSL readings of unannealed S4 sample. Curves S_{n0}, S_{n1}, S_{n2}, S_{n3}, S_{n4} represent unsensitised, 1st sensitised, 2nd sensitised, 3rd sensitised, 4th sensitised, luminescence readings respectively.

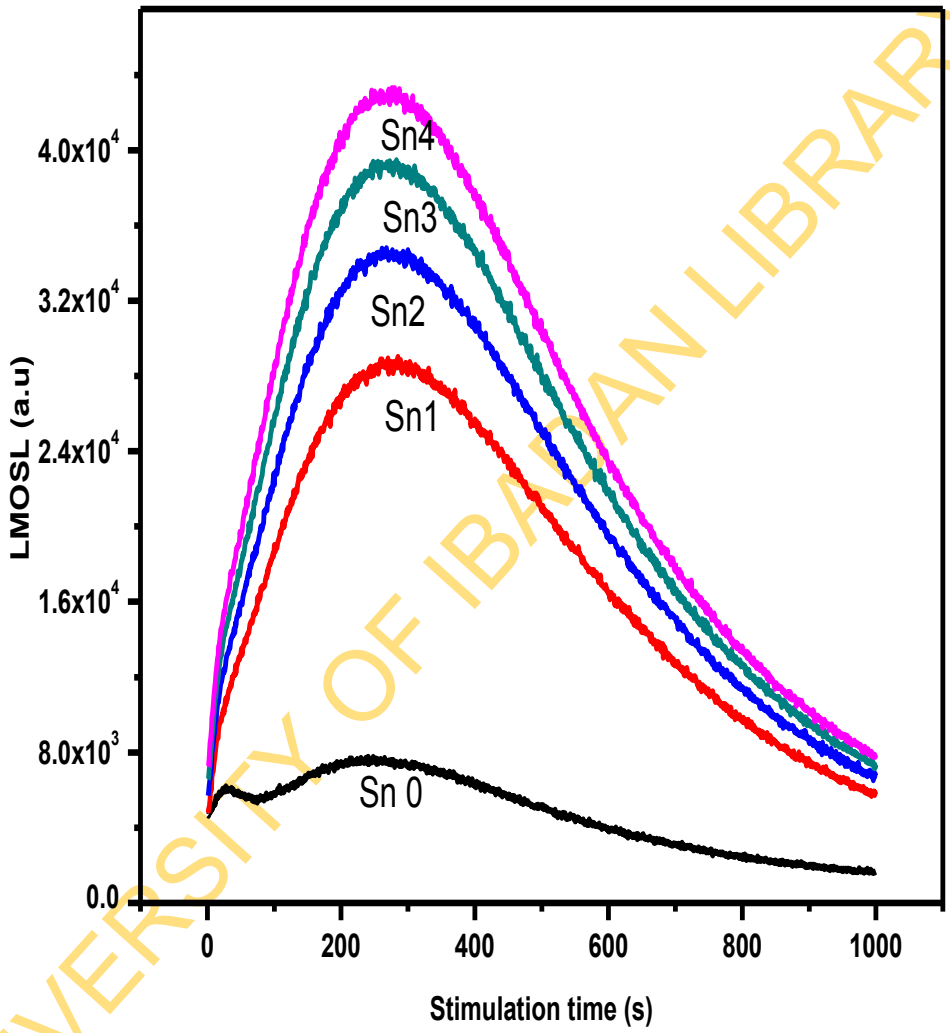

Fig. 4.18: OSL curves showing sensitisations resulting from successive irradiations and LMOSL readings of annealed S4 sample. Curves S_{n0}, S_{n1}, S_{n2}, S_{n3}, S_{n4} represent unsensitised, 1st sensitised, 2nd sensitised, 3rd sensitised, 4th sensitised, luminescence readings respectively.

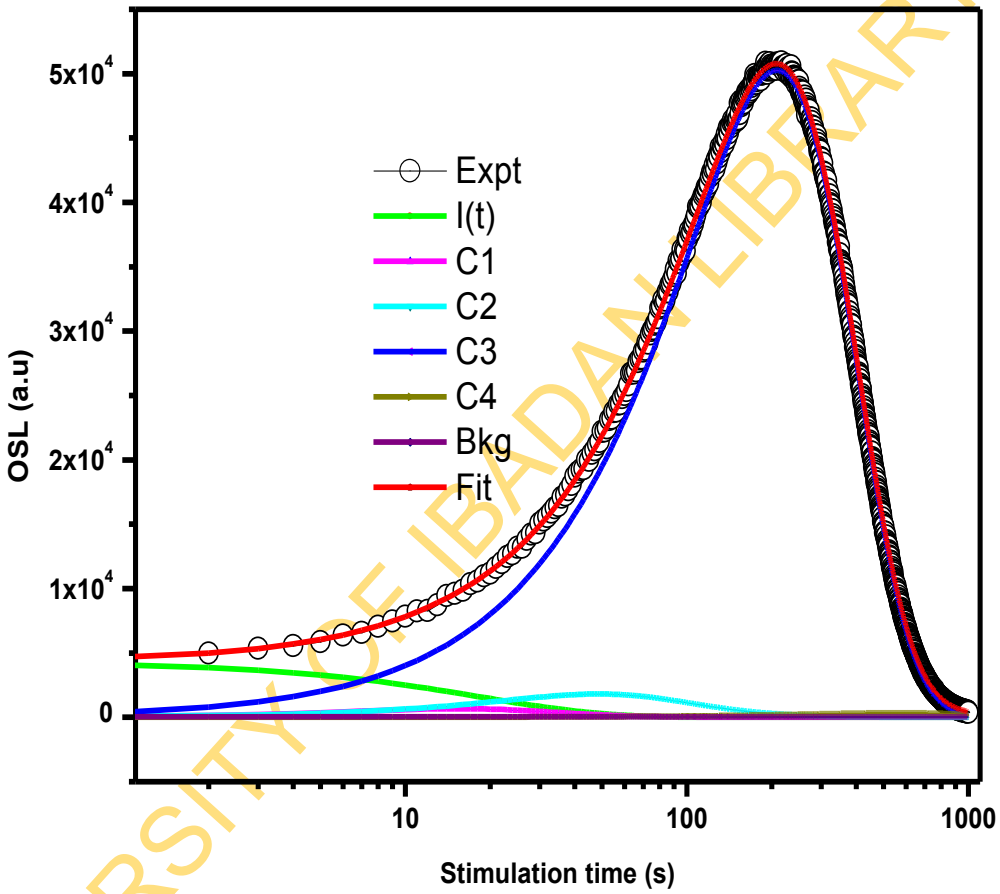

Fig. 4.19: RT-LMOSL curves depicting deconvolution of the LMOSL curves to its respective components unannealed S2 sample. Curves C1, C2, C3, and C4 represent 1st, 2nd, 3rd, and 4th components respectively. Expt. represents experimental data, I(t) represents Bkg. Represents phosphorescence component background and Fit. represents fitted data.

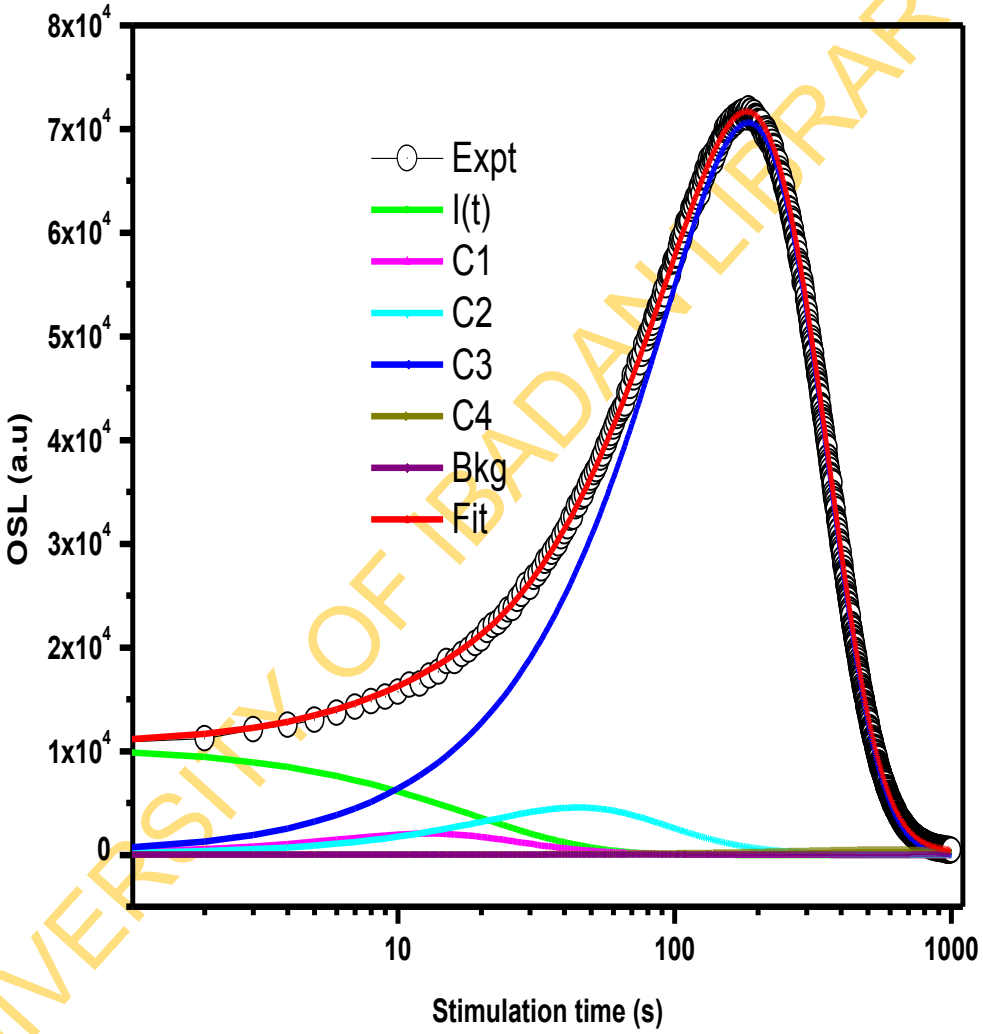

Fig. 4.20: RT-LMOSL curves depicting deconvolution of the LMOSL curves to its respective components for unannealed S4 sample. Curves C1, C2, C3, and C4 represent 1st, 2nd, 3rd, and 4th components respectively. Expt. represents experimental data, I (t) represents Bkg. Represents phosphorescence component background and Fit. represents fitted data.

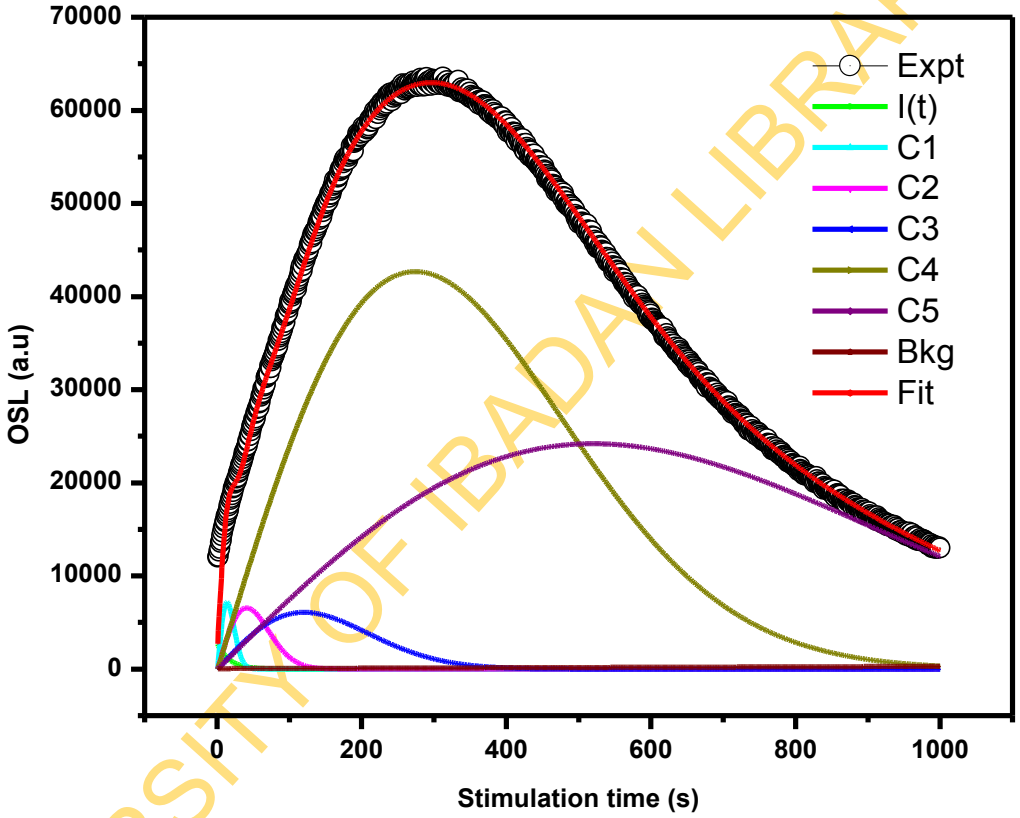

Fig. 4.21: RT-LMOSL curves depicting deconvolution of the LMOSL curves to its respective components annealed S2 sample. Curves C1, C2, C3, C4 and C5 represent 1st, 2nd, 3rd, 4th, 5th components respectively. Expt. represents experimental data, I(t) represents Bkg. Represents phosphorescence component background and Fit. represents fitted data.

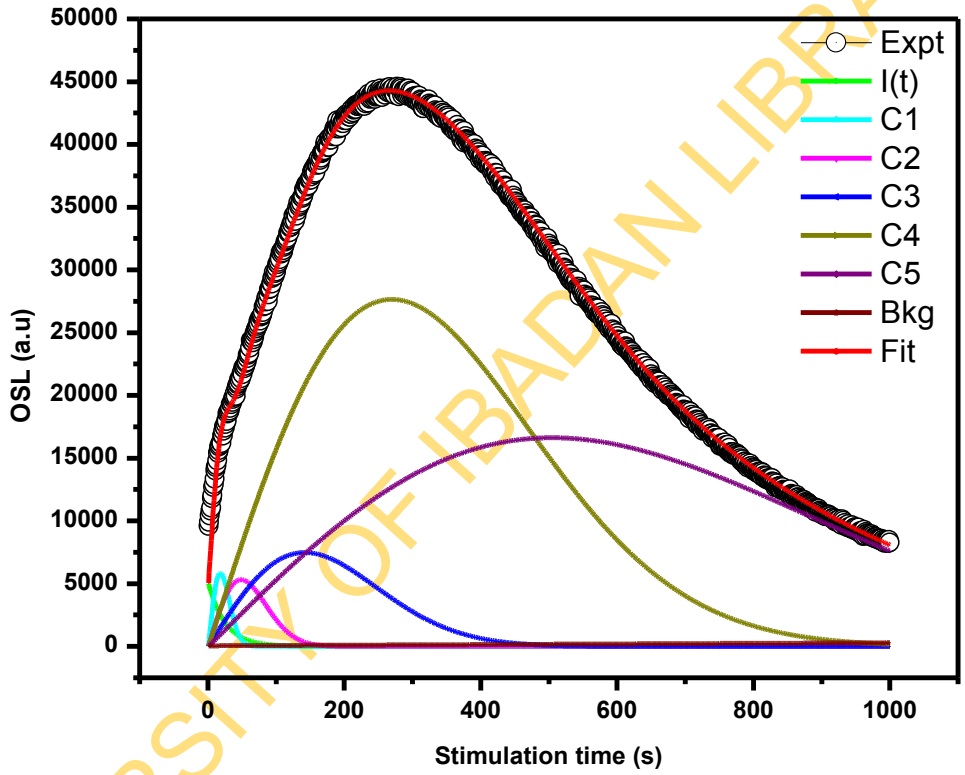

Fig. 4.22: RT-LMOSL curves depicting deconvolution of the LMOSL curves to its respective components annealed S4 sample. Curves C1, C2, C3, C4 and C5 represent 1st, 2nd, 3rd, 4th, 5th components respectively. Expt. represents experimental data, I(t) represents Bkg. Represents phosphorescence component background and Fit. represents fitted data.

annealing. The changes in the nature of the glow-curves and RT-LMOSL components after annealing have been attributed to the alterations made to the recombination pathways and competitions during irradiation and heating. As suggested by Bøtter-Jensen *et al*. (1995) they are as a result of introduction of more traps and recombination centres.

From the objective of this study, it is important to associate each RT-LMOSL component with their corresponding TL peak; most especially 110^{o}C TL peak. Room temperature (RT)-LMOSL component associated with 110^{o}C TL peak has always been described to be the broad, intermediate and intense component among all the RT-LMOSL components (Kiyak et al., 2008; Polymeris et al., 2009). Based on this, C3 is the specific component identified with the 110^{o}C TL peak for both S2 and S4 unannealed samples in this work as could be seen in Figures 4.19 and 4.20. This is, furthermore, confirmed from Table 4.2 which shows the percentage of 110^{o}C TL peak signal to the total TL response and that of each component of the RT-LMOSL signal to the overall OSL signal of each sample. From Table 4.2, the signal of 110^{o}C TL peak is 99.01 and 99.00% of the total signal of the whole TL emission for S2 and S4 unannealed samples respectively. It is C3 that follows the exact trend of dominating percentage in RT-LMOSL signal with 96.75 and 95.24% of the total signal of the whole RT-LMOSL emission for S2 and S4 unannealed samples respectively. The first two RT-LM-OSL components (C1 and C2) are recognized to be the two fast components which are known to be associated with the 325◦C peak (Jain et al., 2003; Kiyak et al., 2008; Polymeris et al., 2009) and the fourth component (C4) is considered as the sum of all slower components (Kitis et al 2010). The C4 is only partially emptied in the LM-OSL measurements therefore, not well defined. Different slow components that is believed to makes up the C4 has been confirmed to be associated with TL trap slightly above 260^{o}C, another around 400^{o}C and even with very stable TL traps beyond 600^{o}C (Jain et al., 2003).

However, in the case of annealed samples (Figures 4.21 and 4.22), five RT-LMOSL components are recognized. The C1, C2 and C3 stand as the three fast components, while the broad, intermediate and intense RT LM-OSL component C4 is identified with 110^{o}C TL peak (Kiyak et al., 2008; Polymeris et al., 2009). As earlier observed for C4 in the case of unannealed samples, the behavior of component C5 is

Table 4.2: Percentage sensitisation signal of each component to the total fitted data

Luminescence Component	S2		S4	
	Unannealed (% of Experimental Data)	Annealed (% of Experimental Data)	Unannealed (% of Experimental Data)	Annealed (% of Experimental Data)
110^{o}CTL Peak	99.01	90.11	99.00	92.83
C1	0.32	0.39	0.67	0.62
C2	1.22	1.12	2.27	1.57
C3	96.75	3.10	95.24	6.52
C4	1.64	49.62	1.67	45.81
C5	-	45.14	-	44.46
OSL Fitted Data	99.93	99.93	99.85	99.61

not of much interest in the present study (Apendix A1), mainly due to the following reasons: (i) the component has not totally decayed after 1000s of stimulation, (ii) this component is considered as the sum of all slower components.

4.2.2 Dependence of 110^{o}C TL peak and RT-LMOSL sensitisations on heating rate of thermal activation

Having identified C3 in unannealed samples and C4 in annealed samples to share the same electron trap with 110^{o}C TL peak, the signal of these components was used as the parallel complementary method to that of 110^{o}C TL peak in this study. With reference to Figures 4.11 to 4.18, both unannealed and annealed S2 and S4 samples exhibited sensitisation after each successive cycle of irradiations and TL/OSL measurements. However, the nature of the glow and OSL curves obtained for the remaining heating rates were similar to this pattern but the only variation observed was from differences in the intensity of the signals. Figures 4.23 to 4.30 better present the dependence of the sensitisation for both TL and RT-LMOSL on heating rate of the preceding TL used for thermal activation for both S2 and S4. As could be seen in Figures 4.23 to 4.30 for the unannealed samples, the level of sensitisation is high for low heating rate and low for the high heating rate. Mostly for unannealed samples, the sensitisation is somewhat decreasing with heating rates generally. However, a careful observation of these figures showed that there are some points in which this heating rate sensitisation dependency trend was distrusted. On the other hand for annealed samples, it is only S2 and TL aspect of S4 that remarkable displayed the above trend of dependence of the sensitisation on heating rates of thermal activation.

4.2.3 Dependence of various components of RT-LMOSL sensitisations on heating rate of thermal activation

The sensitisation of various components of RT-LMOSL is nearly identical to C4 described above. This is shown in Figures 4.31 to 4.34 for the two unannealed and annealed samples, which is sensitisation obtained during the measurement of Part C Step 6 (Sn4) of the protocol. The dependence of the sensitisation on the heating rates of thermal activation is more pronounced in unannealed samples than in the annealed for the two samples. As seen in these figures, the degree of the dependence on the

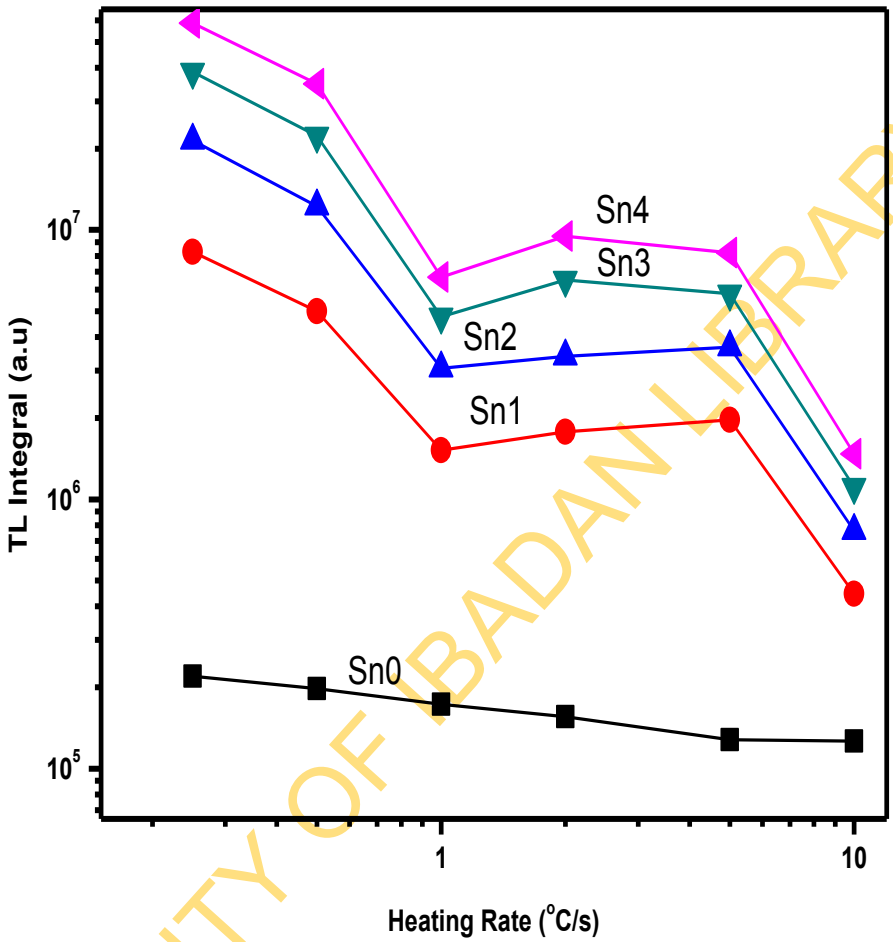

Fig. 4.23: Plots of TL sensitisations against heating rates as function of cycle of measurements for unannealed S2 samples. Curves S_{n0}, S_{n1}, S_{n2}, S_{n3}, S_{n4} represent unsensitised, 1st sensitised, 2nd sensitised, 3rd sensitised, 4th sensitised, luminescence readings respectively

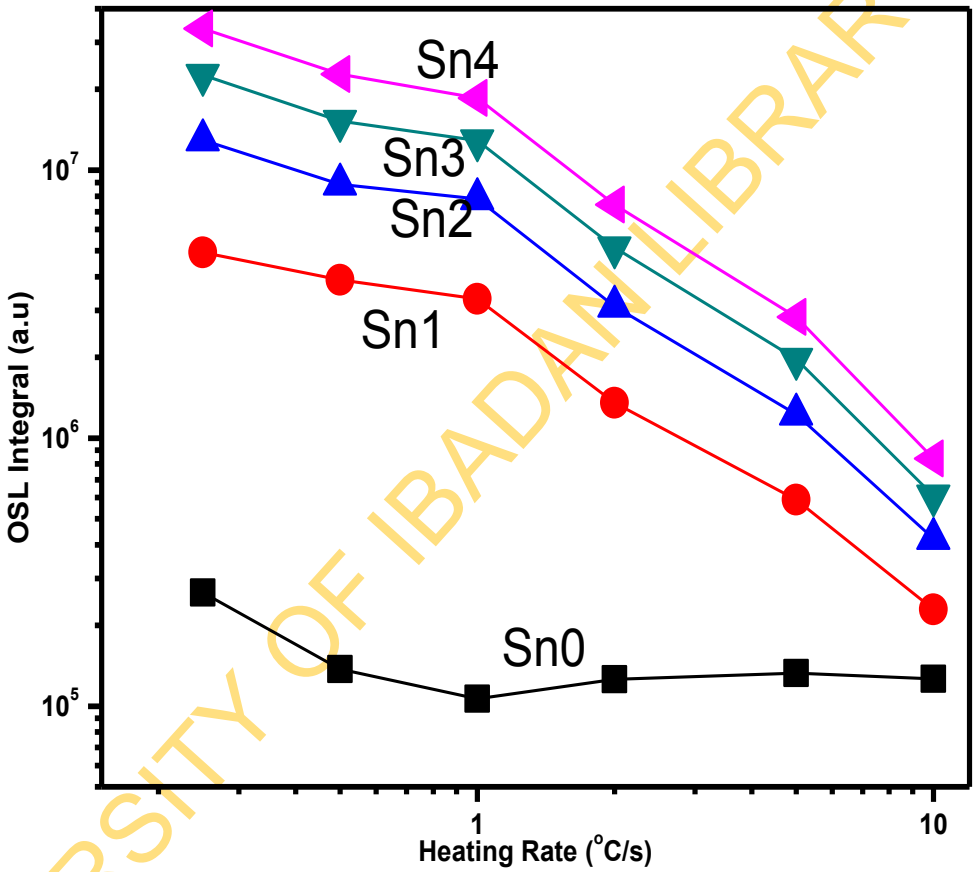

4.24: Plots of RT-LMOSL sensitisations against heating rates as function of cycle of measurements for unannealed S2 samples. Curves S_{n0}, S_{n1}, S_{n2}, S_{n3}, S_{n4} represent unsensitised, 1st sensitised, 2nd sensitised, 3rd sensitised, 4th sensitised, luminescence readings respectively

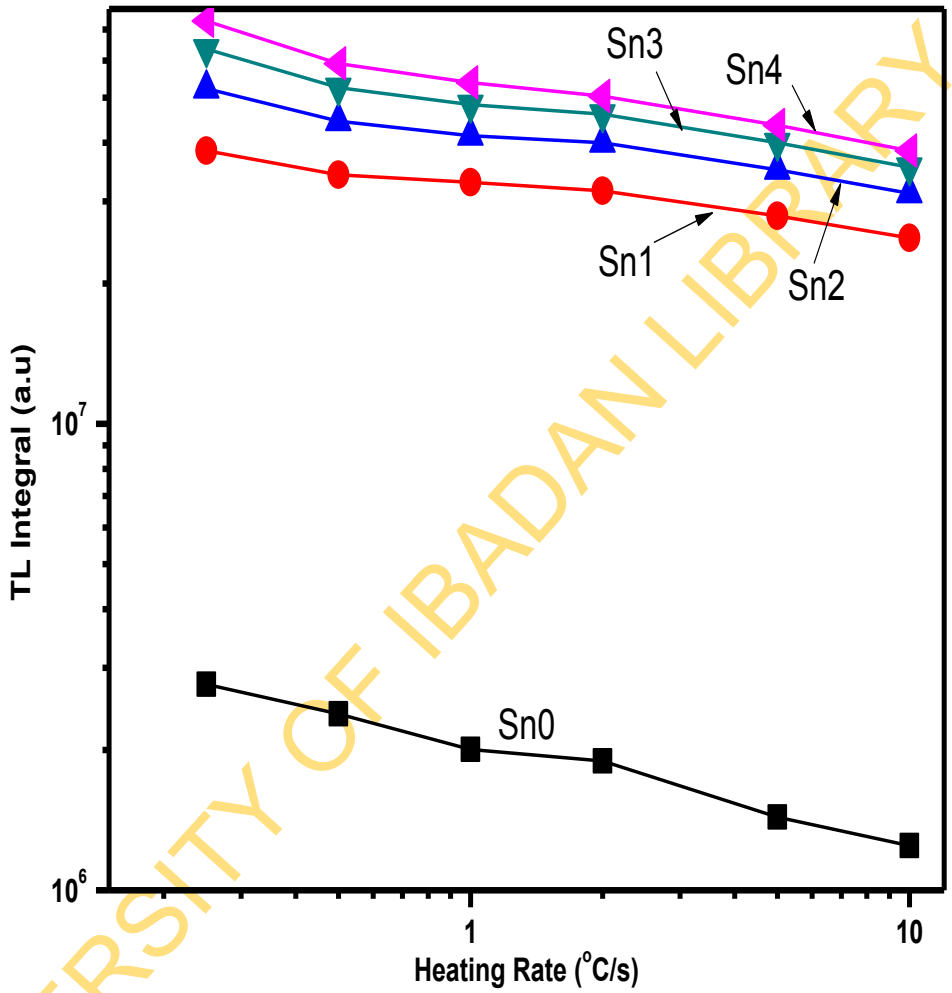

Fig. 4.25: Plots of TL sensitisations against heating rates as function of cycle of measurements for annealed S2 samples. Curves S_{n0}, S_{n1}, S_{n2}, S_{n3}, S_{n4} represent unsensitised, 1st sensitised, 2nd sensitised, 3rd sensitised, 4th sensitised, luminescence readings respectively

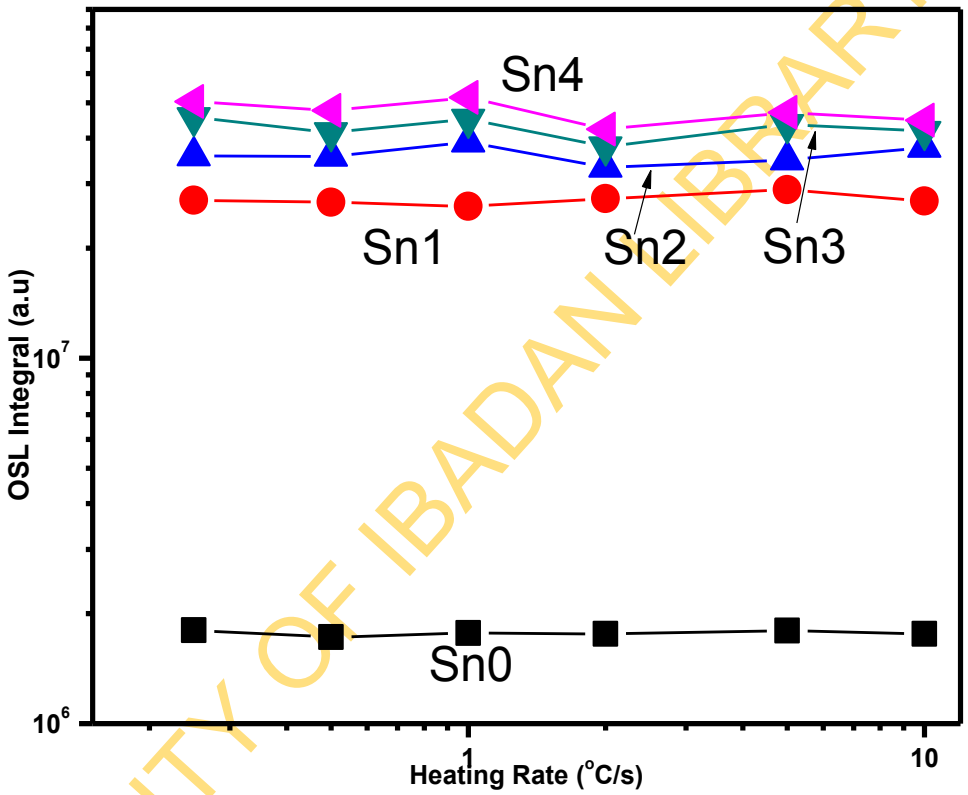

Fig. 4.26: Plots of RT-LMOSL sensitisations against heating rates as function of cycle of measurements for annealed S2 sample. Curves S_{n0}, S_{n1}, S_{n2}, S_{n3}, S_{n4} represent unsensitised, 1st sensitised, 2nd sensitised, 3rd sensitised, 4th sensitised, luminescence readings respectively

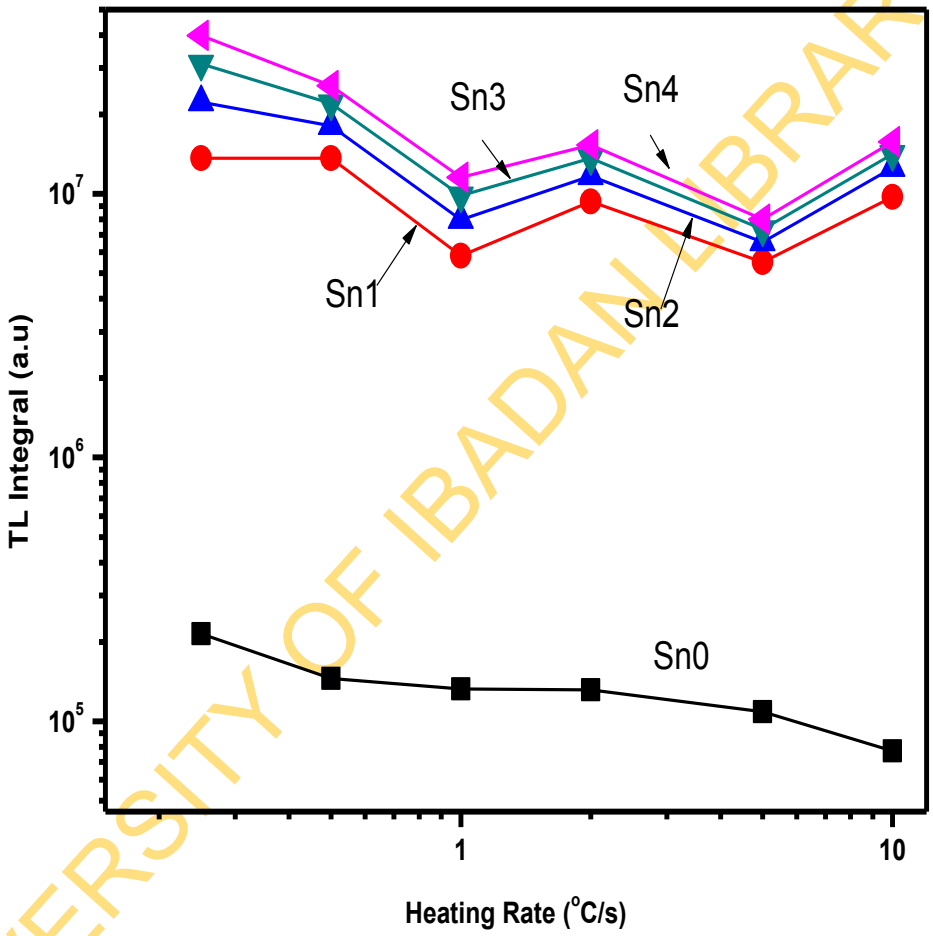

Fig. 4.27: Plots of TL sensitisations against heating rates as function of cycle of measurements for unannealed S4 samples. Curves S_{n0}, S_{n1}, S_{n2}, S_{n3}, S_{n4} represent unsensitised, 1st sensitised, 2nd sensitised, 3rd sensitised, 4th sensitised, luminescence readings respectively

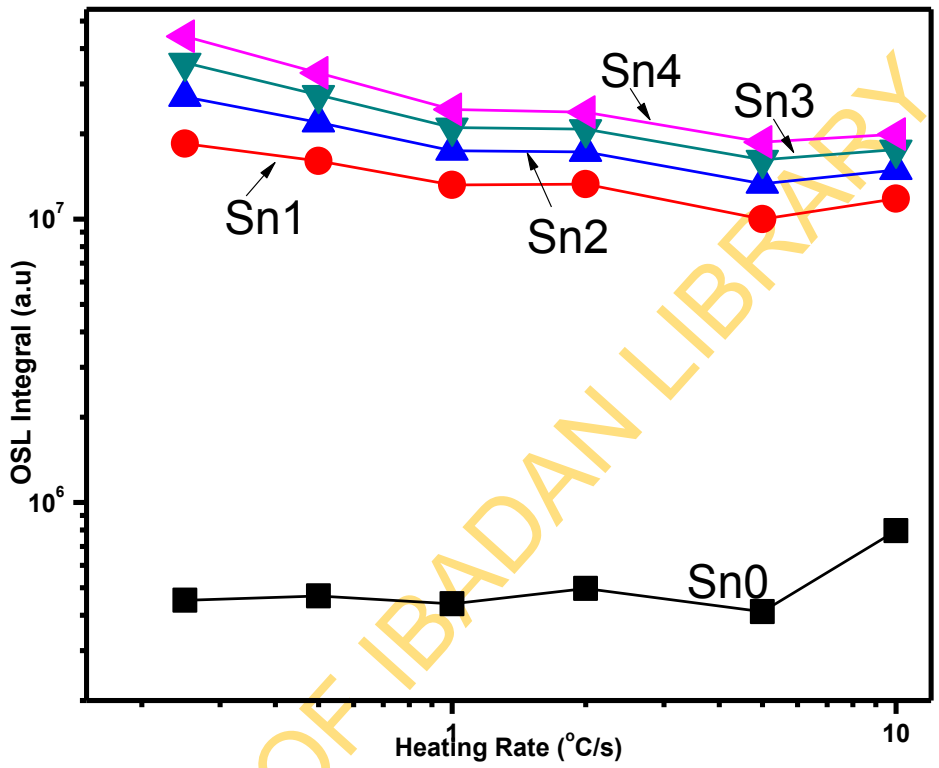

Fig. 4.28: Plots of RT-LMOSL sensitisations against heating rates as function of cycle of measurements for unannealed S4 samples. Curves S_{n0}, S_{n1}, S_{n2}, S_{n3}, S_{n4} represent unsensitised, 1st sensitised, 2nd sensitised, 3rd sensitised, 4th sensitised, luminescence readings respectively

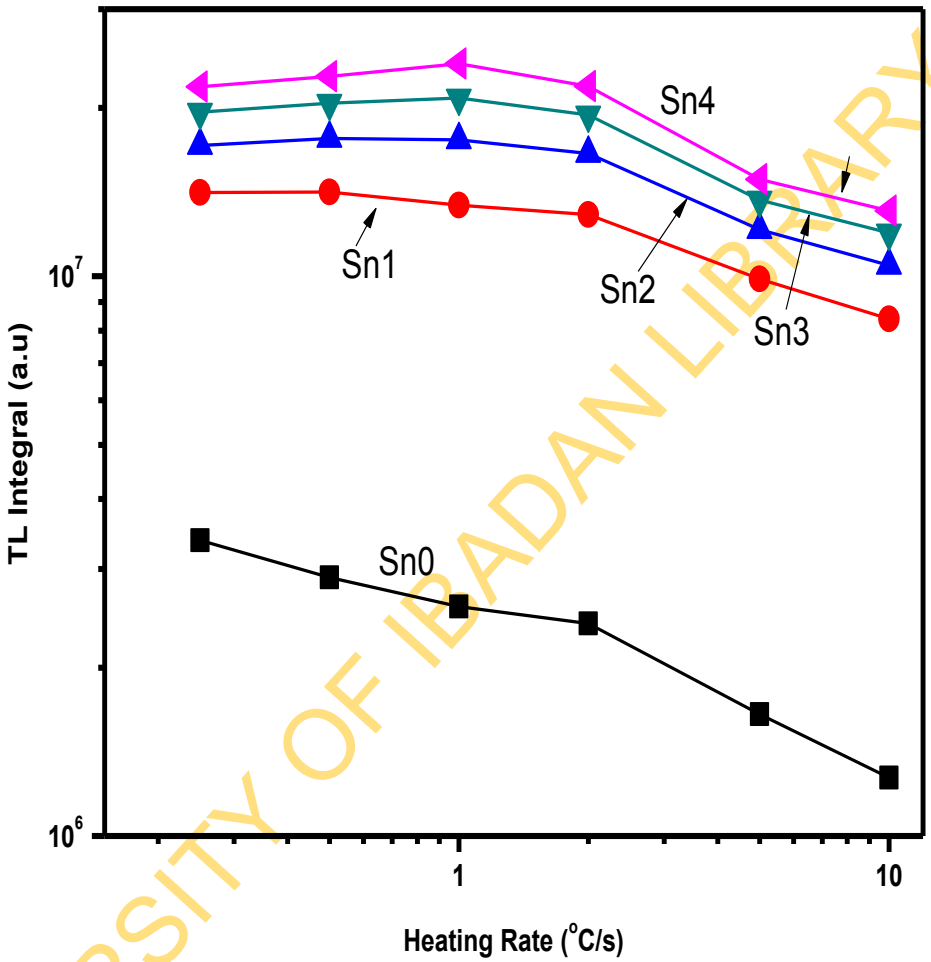

Fig. 4.29: Plots of TL sensitisations against heating rates as function of cycle of measurements for annealed S4 samples. Curves S_{n0}, S_{n1}, S_{n2}, S_{n3}, S_{n4} represent unsensitised, 1st sensitised, 2nd sensitised, 3rd sensitised, 4th sensitised, luminescence readings respectively.

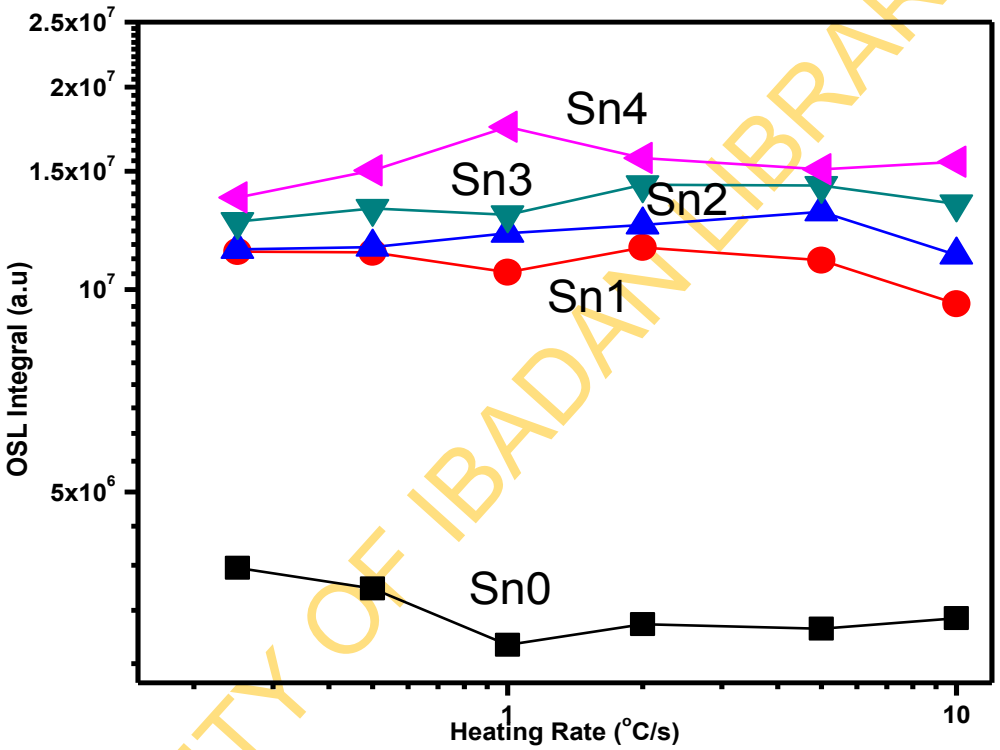

Fig. 4.30: Plots of RT-LMOSL sensitisations against heating rates as function of cycle of measurements for annealed S4 samples. Curves S_{n0}, S_{n1}, S_{n2}, S_{n3}, S_{n4} represent unsensitised, 1st sensitised, 2nd sensitised, 3rd sensitised, 4th sensitised, luminescence readings respectively.

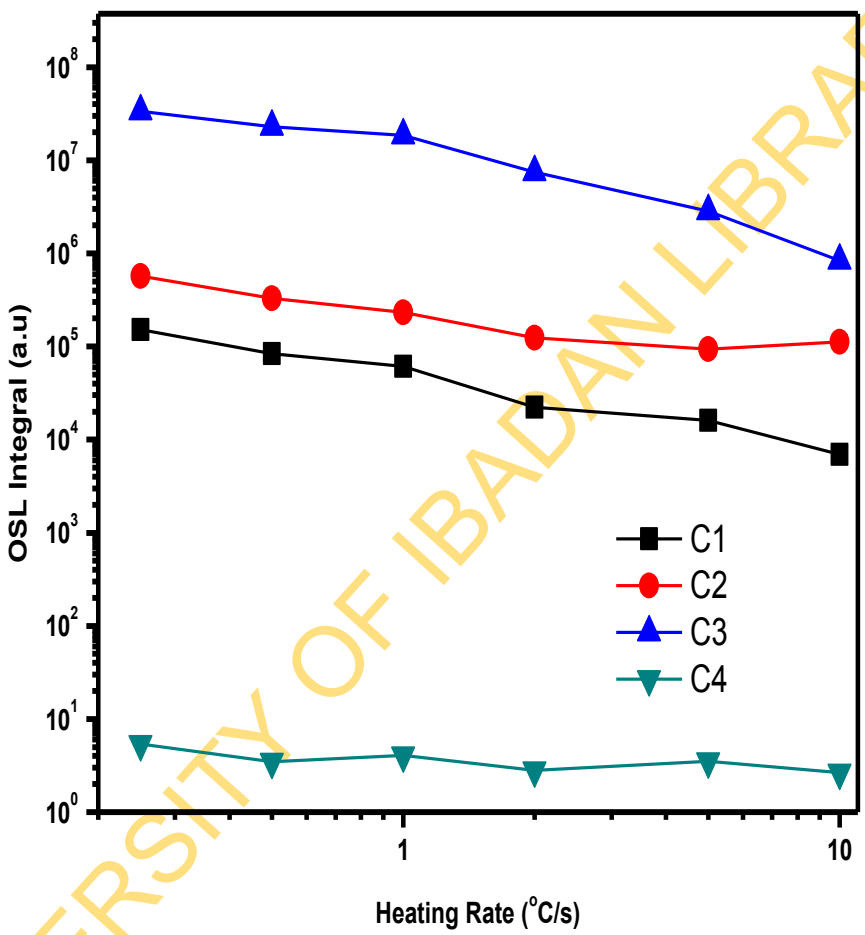

Fig. 4.31. Plots of 4th sensitised of RT-LMOSL components sensitisations against heating rates as function of cycle of measurements for unannealed S2 samples.

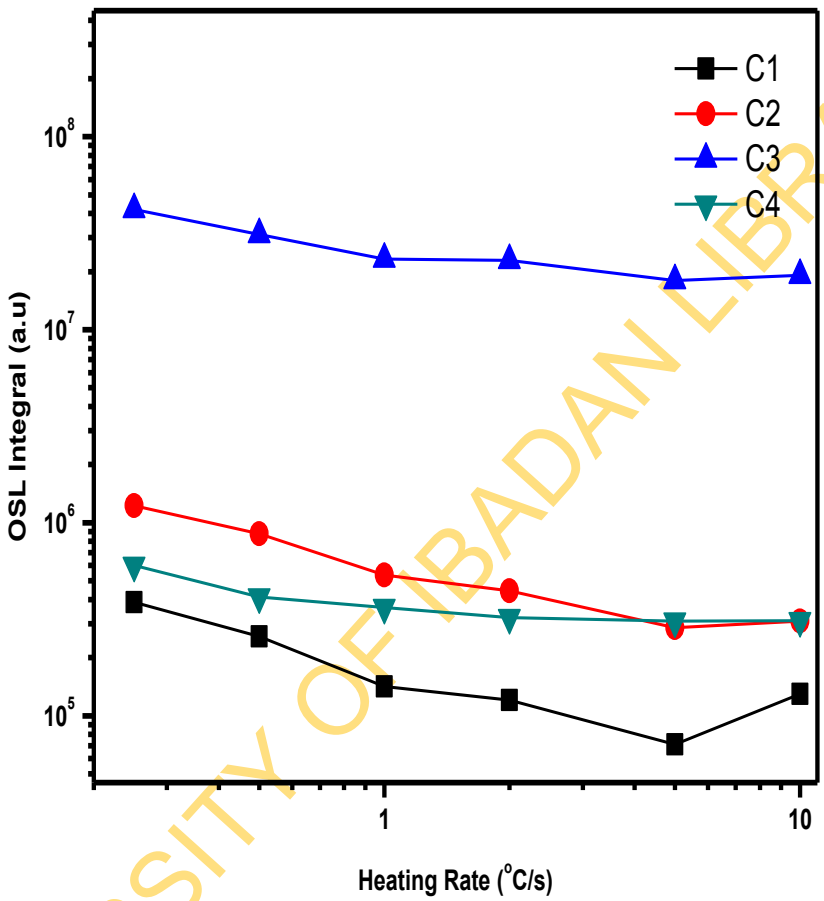

Fig. 4.32. Plots of 4th sensitised of RT-LMOSL components sensitisations against heating rates as function of cycle of measurements for unannealed S4 samples.

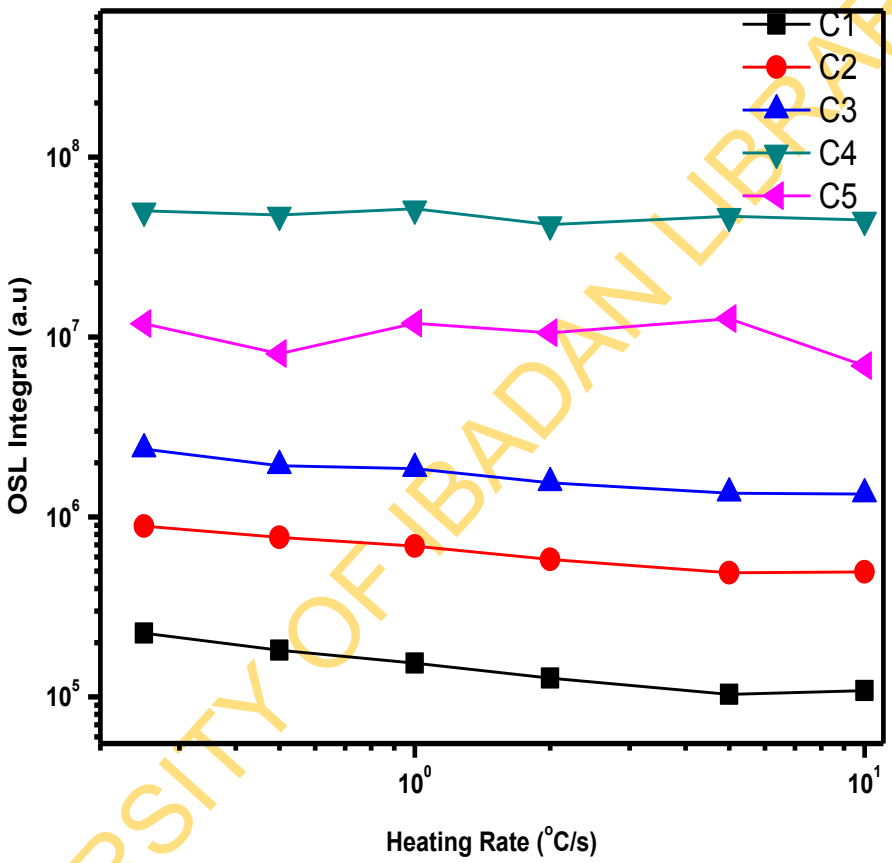

Fig. 4.33. Plots of 4th sensitised of RT-LMOSL components sensitisations against heating rates as function of cycle of measurements for annealed S2 samples.

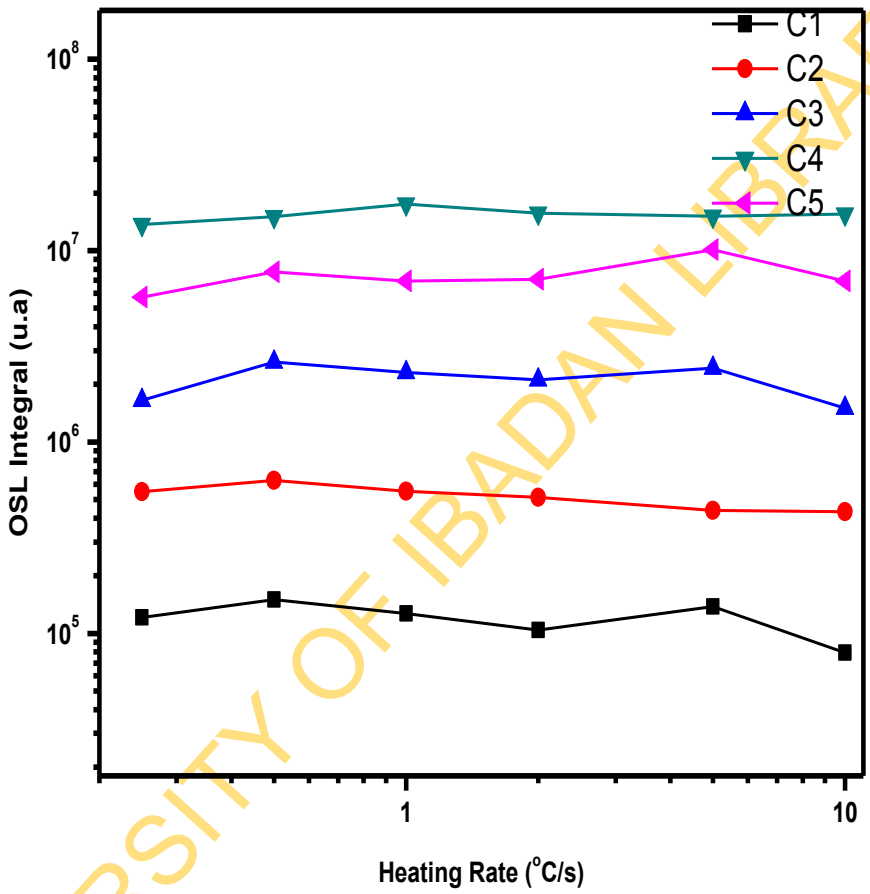

Fig. 4.34. Plots of 4th sensitised of RT-LMOSL components sensitisations against heating rates as function of cycle of measurements for annealed S4 samples.

heating rates of thermal activation in the unannealed samples is more prominent in the fast components, then followed by C3 and less pronounced in C4. While for annealed samples, similar dependence of the sensitisation of all the components on heating rates of thermal activation was observed. However, C4 and C5 of S4 annealed sample did not show note worthy dependence on heating rates of thermal activation.

4.2.4 Dependence of 110^{o}C TL peak and RT LM-OSL sensitisations on TL activation histories

Identification of the exclusive contributions of pre-exposure of quartz sample to a dose of irradiation and the purely thermal activation by way of experiment was one of the major objectives that motivated this work. There are some underlying principles behind each step of the protocol in attempts to separate the contributions of each of the two factors stated above. Although, the same dose of irradiation was maintained in the measurements irrespective of the protocol parts, however, pre-exposure dose (accumulated dose) was varied with the successive cycle of measurements and irradiations. The comparative sensitisations of the various parts of the protocol with respect to heating rate for both unannealed and annealed S2 and S4 samples are presented in Figures 4.35 to. 4.42. In particular, by looking at TL section of the protocol, the key difference between parts A and B of the protocol is the presence of intermediate irradiations that are sandwiched in between the successive cycles of thermal activation in part A that were absent in Part B. Also, the exact differentiation exits respectively between parts C and D that were meant for OSL of the protocol.

Contrarily to what is exhibited in the unannealed samples, a relative higher enhancement in sensitisations of parts A and C over parts B and D respectively was expected based on pre-dose model. This is because the accumulated pre-exposure dose of parts A and C were more than that of parts B and D correspondingly. The two annealed samples excellently displayed this as could be seen in Figures 4.35 to. 4.42. Contrarily, curve S_{n4} do not exhibit any clear sensitisation enhancement over curve S_{n1b} for both TL and RT LMOSL in unannealed samples. The contribution of thermal sensitisation is also reflected in curve S_{n1b} with respect to curve S_{n1} for both TL and RT-LMOSL. The former curve is quantitatively higher than the later.

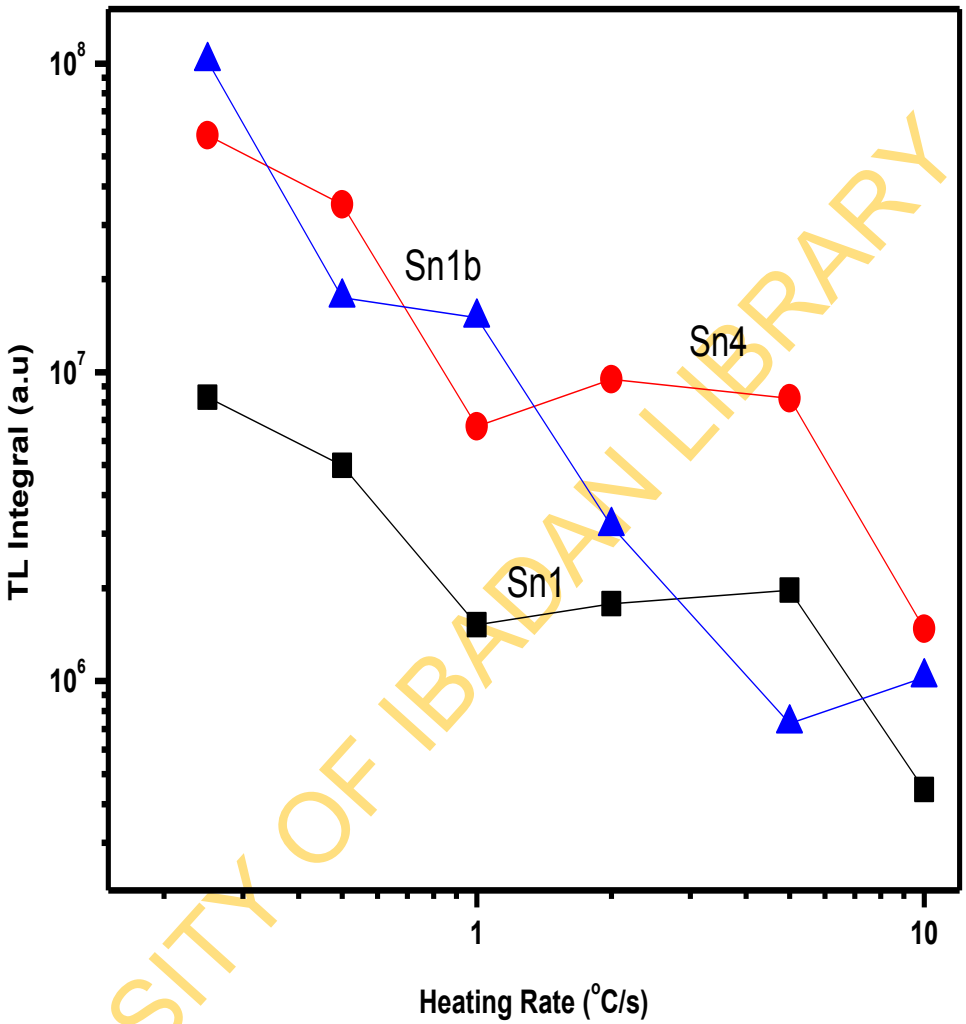

Fig. 4.35: Comparison of TL sensitisations in aliquots with pre-exposure dose and those with thermal activation against heating rates for unannealed S2 sample. Curves S_{n1} and S_{n4} are respectively 1st and 4th sensitisation of successive cycles with pre-exposure dose. S_{n1b} is the last sensitisation of successive cycles without pre-exposure dose.

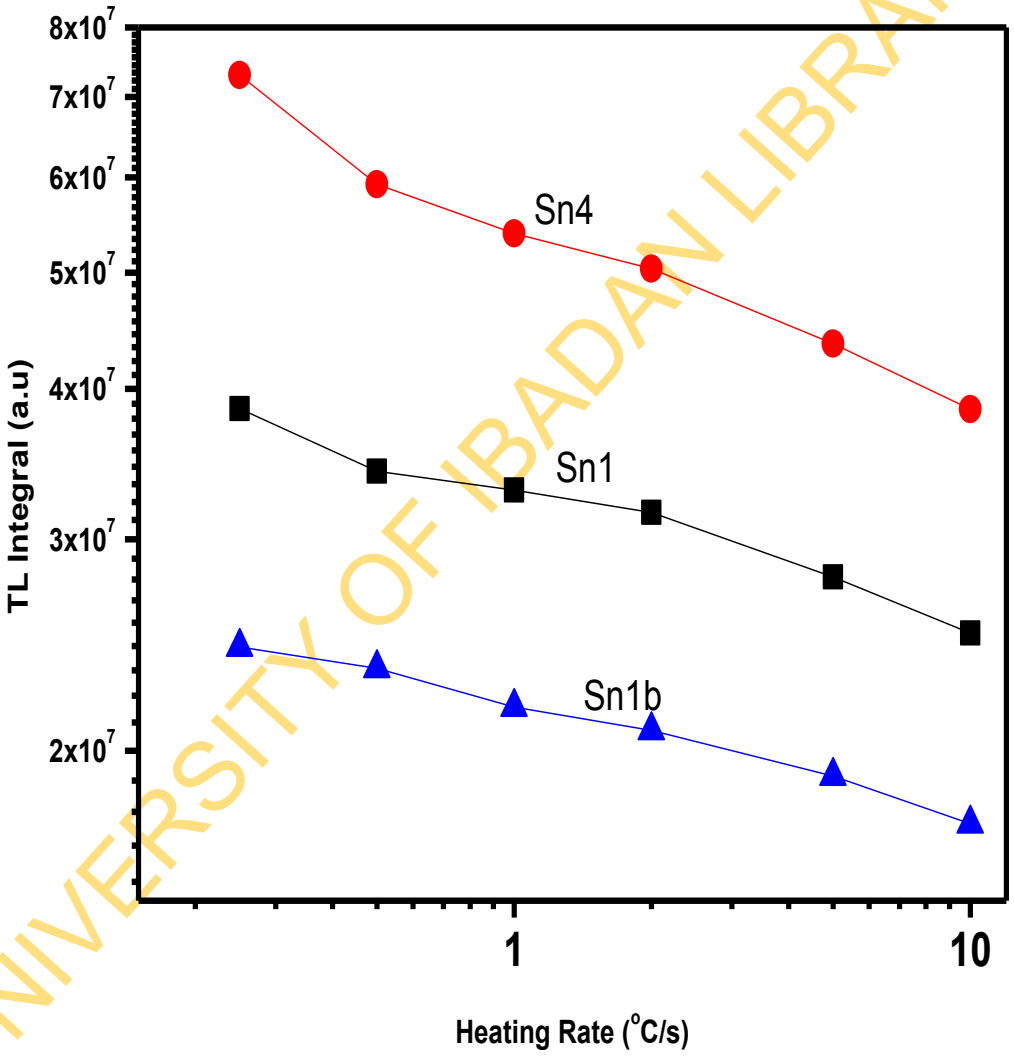

Fig.4.36. Comparison of TL sensitisations in aliquots with pre-exposure dose and those with thermal activation against heating rates for annealed S2 sample. Curves S_{n1} and S_{n4} are respectively 1st and 4th sensitisation of successive cycles with pre-exposure dose. S_{n1b} is the last sensitisation of successive cycles without pre-exposure dose.

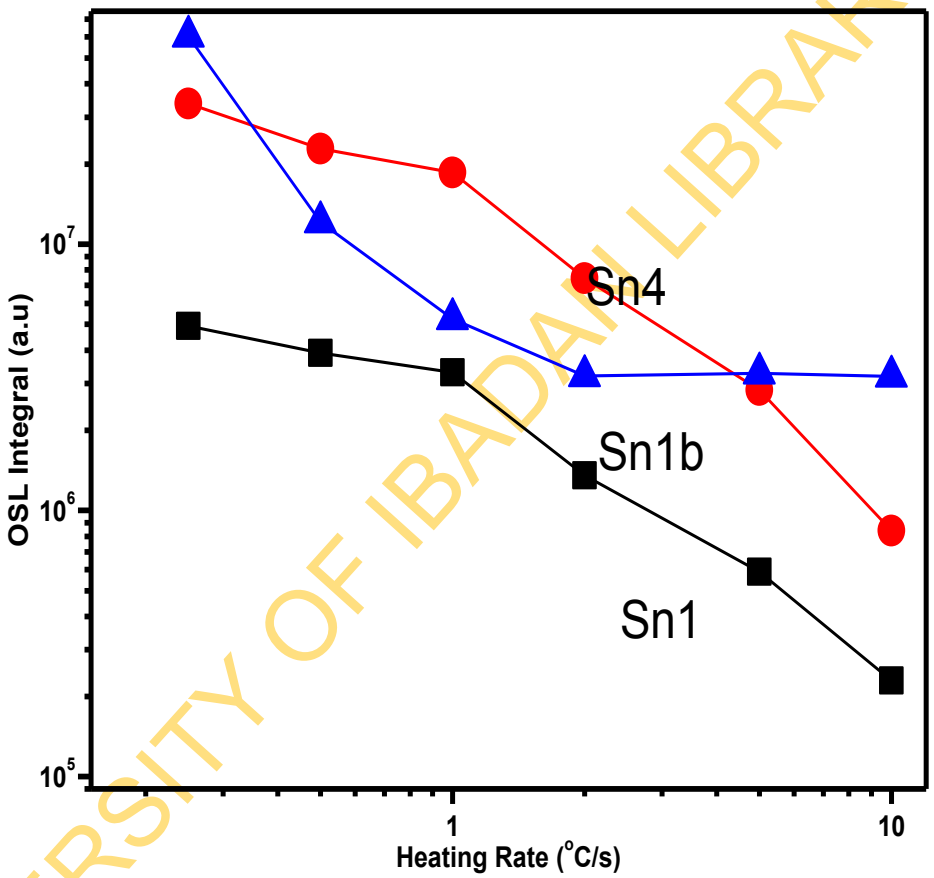

Fig.4.37. Comparison of RT-LMOSL sensitisations in aliquots with pre-exposure dose and those with thermal activation against heating rates for unannealed S2 sample. Curves S_{n1} and S_{n4} are respectively 1st and 4th sensitisation of successive cycles with pre-exposure dose. S_{n1b} is the last sensitisation of successive cycles without pre-exposure dose.

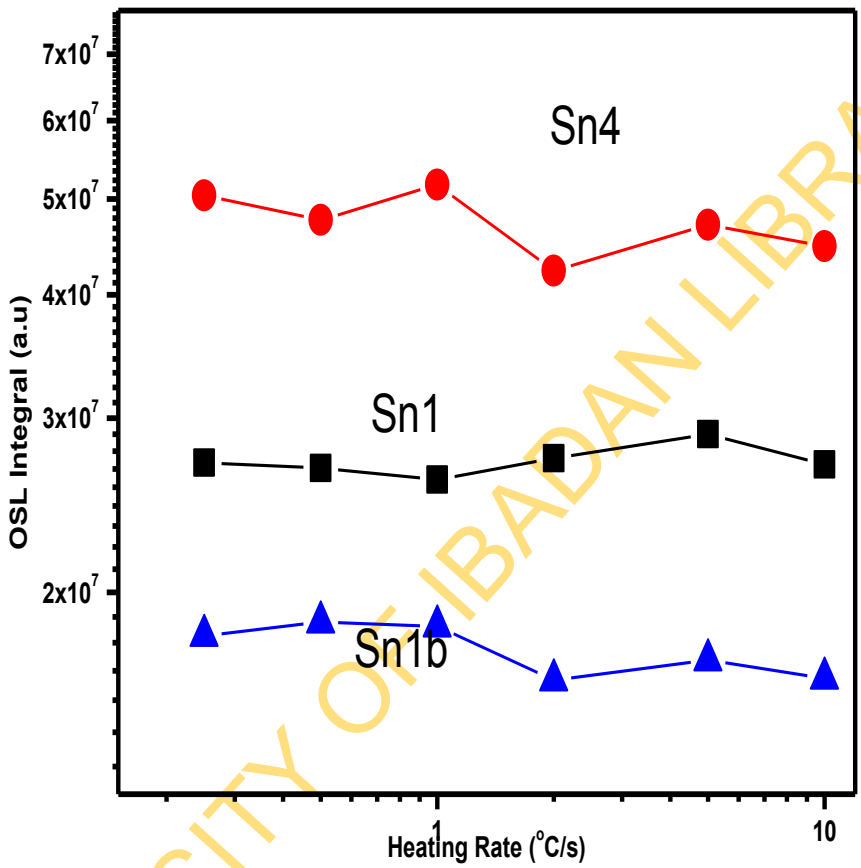

Fig.4.38. Comparison of RT-LMOSL sensitisations in aliquots with pre-exposure dose and those with thermal activation against heating rates for annealed S2 sample. Curves S_{n1} and S_{n4} are respectively 1st and 4th sensitisation of successive cycles with pre-exposure dose. S_{n1b} is the last sensitisation of successive cycles without pre-exposure dose.

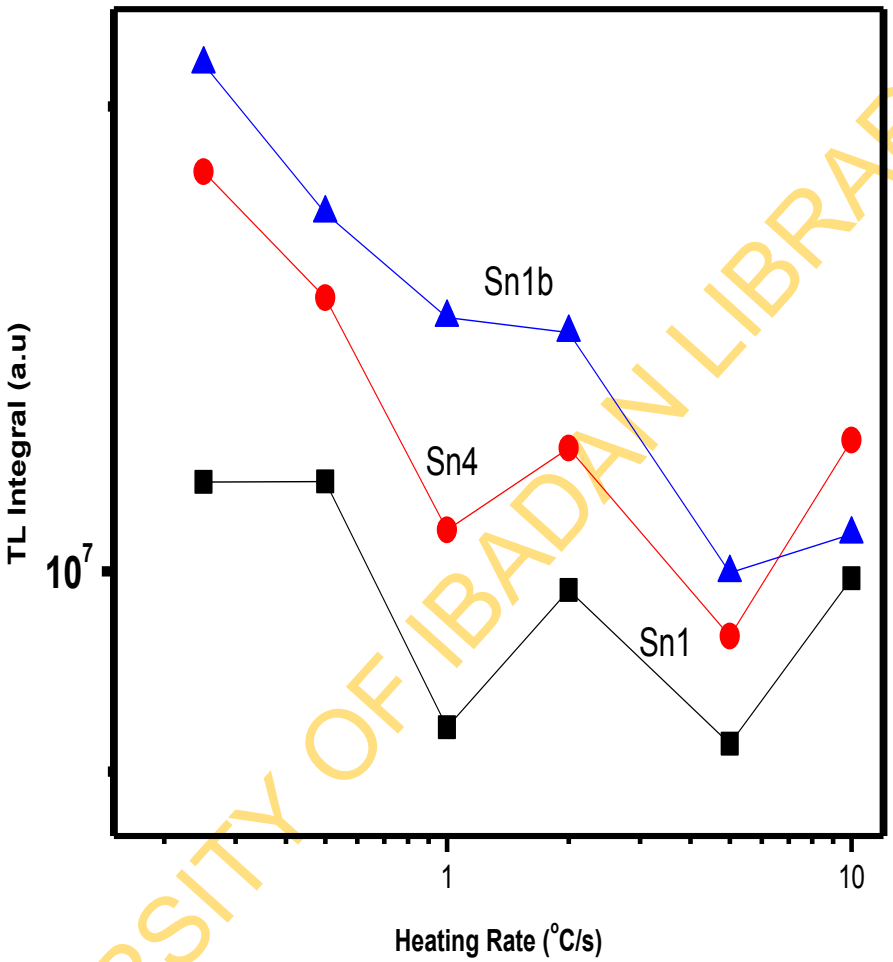

Fig.4.39. Comparison of TL sensitisations in aliquots with pre-exposure dose and those with thermal activation against heating rates for unannealed S4 sample. Curves S_{n1} and S_{n4} are respectively 1st and 4th sensitisation of successive cycles with pre-exposure dose. S_{n1b} is the last sensitisation of successive cycles without pre-exposure dose

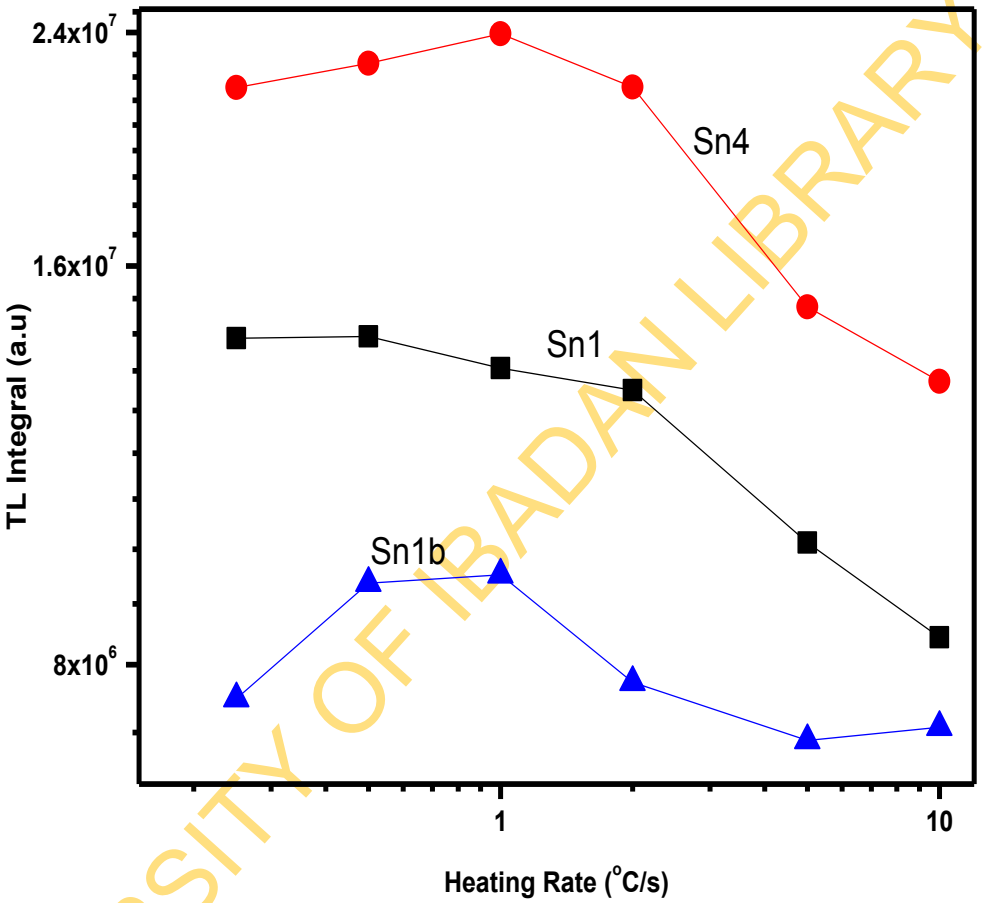

Fig.4.40. Comparison of TL sensitisations in aliquots with pre-exposure dose and those with thermal activation against heating rates for annealed S4 sample. Curves S_{n1} and S_{n4} are respectively 1st and 4th sensitisation of successive cycles with pre-exposure dose. S_{n1b} is the last sensitisation of successive cycles without pre-exposure dose.

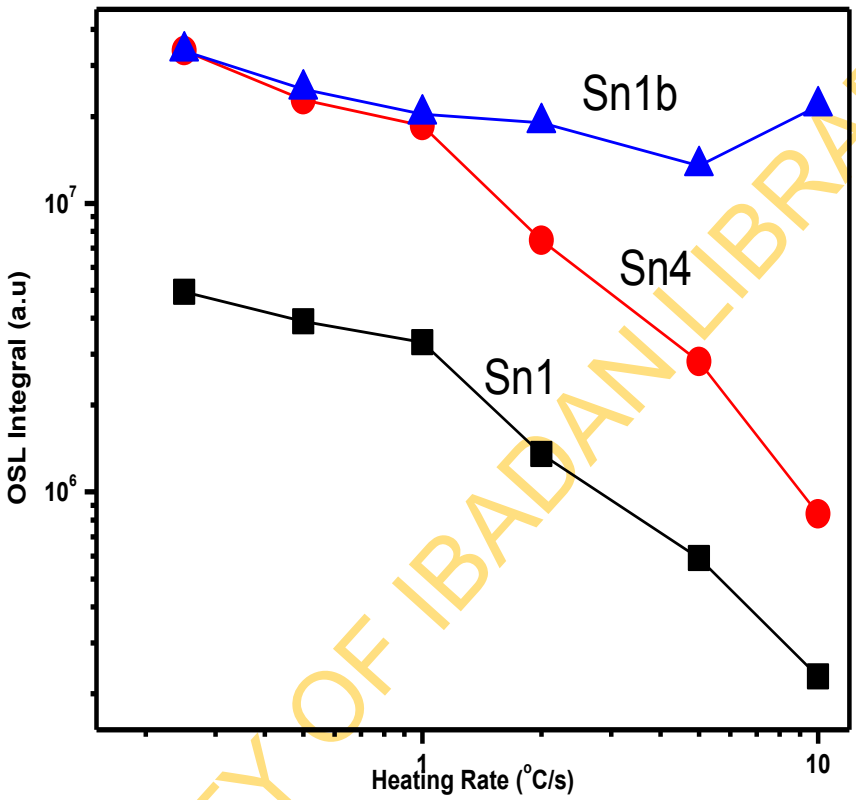

Fig. 4.41. Comparison of RT-LMOSL sensitisations in aliquots with pre-exposure dose and those with thermal activation against heating rates for unannealed S4 sample. Curves S_{n1} and S_{n4} are respectively 1st and 4th sensitisation of successive cycles with pre-exposure dose. S_{n1b} is the last sensitisation of successive cycles without pre-exposure dose.

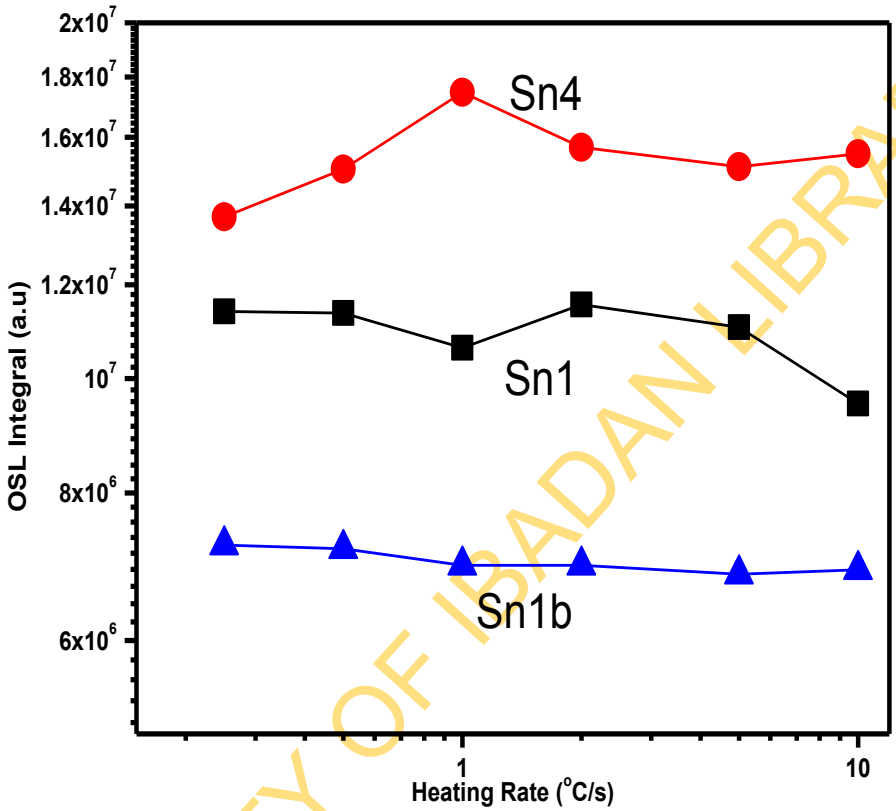

Fig. 4.42. Comparison of RT-LMOSL sensitisations in aliquots with pre-exposure dose and those with thermal activation against heating rates for annealed S4 sample. Curves S_{n1} and S_{n4} are respectively 1st and 4th sensitisation of successive cycles with pre-exposure dose. S_{n1b} is the last sensitisation of successive cycles without pre-exposure dose.

In order to identify the comparative sensitisations resulting from accumulative successive TL readings and irradiations that each of the aliquots has been subjected to, Part A steps 6 and 7 and Part B step 7 and 8 of the protocol were investigated on each of the aliquots. It should be recalled that steps 7 and 8 respectively in parts A and B of the protocols were read at heating rate of 2^{o}C/s for all the aliquots. Curves S_{n5} and S_{n2b} in Figures 4.43 to 4.44 resulted from these measurements for parts A and B of the protocol respectively. Virtually identical trend were exhibited by curves S_{n4} and S_{n1b} as compared with S_{n5} and S_{n2b} correspondingly.

4.2.5 Discussion

The possible reasons behind the unexpected inconsistencies that were observed in the sensitisation dependence of both TL and RT-LMOSL on heating rates of thermal activation are presented below. The sensitisation reproducibility study of the two samples that were presented in section 4.1, were in line with the recently report that quartz aliquots from the same crystal failed to possess sensitisation reproducibility Appendix 1). The observations of the referred were based on 10 different quartz samples that happened to include the present two understudied quartz samples. It was further observed also that this strong variation is removed by high temperature annealing as well as heating up to 500^{o}C, involved in the TL measurements. Therefore, since multiple aliquots were used in the present work, the individual sensitisation of each aliquot is believed to be the major influence behind the alteration in the sensitisation pattern of the TL with respect to heating rates that was observed.

The structure of curve S_{n0} of TL for both unannealed and annealed two samples exhibits a satisfactory trend of sensitisation on heating rate as depicted in Figures 4.23, 4.25, 4.27 and 4.29. With reference to the protocols, it should be born in mind that there was no thermal activation, at all, before TL of Step 4 (part A protocol) that produced curve S_{n0}. The TL reading of Step 2 that preceded curve S_{n0} was only to 180^{o}C which is below thermal activation temperature. Thus, the absence of contribution of thermal activation, which is prone to sensitisation non-reproducibility, in curve S_{n0} is the reason why there is consistency with heating rates in this particular curve for TL part. This adequately revealed the inconsistency that sensitisation non-reproducibility of the multiple aliquots introduced into the sensitisation of curves S_{n1}-S_{n4} that are read after curve S_{n0} which served as thermal activation.

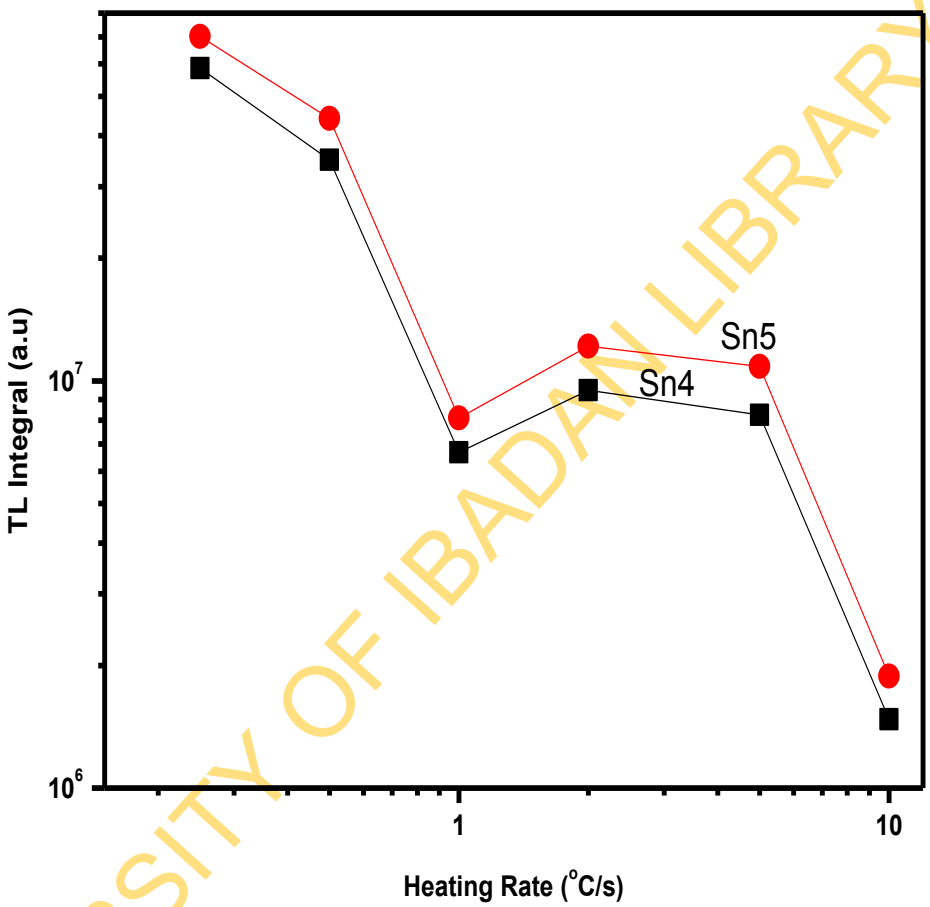

Fig. 4.43: Comparison of 110^{o}C TL peak sensitisations resulting from measurement histories in aliquots with pre-exposure dose for unannealed S2 sample. Curves S_{n4} and S_{n5} are respectively 4th and 5th sensitisations of successive cycles. It should be recalled that S_{n5} was read at HR of 2^{o}C/s

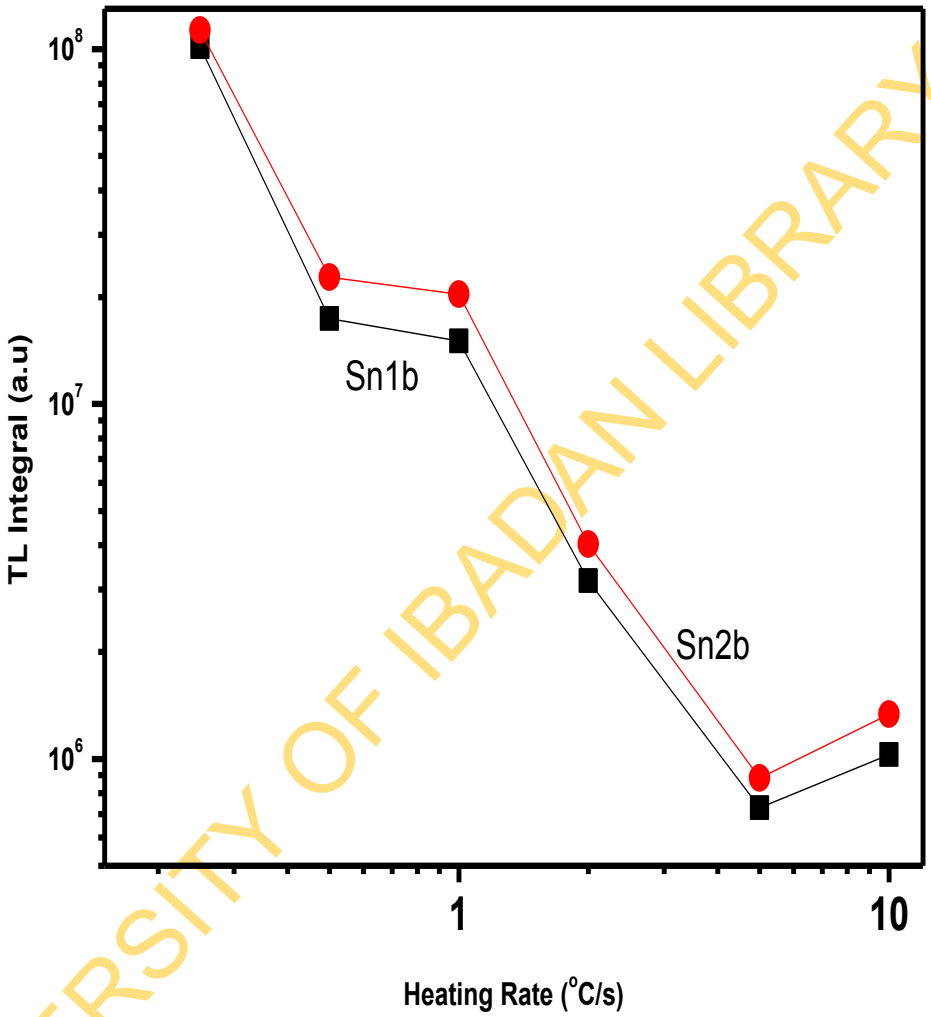

Fig. 4.44: Comparison of 110^{o}C TL peak sensitisations resulting from measurement histories in aliquots without pre-exposure dose for unannealed S2 sample. Curves S_{n1b} and S_{n2b} are respectively the 4th and 5th sensitisation of successive cycles. It should be recalled that S_{n2b} was read at HR of 2^{o}C/s

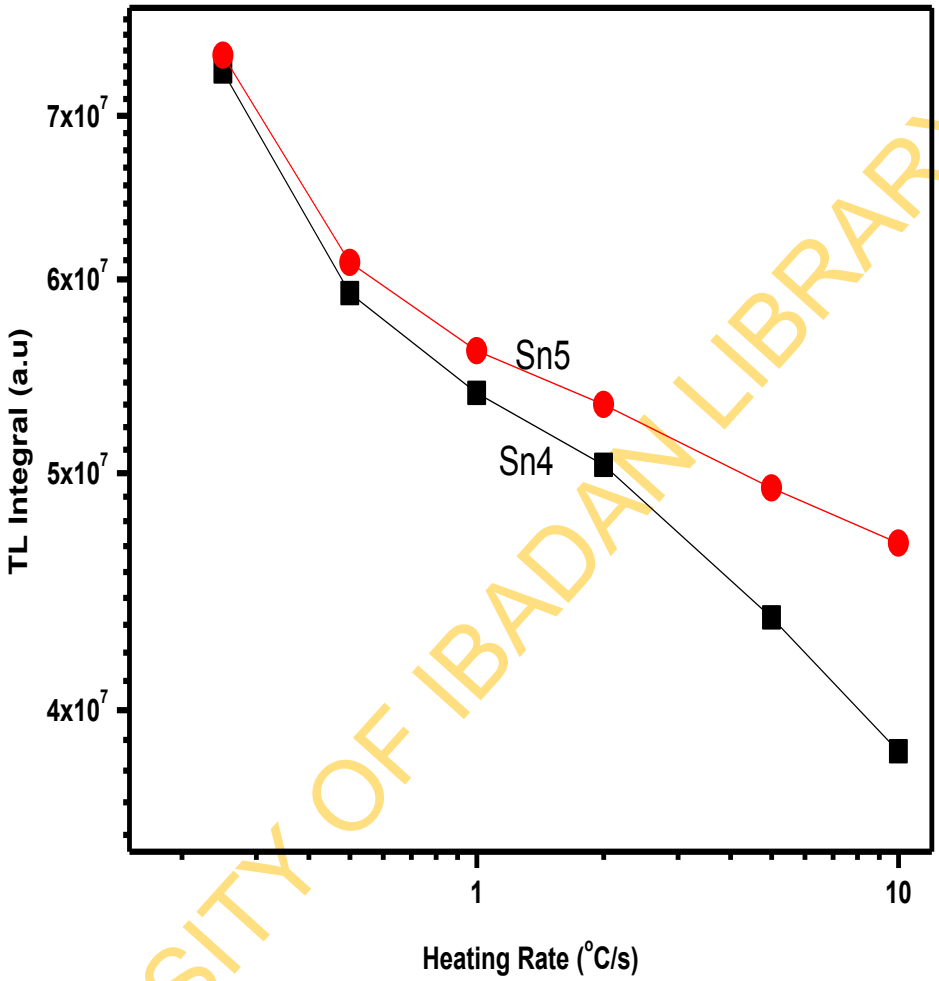

Fig. 4.45: Comparison of 110°C TL peak sensitisations resulting from measurement histories in aliquots with pre-exposure dose for annealed S2 sample. Curves S_{n4} and S_{n5} are respectively 4th and 5th sensitisations of successive cycles. It should be recalled that S_{n5} was read at HR of 2°C/s

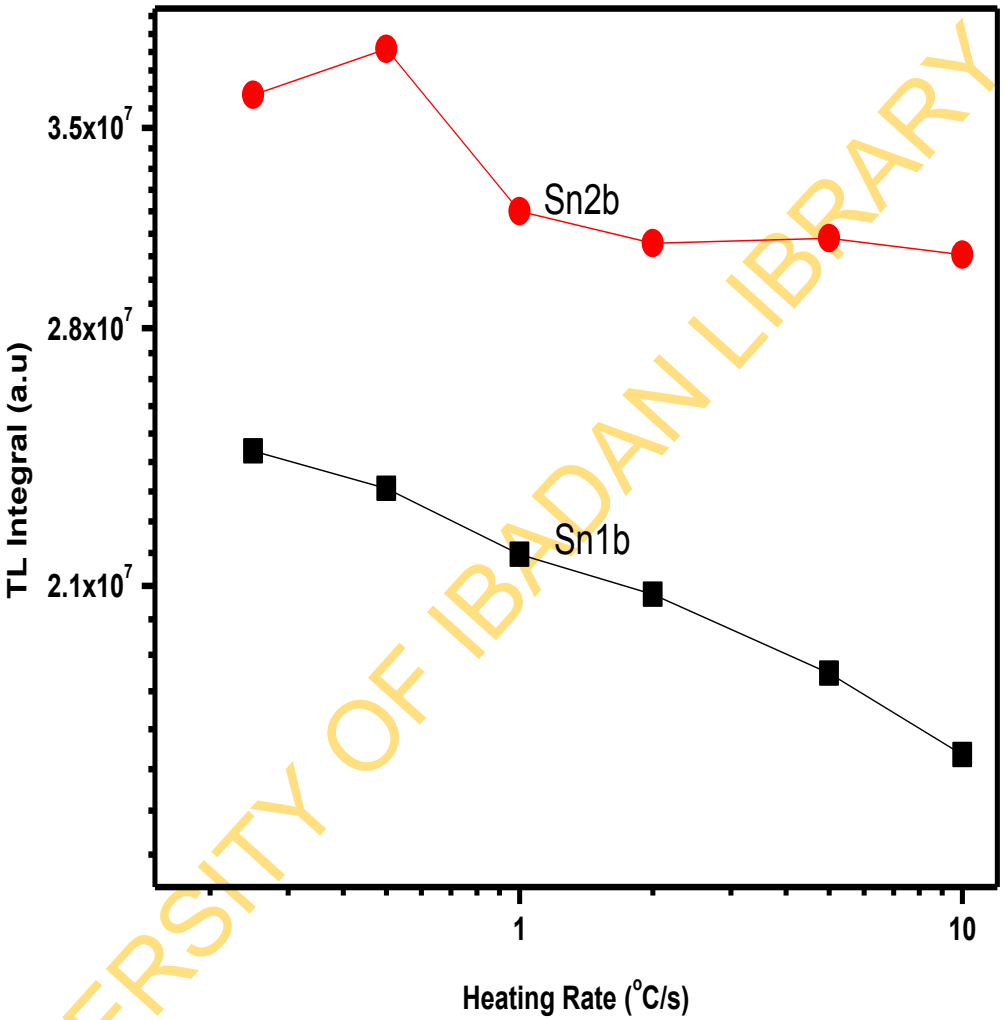

Fig. 4.46: Comparison of 110°C TL peak sensitisations resulting from measurement histories in aliquots without pre-exposure dose for annealed S2 sample. Curves S_{n1b} and S_{n2b} are respectively the 4th and 5th sensitisation of successive cycles. It should be recalled that S_{n2b} was read at HR of 2°C/s

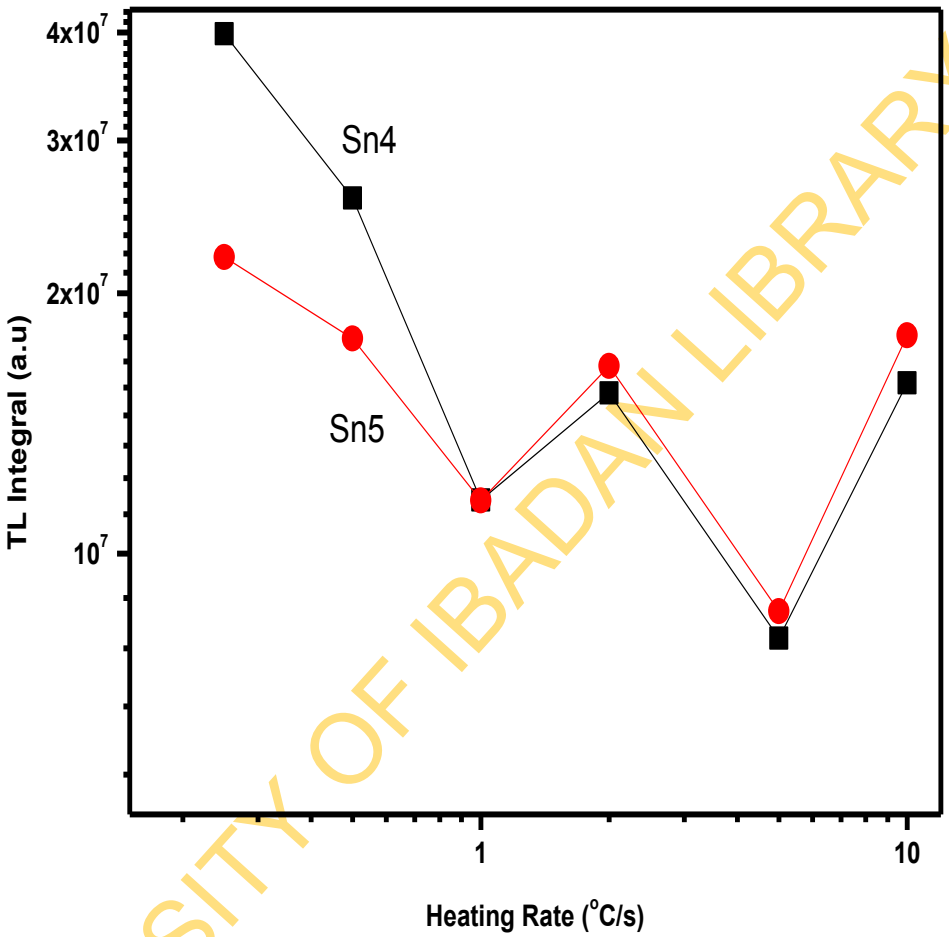

Fig. 4.47. Comparison of 110°C TL peak sensitisations resulting from measurement histories in aliquots with pre-exposure dose for unannealed S4 sample. Curves S_{n4} and S_{n5} are respectively 4th and 5th sensitisations of successive cycles. It should be recalled that S_{n5} was read at HR of 2°C/s

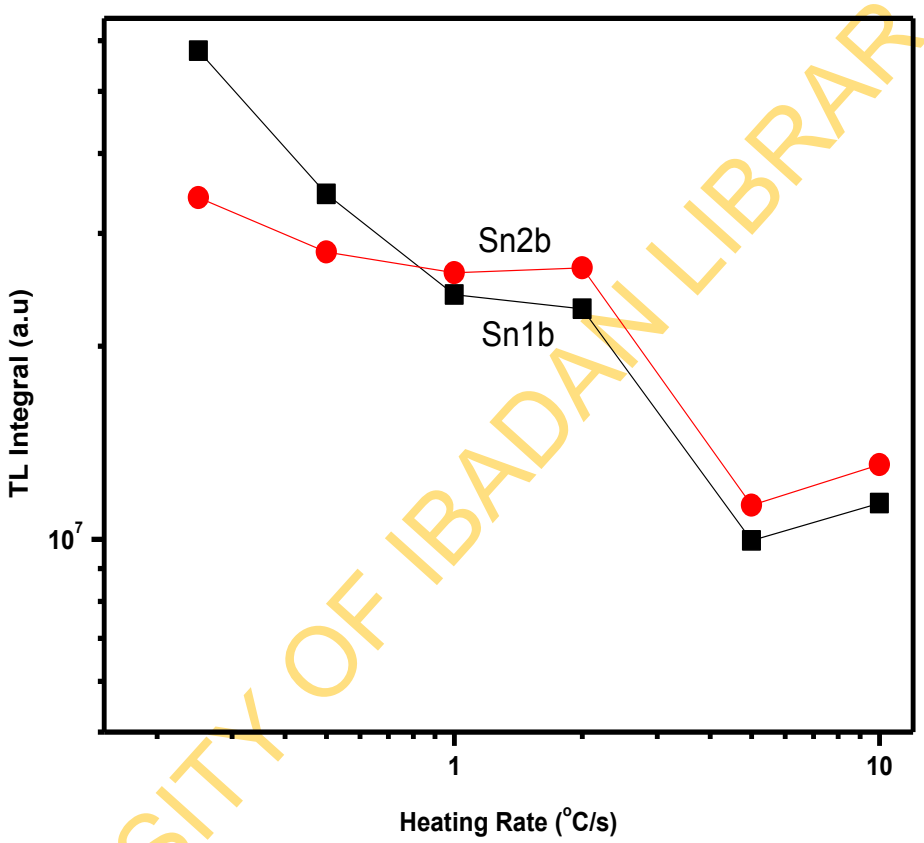

Fig. 4.48: Comparison of 110°C TL peak sensitisations resulting from measurement histories in aliquots without pre-exposure dose for unannealed S4 sample. Curves S_{n1b} and S_{n2b} are respectively the 4th and 5th sensitisation of successive cycles. It should be recalled that S_{n2b} was read at HR of 2°C/s

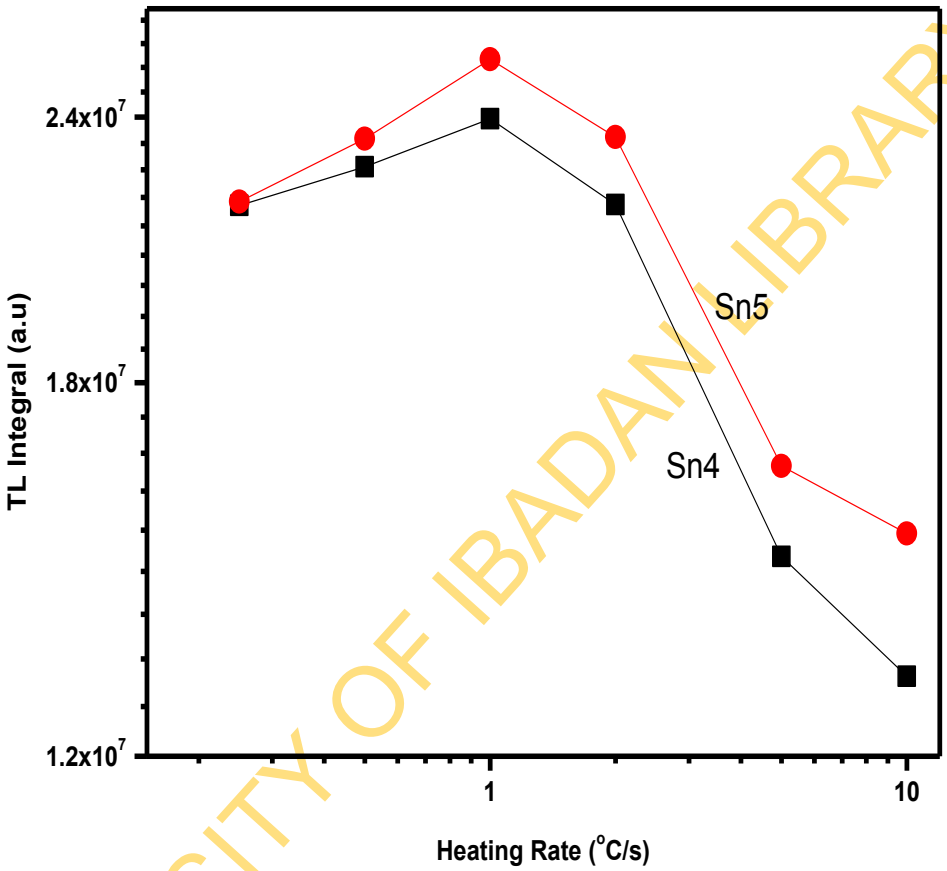

Fig. 4.49: Comparison of 110°C TL peak sensitisations resulting from measurement histories in aliquots with pre-exposure dose for annealed S4 sample. Curves S_{n4} and S_{n5} are respectively 4th and 5th sensitisations of successive cycles. It should be recalled that S_{n5} was read at HR of 2°C/s

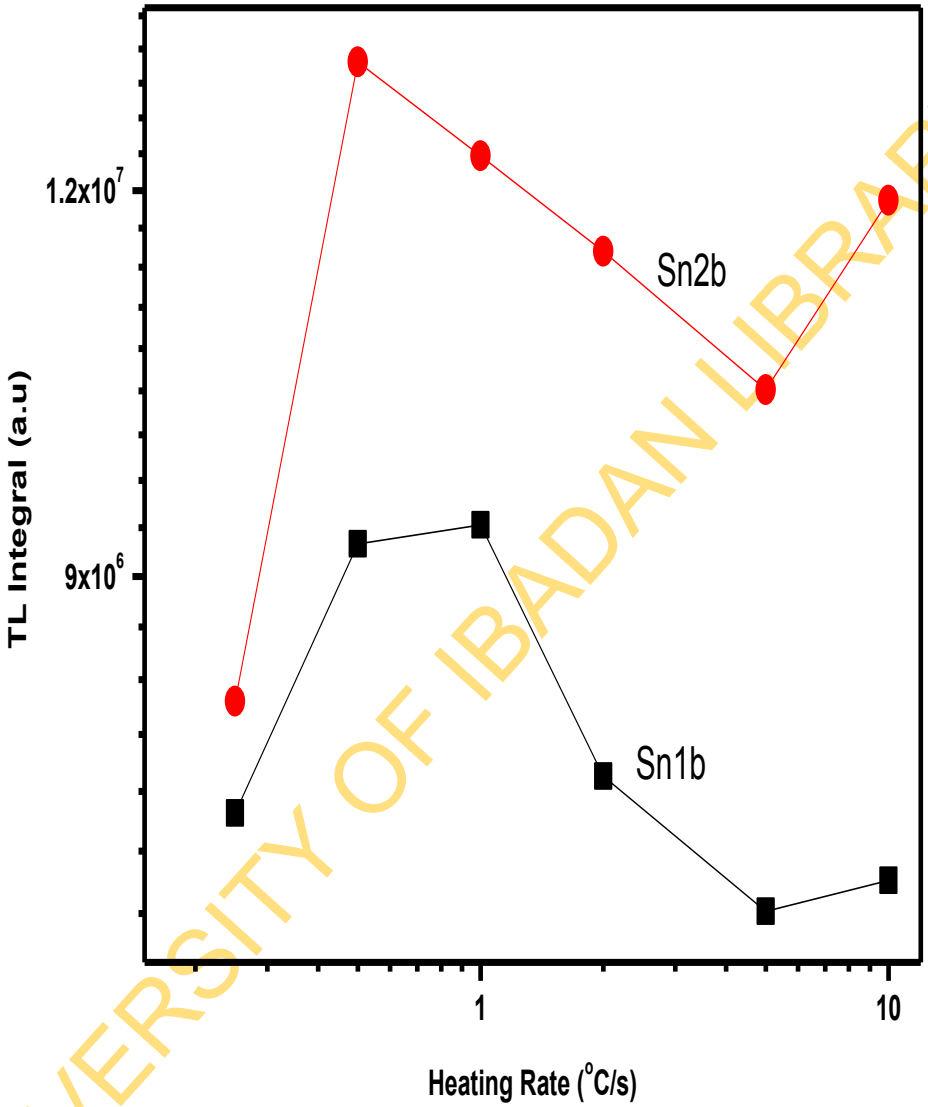

Fig. 4.50: Comparison of 110°C TL peak sensitisations resulting from measurement histories in aliquots without pre-exposure dose for annealed S4 sample. Curves S_{n1b} and S_{n2b} are respectively the 4th and 5th sensitisation of successive cycles. It should be recalled that S_{n2b} was read at HR of 2°C/s

In addition, the sensitisation curves of Figures 4.25 and 4.26 for annealed sample satisfactorily demonstrate the dependence of sensitisation on heating rate that is envisaged. Hence, the curves of figure for annealed S2 demonstrate the true picture of the dependency of sensitisation on heating rate since the level of sensitisation non-reproducibility in annealed samples have been observed to be generally insignificant (Appendix 1).

It was consequently anticipated that normalization of each curve of Figures 4.23 to 4.30 for S2 and S4 unannealed samples to the first sensitised curve, S_{n1}, rather than S_{n0} should present the true dependence of sensitisation on heating rate. The outcome of this normalization is presented in Figures 4.51 and 4.52 that are the true sensitisation dependence on heating rate in which the sensitisation inconsistency has satisfactorily disappeared for the two unannealed samples. The only point where this trend is not observed is after 5^{o}C/s in S4 samples which seems to possess relatively less sensitisation feature as compared with S2.

As it was afore mentioned under observations, it is apparent on the average that there was no special sensitisation contribution made by accumulated pre-exposure dose in parts A and C (curve S_{n4}) over parts B and D (curve S_{n1b}) of both TL and RT-LMOSL in unannealed samples (see Figures 4.35, 4.37, 4.39 and 4.41). It should be recalled that S_{n4} and S_{n1} respectively received accumulated pre-exposure dose that are by factors of 3 and 1 TD higher than the one received by S_{n1b} for both TL and RT LMOSL. In the same way, S_{n4} and S_{n1b} received the similar successive cycles of TA that is factor of 3 higher than the one received by S_{n1}. According to the pre-dose model, sensitisation of S_{n4} was expected to be higher than that of S_{n1b}. Although, sensitisation non-reproducibility that is more pronounced in unannealed sample has certainly contributed to the obvious demarcation of curve S_{n4} sensitisation with respect to curve S_{n1b} that is missing in unannealed samples for both TL and RT-LMOSL. Nevertheless, it can be seen from Figures 4.35, 4.37, 4.39 and 4.41 that

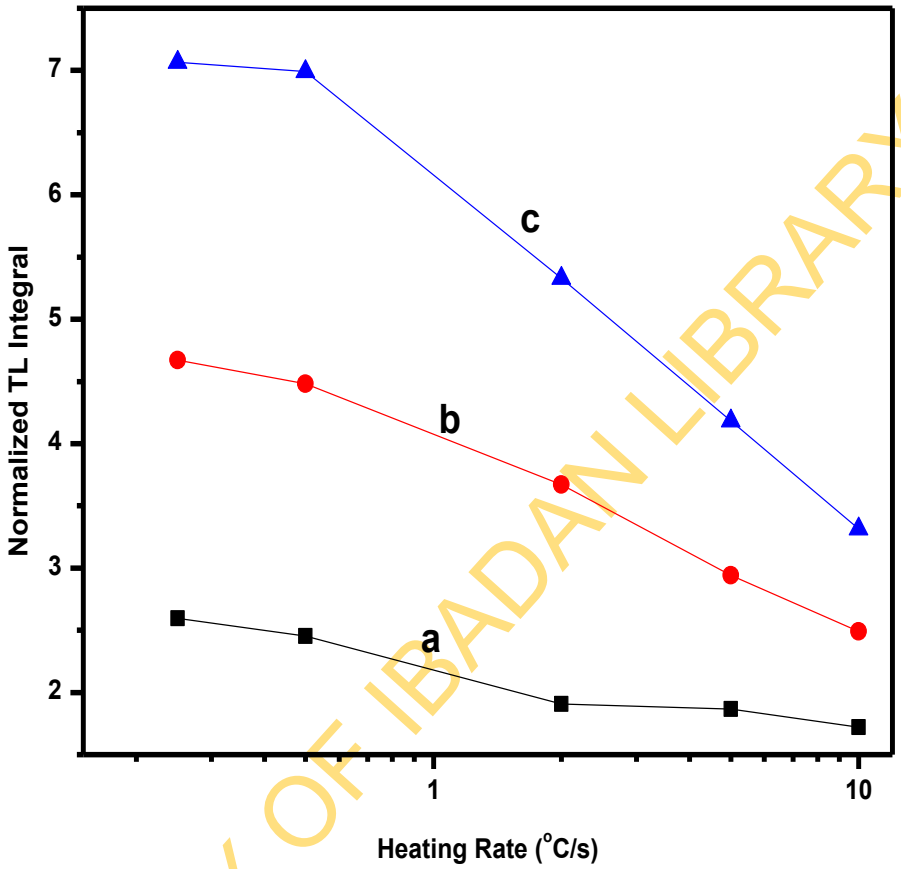

Fig. 4.51. Plots of normalized 110°C TL peak sensitisations against heating rates as function of cycle of measurements for unannealed S2. (a) S_{n2}/S_{n1}, (b) S_{n3}/S_{n1}, (c) S_{n4}/S_{n1} with S_{n1}, S_{n2}, S_{n3}, S_{n4} representing 1st sensitised, 2nd sensitised, 3rd sensitised, 4th sensitised, luminescence readings respectively

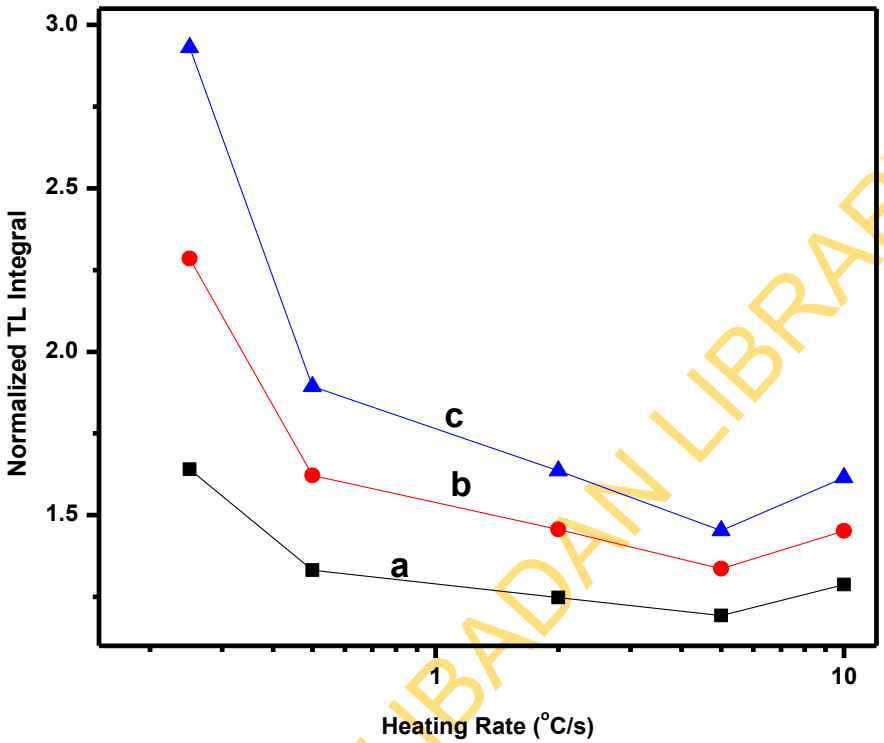

Fig. 4.52. Plots of normalized 110°C TL peak sensitisations against heating rates as function of cycle of measurements for unannealed S4. (a) S_{n2}/S_{n1}, (b) S_{n3}/S_{n1}, (c) S_{n4}/S_{n1} with S_{n1}, S_{n2}, S_{n3}, S_{n4} representing 1st sensitised, 2nd sensitised, 3rd sensitised, 4th sensitised, luminescence readings respectively

curves S_{n4} and S_{n1b} overlap on the average. Even better still, S_{n1b} is always higher for all points of the heating rate 0.25^{o}C/s for the two samples. As presented in Table 4.3, the sensitisation signals at the highest thermal activation of the aliquots of unannealed samples without pre-exposure dose was higher than that of the aliquots with pre-exposure dose by factor of 76.0 % and 79.0 % for TL and RT-LMOSL respectively for S2 while the corresponding factors obtained for S4 were 45.0 % for TL and 14.0 % for RT-LMOSL. In annealed samples, the sensitisation signal of the aliquots with pre-exposure dose was rather higher than that of the aliquots without pre-exposure dose, by factor of 224.0 % for TL and 201.0 % for RT-LMOSL for S2 and for S4, it was by factor of 245.0 % for TL and 217.0 % for RT-LMOSL. The exact sensitisation trend as observed above are displayed by the fast components of S2 and S4 unannealed and annealed samples (Figures 4.53 to 4.56)

Yet, curve S_{n1b} is quantitatively higher than S_{n1} in Figures 4.35, 4.37, 4.39 and 4.41 for unannealed samples. Based on pre-exposure dose received, these observations were contrary to pre-dose model. Thus, the identical sensitisation that both S_{n4} and S_{n1b} share can only be explained on the ground of the similar level of thermal activation the two received as mentioned earlier. Equally, the degree of thermal activation of S_{n1b} that is above that of S_{n1} clarifies why higher sensitisation is in favour of S_{n1b}. The sensitisations of S2 and S4 annealed samples Figures 4.36, 4.38, 4.40 and 4.42 truly and satisfactorily obey pre-dose model in its case contrarily to the case of unannealed samples. Therefore, the inference that could be drawn from these is that contribution of thermal sensitisation and pre-exposure dose are opposite in unannealed and annealed samples. This means that thermal sensitisation is the key contribution of sensitisation in unannealed sample while pre-exposure dose played the chief role in annealed samples sensitisation.

A support to this conclusion is the dependence of the observed sensitisation on heating rates of thermal activation that is more pronounced in unannealed samples as compared with S2 and S4 corresponding annealed samples (Figures 4.23 to 4.30). This is because the dependence of sensitisation on heating rates of thermal activation has been associated with the pure thermal sensitisation (Koul et al., 2010). Although, a common activation temperature of 500^{o}C was used all through, it was the various heating rates that accounted for the different activation heating times. The TL

Table 4.3: Relative sensitisation factor of aliquots with pre-exposure dose and those without pre-exposure dose

Samples	TL		OSL	
	Sensitisation factor without PED for unannealed sample (%)	Sensitisation factor with PED for annealed sample (%)	Sensitisation factor without PED for unannealed sample (%)	Sensitisation factor with PED for annealed sample (%)
S2	76.0	224.0	79.0	201.0
S4	45.0	245.0	14.0	217.0

Key: PED = pre-exposure dose

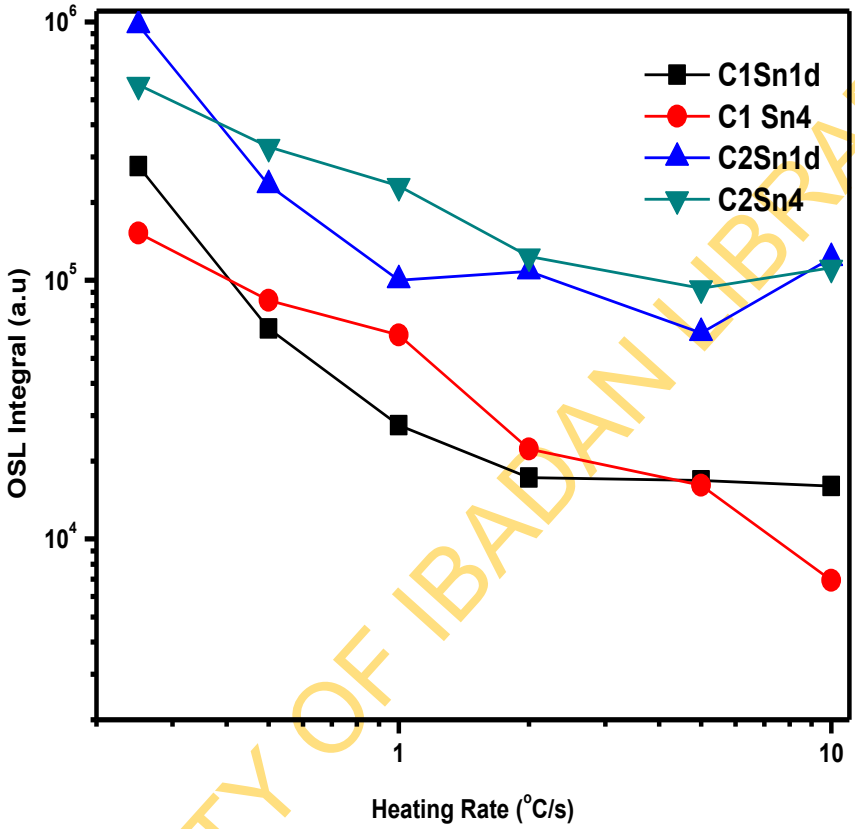

Fig.4.53: Comparison of RT-LMOSL sensitisations in aliquots with pre-exposure dose and those with thermal activation against heating rates for unannealed S2 sample. Curves $C1S_{n4}$ and $C2S_{n4}$ are respectively 4th sensitisation of successive cycles with pre-exposure dose for components C1 and C2 while C1S_{n1b} and C2S_{n1b} are respectively the last sensitisation of successive cycles without pre-exposure dose for components C1 and C2.

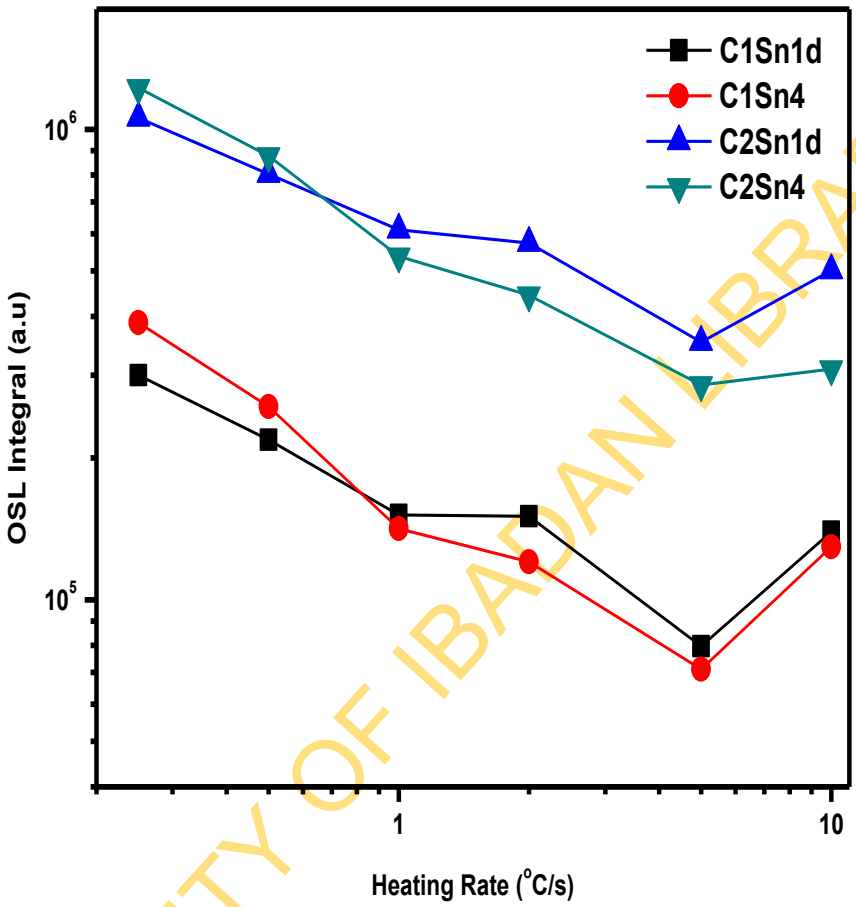

Fig. 4.54: Comparison of RT-LMOSL sensitisations in aliquots with pre-exposure dose and those with thermal activation against heating rates for unannealed S4 sample. Curves $C1S_{n4}$ and $C2S_{n4}$ are respectively 4th sensitisation of successive cycles with pre-exposure dose for components C1 and C2 while C1S_{n1b} and C2S_{n1b} are respectively the last sensitisation of successive cycles without pre-exposure dose for components C1 and C2.

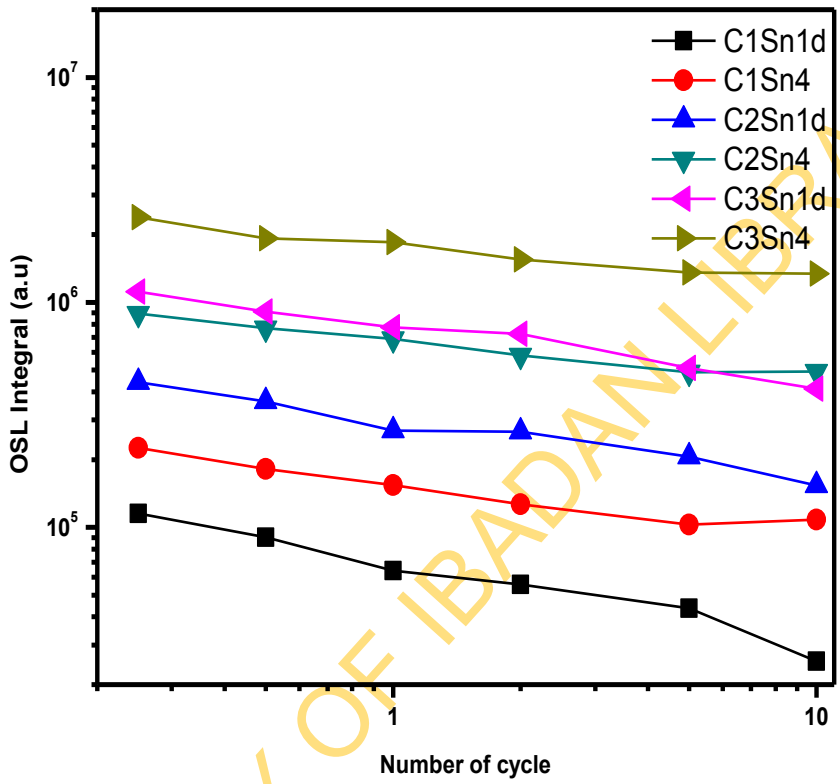

Fig. 4.55: Comparison of RT-LMOSL sensitisations in aliquots with pre-exposure dose and those with thermal activation against heating rates for annealed S2 sample. Curves $C1S_{n4}$, $C2S_{n4}$ and $C3S_{n4}$ are respectively 4th sensitisation of successive cycles with pre-exposure dose for components C1, C2 and C3 while C1S_{n1b}, C2S_{n1b} and C3S_{n1b} are respectively the last sensitisation of successive cycles without pre-exposure dose for components C1, C2 and C3.

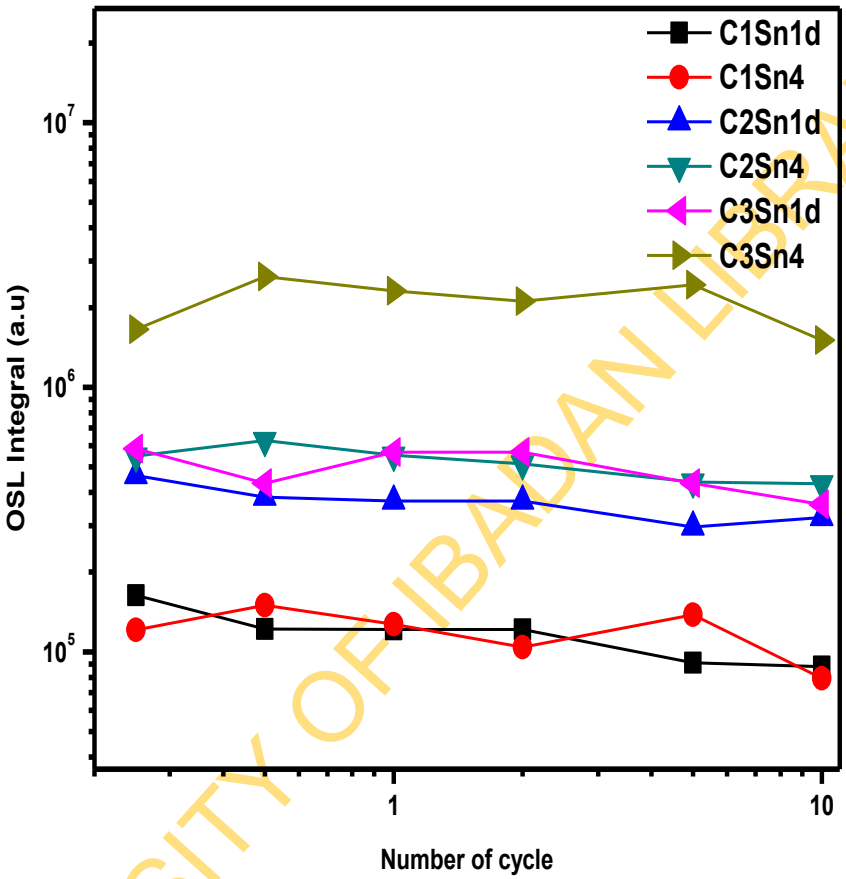

Fig. 4. 56: Comparison of RT-LMOSL sensitisations in aliquots with pre-exposure dose and those with thermal activation against heating rates for annealed S4 sample. Curves $C1S_{n4}$, $C2S_{n4}$ and $C3S_{n4}$ are respectively 4th sensitisation of successive cycles with pre-exposure dose for components C1, C2 and C3 while C1S_{n1b}, C2S_{n1b} and C3S_{n1b} are respectively the last sensitisation of successive cycles without pre-exposure dose for components C1, C2 and C3.

readings at 0.25 and 10^{o}C/s heating rates will result into 2000 and 50s heating time of the aliquots respectively. As indicated by this, an aliquot that was read out at 0.25^{o}C/s would have received heating of 40 times more than the one that was read at 10^{o}C/s heating rate. In real sense, sensitisation of S4 does not practically show any dependence on heating rates of thermal activation while slight dependence on heating rate can be seen in S2 in these figures for annealed samples.

Another argument, which supports this inference is an abrupt change on the sensitivity of all samples between the first (Sn0) and the second (Sn1) TL and RT-LMOSL measurement that is a clear product of pre-dose sensitisation effect (Oniya et al., 2012b). In this same vain, this abruption of sensitisation was more conspicuous in S2 and S4 annealed samples than their unannealed counterpart (Figures 4.11 to 4.18). This was unnoticeable at all in S2 unannealed sample. These observations hereby identify and present distinctive factor that is mostly responsible for sensitisation of each of unannealed and annealed samples of quartz.

The enormous increase in the percentage emission from 1.64 and 1.65% of C4 respectively in S2 and S4 unannealed samples to 45.14 and 44.46% of C5 of their annealed counterparts is informative (Table 4.2). Jain et al., 2003 reported a similar observation for a Korean sample where its OSL is dominated by slower components after annealing. More light is shed on the observations in question by matching each RT-LMOSL component with their corresponding glow peak in curve c Figures 4. 57 to 4. 60. These figures depict the “OSL glow curve” that is the difference between TL glow curve obtained before OSL measurement (Un-bleached TL) and the residual TL (Bleached TL) after OSL stimulation. As a result, Curve c in Figures 4. 57 and 4. 60 corresponds to the total signal of the whole RT-LMOSL emission recorded during the bleaching. Percentage signal of C3 and C4 respectively in unannealed and annealed samples, adequately and quantitatively commensurates with the signal of 110^{o}C TL glow peak in curve c. The same relationship is maintained between the fast components and 325^{o}C TL peak of curve c. But unlike what is observed in unannealed case, the percentage signals, 49.62 and 45.81%, of C4 in respective annealed S2 and S4 samples do not commensurate with those of 110^{o}C TL peaks (Table 4.2). Therefore, as the signal of 110^{o}C TL peak almost completely dominates the entire signal of the TL response, it can be inferred that the electron trap(s) that was

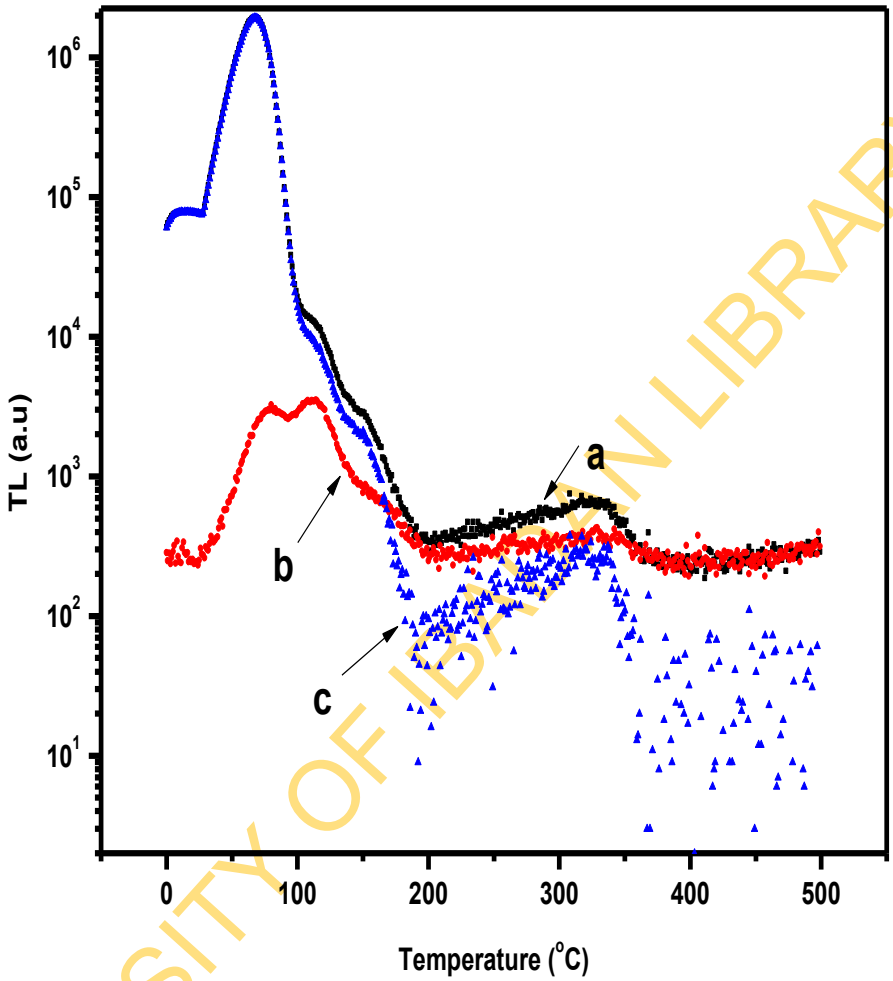

Fig. 4.57. For unannealed S2 represents glow curves (a) C4 (Un-bleached TL) obtained from step 5 of Part A, (b) bleached TL from step 5 of Part C and (c) the "OSL glow curve" which is the different between (a) and (b) .

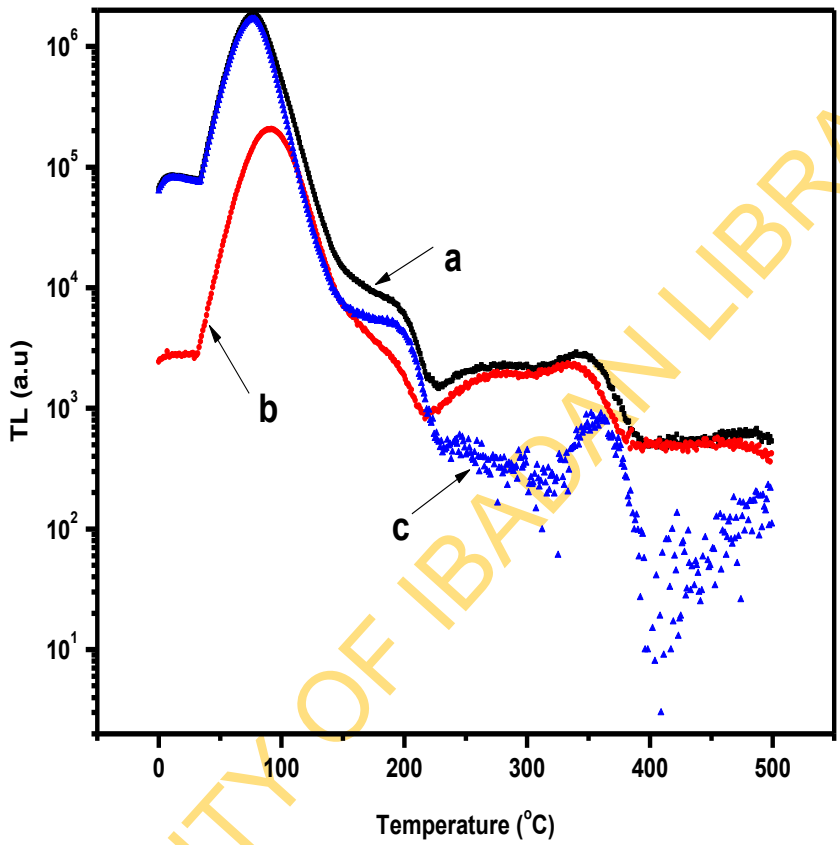

Fig. 4.58. For annealed S2 represents glow curves (a) C4 (Un-bleached TL) obtained from step 5 of Part A, (b) bleached TL from step 5 of Part C and (c) the "OSL glow curve" which is the different between (a) and (b) .

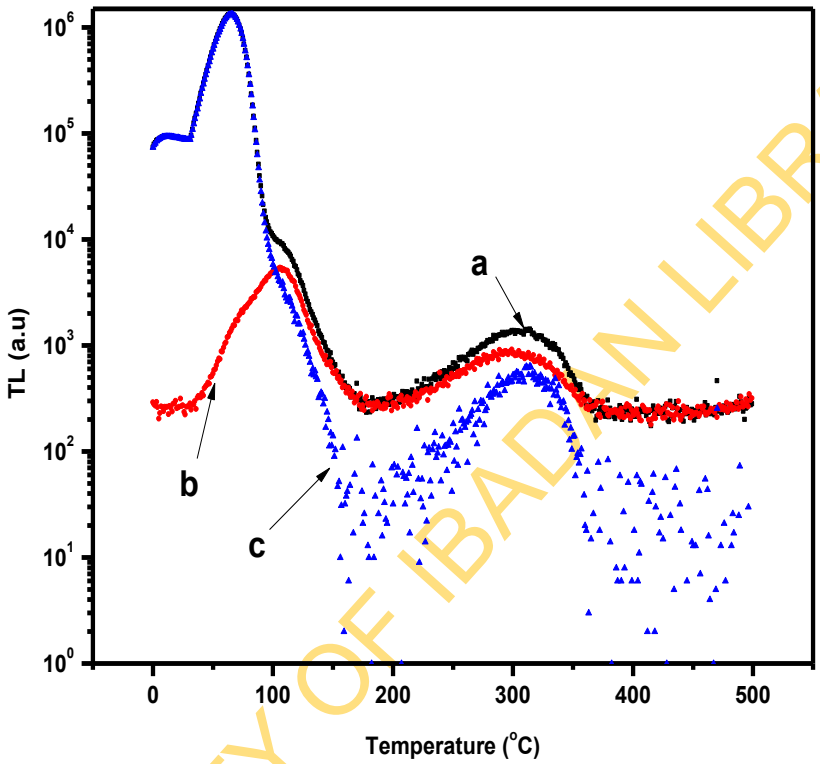

Fig. 4.59. For unannealed S4 represents glow curves (a) C4 (Un-bleached TL) obtained from step 5 of Part A, (b) bleached TL from step 5 of Part C and (c) the "OSL glow curve" which is the different between (a) and (b) .

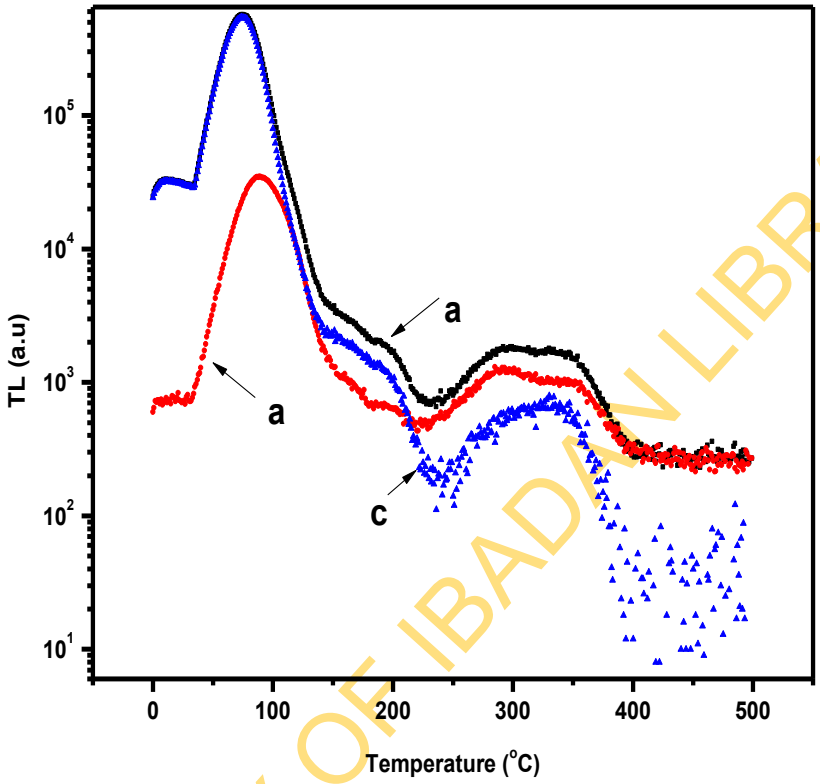

Fig. 4.60. For annealed S4 represents glow curves (a) C4 (Un-bleached TL) obtained from step 5 of Part A, (b) bleached TL from step 5 of Part C and (c) the "OSL glow curve" which is the different between (a) and (b) .

responsible for some of the components that make up the C5 in annealed sample is not depleted during the TL measurement. Hence this further confirmed that some of the components of C5 are associated with electron traps around 600^{o}C as earlier claimed. It could be proposed here that the trap responsible for the slower component in question is activated or created during annealing process. This therefore explains why its response is unnoticed in unannealed samples.

It was important to identify the effect of thermal quenching on the observations. By considering curve S_{n0} in Figures 4.23, 4.25, 4.27 and 4.29 in particular, it shows that these curves were purely determined by thermal quenching effect since there was no sensitisation up to this level. If that is untrue, the structure of curve S_{n0} for RT-LMOSL in Figures 4.24, 4.26, 4.28 and 4.30 also would have shown dependence on heating rates. That curve S_{n0} for RT-LMOSL in Figures 4.24, 4.26, 4.28 and 4.30 do not show significant dependence on heating rates of thermal activation is not far from expectation since all the RT-LMOSL were not read in varied temperature, which would have guaranteed obviously seen thermal quenching effect. Thus, the curve S_{n0} structure of TL is a product of thermal quenching. Also, a close look at curves S_{n1}-S_{n4} in the same Figures 4.23 to 4.30 shows these curves exhibit nearly identical curve nature (exclusive intensity) with S_{n0} that suffers only from thermal quenching. Hence, the cause behind the nature of curves S_{n1}-S_{n4}, which has been claimed to be due to sensitisation as a function of heating rate all along in this work, is prone to be mistaken for thermal quenching.

It is therefore obvious that, the comparative sensitisations resulting from accumulative successive TL readings and irradiations that each of the aliquots were subjected to, clarify the possible mix-up. The pattern of curves S_{n5} and S_{n2b}, which were read using the same heating rate (2^{o}C/s) on all the aliquots earlier used for curves S_{n0}-S_{n4} and S_{n1b} respectively (Figures 4.43 to 4.50) confirmed this. For if the trend of curves S_{n1}-S_{n4} in these figures are truly caused by thermal quenching effect, curve S_{n5} is not supposed to follow any pattern with heating rates. Therefore curve S_{n5} that shows increase of sensitisation with decreasing heating rates solely reflects the dependence of sensitisation on TL reading histories of each aliquot. The same observation was observed for part B that involved no intermediate successive irradiations (see curves S_{n2b} and S_{n1b} in the same Figures 4.43 to 4.50).

Another support for this is seen from RT-LMOSL sensitisation that showed dependence on heating rates exactly like TL counterpart. This is because, all the RT-LMOSL were read in room temperatute and could not have suffered from thermal quenching. In conclusion, the practically indistinguishable trend that is exhibited by curves S_{n5} and S_{n1b} as compared with S_{n4} and S_{n2b} respectively, indicates curves S_{n1}-S_{n4} and S_{n1b} to be the actual sensitisation pattern resulting from the successive cycles of TL luminescence measurements and irradiations.

However, this claim does not completely rule out the contribution of thermal quenching in the curves but rather asserting that it is minimal. The little contribution of thermal quenching effect is only obvious in S4 unannealed samples as seen in Figures 4.47 and 4.48. Given that curve S_{n5} is the next successive TL reading immediately after curve S_{n4}, curve S_{n5} would be expected to always be higher than S_{n4} for all the heating rates. Contrarily, curve S_{n4} happens to be higher than S_{n5} for 0.25 and 0.5C/s heating rates points, while the two curves are almost the same for 1^{o}C/s heating rate, curve S_{n5} takes the lead over S_{n4} for the remaining heating rates points. A similar relation is observed in the same referred figure for part B of the protocol where there were no intermediate irradiations. The above behaviour is the reflection of thermal quenching effect. This is because TL of curve S_{n5} was read using 2^{o}C/s heating rate for all the aliquots and 2^{o}C/s will experience relatively more thermal quenching than 0.25, 0.5 and 1^{o}C/s heating rates. That accounts for the reason why curve S_{n4} takes the lead over S_{n5} for the three low heating rates. In addition, the sensitisation of RT LM-OSL of annealed S4 does not show any dependence on heating rates of thermal activation (Figure 4.30). Therefore, the decrease in sensitisation with heating rate that its TL counterpart displayed after heating rates of 2^{o}C/s (Figure 4.29) is definitely caused by thermal quenching.

Another observation that merits further consideration is the enormous sensitisation that curve S_{n2b} exhibited over S_{n1b} as seen in annealed S2 and S4 samples (Figures 4.46 and 4.50). This was neither seen in unannealed samples (Figures 4.45 and 4.49) even in part A protocol (Figures 4.43, 4.44, 4.47, and 4.48) of the two annealed samples. The original Zimmerman, 1971 model was able to adequately proffer a possible explanation for this. According to Zimmerman, 1971 model, the successive TL readings of the protocol will cause depletion of the *R*-centers. The irradiations that were sandwiched in between successive cycles of thermal activation of part A of the protocol will replenish the depleted *R*-centre after each successive TL readings. Conversely, *R*-

center will be enormously depleted at the end of successive TL readings for part B protocol of which the successive TL readings were not sandwiched with irradiations. This will consequently result in high competition for holes between *L*-centre and *R*-centre during the following administration of TD (Step 5 Part B protocol) prior to the next TL readout to 500^{o}C of Step 6 that produced S_{n1b}. Most of the holes produced by this TD are therefore captured by *R*-centre owing to its heavy depletion and the preferential hole trapping nature (competition) that it possesses over *L*-centre (according to pre-dose model). The consequential effect of this will lead to a relatively intense reduction in TL signal of S_{n1b} as compared with the following pre-dose sensitisation of S_{n2b} that resulted from combined effect of TD of step 5 and TA of TL of step 6 of part B of the protocol. This comparatively reduced signal of S_{n1b} is responsible for the questioned vast sensitisation that curve S_{n2b} exhibited over S_{n1b} of annealed S2 and S4 samples in Figures 4.46 and 4.50 respectively. The absence of this vast depletion accounts for why part A behaved differently from this. The fact that the above observation, which is based on pre dose model, only pertains to annealed samples is another support to the initial inference that two different mechanisms are responsible for sensitisation in unannealed and annealed samples.

The overall sensitisations as observed in this study could be explained under the framework of the existing models as follows. Since the unannealed S2 and S4 samples have not received thermal activations prior to the measurements, the process of cycles of TL readings to 500^{o}C resulted into the pure thermal sensitisation for all the unannealed samples. Moreover, the annealing of the unannealed samples to 900^{o}C for 1 hour is believed to cause the alteration made to the recombination centre and very deep electron traps to attain the peak. This accounts for the relative increase of sensitivity after annealing by factors of 116 and 27 that is demonstrated by S2 and S4 respectively in this study. This therefore makes the contributions of pure thermal sensitisation to become less significant after the annealing (as the case of the annealed S2 and S4 samples) and consequently offers the pre-dose sensitisation the prominent role it played in annealed samples. To buttress this, the relative lesser thermal sensitisation during successive cycles of TL readings to 500^{o}C that was observed in annealed samples could be recalled. The dependence of sensitisation on heating rates observed in this work, which on its own was an evidence of purely thermal sensitisation, also supports the above inferences. This is because it is outstanding in unannealed samples comparably to its annealed samples counterpart.

4.2.6 Implications of results

Thermal sensitisation was observed to be the major mode of sensitisation in unannealed sample while pre-exposure dose played the chief role in annealed samples sensitisation. Therefore, pre-dose technique is not appropriate for unheated sample but rather ideal for fired quartz grains inclusion materials like ceramics, fired sediments and bricks, metallurgy ovens, and other highly fired objects. Furthermore, the protocol used in this study can be employed for authenticity testing to determine which samples have been previously heated. Another insinuation on dating that could be inferred from this work is the observed dependence of the luminescence sensitisation on heating rate used for thermal activation, irradiation dose and TL readout histories. This is important since integrated light output of the 110^{o}C TL peak is sometime employed for mass normalization in TL/OSL dating procedures and luminescence study. Thus, such mass normalization will be erroneous if the concerned aliquots have been subjected to various thermal activations through different heating rates, TL readout histories and irradiation dose. It is therefore suggested that this type of mass normalization be done at the beginning of measurement. However, if that is not possible, these factors as revealed in this work should be taken into consideration. Lastly, due to sensitisation resulting from TL readout histories, the practice of taking background TL measurement after each measurement should be taken into consideration in respect of changes in sensitivity of the concerned aliquot that such treatments could introduce. The parallel pattern of the pre-dose sensitisation that the TL and RT-LMOSL exhibited in this work lend a solid support to the earlier suggestion of Polymeris *et al.*, 2009 to extrapolate the TL pre-dose methodology to the OSL pre-dose effect using only the appropriate component of RT-LMOSL, instead of the initial part of the CW-OSL signal. Therefore, it is here by proposed on the basis of the identical dose response (Polymeris *et al.*, 2009) and the similar pre-dose sensitisation reported in this work for the two methods can serve as complementary dating methods with the motive to use it to authenticate the result obtain with either of them or as an alternative method. It should be noted also that the RT-LMOSL guarantee the avoidance of heating during the luminescence measurement. This in return rules out the possibility of chemiluminescence which makes OSL measurements not necessarily mandatory in nitrogen atmosphere and the total absence of thermal quenching effect.

CHAPTER FIVE

CONCLUSIONS AND RECOMMENDATIONS

5.1 Conclusion

Study of Thermoluminescence (TL) and Optically Stimulated Luminescence (OSL) sensitisations of unannealed and annealed quartz samples using two quartz samples collected from southwestern Nigeria have been carried out. From the results obtained, the following conclusions were drawn:

1. Reproducibility study of the pre-dose sensitisation effect within the same quartz crystal revealed that there is a very good reproducibility between the initial sensitivities in both cases of fired and unannealed samples based on the standard deviation from 10 aliquots of the normalised sensitivity. Heating up to 180 ^{o}C does not influence the sensitivity of the samples. The reproducibility of the pre-dose sensitisation, observed within various aliquots of the same sample, was observed to be much better in annealed than unannealed samples.

2. The contributions of pre-exposure dose and thermal activation on 110^{o}C TL peak and TR-LMOSL sensitivities of two quartz samples showed sensitisation pattern exhibited by 110^{o}C TL peak and RT-LMOSL to be nearly identical. This therefore, supports the model of these two mechanisms to share a common electron trap and recombination centres. The luminescence sensitisation was observed to somewhat decrease with heating rates generally. Furthermore, thermal sensitisation was observed to be the key contribution of sensitisation in unannealed sample while pre-exposure dose played the chief role in sensitisation of annealed samples. Thus, this clarifies the usual mixed up of the two mechanisms.

3. Luminescence sensitisation was observed to decrease with heating rate used for thermal activation mostly in unannealed samples but increase with quantity of pre-exposure dose in annealed samples. However, the sensitisation increased with the number of TL readout for both annealed and unannealed samples.

4. Both the pre-dose sensitisation of TL and RT-LMOSL nearly followed identical pattern. 110^{o}C TL peak were observed to share the same electron traps with component 3 (C3) and component 4 (C4) in unannealed and annealed samples respectively.

5.2 Recommendations

Following the observations in this study and for future luminescence dating and studies, it is recommended that.

1. Pre-dose method of dating is only appropriate for heated quartz samples and not feasible for unannealed samples.
2. Special caution should be exercised while applying specific mass reproducibility correction procedure in the case of geological, unannealed quartz samples, since it could result in erroneous equivalent dose estimation. Generally, the systematic understanding of effects of each step of luminescence protocol on mechanisms describing 110^{o}C TL peak characteristics must be taken into consideration in order to chose appropriate point for sensitivity test and correction for unannealed and annealed samples.
3. Due to sensitisation resulting from TL readout histories, changes in sensitivity of the concerned aliquot should be taken into consideration in the practice of TL background measurements after each TL readings in order to avert introduction of errors in results.
4. The protocol used in this study can be employed for authenticity testing to determine which samples has been previously fired or unannealed and in determination of thermal histories of quartz generally.
5. Heating rate of 1C/s is suggested to be used for the TL reading that serves as thermal activation in pre-dose technique.
6. The pre-dose sensitisation of RT LMOSL can serve as a complementary dating methods to the traditional 110^{o}C TL peak.

REFERENCES

Adamiec, G., 2005. Properties of the 360 and 550 nm TL emissions of the '110^{o}C peak' in fired quartz. *Radiation Measurements.* 39: 105 – 110.

Adamiec, G., Bluszcz, A., Bailey, R., Garcia-Talavera, M., 2006. Finding model parameters. Genetic algorithms and the numerical modelling of quartz luminescence. *Radiation Measurements* 41: 897 – 902.

Afouxenidis, D., Polymeris, G. S., Tsirliganis, N. C., Kitis, G., 2012. Computerised curve deconvolution of TL/OSL curves using a popular spreadsheet program. *Radiation Protection Dosimetry*. 149 (4): 363–370.

Aitken, M. J., 1985. *Thermoluminescence Dating*. Academic Press, London.

Aitken, M. J., Smith, B. W., 1988. Optical dating. recuperation after bleaching *Quaternary Science Reviews*. 7: 387–393.

Aitken, M. J., 1998. *An Introduction to Optical Dating*. Oxford University Press, Oxford.

Asfora, V. K., Guzzo, P, L., Pessis, A-M., Barros, V. S. M., Watanabe, S., Khoury, H. J., 2014. Characterization of the burning conditions of archaeological pebbles using the thermal sensitization of the 110^{o}C TL peak of quartz. *Radiation Measurements*, http://dx.doi.org/10.1016/j.radmeas.2014.04.022.

Bailey, R. M., 2001. Towards a general kinetic model for optically and thermally stimulated luminescence of quartz, *Radiation Measurements*. 33: 17-45.

Bailiff, I. K., 1994. The pre-dose technique, *Radiation Measurements.* 23 (2/3): 471-479.

Bailiff, I. K., 2000. Characteristics of time-resolved luminescence in quartz. *Radiation Measurements.* 32: 401–405.

Balian, H. G., Eddy, N. W., 1977. Figure-of-merit (FOM). an improved criterion over the normalized Chi-squared test for assessing goodness-of-fit of gamma-ray spectral peaks. *Nuclear Instruments and Methods.* 145: 389–395.

Bartnitskaya, T. S., Vlasova, M. V., Zelyavskii, V. B., Kakazei, N. G., Kurdyumov, A. V., Sukhikh, L. L., Chistyakov, V. I., 1992. Defect structure formation in silicon on grinding, *Soviet Powder Metallurgy and Ceramics.* 31: 903-907.

Battaglia, S., Fanzini, M., Leoni, L., 1993. Influence of grinding methods on the 101 X-ray powder diffraction line of a-quartz. in methods and practices in X-ray powder diffraction, ICDD, USA.

Betts, D. S., Townsend, P. D., 1993. Temperature distribution in thermoluminescence experiments. II. Some calculational models. *Journal of Physics D: Applied Physics.* 26**:** 849–857.

Betts, D. S., Couturier, L., Khayarat, A. H,, Luff, B. J., Townsend. 1993. Temperature distribution in thermoluminescence experiments. I. Experimental results. *Journal of Physics D. Applied Physics.* 26: 843–848.

Botter-Jensen, L., 1997. Luminescence techniques. instrumentation and methods. *Radiation Measurements*, 27(5/6): 749-768.

Botter-Jensen, L., Duller, G. A. T., Murray, A. S., Banerjee, D. 1999. Blue light emitting diodes for optical stimulation of quartz in retrospective dosimetry and dating. *Radiation Protection Dosimetry*, 84: 335-340.

Botter-Jensen, L., Bulur, E., Duller, G. A. T., Murray, A. S., 2000. Advances in luminescence instrument systems. *Radiation Measurements*. 32: 523-528.

Botter-Jessen, L., McKeever, S. W. S., Wintle, A. G., 2003a. *Optically stimulated luminescence dosimetry*. Elsevier Science B.V. Amsterdam.

Botter-Jensen, L., Andersen, C. E., Duller, G. A. T., and Murray, A. S. 2003b. Developments in radiation, stimulation and observation facilities in luminescence measurements. *Radiation Measurements.* 37: 535-541.

Bulur, E., 1996. An alternative technique for optically stimulated luminescence (OSL) experiment. *Radiation Measurements.* 26: 701–709.

Chen, R., 1979. Saturation of sensitisation of the 110^{o}C TL peak in quartz and its potential application in pre-dose technique, *Eur. PACT* 3: 325-335.

Chen, R., Kristianpoller, N., Davidson, Z., Visocekas, R., 1981. Mixed-order and second order kinetics in thermally stimulated processes. *Journal of Luminescence*. 23 (3,4): 293–303.

Chen, R., Yang, X. H., McKeever, S. W. S., 1988. Strongly superlinear dose dependence of thermoluminescence in synthetic quartz. *Journal of Physics D: Applied Physics* 21: 1452-1457.

Chen, R., Fogel, G., Kristianpoller, N., 1994. Theoretical account of the sensitisation and de-sensitisation in quartz. *Radiation Measurements.* 23: 277-279.

Chen, R., Mckeever, S. W. S., 1997. *Theory of Thermoluminescence and Related Phenomena*. World Scientific Publishing, Singapore.

Chen, G., Li. S. -H., 2000. Studies of quartz 110 °C thermoluminescence peak sensitivity change and its relevance to optically stimulated luminescence dating. *Journal of Physics D: Applied Physics*. 33: 437-443.

Chen, G., Li, S. -H., Murray, A. S., 2000. Study of the 110 ^{o}C TL peak sensitivity in optical dating of quartz. *Radiation Measurements.* 32: 641–645.

Chen, R., Leung, P. L., 2002. The decay of OSL signals as stretched exponential functions. *Radiation measurements.* 37: 519 – 526.

Chen, R, Pagonis, V., 2003. Modelling thermal activation characteristics of the sensitisation of thermoluminescence in quartz. *Journal of Physics D: Applied Physics.* 36: 1–6.

Chithambo, M. L., Galloway, R. B., 2000. A pulsed light-emitting-diode system for stimulation of luminescence. *Measurement Science Technology* 11: 418–424

Curie, D., 1963. *Luminescence in Crystals*. Wiley, New York.

Deer, W. A., Howie, R. A., Wise, W. S., Zussman, J., 2004. *Rock-Forming Minerals, V4b. Framework Silicates. Silica Minerals, Feldspathoids and the Zeolites*. 2nd edition. Geological society of London, Xv pp +982.

Duller A. T., 1997. Behavioural studies of stimulated luminescence from feldspar. *Radiation Measurements*. 27 (5/6): 663-694.

Duller, G. A. T., 2003. Distinguishing quartz and feldspar in single grain luminescence measurements. *Radiation Measurements* 37: 161–165.

Facey, R., A., 1996. Heating-rate effects in glow peak measurements for thermoluminescent dosimetry, *Health Physics.* 12: 717-720.

Ferreira de Souza, L. B., Guzzo, P. L., Khoury, H. J., 2014. OSL and photo-transferred TL of quartz single crystals sensitised by high-dose of gamma-radiation and moderate heat-treatments. *Applied Radiation and Isotopes*. 94: 93–100.

Figel, M., Goedicke, C., 1999. Simulation of the pre-dose effect of the 100^{o}C TL peak in quartz. *Radiation Protection Dosimetry*. 84: 433–438.

Fleming, S. J., Thompson, J., 1970. Quartz as a heat resistant dosimeter. *Health Physics.* 18: 567–568.

Forman, S. L., Pierson, J., Smith. R. P., Hackett, W. R., Valentine, G., 1994. Assessing the accuracy of thermoluminescence for dating backed sediments beneath late Quaternary lava flows, Snake River plain, Idaho. *Journal of Geophysical Research*. 99 B (8): 15569-15576.

Franklin, A. D., Prescott, J. R., Scholefield, R. B., 1995. The mechanism of thermoluminescence in an Australian sedimentary quartz. *Journal of Luminescence*. 63: 317–326.

Furetta, C., 2003. *Handbook of Thermoluminescence*. World Scientific publishing Co. Pte.Ltd., Singapore.

Galli, A., Martini, M., Montanari, C., Panzeri, L., Sibila, E., 2006. TL of fine-grain samples from quartz-rich archaeological ceramics. dosimetry using the 110 and 210^{o}C TL peaks. *Radiation Measurements*. 41: 1009-1014.

Garlick, G. F. J., Gibson, A. F., 1948. The electron trap mechanism of luminescence in sulphide and silicate phosphors. *Proc. Roy. Soc. London* A60: 574-590.

Gotlib, V. I., Kantorovich, L. N., Grebenshicov, V. L., Bichev, V. R., Nemiro, E. A., 1984. The study of thermoluminescence using the contact method of sample heating. *Journal of Physics D: Applied Physics*. 17: 2097–2114.

Gumnior, M., Preusser, F., 2007. Late Quaternary river development in the southwest Chad Basin. OSL dating of sediment from the Komadugu palaeofloodplain (northeast Nigeria). *Journal of Quaternary Science*. 22: 709–719.

Han, Z. Y., Li, S. H., Tso, M. Y. W., 2000. Effect of annealing on TL sensitivity of granitic quartz, *Radiation Measurements*. 32: 227-231.

Hashimoto, T., Sakaue, S., Ichino, M., 1994. Dependence of TL-property changes of natural quartzes on aluminum contents accompanied by thermal annealing treatment. *Radiation Measurements*. 23: 293-299.

Horowitz, Y. S., 1984. *Thermoluminescence and Thermoluminescent dosimetry*, volume Vol.1. CRC Press.

Horowitz, Y. S. Yossian, D., 1995. Computerized glow curve deconvolution . application to thermoluminescence dosimetry. *Radiation Protection Dosimetry*. Spec. Issue, 60.

Huntley, D. J., Godfrey-Smith, D. I., Thewalt, M. L. W., 1985. Optical dating of sediments. *Nature*. 313: 105–107.

Huntley, D. J., Godfrey-Smith, D. I., Haskell, E. H., 1991. Light-induced emission spectra from some quartz and feldspars. *Nuclear Tracks and Radiation Measurements*. 18: 127-131.

Hutt, G., Jaek, I., and Tchonka, J., 1988. Optical dating. K-feldspars optical response stimulation spectra. *Quaternary Science Reviews*, 7: 381-385.

Ivliev, A. I., Kashkarov, L. L., Kalinina, G. V., 2006. Comparative Thermoluminescence characteristics of the different origin natural quartz. Electronic Scientific Information Journal. *Herald of the Department of Earth Science RAS.* 1(24): 1-2.

Jain, M., Murray, A.S., Bøtter-Jensen, L., 2003. Characterisation of blue-light stimulated luminescence components in different quartz samples. implications for dose measurements. *Radiation Measurements*. 37: 441–449.

Jones, C. E., Embree, D., 1976. Correlations of the 4.77-4.28eV luminescence band in silicon dioxide with oxygen vacancy. *Journal of Applied Physics*. 47: 5365-5371.

Kitis, G., Spiropulu, M.. Papadopoulos, J., Charalambous, S., 1993. Heating rate effects on the TL glow-peaks of three thermoluminescent phosphors. *Nuclear Instruments and Methods in Physics Research*. 73: 367-372.

Kitis, G. Gomez-Ros, J. M. Tuyn, J. W. N., 1998 . Thermoluminescence glowcurve deconvolution functions for first, second and general orders of kinetics. *Journal of Physics D. Applied Physics*. 31: 2636-2641.

Kitis, G., Tuyn, J. W. N., 1998. A simple method to correct for the temperature lag in TL glow-curve measurements. *Journal of Physics D: Applied Physics*. 31: 2065–2073.

Kitis, G., 2001. TL glow-curve deconvoluion functions for various kinetic orders and continuous trap distribution. Acceptance criteria for E and s values. *Journal of Radioanalytical and Nuclear Chemistry*. 247 (3): 697-703.

Kitis, G., Pagonis, V., 2008. Computerized curve deconvolution analysis for LM-OSL. *Radiation Measurements*. 43(2/6): 737 – 741.

Kitis, G., Kiyak, N. G., Polymeris, G. S. Tsirliganis, N. C., 2010. The correlation of fast OSL component with the TL peak at 325^{o}C in quartz of various origins. *Journal of Luminescence*. 130: 298–303.

Kitis, G., Pagonis, V., 2013. Analytical solutions for stimulated luminescence emission from tunneling recombination in random distributions of defects. *Journal of Luminescence*. 137 : 109–115.

Kiyak, N. G., Polymeris, G. S., Kitis, G., 2007. Component resolved OSL dose response and sensitisation of various sedimentary quartz samples. *Radiation Measurements*. 42: 144–155.

Kiyak, N. G., Polymeris, G. S., Kitis, G., 2008. LM–OSL thermal activation curves of quartz. relevance to the thermal activation of the 110^{o}C TL glow peak. *Radiation Measurements* 43: 263–268.

Koul, D. K., Nambi, K. S. V., Singhvi, A. K., Bhat, C. L., Gupta, P. K., 1996. Feasibility of estimating firing temperature using 110 ^{o}C TL peak of quartz, *Applied Radiation and Isotope*. 47: 191-196.

Koul, D. K., Chougaonkar, M. P., 2007. The pre-dose phenomenon in the OSL signal of quartz. *Radiation Measurements* 42: 1265–1272.

Koul, D. K., 2008. 110^{o}C TL glow peak of quartz – a brief review. *Pramana.* 71: 1209-1229.

Koul, D. K., Polymeris, G. S., Tsirliganis, N. C., Kitis, G., 2010. Possibility of pure thermal sensitisation in the pre-dose mechanism of the 110^{o}C TL peak of quartz. *Nuclear Instruments and Methods in Physics Research* B. 268: 493–498.

Koul, D. K., Polymeris, G. S., 2013. Impact of firing on the optically stimulated luminescence of geological quartz. *AIP Conference Proceedings*. 1512: 916–917.

Koul, D. K., Patil, P. G., Oniya, E. O., Polymeris, G. S., 2014. Investigating the thermally transferred optically stimulated luminescence source trap in fired geological quartz. *Radiation Measurement*. 62(2014), 60–70.

Krbetschek, M. R., Gotze, J., Dietrich, A., Trautmann, T., 1997. Spectral information from minerals relevant for luminescence dating. *Radiation Measurements*. 27(5/6): 695-748.

Lersen, N. A., 1997. Dosimetry based on thermally and optically stimulated luminescence. Dissertation submitted June 1997 for the Ph.D degree at the Niels Bohr Institute, University of Copenhagen.

Li, S.-H., Yin, G.-M., 2001. Luminescence dating of young volcanic activity in China, *Quaternary Science and Reviews*. 20: 865-868.

Li, S.-H., 2002. Luminescence sensitivity changes of quartz by bleaching, annealing and uv exposure. *Radiation Effects and Defects in Solids.* 157: 357–364.

May, C. E., Partridge, J. A., 1964. Thermoluminescence kinetics of alpha irradiated alkali halides. *J. Chem. Phys.* 40. 1401-1409.

McKeever, S. W. S., Strain, J. A., Townsend, P. D., Udval, P., 1983. Effects of thermal cycling on the thermoluminescence and radioluminescence of quartz. *PACT 9:* 123-132.

McKeever, S. W. S., 1991. Mechanisms of thermoluminescence production, some problems and a few answers. *Nuclear Tracks and Radiation Measurements* 18: 5-12.

McKeever, S. W. S., Chen, R., 1997. Luminescence models. *Radiation Measurements.* 27(5/6): 625-661.

McKeever, S. W. S., Bùtter-Jensen, L., Agersnap Larsen, N., Duller, G. A. T., 1997. Temperature dependence of OSL decay curves. experimental and theoretical aspects. *Radiation Measurements.* 27(2): 161-170.

Michael, C. T., Zacharias, N., Maniatis, Y., Dimotikali, D., 1997. A new technique (foil technique) for measuring the natural dose in TL dating and its application in the dating of a mortar containing ceramic fragments. *Ancient TL*. 15(2/3): 36–42.

Mott, N. F., Gurney, R. W., 1948. *Electronic Processes in Ionic Crystals*, 2nd ed. Oxford University Press, London.

Murray, A. S., Roberts, R. G., 1998. Measurement of the equivalent dose in quartz using a regenerative-dose single aliquot protocol. *Radiation Measurements* 29(5): 503 – 515.

Murray, A. S., Wintle, A. G., 2000. Luminescence dating of quartz using an improved single-aliquot regenerative-dose protocol. *Radiation Measurements*. 32: 57–73.

Nanjundaswamy, R., Lepper, K., McKeever, S. W. S., 2002. Thermal quenching of thermoluminescence in natural quartz. *Radiation Protection Dosimetry*. 100: 305-308.

Ogundare, F. O., Chithambo, M. L., Oniya, E. O., 2006. Anomalous behaviour of thermoluminescence from quartz. A case of glow peaks from a Nigerian quartz. *Radiation Measurements*. 41: 549-553.

Ogundare, F. O., Chithambo, M. L., 2007a. Thermoluminescence kinetic analysis of quartz with a glow peak that shifts in an unusual manner with irradiation dose. *Journal of Physics D. Applied Physics*. 40: 247–253.

Ogundare, F.O., Chithambo, M.L., 2007b. Time resolved luminescence of quartz from Nigeria. *Optical Materials.* 29: 1844–1851.

Ogundare, F. O., Chithambo, M. L., 2008. The influence of optical bleaching on lifetimes and luminescence intensity in the slow component of optically stimulated luminescence of natural quartz from Nigeria. *Journal of Luminescence*. 128: 1561–1569.

Oniya, E. O., Polymeris, G. S., Tsirliganis, N. C., Kitis, G., 2012a. On the pre-dose sensitization of the various components of the LM-OSL signal of annealed quartz; Comparison with the case of 110^{o}C TL peak. *Radiation Measurements*. 47: 864-869.

Oniya, E. O., Polymeris, G. S., Tsirliganis, N. C., Kitis, G., 2012b. Sensitization of high temperature thermoluminescence glow-curve peaks in various quartz samples. *Geochronometria*. 39(3): 212-220.

Pagonis, V., Kitis, G., Furetta, C., 2006. *Numerical and Practical Exercises in Thermoluminescence.* Springer Science+Business Media, Inc. New York.

Pagonis, V., Kitis, G., 2012. Prevalence of first-order kinetics in thermoluminescence materials: An explanation based on multiple competition processes. *Physica Status Solidi B.* 249(8): 1590–1601.

Petrov, S. A., Bailiff, I. K., 1996. Thermal quenching and the Initial Rise technique of trap depth evaluation. *Journal of Luminescence*. 65: 289-291.

Piters, T. M., Bos, A. J. J., 1994. Effects of nonideal heat transfer on the glow curve in thermoluminescence experiments. *Journal of Physics D: Applied Physics*. 27: 1747–1756.

Polymeris, G. S., Afouxenidis, D., Tsirliganis, N. C., Kitis, G., 2009. The TL and room temperature OSL properties of the glow peak at 110 ^{o}C in natural milky quartz. A case study. *Radiation Measurements.* 44: 23–31.

Polymeris, G. S., 2015. OSL at elevated temperatures: Towards the simultaneous thermal and optical stimulation. *Radiation Physics and Chemistry*. 106: 184–192.

Prescott, J. R., Robertson. G. B., 1997. Sediment dating by luminescence. a review. *Radiation Measurements*. 27: 893-922.

Preusser, F., Chithambo, M. L., Götte, T., Martini, M., Ramseyer, K., Sendezera, E. J., Susino, G. J., Wintle, A. G., 2009. Quartz as a natural luminescence dosimeter. *Earth-Science Reviews.* 97: 184–214.

Randall, J. T., Wilkins, M. H. F., 1945. Phosphorescence and electron traps II- The interpretation of long period phosphorescence. *Proct. R. Soc. London Ser.* A, 184: 390-407.

Ranjbar, A. H., Durrani, S. A., Randle, K., 1999. Electron spin resonance and thermoluminescence in powder form of clear fused quartz; Effects of grinding, *Radiation Measurements*. 30: 73-81.

Rendell, H. M, Townsend, P. D., Wood, R. A., Luff, B. J., 1994. Thermal treatment and emission spectra of TL from quartz, *Radiation Measurements*. 23: 441-449.

Roberts, R. G., 1997. Luminescence dating in archaeology from origins to optical. *Radiation Measurements*. 27: 819-892.

Sadek, A. M., Eissa, H. M., Basha, A. M., Kitis, G., 2014. Resolving the limitation of the peak fitting and peak shape methods in the determination of the activation energy of thermoluminescence glow peaks. *Journal of Luminescence*. 146: 418–423.

Sawakuchi, G. O., Okuno, E. 2004. Effect of high gamma doses in quartz. *Nuclear Instruments and Methods in Physics Research*. B. 218: 217-221.

Schilles, T. Poolton, N. R. J., Bulur E., Bøtter-Jensen L., Murray A. S., Smith G. M., Riedi P C., Wagner G. A., 2001. A multi-spectroscopic study of luminescence sensitivity changes in natural quartz induced by high-temperature annealing. *Journal of Physics D. Applied Physics*. 34: 722–731.

Singhvi, A. K., Krbetschek, M. R., 1996. Luminescence dating of arid zone sediments. A review and perspective. *Ann. Arid Zone*. 35 (3): 249 – 279.

Smith, B. W., Rhodes, E. J., Stokes, S., Spooner, N. A., 1990. The optical dating of sediments using quartz. *Radiation Protection Dosimetry*. 34: 75-78.

Spooner, N. A., Questiaux, D. G., 1989. Optical dating - Achenheim beyond the Eemian using green and infrared stimulation. Proceedings of Workshop on Long and Short Range Limits in Luminescence Dating. In. Occasional Publication 9, Research Laboratory for Archaeology and the History of Art, Oxford.

Spooner, N. A., 1994. On the optical dating signal from quartz. *Radiation Measurements*. 23: 593-600.

Stokes, S., 1994. The timing of OSL sensitivity changes in a natural quartz. *Radiation Measurements*. 23: 593–600.

Stoneham, D., Stokes, S., 1991. An investigation of the relationship between the 110 ^{o}C TL peak and optically stimulated luminescence in sedimentary quartz. *Nuclear Tracks and Radiation Measurements* 18: 119–123.

Subedi, B., Oniya, E., Polymeris, G.S., Afouxenidis, D., Tsirliganis, N. C., Kitis, G., 2011. Thermal quenching of thermoluminescence in quartz samples of various origin. *Nuclear Instruments and Methods in Physics Research* B. 269: 572–581.

Takeuchi, A., Nagahama, H., Hashimoto, T., 2006. Surface resetting of thermoluminescence in milled quartz grains, *Radiation Measurements* 41(7/8): 826-830.

Takeuchi, A., Hashimoto, T., 2008. Milling-induced reset of thermoluminescence and deformation of hydroxyl species in the near-surface layers of quartz grains, *Geochronometria*. 32: 61-68.

Taylor, G. C., Lilley, E., 1982. Effect of clustering and precipitation on thermoluminescene in LiF (TLD-100) crystals. *Journal of Physics D: Applied Physics*. 15: 1253-1263.

Topaksu, M., Dogan, T., Yüksel, M., Kurt, K., Topak, Y., Yegingil, Z., 2014. Comparative study of the thermoluminescence properties of natural metamorphic quartz belonging to Turkey and Spain. *Radiation Physics and Chemistry*. 96: 223–228.

Wintle, A. G., 1973. Anomalous fading of thermoluminescence in mineral samples. *Nature*. 245: 143–144.

Wintle, A. G.,1975. Thermal Quenching of Thermoluminescence in Quartz. *Geophys. J. Roy. Astronom. Sot.* 41: 107-113.

Wintle, A. G., 1997. Luminescence dating. laboratory procedures and protocols. *Radiation Measurements*. 27(5/6): 769-817.

Wintle, A. G., Murray, A. S., 1998. Towards the development of a preheat procedure for OSL dating of quartz. *Radiation Measurements*. 29: 81–94.

Wintle, A. G., Murray, A. S., 1999. Luminescence sensitivity changes in quartz. *Radiation Measurements*. 30: 107–118.

Wintle, A. G., Murray. A. S., 2006. A review of quartz optically stimulated luminescence characteristics and their relevance in single-aliquot regeneration dating protocols. *Radiation Measurements*. 41: 369 – 391.

Yang, X. H., McKeever, S.W.S., 1990. The pre-dose effect in crystalline quartz, *Journal of Physics D: Applied Physics*. 23: 237-244.

Zimmerman, J., 1971. The radiation-induced increase of the 110^{o}C thermoluminescence sensitivity of fired quartz, *Journal of Physics. C: Solid State Physics*. 4: 3265-3276.

APPENDIX 1

Nuclear Instruments and Methods in Physics Research B 274 (2012) 105–110

Contents lists available at SciVerse ScienceDirect

Nuclear Instruments and Methods in Physics Research B

journal homepage: www.elsevier.com/locate/nimb

In-homogeneity in the pre-dose sensitization of the 110 °C TL peak in various quartz samples: The influence of annealing

George S. Polymeris [a,b,*], Ebenezer O. Oniya [a,d], Nnamdi N. Jibiri [e], Nestor C. Tsirliganis [a], George Kitis [c]

[a] Laboratory of Radiation Applications and Archaeological Dating, Department of Archaeometry and Physicochemical Measurements, Cultural and Educational Technology Institute, Athena, Research and Innovation Center in Information, Communication and Knowledge Technologies, Tsimiski 58, GR-67100 Xanthi, Greece
[b] ISIK University, Faculty of Science and Arts, Physics Department, Şile 34980, Istanbul, Turkey
[c] Aristotle University of Thessaloniki, Nuclear Physics Laboratory, 54124 Thessaloniki, Greece
[d] Physics and Electronics Department, Adelaunle Ajasin University, PMB 01 Akungba Akoko, Nigeria
[e] Department of Physics, University of Ibadan, Ibadan, Nigeria

ARTICLE INFO

Article history:
Received 8 June 2011
Received in revised form 29 November 2011
Available online 13 December 2011

Keywords:
Quartz
Thermoluminescence (TL)
110 °C TL glow-peak
Pre-dose effect
Sensitization
Aliquot – to – aliquot scatter

ABSTRACT

The pre dose sensitization effect of the 110 °C TL glow peak of quartz is a basic tool in thermoluminescence and optically stimulated luminescence dating and retrospective dosimetry. In the present work, a homogeneity study was performed on pre dose sensitization in grains obtained from large quartz crystals samples collected from 10 different origins. The aliquot to aliquot scatter of the pre dose sensitization of the 110 °C TL peak within each quartz crystal was monitored. The influence of the annealing on this scattering was also studied. Therefore, the investigation was applied to the un fired "as is" samples as well as to samples annealed at 900 °C for 1 h following cooling to room temperature in air. The results showed that in the case of "as is" quartz the sensitization effect vary strongly within each aliquot of the same quartz sample. This strong variation is removed by both the high temperature annealing as well as heating up to 500 °C, involved in the TL measurements. These results are generally discussed in the framework of existing models and applications of the effect.

1. Introduction

SiO_2 (silica) makes up 12.6% by weight of the Earth's crust as crystalline quartz and amorphous silica [1]. Quartz is the main material for retrospective dosimetry and for dating archeological pottery and geological sediments using both thermoluminescence (TL) as well as optically stimulated luminescence (OSL). Among the various TL glow peaks of quartz, the one which was found at just about 100 °C for a heating rate of 5 °C/s is known as the 110 °C TL peak [2]. This specific TL peak in quartz is known to decay at room temperature (RT) with a half-life of the order of an hour [3]. Therefore this peak can be seen in all quartz, whether natural or artificial [4] provided that it has been irradiated less than a few hours before measurement. Nevertheless, though unstable at RT, the 110 °C TL glow peak of quartz, has worked very efficiently due to its pre-dose sensitization property [5]. The pre-dose thermoluminescence technique of dating [6] is unique in its ability to measure radiation doses of as small as 10 mGy in contemporary ceramic materials such as bricks, tiles and porcelain plumbing fixtures [7]. Therefore, it is a well-established technique in both retrospective dosimetry and dating [8]. The main idea behind the use of both this technique and peak is to monitor the increase in the sensitivity rather than the, conventional, accumulation of TL [9], since the response of the 110 °C TL peak to a small test dose can be enhanced by heating to temperatures above 200 °C [10]. Utilizing this sensitization, the 110 °C TL glow peak of quartz has been attempted for the firing temperature assessment of ceramics also [11–13].

A workable TL peak at a temperature as low as 110 °C is a big advantage in TL measurements for a number of reasons, namely: (a) studying the TL resulting from charge release from this trap is not difficult and no instrumental limitation is implied, as the unwanted effects occurring due to heating at much higher temperatures can be avoided, (b) this TL peak is ubiquitously present in all quartz samples, natural or artificial, annealed and as-is, (c) several features of the 110 °C TL glow-peak were proved to be universal or prevalent, such as its main structure (shape, peak position and trapping parameters [14]) as well as its thermal quenching behavior [15], (d) due to its simplicity and non-composite nature, the 110 °C TL peak does not require de-convolution, (e) lastly, the 110 °C TL peak is sensitive and consequently, its study therefore does not require large doses of irradiation in the laboratory.

* Corresponding author at: Laboratory of Radiation Applications and Archaeological Dating, Department of Archaeometry and Physicochemical Measurements, Cultural and Educational Technology Institute, Athena, Research and Innovation Center in Information, Communication and Knowledge Technologies, Tsimiski 58, GR-67100 Xanthi, Greece. Tel.: +30 2541078787; fax: +30 2541063656.
E-mail address: polymers@auth.gr (G.S. Polymeris).

0168-583X/$ – see front matter © 2011 Elsevier B.V. All rights reserved.
doi:10.1016/j.nimb.2011.12.001

Given all the aforementioned reasons, the pre-dose methods are basically centered on the 110 °C TL peak, thus, the pre-dose sensitization of the latter glow-peak has also become the subject of numerous studies in respect to:

(i) Its response to combined annealing and irradiation [4,5,16,17].
(ii) Its response to either irradiation [18] or thermal treatment [9,19].
(iii) The recombination center as well as the emission wavelength which are responsible for pre-dose effect, namely the emission at 370 nm which occurs due to $[H_3O_4]^0$ hole centers, silicon vacancies that are occupied by three hydrogen atoms and a trapped hole [20–22].
(iv) The sensitization and superlinearity in quartz, which are phenomena intimately related to each other [23–26].
(v) A comparative study of the pre-dose effect for different types, annealing temperatures and origins of quartz [26,27].
(vi) Explanation and modeling of the effect [28–32].
(vii) Its usefulness to monitor the sensitization of the OSL signal in various dating protocols [2,3,33–42].

One among the uncertainties encountered on the extensively studied phenomenon of sensitization of 110 °C TL peak is the degree of sensitization that changes from sample to sample. The complexity of this peak, just like other quartz luminescence properties, is always attributed to the different crystallization environments during formation of respective sedimentary quartz samples that varies from location to location [43,44]. Nevertheless, even within the same quartz sample, 'grain to grain' variation has been also reported for the case of some sedimentary quartz samples [44–46], leading to the devising of a 'Single grain OSL attachment'. Grain to grain variation has been reported to happen as a result of different grain to grain origin, and various irradiations, thermal and optical/bleaching histories that each grain might have possessed during transportation. Each one of these factors is widely known to be highly influential on pre-dose sensitization [4,5,9,16–19]. Ideally, the same degree of pre-dose sensitization is expected from all the grains of any crystalline quartz. This assumption results from the fact that all the grains are (i) from a common origin, (ii) and possess the same irradiations, thermal and optical/bleaching histories. However averaging effect over many grains is generated by using an aliquot with a layer of grains of quartz. Still disc to disc variations are expected due to statistical reasons but in that case these variations are expected to be very low. Therefore, large variation in sensitization that is exhibited by different grains of a crystalline quartz sample should arise from the intrinsic nature of the crystal and not from prevailing external factors. Should such characteristic exist, it is expected to shed more light on the complexity nature of quartz luminescence characteristics; and subsequently be of high assistance in all luminescence area of applications. Based on the above, the aim of this work was to study the homogeneity of the pre-dose sensitization of the 110 °C TL peak within the same quartz crystal for several quartz samples of various origins by assessing the aliquot – to – aliquot scattering. The influence of the annealing to this scattering was also studied. To the best of the author's knowledge, no similar study is reported in literature, despite the voluminous literature dealing with the 110 °C TL peak in quartz.

2. Experimental procedure

The original quartz samples were large crystals of hydrothermal and metamorphic origins which occurred in vein-associated metamorphic rocks. In order to make the study to be universal, 10 different quartz samples were collected from different origins spanning through Africa, Europe and Asia. The laboratory code names, locations and types of each of the 10 quartz samples are presented in Table 1. Each natural crystal quartz sample was crushed and smashed in an agate mortar. Grains of dimensions between 90 and 150 μm were obtained by sieving, cleaned in acetone and dried in the air. Two types of measurements were performed on each of the ten samples. The first sets were performed to 'as is' (unfired) material while for the second sets the material was previously annealed at 900 °C for 1 h and allowed to cool to room temperature in the air afterwards. For each set, 10 aliquots of equal mass of about 5 mg were analysed in this work with aim of observing variation in the sensitization among ten aliquots of the same sample.

All the TL measurements on the quartz samples were carried out using a RISØ TL/OSL reader (model TL/OSL–DA–15) equipped with a 0.075 Gy/s $^{90}Sr/^{90}Y$ β ray source [46]. The reader was fitted with a 9635QA photomultiplier tube. The detection optics consisted of a 2.5 mm Hoya U-340 ($\lambda_p \sim 340$ nm, FWHM 80 nm) filter. All measurements were performed in a nitrogen atmosphere with a constant heating rate of 1 °C/s in order to avoid significant temperature lag, up to a maximum heat temperature of 500 °C. The experimental protocol used was the following:

Step 1: Give a TD to a natural sample having its Natural TL as NTL.
Step 2: Measure TL up to 180 °C. This step measures the sensitivity S_{01} of the TL glow-peak at "110 °C" acting additionally as a mass normalization.
Step 3: Give the same TD and measure TL up to 500 °C. This step (a) measures the sensitivity S_{02} of the TL glow-peak at 110 °C and (b) acts as a thermal activation the sample.
Step 4: Give the same TD and measure TL up to 500 °C. This step (a) measures the sensitivity S_1 of the TL glow-peak at 110 °C and (b) acts as a thermal activation the sample again.

Table 1
Laboratory code name, origin and test dose administered for both 'as is' and annealed samples.

Sample's laboratory name	Sample origin	TD administered, 'as is' (Gy)	TD administered, annealed (Gy)
A1	Nepal, Asia	5	2
B2	Nepal, Asia	2	0.5
Kilkis	Greece, Europe	5	2
Koupa	Greece, Europe	5	2
S1	Nigeria, Africa	5	0.5
S2	Nigeria, Africa	2	1
S3	Nigeria, Africa	5	0.5
S4	Nigeria, Africa	2	0.5
S6	Nigeria, Africa	5	0.5
S8	Nigeria, Africa	5	0.5

Table 2
Case of un-fired quartz: Column S_{01} (%) describes the reproducibility of the 10 samples by means of (Standard Deviation/Mean). In a similar manner column NTL (%) describes the reproducibility of the 10 samples based on the NTL signal. Column (S_{02}/S_{01}) gives the variation of the sensitivity due to heating up to 180 °C, column (S_1/S_{01}) gives the variation of the sensitivity due to first thermal activation up to 500 °C and column (S_2/S_{01}) gives the variation of the sensitivity due to second thermal activation up to 500 °C. Due to the very high variation in the cases of (S_1/S_{01}) and (S_2/S_{02}) the mean, minimum and maximum values of the 10 measurements are also given.

Quartz	S_{01} (%)	NTL (%)	S_{02}/S_{01}	S_1/S_{01} min–mean–max	S_2/S_{01} min–mean–max	S_2/S_1 min–mean–max
A1	5.7	2.6	1.26 ± 0.03	1.98–3.7 ± 1.1–5.66	4–7.62 ± 3.4–15	1.44–2.05 ± 0.40–2.10
B2	11.5	5	1.2 ± 0.15	5.5–12.2 ± 4.8–18.9	10–22.37 ± 8.9–35	1.70–1.82 ± 0.06–1.90
Kilkis	21	–	1.01 ± 0.04	15.8–25.2 ± 18.8–60.0	22–34 ± 24.6–81	1.22–1.34 ± 0.10–1.43
Koupa	13	4.6	0.98 ± 0.02	11.8–24.4 ± 10–39.5	13–26.2 ± 10.2–41.5	1.02–1.09 ± 0.05–1.21
S1	4.8	11.7	1.19 ± 0.01	597– 1048 ± 225–1277	709–1203 ± 243–1444	1.12–1.15 ± 0.03–1.19
S2	12.8	6.6	1.16 ± 0.02	3.9–26.6 ± 12.4–44.3	24–60.9 ± 19.3–193	1.80–2.05 ± 0.12–2.16
S3	4.8	4.8	1.06 ± 0.02	15–115.5 ± 73–234	85– 205.7 ± 69.7–310	1.30–1.36 ± 0.04–1.39
S4	5.9	7.5	1.03 ± 0.01	24–80.1 ± 41.8–58	35–114.3 ± 58.8–227	1.31–1.43 ± 0.07–1.45
S6	5.5	2.4	0.89 ± 0.03	19.4–38 ± 14.5–57.9	29–77.3 ± 38.7–138	1.47–2.02 ± 0.27–2.39
S8	6.9	2.1	1.05 ± 0.02	4.1–5.6 ± 1.44–7.8	7–11.4 ± 3.1–16	1.67–2.05 ± 0.25–2.32

Step 5: Give the same TD and measure TL up to 500 °C. This step measures the further sensitization S_2 of the TL glow-peak at 110 °C.

Step 6: Steps 1–5 are applied for 10 different aliquots of the same quartz kind.

The same protocol was used in case of fired samples except for the measurement of NTL. The test dose (TD) administered to each of the 10 quartz samples (both 'as is' and annealed) are presented in Table 2.

3. Experimental results

3.1. "As is" quartz

According to the above mentioned experimental protocol, the sensitivity S_{01} was the "natural" sensitivity obtained without any treatment. The sensitivity S_{02} was due to the heating up to 180 °C, for which the sensitization is considered to be negligible. So, it was generally adopted as the temperature used to erase the TL glow-peak at 110 °C in the most of TL/OSL protocols. The sensitivities S_1 and S_2 were due the first and second thermal activation up to 500 °C correspondingly. Since the quartz samples were not subjected to any previous heating, an abrupt change on the sensitivity of all samples between the first and the second TL measurement was expected. Indeed, this abrupt transition from both the "natural" sensitivity S_{01} and the sensitivity S_{02} without any previous thermal activation to the pre-dosed one S_1 was clearly visible in the case of the TL peak at 110 °C of all quartz samples studied. In a few cases, the sensitization was also extended to the satellite peak at the high temperature part of the 110 °C TL peak.

However, the most interesting result arises from the different level of sensitization that takes place in various aliquots of the same quartz sample. Fig. 1 presents glow curves for the 10 different quartz samples that were subjected to present study. In all plots, curve (a) represents the glow-curve of NTL plus the test dose (S_{02}, step 3, without any thermal activation). Both curves (b) and (c) correspond to the glow-curve after the first thermal activation (S_1, step 4). However, since the sensitization level was not the same throughout all the aliquots of each quartz sample, curve (b) corresponds to the aliquot for which the minimum sensitivity S_1 of 110 °C TL peak was monitored, while curve (c) to the respective aliquot with maximum S_1 sensitivity.

In the present work, all sensitivities were normalized over the "natural" sensitivity S_{01}; this ratio of artificial sensitivities over the "natural" sensitivity (i.e. normalization) will be called sensitization factor hereafter. The results concerning the homogeneity of the pre-dose sensitization effects are summarized in Table 2. The second column [S_{01} (%)] describes the reproducibility of the 10 samples by means of the standard deviation (SD) over the mean value of the 10 S_{01} measurements of the 110 °C TL glow-peak. In the cases of the "as is" quartz the sample reproducibility can be also measured through their NTL signal. This is shown in the third column *[NTL (%)]*. As this column further reveals, except in one case, the reproducibility of the samples based on the TL peak at 110 °C was kept well less than 10%, whereas the results were much better for the NTL signal. The influence of the pre-heat up to 180 °C on the sensitivity of 110 °C TL peak was not seen to be appreciable as depicted in column [S_{02}/S_{01}] of Tables 2 and 3. Therefore, this temperature can be used safely for the thermal cleaning.

Nevertheless, the main interest was revealed by the results of column [S_1/S_{01}], which gives the variation of the sensitization factor due to first thermal activation up to 500 °C. A variation of the sensitization for different quartz types could be expectable. However, the sensitization factor between different aliquots of the same quartz type was also widely varying. This variation was well beyond expectation, based on the original state and origin of the samples, as well as, on the good reproducibility resulted from the TL of 110 °C TL peak and the NTL shown in Table 2 and discussed above. The results of column [S_2/S_{01}], which provides with the variation of the sensitization due to second thermal activation up to 500 °C, behave similarly. So, the second pre-dose measurement confirms the variation observed in its first measurement of this emission in case of all the samples.

3.2. Quartz fired at 900 °C

Results for annealed quartz samples are presented in Fig. 2 and Table 3. Similar to Fig. 1, in all plots curve (a) represents the glow-curve measured without any previous stimulation, according to step 3 of the protocol (S_{02}). Both curves (b) and (c) correspond to the glow-curve indicating the minimum and maximum sensitization respectively after the first thermal activation ($S1$, step 4). The first dose acts as pre-dose and so the sensitization recorded in this case will be the pre-dose sensitization. However in some cases like samples B2 and S6 it was negligible. Nevertheless, in other quartz samples the sensitization was extended to all TL glow-peaks up to 300 °C, without being limited only to the TL glow-peak at 110 °C.

Table 3 summarizes the results concerning the homogeneity of the pre-dose sensitization effects on the annealed samples. Column [S_{01} (%)] describes the reproducibility of the 10 samples by means of the standard deviation (SD) over the mean value of the 10 measurements of the 110 °C TL glow-peak. As it is seen the reproducibility based on the TL peak at 110 °C was kept well less than 10%. The influence of the pre-heat up to 180 °C on the sensitivity of 110 °C TL peak is given in column [S_{02}/S_{01}], where one can see that in 7 over the 10 quartz samples the influence was less than

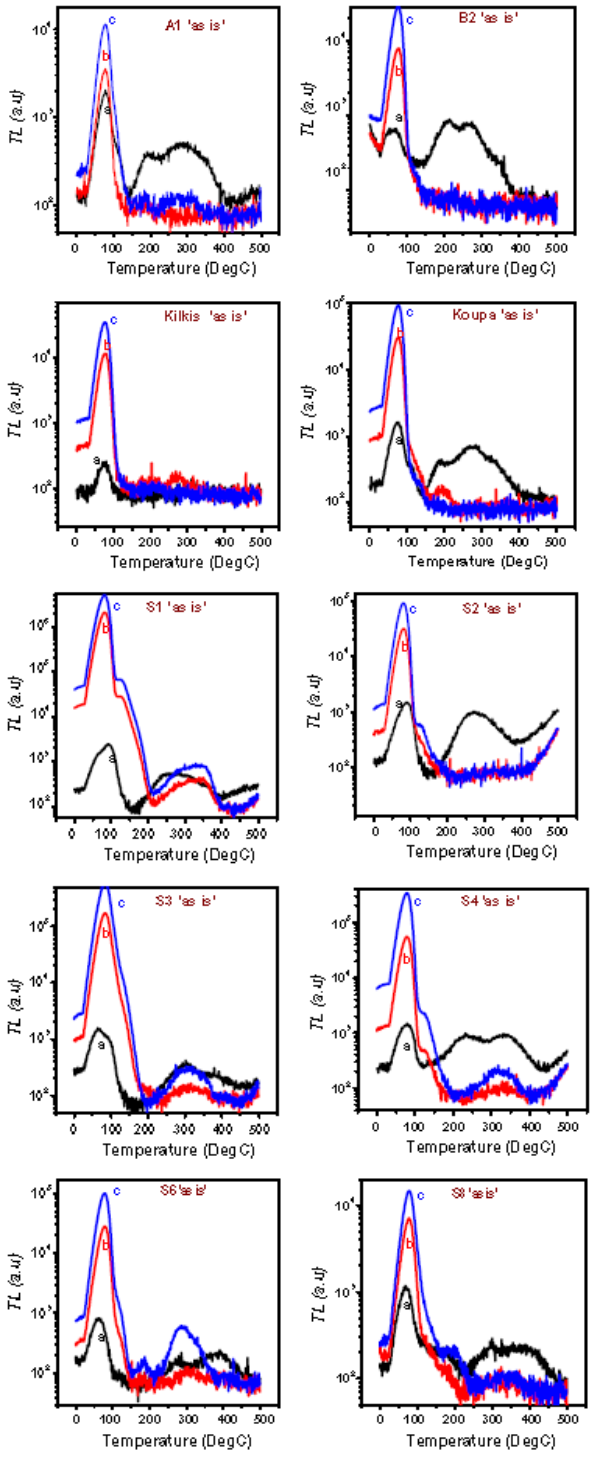

Fig. 1. TL glow curves for all 'as is' samples. In each plot, curve (a) corresponds to the sensitization without previous thermal activation (S_{02}). Both curves (b) and (c) correspond to the glow-curve after the first thermal activation (S_1) at 500 °C, indicating the minimum and maximum sensitization respectively. For details of test doses please refer to Table 1.

Table 3
Case of fired quartz: Column S_{01} (%) describes the reproducibility of the 10 samples by means of (Standard Deviation/Mean). Column (S_{02}/S_{01}) gives the variation of the sensitivity due to heating up to 180 °C, column (S_1/S_{01}) gives the variation of the sensitivity due to first thermal activation up to 500 °C and column (S_2/S_{01}) gives the variation of the sensitivity due to second thermal activation up to 500 °C.

Quartz	S_{01} (%)	S_{02}/S_{01}	S_1/S_{01}	S_2/S_{01}
A1	6	1.124 ± 0.014	55.9 ± 2.76	83.9 ± 3.8
B2	9	1.001 ± 0.005	1.46 ± 0.05	1.84 ± 0.13
Kilkis	14	1.21 ± 0.12	13.67 ± 1.65	18.86 ± 3.18
Koupa	8	1.24 ± 0.06	27.21 ± 2.2	34.8 ± 3.07
S1	5.6	1.005 ± 0.007	5.21 ± 0.18	8.31 ± 0.34
S2	6.5	1.11 ± 0.008	17 ± 1.07	21.5 ± 1.7
S3	5.1	1.01 ± 0.006	8.38 ± 0.3	11.9 ± 0.5
S4	13	0.95 ± 0.01	4.8 ± 0.35	5.75 ± 0.4
S6	5.4	0.97 ± 0.001	1.21 ± 0.03	1.34 ± 0.03
S8	4.7	1.007 ± 0.02	2.83 ± 0.06	2.89 ± 0.07

5% and in other 3 cases it is extended up to 20%. Therefore, this temperature can be used safely for the thermal cleaning of the 110 °C TL glow-peak for annealed samples as well.

Once again, the main interest arises from the data of column [S_1/S_{01}], which describes the variation of the sensitivity due to first thermal activation up to 500 °C. In the case of fired quartz and contrary to what was observed for "as is" quartz, there was an excellent reproducibility of the sensitization factor between the 10 measurements of each quartz sample. The results of column (S_2/S_{01}), which gives the variation of the sensitivity due to second thermal activation up to 500 °C, gave also a better than the as-is sample reproducibility in the sensitization factor.

4. Discussion

The sensitization of a quartz sample is influenced by its thermal and radiation history. The original quartz samples were not of sedimentary origin, but instead large crystals of hydrothermal and metamorphic origins which occurred in vein-associated metamorphic rocks. Consequently, the different grains of the same sample were subjected to the same conditions of both heating and irradiation. Therefore, based on their origin, similar pre-dose sensitization was expected for various aliquots derived from these samples. In order to explain the large variation in the sensitization observed in case of various aliquots of a sample the following phenomena are proposed.

The sensitization of the same quartz samples after annealing does not yield the same discrepancy, indicating the importance of heating to reduce the in-homogeneity. The most probable cause could be the gridding and milling of the samples. In general, any treatment of quartz by mechanical actions such as grinding, milling, crushing, sawing and cutting, may result in the production of defect structures [47–50]. These procedures result mostly in the formation of defects such as dislocations in the outer surface of the grains [48]. The surface alterations following a prolonged grinding, which results in significant changes in the physical and chemical characteristics of the material, have been reported in the literature [51]. Formation of free radicals results from the production of large amounts of new fracture surfaces in small quantities of the material. These new surfaces create broken bonds which lay in regions a few nm below the surface.

The defect creation is related to the methods and conditions of treatment [52]. The influence of crushing and milling on TL seems to be minimised if HF treatment is applied, since the near-surface layer is usually removed by HF etching [53]. In the present study, HF etching was not applied. Therefore the creation and presence of these defects affect the TL sensitivity of the as-is samples. However, certain changes seem to occur in the quartz lattice with

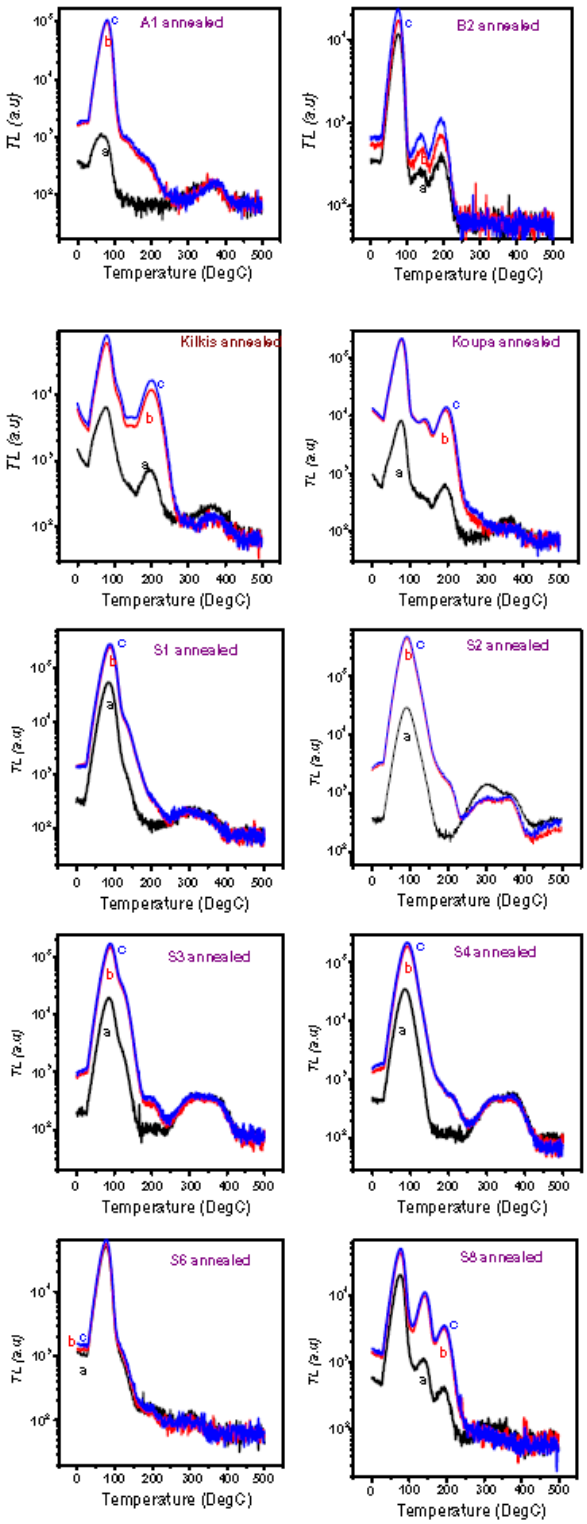

Fig. 2. As in Fig. 1 but for all annealed samples. The details of test doses employed for these measurements are listed in Table 1.

heating at 500 °C, such as annealing of these defects, result in dilution of grinding effects. Therefore, in the case of the annealed samples the sensitization is much more uniform for all aliquots of the same quartz sample. This latter argument is further supported by the column $[S_2/S_1]$ of Table 2 of the 'as is' samples case. Besides the large variation of the sensitization factor S_1 due to first thermal activation up to 500 °C in all quartz samples, the ratio S_2/S_1 of various aliquots is consistent. In 7 out of the 10 quartz samples the standard deviation of the mean ratio S_2/S_1 is less than 7% and in other 3 cases it is extended up to the maximum value of 17%. Therefore, it seems that heating up to 500 °C, even though instantaneous, could merely anneal the dislocations, resulting thus in much more uniform sensitization ratio S_2/S_1.

Despite that 110 °C TL peak in quartz is not stable, a number of applications aside pre-dose dating technique, have been proposed by taking advantage of its sensitization. Among these, Stokes [33] suggested the applicability of the 110 °C TL peak as a sensitivity monitor in a single-aliquot additive dose protocol. A linear relationship between sensitivity changes in the 110 °C TL peak of quartz and in its OSL emission was reported first by Stoneham and Stokes [38], providing evidence for a strong link between the two luminescence signals. Consequently, similar in-homogeneity is expected also to the OSL emission of the same quartz samples. However, implications of this in-homogeneity to OSL are limited due to single aliquot procedures applied. The same insignificant implication applies to the pre-dose dating technique, which is theoretically based on pre-dose sensitization involving (i) single aliquot procedure it involves and (ii) samples extracted from pottery [28].

Nevertheless, the 110 °C TL peak in quartz is used for normalization and sensitivity correction in many multiple-aliquot protocols, such as the foil technique [54]. In the framework of similar protocols, a second TL measurement is performed after the main measurement for each aliquot used. The same dose is applied to all aliquots. The intensity of the 110 °C TL peak of all these second TL measurements is used for both mass reproducibility monitor and correction. Based on the results presented so far in the present study, this procedure could be successfully applied only in the case of heated quartz, although still a relatively increased error is expected. Unfortunately, special caution should be exercised while applying this specific mass reproducibility correction procedure in the case of geological, unfired quartz samples, since it could result in erroneous equivalent dose estimation.

5. Conclusions

The general experimental conclusions for both fired and unfired samples can be summarized as follows: There is a very good homogeneity between the initial sensitivities in both cases of fired and unfired samples. Heating up to 180 °C does not influence the sensitivity of the samples. The homogeneity of the pre-dose sensitization, recorded with various aliquots of the same sample, was observed to be much better in annealed than unfired samples. Even heating up to 500 °C, as incorporated in the TL measurement, was seen to improve the homogeneity of the pre-dose sensitization.

References

[1] M.R. Krbetschek, J. Götze, A. Dietrich, T. Trautmann, Spectral information from minerals relevant for luminescence dating, Radiat. Meas. 27 (1997) 695–748.
[2] A.G. Wintle, Luminescence dating: laboratory procedures and protocols, Radiat. Meas. 27 (5/6) (1997) 769–817.
[3] G.S. Polymeris, D. Afouxenidis, N.C. Tsirliganis, G. Kitis, The TL and room temperature OSL properties of the glow peak at 110 C in natural milky quartz: a case study, Radiat. Meas. 44 (2009) 23–31.
[4] S.A. Petrov, I.K. Bailiff, The '110 C' TL peak in synthetic quartz, Radiat. Meas. 24 (4) (1995) 519.
[5] I.K. Bailiff, The pre-dose technique, Radiat. Meas. 23 (2/3) (1994) 471.
[6] S. Fleming, Thermoluminescence Techniques in Archaeology, Clarendon Press, 1979.

[7] H.Y. Goksu, I.K. Bailiff, V.B. Mikhailik, New approaches to retrospective dosimetry using cementitious building materials, Radiat. Meas. 37 (2003) 323–327.
[8] N. Itoh, D. Stoneham, A.M. Stoneham, The predose effect in thermoluminescent dosimetry, J. Phys.: Condens. Mat. 13 (2001) 2201.
[9] D.K. Koul, G.S. Polymeris, N.C. Tsirliganis, G. Kitis, Possibility of pure thermal sensitization in the pre-dose mechanism of the 110 °C TL peak of quartz, Nucl. Instru. Meth. Phys. Res. B 268 (2010) 493–498.
[10] Z.Y. Han, S.H. Li, M.Y.W. Tso, Effect of annealing on TL sensitivity of granitic quartz, Radiat. Meas. 32 (2000) 227.
[11] C.M. Sunta, M. David, PACT 6 (1982) 460.
[12] D.K. Koul, K.S.V. Nambi, A.K. Singhvi, C.L. Bhat, P.K. Gupta, Feasibility of estimating firing temperature using 110 °C TL peak of quartz, Appl. Radiat. Isot. 6, 191.
[13] G.S. Polymeris, A. Sakalis, D. Papadopoulou, G. Dallas, G. Kitis, N.C. Tsirliganis, Firing temperature of pottery using TL and OSL techniques, Nucl. Instru. Meth. Phys. Res. A 580 (2007) 747–750.
[14] V. Pagonis, E. Tatsis, G. Kitis, G.C. Drupieki, Radiat. Prot. Dosim. 100 (2002) 373.
[15] B. Subedi, E. Oniya, G.S. Polymeris, D. Afouxenidis, N.C. Tsirliganis, G. Kitis, Thermal quenching of thermoluminescence in quartz samples of various origin, Nucl. Instru. Meth. Phys. Res. B 269 (2011) 572–581.
[16] X.H. Yang, S.W.S. McKeever, Characterization of the pre-dose effect using ESR and TL, Nucl. Tracks Radiat. Meas. 14 (1988) 75.
[17] V. Pagonis, G. Kitis, R. Chen, Applicability of Zimmerman predose model in the thermoluminescence of predosed and annealed synthetic quartz samples, Radiat. Meas. 37 (2003) 267.
[18] M. David, Thermoluminescence of quartz – Part VII: radiation sensitization of first peak, Indian J. Pure Appl. Phys. 19 (1981) 1048.
[19] M. David, C.M. Sunta, A.K. Ganguly, TL of quartz part II: sensitization by thermal treatment, Indian J. Pure Appl. Phys. 15 (1977) 277.
[20] X.H. Yang, S.W.S. McKeever, The pre-dose effect in crystalline quartz, J. Phys. D: Appl. Phys. 23 (1990) 237.
[21] A.G. Wintle, A.S. Murray, Luminescence sensitivity changes in quartz, Radiat. Meas. 30 (1999) 107–118.
[22] T. Schilles, N.R.J. Poolton, E. Bulur, L. Botter-Jensen, A.S. Murray, G.M. Smith, P.C. Riedi, G.A. Wagner, A multi-spectroscopic study of luminescence sensitivity changes in natural quartz induced by high temperature annealing, J. Phys. D: Appl. Phys. 34 (2001) 722.
[23] R. Chen, X.H. Yang, S.W.S. McKeever, Strongly superlinear dose dependence of thermoluminescence in synthetic quartz, J. Phys. D: Appl. Phys. 21 (1988) 1452.
[24] C. Charitidis, G. Kitis, C. Furetta, S. Charalambous, Superlinearity of synthetic quartz; dependence on predose, Radiat. Prot. Dosim. 84 (1–4) (1999) 95–98.
[25] C. Charitidis, G. Kitis, C. Furetta, S. Charalambous, Superlinearity of synthetic quartz; dependence on the firing temperature, Nucl. Instru. Meth. Phys. Res. B 168 (2000) 404–410.
[26] G. Polymeris, G. Kitis, V. Pagonis, 2006. The effects of annealing and irradiation on the sensitivity and superlinearity properties of the 110 °C thermoluminescence peak of quartz, Radiat. Meas. 41 (2006) 554–564.
[27] G. Kitis, V. Pagonis, R. Chen, G.S. Polymeris, A comprehensive comparative study of the pre-dose effect for three quartz crystals of different origins, Radiat. Prot. Dosim. 119 (1–4) (2006) 438.
[28] J. Zimmerman, The radiation-induced increase of the 110 °C thermoluminescence sensitivity of fired quartz, J. Phys. C: Solid State Phys. 4 (1971) 3265.
[29] R. Chen, P.L. Leung, Modeling the pre-dose in thermoluminescence, Radiat. Prot. Dosim. 84 (1999) 43.
[30] R.M. Bailey, Towards a general kinetic model for optically and thermally stimulated luminescence of quartz, Radiat. Meas. 33 (2001) 17.
[31] R.M. Bailey, Paper I – Simulation of dose absorption in quartz over geological time scales and its implication for the precision and accuracy of optically dating, Radiat. Meas. 38 (2004) 299.
[32] R. Chen, V. Pagonis, Modelling thermal activation characteristics of the sensitization of thermoluminescence in quartz, J. Phys. D Appl. Phys. 37 (2004) 159–164.
[33] S. Stokes, The timing of OSL sensitivity changes in a natural quartz, Radiat. Meas. 23 (1994) 593–600.
[34] A.S. Murray, R.G. Roberts, Measurement of the equivalent dose in quartz using a regenerative-dose single aliquot protocol, Radiat. Meas. 29 (1998) 503–515.
[35] A.S. Murray, A.G. Wintle, Luminescence dating of quartz using an improved single-aliquot regenerative-dose protocol, Radiat. Meas. 32 (2000) 57–73.
[36] A.G. Wintle, A.S. Murray, A review of quartz optically stimulated luminescence characteristics and their relevance in single-aliquot regeneration dating protocols, Radiat. Meas. 41 (2006) 369–391.
[37] M.J. Aitken, B.W. Smith, Optical dating: recuperation after bleaching, Quatern. Sci. Rev. 7 (1988) 387–393.
[38] D. Stoneham, S. Stokes, An investigation of the relationship between the C TL peak and optically stimulated luminescence in sedimentary quartz, Nucl. Tracks Radiat. Meas. 18 (1991) 119–123.
[39] L. Bøtter-Jensen, N. Agersnap Larsen, V. Mejdahl, N.R.J. Poolton, M.F. Morris, S.W.S. McKeever, Luminescence sensitivity changes in quartz as a result of annealing, Radiat. Meas. 24 (1995) 535–541.
[40] G. Chen, S.-H. Li, A.S. Murray, Study of the 110 °C TL peak sensitivity in optical dating of quartz, Radiat. Meas. 32 (2000) 641–645.
[41] N.G. Kiyak, G.S. Polymeris, G. Kitis, Component resolved OSL dose response and sensitization of various sedimentary quartz samples, Radiat. Meas. 42 (2007) 144–155.
[42] N.G. Kiyak, G.S. Polymeris, G. Kitis, LM-OSL thermal activation curves of quartz: relevance to the thermal activation of the 110 °C TL glow peak, Radiat. Meas. 43 (2008) 263–268.
[43] W.A. Deer, R.A. Howie, W.S. Wise, J. Zussman, Rock-Forming Minerals, Framework Silicates: Silica Minerals, Feldspathoids and the Zeolites, second ed, 4B, The Geological Society, London, 1994.
[44] F. Preusser, M. Chithambo, T. Götte, M. Martini, K. Ramseyer, E.J. Sendezera, G.J. Susino, A.G. Wintle, Quartz as a natural luminescence dosimeter, Earth Sci. Rev. 97 (2009) 184–214.
[45] G.A.T. Duller, Distinguishing quartz and feldspar in single grain luminescence measurements, Radiat. Meas. 37 (2003) 161–165.
[46] L. Botter-Jensen, E. Bulur, G.A.T. Duller, A.S. Murray, Advances in luminescence instrument systems, Radiat. Meas. 32 (2000) 523–528.
[47] S.W.S. McKeever, Thermoluminescence of Solids, Cambridge University Press, Cambridge, 1985.
[48] A.H. Ranjbar, S.A. Durrani, K. Randle, Electron spin resonance and thermoluminescence in powder form of clear fused quartz; effects of grinding, Radiat. Meas. 30 (1999) 73–81.
[49] A. Takeuchi, H. Nagahama, T. Hashimoto, Surface resetting of thermoluminescence in milled quartz grains, Radiat. Meas. 41 (7–8) (2006) 826–830.
[50] A. Takeuchi, T. Hashimoto, Milling-induced reset of thermoluminescence and deformation of hydroxyl species in the near-surface layers of quartz grains, Geochronometria 32 (2008) 61–68.
[51] S. Battaglia, M. Fanzini, L. Leoni, Influence of grinding methods on the 101 X-ray powder diffraction line of a-quartz: in methods and practices in X-ray powder diffraction, ICDD, USA, 1993.
[52] T.S. Bartnitskaya, M.V. Vlasova, V.B. Zelyavskii, N.G. Kakazei, A.V. Kurdyumov, L.L. Sukhikh, V.I. Chistyakov, Defect structure formation in silicon on grinding, Soviet Powder Metall. Ceram. 31 (1992) 903–907.
[53] T. Nakagawa, T. Hashimoto, Sensitivity changes of OSL and RTL signal from natural quartz with annealing treatment, Radiat. Meas. 37 (2003) 397–400.
[54] C.T. Michael, N. Zacharias, Y. Maniatis, D. Dimotikali, A new technique (foil technique) for measuring the natural dose in TL dating and its application in the dating of a mortar containing ceramic fragments, Ancient TL 15 (2–3) (1997) 36–42.

APPENDIX 2

Phys. Status Solidi A 210, No. 11, 2463–2470 (2013) / DOI 10.1002/pssa.201329177

Influence of entire glow-curve structure of quartz on MATAC of its 110 °C TL glow peak

Ebenezer O. Oniya[*,1,2,3], George S. Polymeris[,2], Nnamdi N. Jibiri[3], Nestor C. Tsirliganis[2], Israel A. Babalola[3], and George Kitis[4]**

[1] Physics and Electronics Department, Adekunle Ajasin University, PMB 01, 342111, Akungba Akoko, Nigeria
[2] Laboratory of Radiation Applications and Archaeological Dating, Department of Archaeometry and Physicochemical Measurements, R.C. "ATHENA", Tsimiski 58, 67100 Xanthi, Greece
[3] Department of Physics, University of Ibadan, Ibadan, Nigeria
[4] Aristotle University of Thessaloniki, Nuclear Physics Laboratory, 54124 Thessaloniki, Greece

Received 13 March 2013, revised 15 July 2013, accepted 18 July 2013
Published online 2 September 2013

Keywords glow curve, predose effect, quartz, radiation quenching, thermal activation curve, thermoluminescence

* Corresponding author: e-mail eoniya@hotmail.com, Phone: +2348035033421
** e-mail polymers@auth.gr, Phone: +306974470133

Understanding the complex nature of luminescent characteristics of quartz requires adequate knowledge of charge trafficking among electron and hole traps during excitation and stimulation of materials. These quantities, which are difficult to measure and mostly studied through modelling and theoretical approaches, influence the charge trafficking among the traps. This study aimed at employing a designed TL sequence, with a focus on reservoirs and competitors, to study factors affecting the shape of thermal activation curve/characteristics (TACs) of the 110 °C TL glow peak of quartz. The materials under investigations were two quartz samples from Nigeria that were annealed at 800 °C for 1 h. The results showed the structure of the TAC to be related to the nature of the glow curves (in particular high peaks) obtained during the thermal activation. The roles of reservoirs and competitors in luminescence characteristics have been used to explain the property of the 110 °C TL peak of two quartz samples in the present study. This report is among the first experimental attempts to monitor effects directly correlated to the presence of these concepts.

1 Introduction Modelling of the properties and applications of the thermoluminescence (TL) glow peak at "110 °C" is a widespread field of study in TL and optically stimulated luminescence (OSL) research [1–8]. Existing models are generally divided into two groups, one dealing with the TL dose response properties, whereas the second group studies the predose effect. In most cases, the TL dose response of the 110 °C TL glow peak is explained by models involving competition during both irradiation and heating stages by giving much attention to the competition during heating in cases of a high degree of superlinear TL dose response [1, 9, 10]. On the other hand, the predose sensitization is explained by models involving a thermal transfer of holes from holes traps known as reservoirs (R-centers) to recombination centers [11]. Recombination centers that produce visible light are called luminescence centers (L-centers). Any electron traps that are thermally disconnected in the temperature region at which the TL glow peak at "110 °C" is excited act as competitor. Usually, they are relatively deep traps; those with measurable maximum temperature (T_m) around 350–500 °C. Very deep traps (VDT) with $T_m > 500$ °C also act as competitor. The concept of a reservoir could include any hole trap that is thermally excited and releases holes into the valence band when the temperatures exceed 200 °C.

In general, mechanisms of the luminescence of quartz as a natural dosimeter are full of complexity [1, 2, 4, 12]. One way towards comprehending this intricacy is to understand the system of charge trafficking during each step of treatments administered to quartz in luminescence measurements. This charge interchange basically involves swapping of electrons and holes among the measurable electron traps

and hole centers, inclusive of competitors and reservoirs within the material. Unlike the common electron traps and hole centers that are experimentally quantifiable, reservoirs and competitors associated with VTD have been so far a conceptual idea of TL and OSL theory and modelling. The idea of charge trafficking among competitors and reservoirs has been employed to explain many issues in luminescence characteristics. Among these are supralinearity [1], thermal sensitization [13], predose sensitization [11] and even some complicated phenomena in predose effects like UV reversal and radiation quenching.

The complex luminescence nature of quartz has invariably led to multifarious opinions and models that are proposed on some luminescent phenomena. An example is the predose effect that it is a well-established technique in both retrospective dosimetry and dating [11, 14]. Zimmerman [11], in her own case suggested that the UV reversal is associated with the transfer of holes from L-traps to R-traps during exposure of sample to UV light. By contrast, McKeever [15] linked UV reversal to the optical release of electrons from deep traps that recombine with captured holes in $(H_3O_4)^0$ centers.

Furthermore, two different models have been utilized to explain radiation quenching effect. Using the Zimmerman [11] model, Aitken [16], attributed the radiation quenching effect to the removal of holes captured at L-centers as recombination occurs during irradiation leading to diminution in sensitivity of subsequent luminescence measurement. This model is contrary to the model of Bailey [3] in which he proposed that recombination is allowed at the R-center unlike the model of Zimmerman [11], and that the concentration of holes captured at both L- and R-centers increases with dose. Using these, he argued that it is an increase in competition for free charges, during both irradiation with test dose (TD) and during heating (TL readout) from the R-centers that produces the quenching effect.

Another issue that has been a subject of concern is the mechanism behind the usual decrease in value of the sensitivity in multiple aliquots thermal activation curve (MATAC) of the 110 °C TL peak of quartz after the maximum thermal activation temperature (TAT) [12, 19–23]. Aitken [16] attributed this to thermal deactivation, which he presumed to be due to a direct thermal eviction of holes from L-centers into the valence band. Conversely, this is contrary to the predose model in which L-center is assumed to be much further from the valence band so that once a hole is captured at an L-center, it cannot be thermally released back to the valence band. Figel and Geodicke [19] proposed a model that takes care of the possibility of thermal eviction of holes from L-centers into the valence band. These authors argued that recombination of electrons captured at high TL peaks beyond the maximum TAT during further thermal activation will lead to depletion of already enriched captured holes at L-centers. Consequently, a reduced TL sensitivity will follow. Lastly, a model of probable recombination of electrons at L-centers during subsequent irradiation after thermal activation was proposed by Chen and Pagonis [12] to explain this nominal decrease of sensitization after TAT.

Based on the model of Figel and Geodicke [19], it is herein envisaged that the structure of the glow curve of thermal activation TL if recorded (which is quantifiable measure of the recombination process) should be related to MATAC. Therefore, this study aimed at employing a designed TL sequence with a focus on charge trafficking among reservoirs and competitors to study the factor responsible for the shape of MATAC of the 110 °C TL glow peak of quartz. This work, which is among the first experimental attempts to directly monitor effects associated with the presence of reservoirs and competitors, is envisaged to shed more light on the complex nature of quartz luminescence generally.

2 Materials and methods

2.1 Sample preparation Two different quartz samples collected from Oro, in Kwara State and Ijero Ekiti, in Ekiti State, all from Nigeria, were analysed in this work. They were given laboratory names S2 and S4, respectively. Grains of dimensions 90–150 μm were obtained from each natural crystal quartz samples, after smashing in an agate mortal and sieving. It is desirable in this work that the samples should have known radiation and thermal histories. Hence, the known radiation and thermal history are both obtained by a high-temperature annealing. The samples were annealed at 800 °C for 1 h. This temperature was selected because it erases any history and, furthermore, it is lower than the temperature of about 870 °C, where an irreversible phase change takes place in quartz. Mass reproducibility was strictly kept within 3–5%.

All the TL and OSL measurements on the quartz samples were carried out using a RISØ TL/OSL reader (model TL/OSL–DA–15) equipped with a 0.075 Gy/s $^{90}Sr/^{90}Y$ β-ray source [24]. The reader was fitted with a 9635QA photomultiplier tube. The detection optics consisted of a 7.5-mm Hoya U-340 ($\lambda_p \sim 340$ nm, FWHM 80 nm) filter. All measurements were performed in a nitrogen atmosphere with a constant heating rate of 1 °C s^{-1} in order to avoid significant temperature lag, up to a maximum temperature of 500 °C. The test dose and range of doses administered to each of the quartz samples are accordingly indicated in the experimental protocol presented below.

2.2 Experimental protocol The experimental protocol used in this study and the respective implications of each step of the protocol on mechanisms describing 110 °C TL peak characteristics are presented in Table 1. Test dose s(TD) administered to S2 and S4 samples were 1 and 0.5 Gy, respectively.

3 Results Each experimental point presented in this section is an average value of two TL runs made on two separate aliquots. The standard deviation in all cases was less than 5% of the respective mean value. Glow curves shown in

Table 1 Experimental protocol used in this study.

step	description	significance
1	give test dose (TD) to an aliquot and TL readout up to 180 °C	meant for mass normalization
2	give a predose of 20 Gy to the same aliquot	pre-exposure dose is delivered
3	TL readout up to temperature T_i that is activation temperature for the predose sensitization	thermal activation to different TATs of pre-exposure dose leading to predose effect sensitization
4	give dose D_i to the same aliquot (i −TD, 2TD, 4TD, 8TD, 16TD, 32TD, 64TD Gy)	hole and electron traps are filled. also, loss of electrons through recombination takes place during irradiation [12]
5	TL readout up to 180 °C on the same aliquot	loss of captured holes at the L-centers due to recombination that produces 110 °C TL signal takes place
6	give TD and TL readout up to 500 °C	measures sensitivity resulting from previous steps
7	repeat steps 1–6 for a new aliquot and a new dose D_i but at the same activation temperature T_i	additive dose of step 4 is varied.
8	repeat steps 1–7 for a new aliquot and a new activation temperature T_i (180, 250, 300, 350, 400, 450 and 500 °C)	at different TATs (i) all traps in the temperature below T_i are emptied, (ii) transfer of holes from R-center to L-center for TAT between 250 °C and T_i causes sensitization and (iii) electrons which are depleted from traps below temperature range of T_i recombine with holes at L-centers

Fig. 1 resulted from TL of step 3 for the two samples. This figure is a product and evidence of recombination of the captured electrons at the respective TL traps with the available captured holes at the L-centers during thermal activation of step 3. The overall TL dose-response curves of the 110 °C TL glow peak obtained from steps 4 and 5 for the two samples are similar. The index $f(D)$ [25] in Eq. (1) was evaluated to test the linearity of the dose-response curves. The plots of index $f(D)$ for the two samples are shown in Fig. 2. As this figure reveals, S2 is sublinear even for the lowest dose for all TATs except for that of 180 °C TAT that is linear up to 2 Gy. On the other hand, S4 is sublinear throughout with the exception of 250 and 500 °C TATs that are linear up to 1 and 2 Gy, respectively.

$$f(D) = \frac{(\mathrm{TL}_i/D_i)}{(\mathrm{TL}_1/D_1)}, \qquad (1)$$

where $\mathrm{TL}_i(D)$ is the sample TL response corresponding to dose D_i, and D_1 is the normalization dose in the initial linear region, $f(D_1)$ is the sample TL response corresponding to dose D_1 (by this definition $f(D) > 1$, $f(D) = 1$, and $f(D) < 1$, respectively, imply supralinearity, linearity and sublinearity).

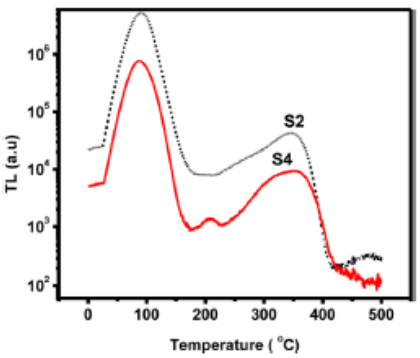

Figure 1 Glow curves recorded during thermal activation to 500 °C of step 3 for the two samples.

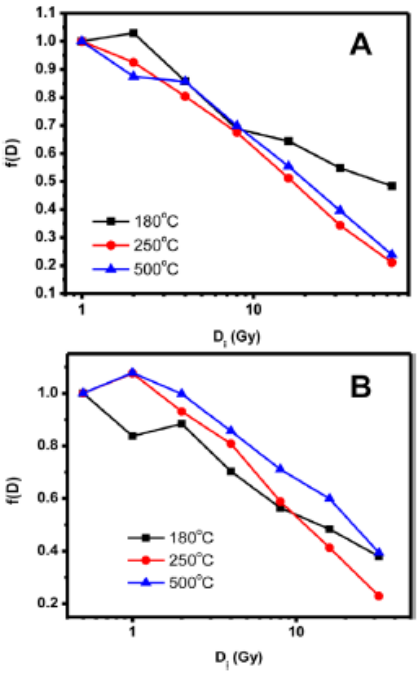

Figure 2 Representative of factor $f(D)$ versus dose for three TATs: (A) and (B) for S2 and S4 samples, respectively.

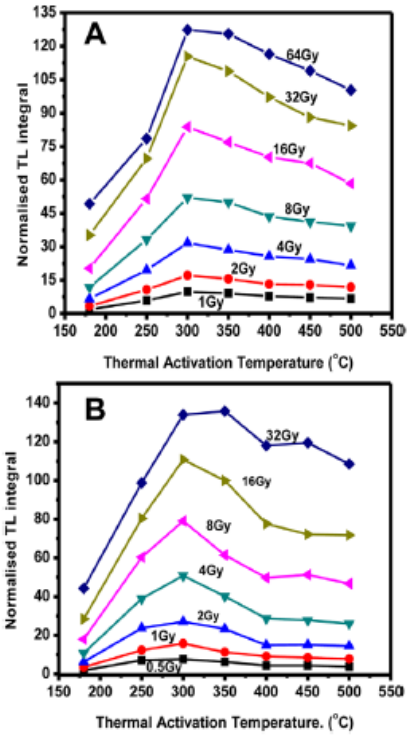

Figure 3 MATACs as a function of dose, normalized over the initial signal of step 1 of the protocol: (A) and (B) for S2 and S4 samples, respectively.

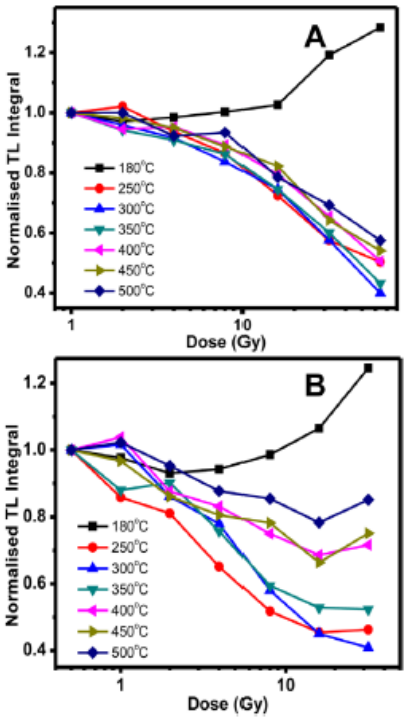

Figure 4 Sensitivity to TD of the TL glow peak at 110 °C following the additive dose of step 6: (A) and (B) for S2 and S4 samples, respectively. Recall that this is not a dose-response curve. The doses in the figure were only employed to identify each aliquot with additive doses D_i of the previous step 4. Each curve was normalized to the signal of 180 °C TAT for all doses D_i.

Figure 3 shows the clear differentiation in sensitivity at diverse TATs where the integrated TL output of the TL glow peak at 110 °C is plotted as a function of TAT for various doses. The results are very interesting since the structure of MATAC does not depend on the additive doses. Nevertheless, the thermal sensitization of both samples under consideration in this work attains a maximum TAT at 300 °C and thereafter decreases in value versus TATs.

The outputs of a fixed TD and TL of step 6 following additive doses and TL of steps 4 and 5, respectively, for 110 °C TL peak are shown in Fig. 4. Since an equal fixed TD was applied to all the aliquots, Fig. 4 provides a measure of sensitization (sensitivity monitor) arising from the combined effect of steps 1–5. It is evident from this figure that it is only TAT of 180 °C that shows a sense of sensitization for both S2 and S4. It is desensitization in general that is exhibited for the remaining TATs with additive doses. However, there is a slight increase in sensitivity at 32 Gy after the peak of desensitization at 16 Gy in S4 sample. This desensitization is well illustrated in Fig. 5.

The net degree of relatively deep electron traps (TL peaks between 350 and 500 °C) filling is reflected in the integrated TL output from 180 up to 500 °C in the glow-curve obtained in step 6. These results are shown in Fig. 6 for the two quartz samples used. Unlike that of the 110 °C (Fig. 4), the TL of high TL peaks, in its case, is a dose-response curve. Basically, TL of step 6 for the high-temperature TL peak is the combined product of doses resulting from additive doses of step 4 and the TD of step 6 together with the unclean part of predose of 20 Gy depending on the TAT of step 5. As is seen in Fig. 6, the TL of the high-temperature TL peaks due to the predose of 20 Gy is not thermally cleaned for TATs in the range between 180 and 300 °C. Most especially in S4, the additive doses up to 2 Gy in step 4 cannot be distinguished from the predose of 20 Gy, so the TL output is more or less stable. However, as the additive dose exceeds 4 Gy the new TL is increased above the level of that that is due to 20 Gy. For TAT above 400 °C the TL of the high-temperature TL peaks is thermally cleaned, so that the series of doses in step 4 induces the well-known TL dose-response curves.

The glow curves obtained for each aliquot for all TATs and dose D_i used in the present study can be grouped into four. Since the overall results of S2 and S4 are nearly identical, each plot in Fig. 7 of S4 is used to represent each group for the two samples. For the two figures, plot (A) is for aliquot with TAT 180 °C and dose D_i of TD (0.5 Gy), (B) is aliquot with TAT of 180 °C and dose D_i of 8 Gy, (C) is aliquot with TAT of 450 °C and dose D_i of TD (0.5 Gy), and

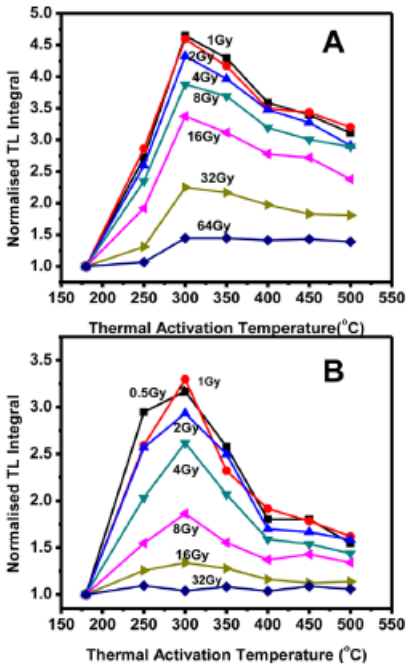

Figure 5 MATACs as a function of preceding additive dose: (A) and (B) for S2 and S4 samples, respectively. The doses in Gy were employed to identify each aliquot with additive doses D_i of previous step 4. Each curve was normalized to the signal of 180 °C TAT for all doses D_i.

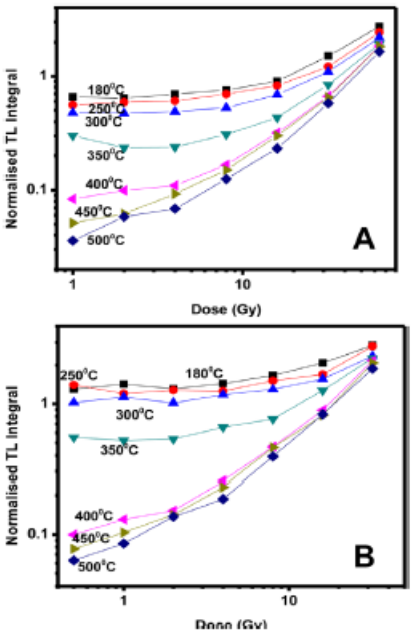

Figure 6 Integrated TL light output of the TL glow peak above 150 °C as a function of dose: (A) and (B) for S2 and S4 samples, respectively. Each curve corresponds to TATs in °C, which acts as a partial thermal cleaning of the TL due to a predose of 20 Gy.

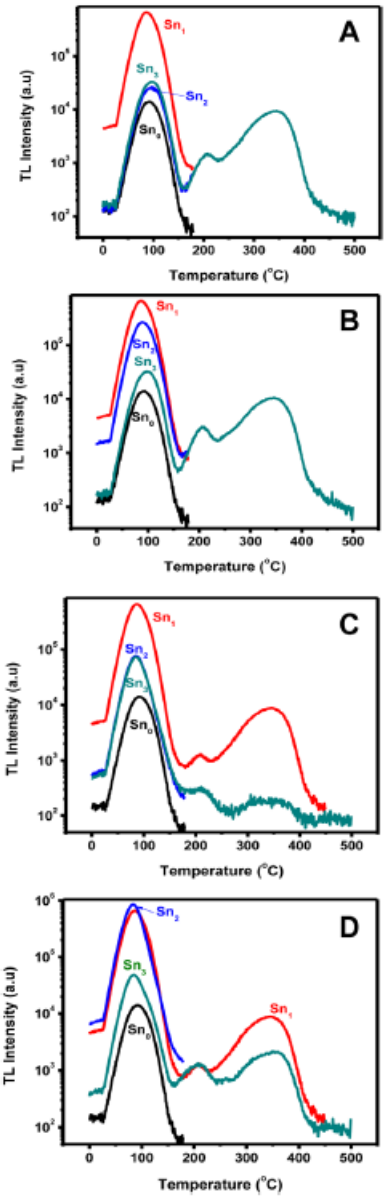

Figure 7 TL glow curves showing sensitizations of each step of TL reading of the protocol for S4. In all Sn_0, Sn_1 Sn_2 and Sn_3 represent glow curve of Steps, 1, 3, 5 and 6, respectively of: (A) aliquot with TAT 180 °C and dose D_i TD (0.5 Gy), (B) aliquot with TAT 180 °C and dose D_i 8 Gy, (C) aliquot with TAT 450 °C and dose D_i TD (0.5 Gy), (D) aliquot with TAT 450 °C and dose D_i 8 Gy.

lastly (D) is aliquot with TAT of 450 °C and dose D_i of 8 Gy (refer to Fig. 7).

4 Discussion All the observed results above can be explained by understanding the effects of each step of the protocol on mechanisms of the 110 °C TL peak

characteristics in general. In plot (A) Fig. 7, none of the curves was previously heated beyond 180 °C. Thus, they are not thermally sensitized. Sn_0 that received only a TD possesses the least response as expected. In that order, Sn_1 that received 20 Gy has the highest response. Since Sn_2 and Sn_3 were not previously and thermally sensitized and only received a TD, they are expected to yield the same response as Sn_0, by contrast with the higher sensitivity they possess than Sn_0. The reason for this is simply due to the competition effect that is evident in the massive filling of the high-temperature part of Sn_3. This is unnoticeable in S2, thus implying that the competition effect is more prevalent in S4 than S2. The higher sensitivity of Sn_2 in Plot (B) is justified by the higher TD (16TD) it received more than that of its counterpart in plot (A). The exact competition effect, as explained above, offers Sn_3 higher sensitivity over Sn_0. What makes plot (C) different from plot (A) is the TAT of 450 °C the former received. The consequential effect of this is the predose sensitization arising from the contribution of the reservoir when its thermally released holes are subsequently captured in the L-center. This fact offers Sn_2 and Sn_3 higher sensitization in plot (C) than what is portrayed in plot (A). The only difference between plots (C) and (D) is the 16-fold of dose D_i that the latter received than the former. The effect of this is reflected in the high signals of Sn_2 and the high-temperature aspect of Sn_3 of plot (D). It is worthy of note that Sn_2, having been thermally sensitized, possesses a more intense signal than Sn_1 that received higher dose (20 Gy), mainly because Sn_1 was not thermally sensitized in its case. The sensitivity of the 110 °C TL peak shown in Fig. 3 is a product of two factors. The thermal activation in step 3 causes (i) sensitization resulting from transfer of holes from the R-center to the L-center (predose effect) and (ii) desensitization because of the competition effect from depletion of electron traps that are unstable up to TAT. The model of Figel and Geodicke [19] is employed to explain the usual decrease in the MATAC beyond the maximum TAT that is also observed in this study. In view of the results reported by Chen and Pagonis [12], these authors commented that it is hard to tell whether the peak shape of the TAC reported by Figel and Goedicke [19] results indeed from the thermal release of electrons from the competitor as suggested by them, or would be observed anyway, without the thermal release from the deep traps. There are two ways to verify this. The first is to find out if recombination takes place during the thermal activation process. The second way is to check if the structure of the glow curves (mainly high temperature peaks) recorded during TAC, is related to their respective MATACs of the 110 °C TL peak. Each of the glow curves in Fig. 1 and Sn_1 in plots (C) and (D) of Fig. 7, which is a product of TL recorded during thermal activation to 500 °C of step 3, provides evidence of recombination during the thermal activation process. The other verification can be observed in the structure of the high-temperature peak in the glow curves of S2 and S4 samples in Fig. 1 as compared with their respective MATACs in Fig. 3.

With reference to Fig. 1, a temperature of 410 °C forms the rising part of another TL peak around 490 °C for S2 that is absent in S4. Thus, this implies that the loss of sensitization due to recombination of electrons at L-centers will reduce drastically beyond 400 °C for S4 as compared with S2 since the ~490 °C TL peak of S2 will still contribute to the additional loss of sensitization. The outcome of this for S4 is the sharp transition in its MATAC at 400 °C, whereas this is missing in S2, as is evident in Fig. 3. The abrupt drop off in the gradual loss of sensitization that remains more or less stable up to 500 °C in S4 that is absent in S2 is a product of this. In agreement with the above fact, a similar observation, even a sharper transition of sensitization at 400 °C, is demonstrated in TL of step 6 following a fixed TD (Fig. 5).

The high-temperature peak of 610 °C that Figel and Geodicke [19] calculated in their theoretical work was always higher than the maximum TAT of the TACs, although, such high temperature peak can rarely be observed experimentally. The high-temperature peak for the two understudied samples here are about 350 °C, while the temperature of the maximum TAT of the TACs is 300 °C. Based on their model, the depletion of occupied holes at L-centers in the process of recombination of captured electron at TL peaks reaches its maximum at the temperature of the high TL peak. Therefore, the decrease in the MATACs of the 110 °C TL peak must take place before this temperature. Thereby, this offers the temperature of the high TL peak to be always higher than the maximum TAT of the TACs.

It can be summarized that this effect (i.e. loss of holes at L-centers due to recombination of electrons with captured holes at L-centers during thermal activation) takes place concurrently with the transfer of holes from R-centers to L-centers (predose effect), starting from the onset of thermal activation. It merely happens that the latter stops suppressing the former when the maximum TAT is reached. If this has not taken place, a plateau is expected according to the predose effect.

The results presented in this work for the two quartz samples seem to be the first experimental confirmation of the Figel and Geodicke [19] model by considering the relationship between MATACs and glow curves. Also, this report is among the first experimental attempts to monitor effects directly correlated to the presence of reservoirs and competitors. It should be clearly stressed here that the model of Chen and Pagonis [12] to explain the usual decrease of sensitization after TAT, is not disputed by this work. Rather, the model of these authors is difficult to establish experimentally within the scope of this work.

The observed desensitization with additive dose of dose-response curves in Fig. 4 and MATACs in Fig. 5 deserves plausible explanations. The sensitization due to competitor is distinguished from that of thermal activation in aliquots with 180 °C TAT for the two samples as depicted in Fig. 4 as well as Sn_2 and Sn_3 in both plots (A) and (B) of Fig. 7. Thermal activation has little effect on these sets of samples since they

were never heated beyond 180 °C. Likewise, the concentration of electrons in deep traps that are due to the accumulated dose resulting from predose of 20 Gy, additive dose D_i, and the fixed TD are intact up to the TL readout up to 180 °C of step 6 (Sn_3 in plots (A) and (B) of Fig. 7). Consequently, any changes in its sensitivity are solely due to the competition effect that in turn is a function of deep traps filling. Hence, as the dose D_i increases the concentration of electrons in deep traps, which can act as potential competitors, also increases. In other words, the available numbers of competitors are decreased. According to the competition idea when the number of competitors is decreased the sensitivity of the TL peak (the 110 °C in the present case) due to the active trap is expected to increase [1, 9, 10]. This competition model is verified by the results of 180 °C TAT that show an increase in sensitization to the fixed TD. In Fig. 7, this causes sensitization of both curves Sn_2 and Sn_3 over Sn_0 in plot (A) and also Sn_3 over Sn_0 in plot (B). Furthermore, no other factor than this effect could have caused the sensitization of Sn_2 to be higher than that of Sn_3 in plot (A) of Fig. 7 based on existing models.

Conversely, a decrease of sensitization with additive doses D_i for TAT of 250 to 500 °C is exhibited by the two samples. At any rate, this observation is explainable in view of the fact that predose sensitization could not be derived from the additive dose D_i of step 4 since it was never activated up to this point of step 6. Accordingly, the desensitization is consequently traceable to case (ii) above only and, in fact, caused by the "radiation quenching" phenomenon. Going by way of the model suggested by Aitken [16], the TL of step 6 is similar to $S_N^{\perp}$ of Baillif [17], which he termed the 'measurement of the radiation quenched sensitivity'. The sensitivity to a fixed TD of TL of step 5 and immediate TL of step 6 for all the TATs are presented in Table 2 in order to establish the quenching in step 6 relatively to step 5 for the two samples. It is clear from this table that the sensitivity to the same TD is always quenched in step 6 comparatively to step 5 for 250 °C TAT and above. In short, the sensitization rather than desensitization of step 6 for 180 °C TAT is in conformity with the mechanisms of the 110 °C TL peak in general. This is on the basis of the reality that holes were not thermally transferred to the L-center from the R-center and the available captured holes at the L-centers are merely the proportion derived from the TDs in only steps 5 and 6. Therefore, desensitization is not expected in step 6 for 180 °C TAT but sensitization that is traceable to the competition effect since the cumulative dose in steps 6 is higher (high-temperature aspect of Sn_3 in plots (A) and (B) of Fig. 7). In the case of 250 °C TAT and beyond, in addition to the contributions of the TDs, the population of the captured holes at L-centers in step 5 are derived from the thermal activation of step 3. For step 6, the only additional contribution to those gained from the TD is the residual of the thermally activated holes that survived step 5 holes depletion.

Table 2 Comparison of TL sensitivity to a TD of steps 5 and 6 of the protocol for the two samples.

*TAT$_i$ (°C)	normalized TL integral (a.u.)			
	S2		S4	
	step 5	step 6	step 5	step 6
180	1.91	2.09	1.90	2.35
250	5.80	5.70	7.14	6.93
300	9.82	9.73	7.63	7.45
350	9.07	8.99	6.24	6.06
400	7.72	7.51	4.34	4.24
450	7.23	7.10	4.38	4.24
500	6.67	6.50	3.75	3.64

Pagonis et al. [18] theoretically observed radiation quenching not be only caused by recombination that occurs during irradiation (step 4) as proposed by Aitken [16]. Rather, the TL (of Step 5 as in this work), which is a preheating that is meant for removal of the 110 °C TL peak that customarily follows a laboratory calibration beta-dose, definitely contributes to the radiation-quenched sensitivity also. This is experimentally observed in this study, because the recombination of step 5, which is measurable and quantifiable, as is evident in Fig. 3 and Sn_1 in plots (C) and (D) of Fig. 7), also resulted into depletion of captured holes at L-centers, implying that the greater the available additive dose D_i (Fig. 3) to cause depletion of the captured holes in step 5, the more pronounced the observed desensitization in step 6 (Figs. 4 and 5). As observed, the TL signal of steps 6 (Figs. 4 and 5) is somewhat inversely dependent on the TL signal of step 5 (Fig. 3). Thus, Fig. 5 is a reflection of the degree of the depletion of the pumped holes at L-centers as predetermined by the additive dose D_i of step 4 (Fig. 3).

Aliquots with the least additive dose D_1 for the two samples exhibited the highest sensitivity to the TD of the immediate step (Fig. 5). This accounts for why the sensitivity decreases with the additive dose D_i for all the TAT, since the degree of the survival of the pumped holes depletes with additive dose also. Particularly in S4, the radiation-quenching effect reached its maximum at 16 Gy when recombination resulting from irradiation and TL of Steps 4 and 5, respectively, has caused nearly total depletion of the already pumped holes at the L-center (Figs. 4 and 5). The filling of competitors by subsequent dose D_i at 32 Gy invariably causes the quenching effect less effective and at the same time makes the competition impact obvious. The result of this is the increase of sensitization at dose 32 Gy after 16 Gy. The fact that the competition effect is more prevalent in S4 seems to justify why this observation is only limited to this sample. This, therefore, indicates that this high dose has nullified the sensitization resulting from predose effects of steps 2 and 3 that the aliquots possessed. Consequently, the MATAC seems not to be TAT dependent any longer.

5 Conclusions In this work, the results of the two quartz samples showed the structure of the MATAC to be

predetermined by the nature of the glow curves (in particular the high-temperature TL peaks) obtained during the thermal activation. This relationship could be helpful in predicting MATAC of a given quartz based on the structures of its high temperature glow peak. This could be therefore helpful in the selection of preheat temperature as applicable in the SAR dating protocol. The roles of reservoirs and competitors in luminescence characteristics have been used to explain the property of the 110 °C TL peak of two quartz samples in the present study. This report is among the first experimental attempts to monitor these effects directly correlated to the presence of reservoirs and competitors. The competition effect was observed to be more prevalent in S4 than S2. It is suggested that all the measurements undertaken be extended to diverse quartz types and different origins.

Acknowledgements E.O.O. is profoundly grateful to the Adekunle Ajasin University and Education Trust Fund (ETF) Nigeria for financial support.

References

[1] R. Chen and S. W. S. Mckeever, Theory of Thermoluminescence and Related Phenomena (World Scientific Publishing, Singapore, 1997).
[2] S. W. S. Mckeever and R. Chen, Radiat. Meas. **27**(5), 625 (1997).
[3] R. M. Bailey, Radiat. Meas. **33**, 17 (2001).
[4] F. Preusser, M. L. Chithambo, T. Götte, M. Martini, K. Ramseyer, E. J. Sendezera, J. Susino, and A. G. Wintle, Earth-Sci. Rev. **97**, 184 (2009).
[5] R. Chen and P. L. Leung, J. Phys. D: Appl. Phys. **31**, 2628 (1998).
[6] R. Chen and P. L. Leung, Radiat. Protect. Dosim. **84**, 43 (1998).
[7] V. Pagonis, G. Kitis, and R. Chen, Radiat. Meas. **37**, 267 (2003).
[8] G. Polymeris, G. Kitis, and V. Pagonis, Radiat. Meas. **41**, 554 (2006).
[9] R. Chen and G. Fogel, Radiat. Protect. Dosim. **47**, 23 (1993).
[10] R. Chen and S. W. S. McKeever, Radiat. Meas. **23**(4), 667 (1994).
[11] J. Zimmerman, J. Phys. C: Solid State Phys. **4**, 3265 (1971).
[12] R. Chen and V. Pagonis, J. Phys. D: Appl. Phys. **36**, 1 (2003).
[13] L. Bøtter-Jensen, L. N. Agersnap, V. Mejdahl, N. R. J. Poolton, M. F. Morris, and S. W. S. McKeever, Radiat. Meas. **24**, 535 (1995).
[14] N. Itoh, D. Stoneham, and A. M. Stoneham, J. Phys.: Condens. Matter **13**, 2201 (2001).
[15] S. W. S. McKeever, Nucl. Tracks Radiat. Meas. **18**, 5 (1991).
[16] M. J. Aitken, Thermoluminescence Dating (Academic Press, London, 1985).
[17] I. K. Bailiff, Radiat. Meas. **23**(2/3), 471 (1994).
[18] V. Pagonis, E. Balsamo, C. Barnold, K. Duling, and S. McCole, Radiat. Meas. **43**, 1343 (2008).
[19] M. Figel and C. Goedicke, Radiat. Protect. Dosim. **84**, 433 (1999).
[20] G. Kitis, V. Pagonis, R. Chen, and G. Polymeris, Radiat. Protect. Dosim. **119**(1–4), 438 (2006).
[21] G. Kitis, V. Pagonis, and R. Chen, Radiat. Meas. **41**, 910 (2006).
[22] G. Adamiec, M. Garcia-Talavera, R. M. Bailey, and P. Iniguez de la Torre, Geochronometria **23**, 9 (2006).
[23] G. Adamiec, A. Bluszcz, R. Bailey, and M. Garcia-Talavera, Radiat. Meas. **41**, 897 (2006).
[24] L. Bøtter-Jensen, E. Bulur, G. A. T. Duller, and A. S. Murray, Radiat. Meas. **32**, 523 (2000).
[25] E. F. Mische and S. W. S. McKeever, Radiat. Protect. Dosim. **29**, 159 (1989).